FINAL REPORT

Report No. FL/DOT/MO/340/88
State Project No. 99700-7375-119

WPI 0510413
UF Project 4910450420712

TEST OF THE PUNCHING SHEAR STRENGTH OF LIGHTLY REINFORCED ORTHOTROPIC BRIDGE DECKS

C.O. Hays
J.M. Lybas
J.O. Guevara

August 1988

Structures and Materials Research Report No. 88-3

Department of Civil Engineering
College of Engineering
UNIVERSITY OF FLORIDA
Gainesville

Engineering & Industrial Experiment Station

TECHNICAL REPORT STANDARD TITLE PAGE

1. Report No.	2. Government Accession No.	3. Recipient's Catalog No.
FL/DOT/M0340-88		

4. Title and Subtitle	5. Report Date
Tests of the Punching Shear Strength of Lightly Reinforced Orthotropic Bridge Decks	August 1988
	6. Performing Organization Code
7. Author(s)	8. Performing Organization Report No.
Cliff O. Hays, John M. Lybas, and Jose O. Guevara	4910450420712
9. Performing Organization Name and Address	10. Work Unit No.
University of Florida Department of Civil Engineering 345 Weil Hall Gainesville, FL 32611	11. Contract or Grant No.
12. Sponsoring Agency Name and Address	13. Type of Report and Period Covered
FL Dept of Transportation Materials Office P.O. Box 1029 Gainesville, FL 32602 FL Dept of Transportation Bureau of Environment 605 Suwannee St. M.S.37 Tallahassee, FL 32301	Final Report May 8, 1987 - Aug 31, 1988
	14. Sponsoring Agency Code 99700-7375-119

15. Supplementary Notes

Prepared in cooperation with the Federal Highway Administration

16. Abstract

The AASHTO provisions for concrete bridge decks, based on design for flexure are very conservative, primarily because the horizontal expansion of the bottom surface of the slab caused by flexural strains are restrained by the longitudinal girders and other parts of the bridge system. Canadian research on both small scale models and prototype bridges indicated strengths for far in excess of that required by normal wheel loads. The Ontario Highway Bridge Design Code has adopted a simple empirical design approach for bridge decks, allowing 0.3% orthotropic reinforcement top and bottom in both directions, when certain requirements are met. In 1971, scale model tests were performed by the New York Highway Department (2) that confirmed the general behavior of the bridge decks observed in the Ontario research. Recently an extensive research program has been carried on at the University of Texas on a full scale laboratory model.

A series of laboratory tests on approximately one-half scale models of concrete bridge decks built with the 0.3% orthotropic reinforcement are underway at the University of Florida. This report documents the first year of the study involving the static application of simulated wheel loads to three specimens. Static load capacities for all tests, when converted to a full scale 8" deck thickness, gave more than an adequate factor-of-safety for typical highway legal tandem loads. A fourth specimen will be constructed and tested in the second year of the project. This specimen will be subjected to a large number of cyclic loads and then subjected to static loading to failure. The second year's testing will include three specimens with slabs cast on standard size bulb-tee girders, as recently adopted in Florida. Additional work is planned to thoroughly analyze the results of all tests comparing the observed behavior to finite element and other analytical models.

17. Key Words	18. Distribution Statement
Bridge decks, Orthotropic Reinforcement Punching Shear Laboratory Testing	No restrictions. This document is available to the public through the National Technical Information Service, Springfield, VA, 22161

19. Security Classif. (of this report)	20. Security Classif. (of this page)	21. No. of Pages	22. Price
Unclassified	Unclassified	201	

Form DOT F 1700.7 (8-69)

Final Report

TESTS OF THE PUNCHIN SHEAR STRENGTH OF LIGHTLY REINFORCED OR OTROPIC BRIDGE DECKS

State Project No.:	9700-7375-119
OF Project No.:	910450420712
WPI No.:	510413

by

Clifford 0. Hays, Jr.

John M. Lybas

Jose 0. Guevara

Engineering and Industrial Experiment Station

College of Engineering

Department of Civil Engineering

University of Florida

Gainesville, Florida

Submitted to

Florida Department of Transportation

August 1988

METRIC CONVERSION FACTORS

Approximate Conversions to Metric Measures

Symbol	When You Know	Multiply by	To Find	Symbol
		LENGTH		
in	inches	*2.5	centimeters	cm
ft	feet	30	centimeters	cm
yd	yards	0.9	meters	m
mi	miles	1.6	kilometers	km
		AREA		
in^2	square inches	6.5	square centimeters	cm^2
ft^2	square feet	0.09	square meters	m^2
yd^2	square yards	0.8	square meters	m^2
mi^2	square miles	2.6	square kilometers	km^2
	acres	0.4	hectares	ha
		MASS (weight)		
oz	ounces	28	grams	g
lb	pounds	0.45	kilograms	kg
	short tons (2000 lb)	0.9	tonnes	t
		VOLUME		
tsp	teaspoons	5	milliliters	ml
Tbsp	tablespoons	15	milliliters	ml
fl oz	fluid ounces	30	milliliters	ml
c	cups	0.24	liters	l
pt	pints	0.47	liters	l
qt	quarts	0.95	liters	l
gal	gallons	3.8	liters	l
ft^3	cubic feet	0.03	cubic meters	m^3
yd^3	cubic yards	0.76	cubic meters	m^3
		TEMPERATURE (exact)		
°F	Fahrenheit temperature	5/9 (after subtracting 32)	Celsius temperature	°C

*1 in = 2.54 (exactly). For other exact conversions and more detailed tables, see NBS Misc. Publ. 286, Units of Weights and Measures, Price $2.25, SD Catalog No. C13.10.286.

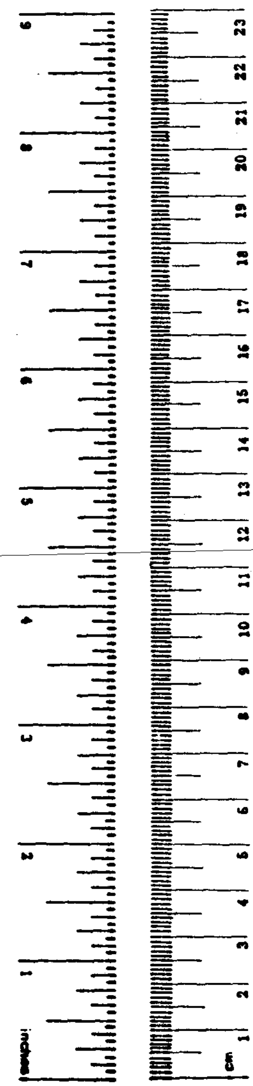

Approximate Conversions from Metric Measures

Symbol	When You Know	Multiply by	To Find	Symbol
		LENGTH		
mm	millimeters	0.04	inches	in
cm	centimeters	0.4	inches	in
m	meters	3.3	feet	ft
m	meters	1.1	yards	yd
km	kilometers	0.6	miles	mi
		AREA		
cm^2	square centimeters	0.16	square inches	in^2
m^2	square meters	1.2	square yards	yd^2
km^2	square kilometers	0.4	square miles	mi^2
ha	hectares (10,000 m^2)	2.5	acres	
		MASS (weight)		
g	grams	0.035	ounces	oz
kg	kilograms	2.2	pounds	lb
t	tonnes (1000 kg)	1.1	short tons	
		VOLUME		
ml	milliliters	0.03	fluid ounces	fl oz
l	liters	2.1	pints	pt
l	liters	1.06	quarts	qt
l	liters	0.26	gallons	gal
m^3	cubic meters	35	cubic feet	ft^3
m^3	cubic meters	1.3	cubic yards	yd^3
		TEMPERATURE (exact)		
°C	Celsius temperature	9/5 (then add 32)	Fahrenheit temperature	°F

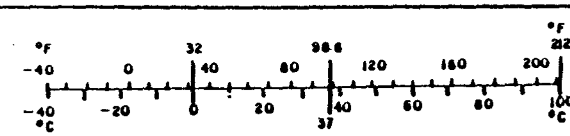

INDEX

CHAPTER ONE

INTRODUCTION

It is well known that the AASHTO (1) provisions for concrete bridge decks, based on design of the slab for flexure are very conservative. Apparently the primary reason for the conservatism is that the horizontal expansion of the bottom surface of the slab caused by flexural strains are restrained by the longitudinal girders and other parts of the bridge system. This induces compression in the slab, increasing the failure load, and is referred to as arching action.

1.1 Previous Research and Implementation

Research performed by the Ontario Ministry of Transportation (3,4,5,6), on both small scale models and prototype bridges indicated strengths under a two tire loading to be far in excess of that required by normal wheel loads on Canadian or American highways. The Ontario research emphasized the importance of lateral confinement and the associated arching action on the strength of the deck.

Based on the punching shear research the Ontario Highway Bridge Design Code, OHBDC (8), adopted a simple empirical design approach for bridge decks, allowing 0.3% orthotropic reinforcement top and bottom in both directions,

when certain requirements relative to slab thickness, transverse span-to-thickness ratio, transverse span, diaphragms, overhangs, and other parameters are met.

Considerable interest has been shown in developing a OHBDC-like design approach for application in the United States. It has been estimated by the FDOT engineers that the use of 0.3 % orthotropic reinforcement could save from one fourth to one half the quantity of reinforcement in typical bridge decks.

Also, reducing the quantity of deck steel has advantages in reducing congestion in the deck during placement of the concrete and in reducing the conduits for corrosion to enter. However, there are several differences between Canadian and US practice in bridge construction, which led several states to do research on punching shear.

As early as 1971, scale model tests were performed by the New York Highway Department (2) that confirmed the general behavior of the bridge decks observed in the Ontario research. Recently an extensive research program has been carried on at the University of Texas on a full scale laboratory model. The Texas tests (7,9,10) were made on a full scale model of a 7-1/2" thick deck supported on three steel girders spaced at 7'-0" center-to center. The overall deck dimensions in plan were 20' by 50'. Half of the bridge was constructed using stay-in-place panels and the other half was of conventional cast-in-place construction.

First the bridge was supported as a simply supported bridge with the girders having a span of 49' - 0". Four wheel loads were applied simultaneously to represent a two axle truck straddling the center girder. The bridge was statically loaded to wheel load of 60 kips and then subjected to cyclic wheel loads of approximately 26 kips for 5,000,000 cycles. After the cyclic loading the wheel loads were again applied statically, this time to a load of 40 kips. The bridge performed well in all areas.

The same bridge used in the first series of tests was then subjected to a loading to simulate the behavior of a continuous girder bridge in the negative moment region. The bridge was loaded with four concentrated loads to represent a tandem with two axles and four wheel loads. Static and cyclic tests were performed. Again the bridge behaved well under the static and cyclic loading.

Then, single point and double point concentrated load tests were made to failure in both the cast-in-place and stay-in-place portions of the deck. The single point failure loads exceeded 140 kips for the cast-in-place deck. Total load for the two point failure test exceeded 200 kips for the cast-in place deck. The corresponding failure loads for the stay-in-place portion of the deck were even higher.

Finally, additional tests were made on a skewed slab specimen which performed well under monotonic failure loading. The Texas researchers showed that the beneficial effects of lateral confinement exist even prior to cracking of the deck and the development of yield lines. This is important; because it shows that stresses in the steel even at service load levels may be substantially less than that given by AASHTO criteria.

The Texas tests are very encouraging. However, they only involved one span-to-thickness ratio for the slab, 11.2. The OHBOC allows the simplified orthotropic design for values up to 15. Also, the Texas research, like the Ontario research, did not involve tests in the overhanging areas of the slab.

1.2 Scope of Florida Tests

A series of laboratory tests on approximately one-half scale models of concrete bridge decks built with the 0.3% orthotropic reinforcement, consistent with the Ontario empirical design approach, are underway at the University of Florida. These tests are meant to extend and enhance the prior research, and provide data on the feasibility of using the empirical approach for bridge deck design in Florida and other states.

The major differences between Canadian and American practice with regards to bridge deck construction are as follow. First, it is common practice in many states to use deck thicknesses less than the Ontario minimum of

8.85 inches. The test specimens reflect this, and additionally incorporate transverse span-to-thickness ratios up to 22, greater than the Ontario maxinum of 15. Using these higher span-to-thickness ratios would permit using fewer longitudinal girders than would normally be required for a particular bridge structure, with obvious cost savings.

Second, bulb-tee girders, currently finding application in Florida and other states, will be incorporated into several specimens. As the flanges of these girders are quite wide, and tapered in thickness, the definition of span-to-thickness ratio is not so straightforward as for a deck, on steel girders, and the tests will be designed to study this.

Third, the Ontario tests did not include loads applied to overhanging edges of slabs, and the Florida tests will include this. While the capacity for confinement in overhangs, and therefore arching, would be slight, some tests are warranted, especially considering the edge stiffening affects of the parapets normally used at slab edges. This report documents the first year of the study involving the static application of simulated wheel loads to three specimens.

1.3 Additional Studies

Based on the performance of the three specimens tested statically, a fourth specimen will be constructed and tested in the second year of the proj-ect:. This specimen will be subjected to a large number of cyclic loads and them subjected to static loading to failure. The second year's testing will include three specimens with slabs cast on standard size bulb-tee girders, as recently adopted in Florida.

Additional work is planned to thoroughly analyze the results of all tests comparing the observed behavior to finite element and other analytical models.

Chapter 2

TEST PROGRAM AND PROCEDURES

2.1 Size and Scale Facto s of Test Specimens

The general cross-section of the three specimens are shown in Figure 1. The same three simple span steel girders were used to support all three decks. Sacrificial steel plates were bolted to the girders to transfer the horizontal shear forces between the slab and the girders and yet permit the easy removal of the decks after each specimen was tested.

A parapet was located on one side of he specimens while the other side had only a plain overhang. The model parapet dimensions were chosen to approximate the flexural and torsional stiffness properties of a standard FDOT parapet at the appropriate scale.

The center-to-center spacing between he girders is S, the overhang distance on the side of the bridge with the parapet is A and the overhang distance on the other side of the bridge is B.

In any test program the range of variable that can be looked at is finite. When large specimens are involved this is even more true. After considerable discussion with the FDOT and after the excellent performance of the first specimen it was decided to hold all parameters for the prototype essentially constant in the three tests except or the slab span-to-thickness ratios. The scale factors were selected to be as close to 2.0 as possible and give the desired span-to-thickness ratios, subject to the limitations on the available width of the specimen between laboratory hold downs.

The three specimens were designed to have span-to-thickness ratios (S/T), of 18, 20 and 22, with the overhang-to-thickness ratios, (A/T) and (B/T), increasing proportionally. The nominal deck thicknesses were selected on the

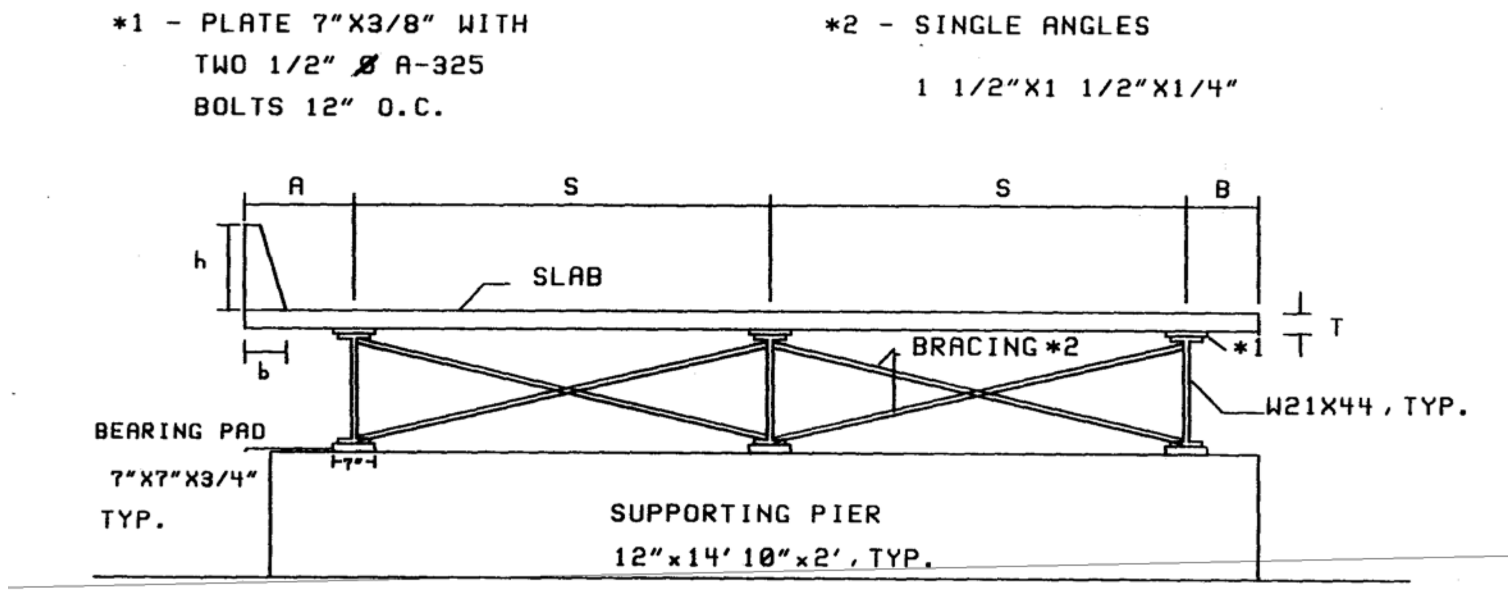

SPECIMEN	T	S	A	B	S/T	A/T	B/T	h	b	SCALE FACTOR
1	4 11/32	80	21.0	13.5	18.4	4.8	3.1	15.5	7.5	1.84
2	3 11/16	75 3/8	28.0	18.5	20.4	7.6	5.0	15.5	7.5	2.17
3	3 3/16	71 7/8	32.0	22.0	22.5	10.0	6.9	12.2	6.5	2.51

Figure 1 General Test Cross-Section

models to imply an eight (8) inch deck at full scale. After construction the deck thickness was measured using a surveyors level and the results are shown in Appendix 0. The table in Figure 1. shows the S/T, A/T, and B/T ratios computed using the average thicknesses of the decks. The scale factors shown in the table were computed using the average measured deck thicknesses to give a prototype or full scale deck thickness of inches.

The first specimen was constructed entirely with University of Florida personnel and was satisfactory in all respects except for the finishing of the top of the concrete deck. Due to the large volume of concrete and large surface area to be finished, the deck's top surface was not finished as well as desired. For the second and third test specimens, Durastress Concrete provided professional concrete finishers to assist in the placement and finishing of the concrete in the deck. Both the second and third specimens had a uniform high quality finish of the deck top.

Figure 2. shows a plan view of the specimens. The simple span length of all specimens was 24'-11" and the length of the steel beams and deck was 25'8". Corresponding span length at full scale ranged from approximately 45 to 62 feet. The x-braces were welded to the top and bottom flanges of the girders at the three longitudinal positions shown in Figure 2.

2.2 Material Properties of Specimens

For a scale factor of approximately 2, the maximum size aggregate should be approximately 3/8". Thus, the coarse aggregate used was FDOT designation #89. Because of the volume of concrete in the deck it was advisable to use a ready mix concrete. The concrete mix was a FDOT type II with a a design strength of 3,400 psi. Average compressive strengths at 28 days were 5590 psi, 5980 psi, and 5720 psi for specimens 1, 2, and 3, respectively.

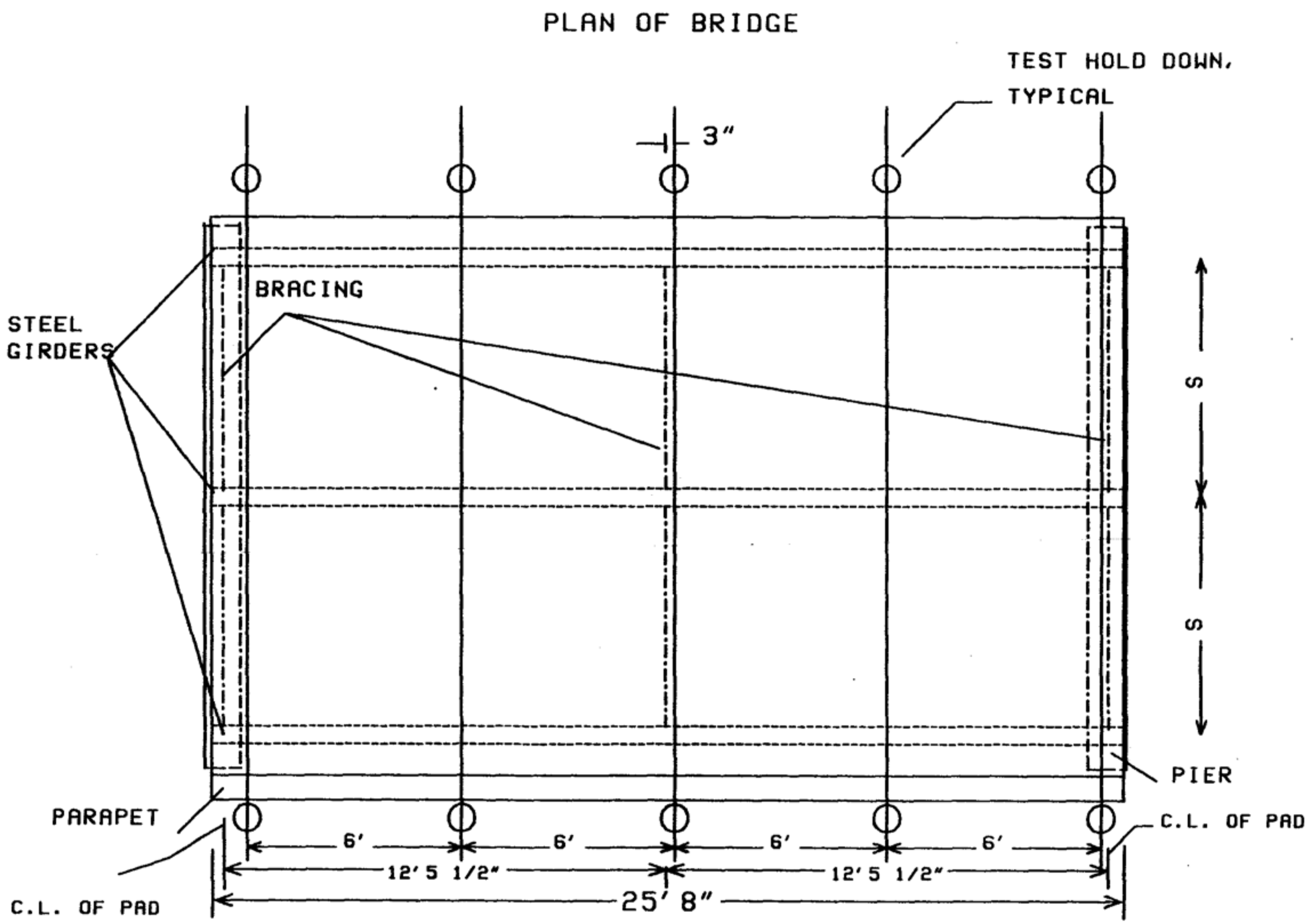

Figure 2 Plan View of Test Specimens

Complete cylinder compressive and flexural modulus of rupture test results are shown in Appendix F. ,Also, Appendix F contains an aggregate gradation curve and typical concrete mix proportions.

It is difficult to obtain deformed reinforcement for scale modeling of tests even for one-half scale testing. For the .370 orthographic reinforcement in an 8" deck a typical reinforcement pattern would be #4 @ 12". For a scale factor of 2.0, this implies #2 0 6". Deformed wire of approximately the same size as a #2 bar is available (0.05 si); however, the wire is usually cold drawn and has higher strength and less ductility than conventional reinforcement. Ivey Steel in Jacksonville Florida cooperated with the University of Florida to provide a steel wire with good ductility and a yield stress close to that for conventional reinforcement.

The Stress-strain curve for the reinforcing wire is shown in Appendix F. The wire used in the specimens was nominal y a D5 (.05 si). However, the computed area based on weight is only about 0 0477 si. Using the .0477 area gives a yield stress of about 76 ksi. However, using the nominal area of 0.05 si gives a yield stress of only 72 ksi. T e stress-strain curve exhibits a definite yield plateau and has quite good ductility.

Figure 3. shows the spacing of the reinforcing wire for the specimens. The primary reinforcement was the D5 wires at 6" on centers both ways top and bottom in the deck. The cover to the transverse top and bottom bars was 1". On the side without the parapet, extra transverse top bars were used with the same spacing as the primary reinforcement. In addition, for specimen No. 1 only, extra transverse reinforcement similar to that on the free edge was used on the side with the parapet. Extra later 1 reinforcement was used in the end section to provide additional support at the discontinuous end of the slab as shown in Figure 3.

S	Sr
80″	6″
75 3/8″	6 1/2″
71 7/8″	7 1/2″

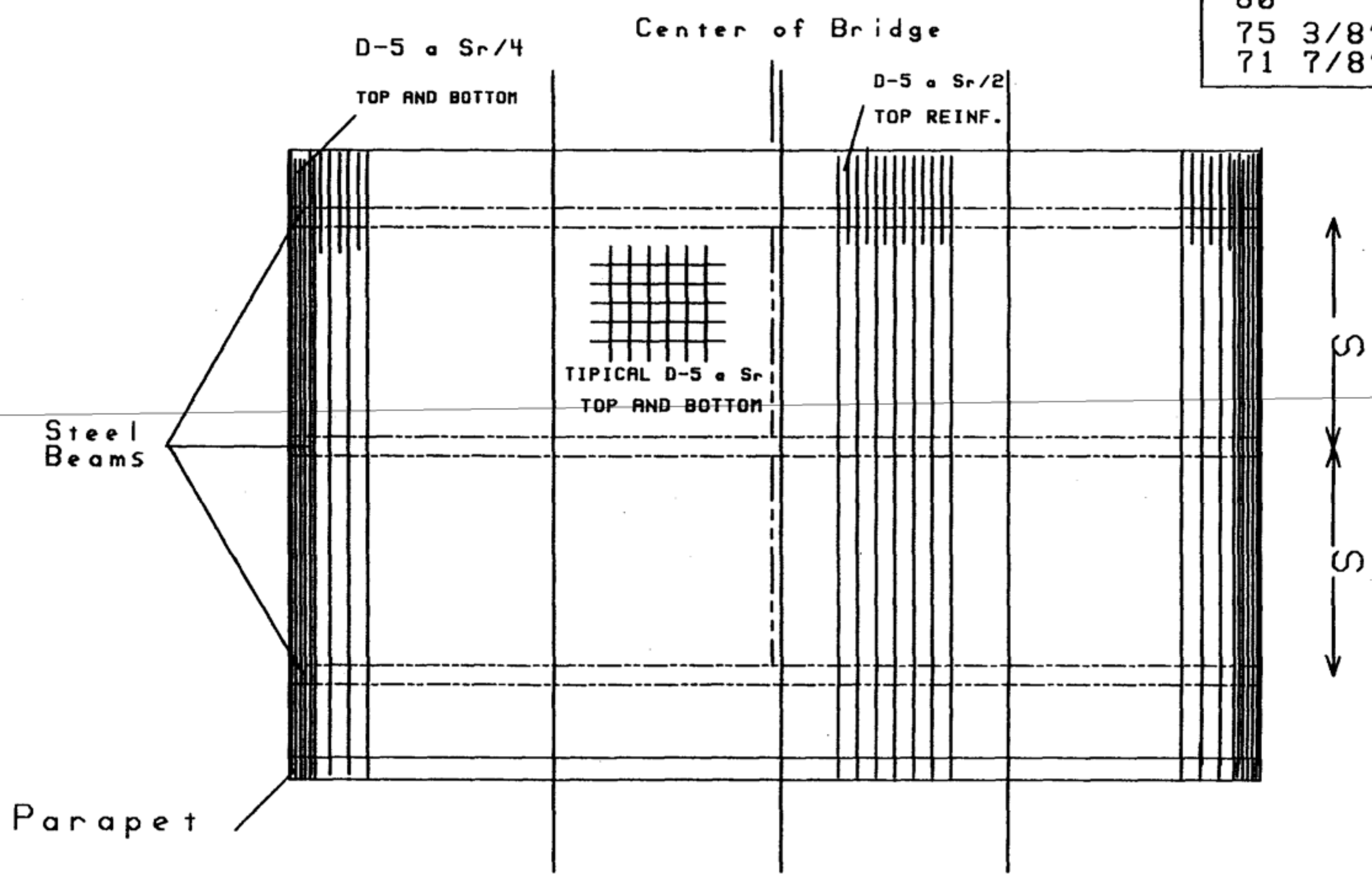

Figure 3 Reinforcement Spacing for Specimens

Figure 4. is a photograph of specimen number three showing the general layout of the specimen.

2.3 Loading And Instrumentation

By loading the deck in a variety of locations, the relative effects of the parapet, the free overhang, and the confinement of the interior spans could be observed. The loading positions and patterns for the three specimens are shown in Figures 5, 6, and 7, respectively. Loads were applied to the deck through heavy steel plates, shaped an sized to model the imprint of one dual wheel formation at half scale.

Loading on the first specimen represented either one set of dual tires or two sets of dual tires belonging to separate trucks passing close to one another. However, when the (S/T) ratio was et for the second and third tests it became apparent that the effect of a full tandem of loads should be investigated. Thus, for the second and third specimens, four loads representing a full tandem wheel formation of one tuck were applied. In all discussions of test loads, the entire load on the test is given, whether it is distributed to one, two, or four wheel plates.

Figure 8. shows a view of the load assembly used to apply the tandem loads. Two 6" deep steel W sections were supported on rollers that were placed on top of the four wheel pads. A 6" deep steel W section spanned between the two lower steel sections and was loaded by the vertical hydraulic ram. The ram jacked against a longitudinal beam that spanned between two lateral frames that spanned over the specimen. Rollers were not used under the lower steel W section for specimen numb r two; thus, the loading might not have been exactly equally distributed for those tests.

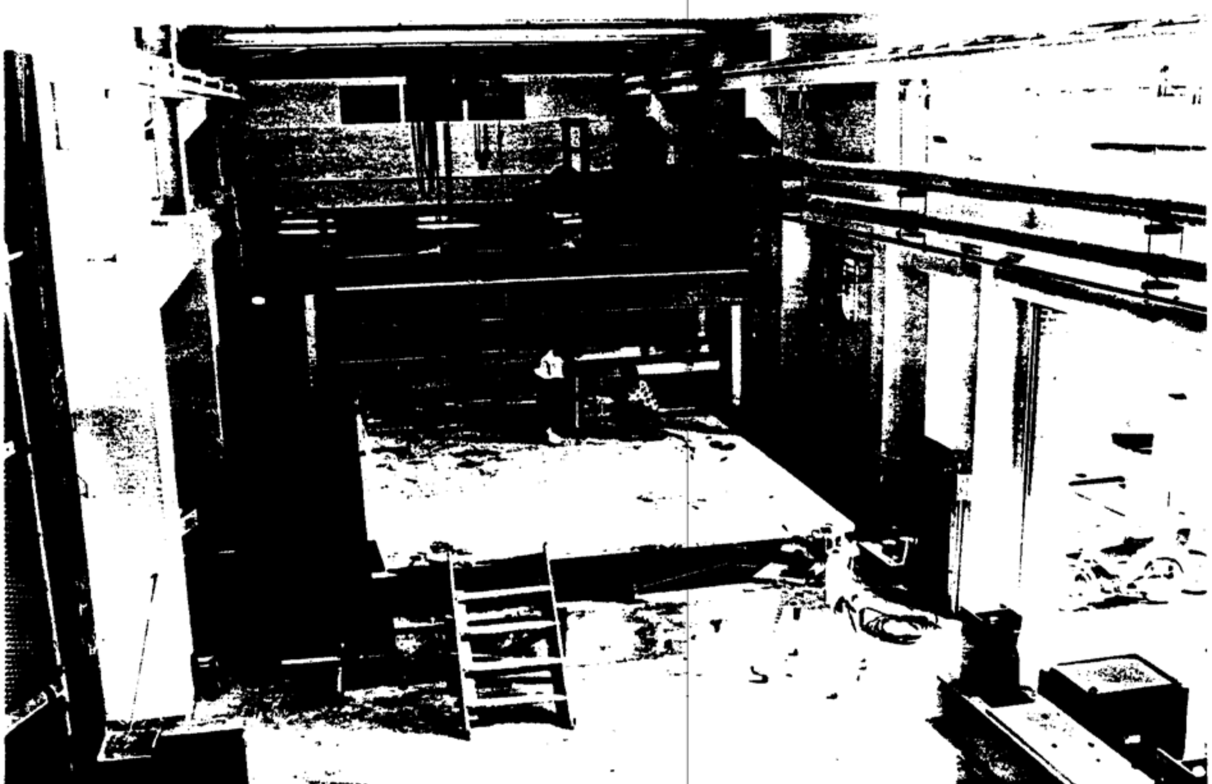

Figure 4 General Layout of Test Specimens

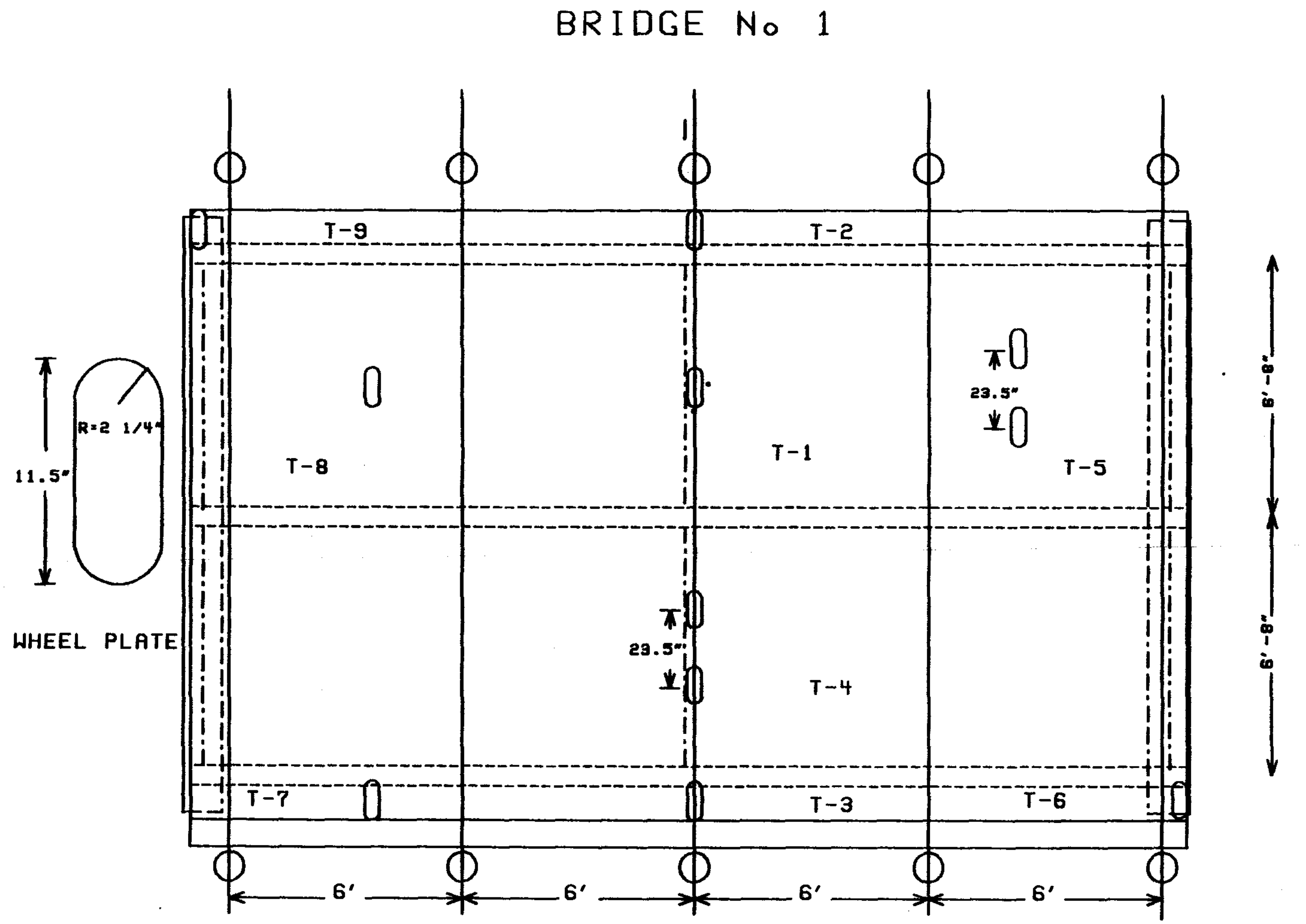

Figure 5 Loading Positions for Specimen One

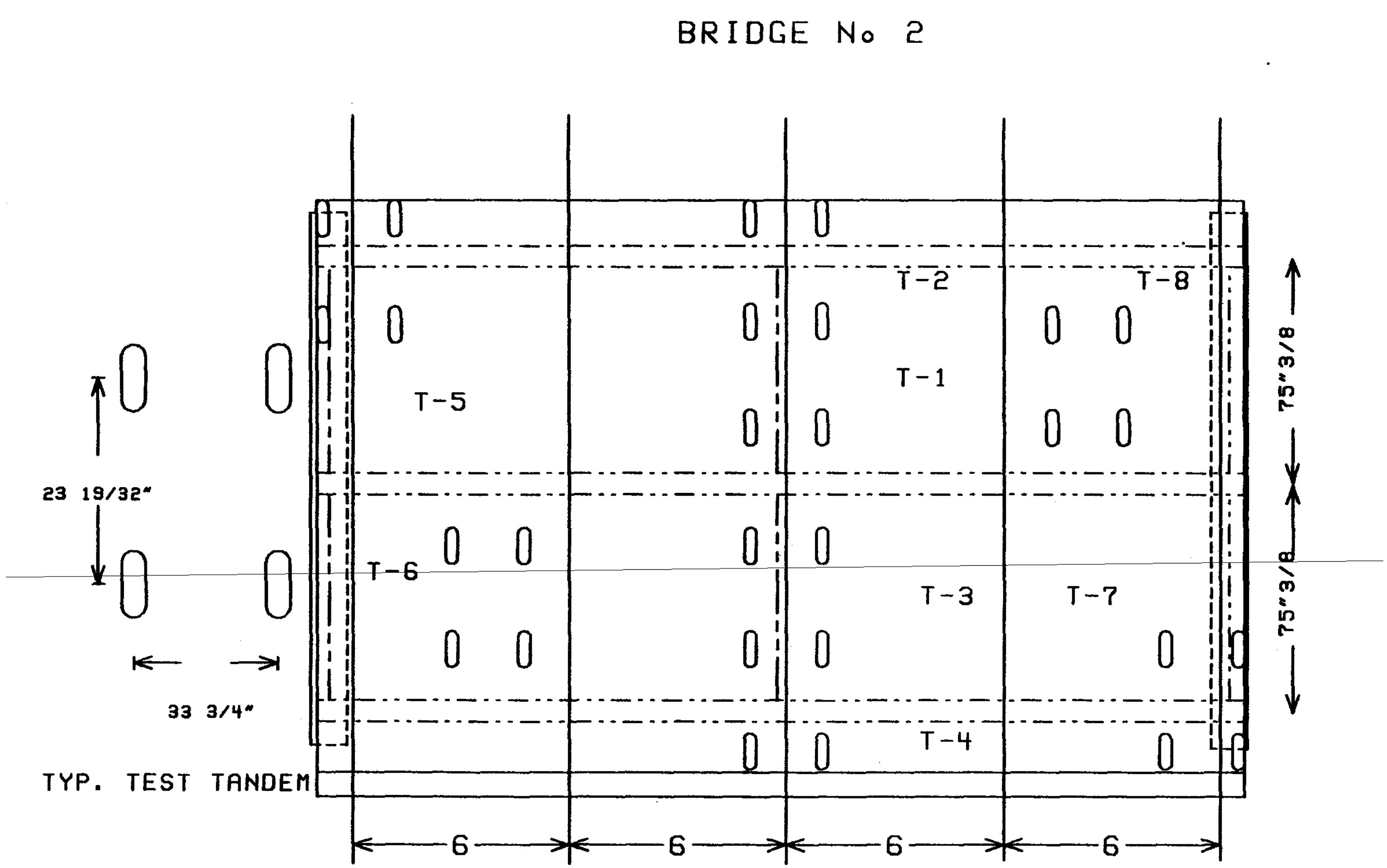

Figure 6 Loading Positions for Specimen Two

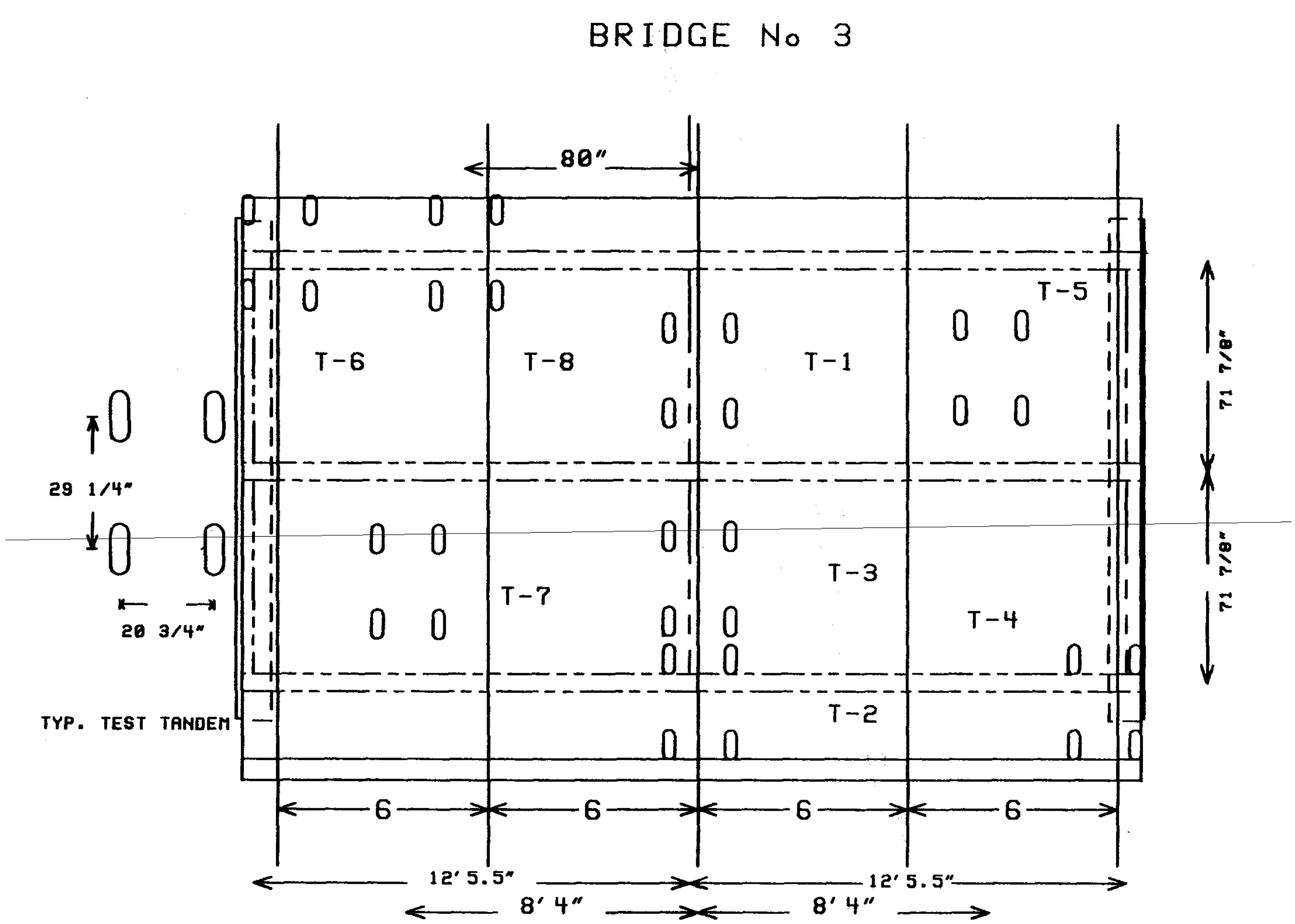

Figure 7 Loading Positions for Specimen Three

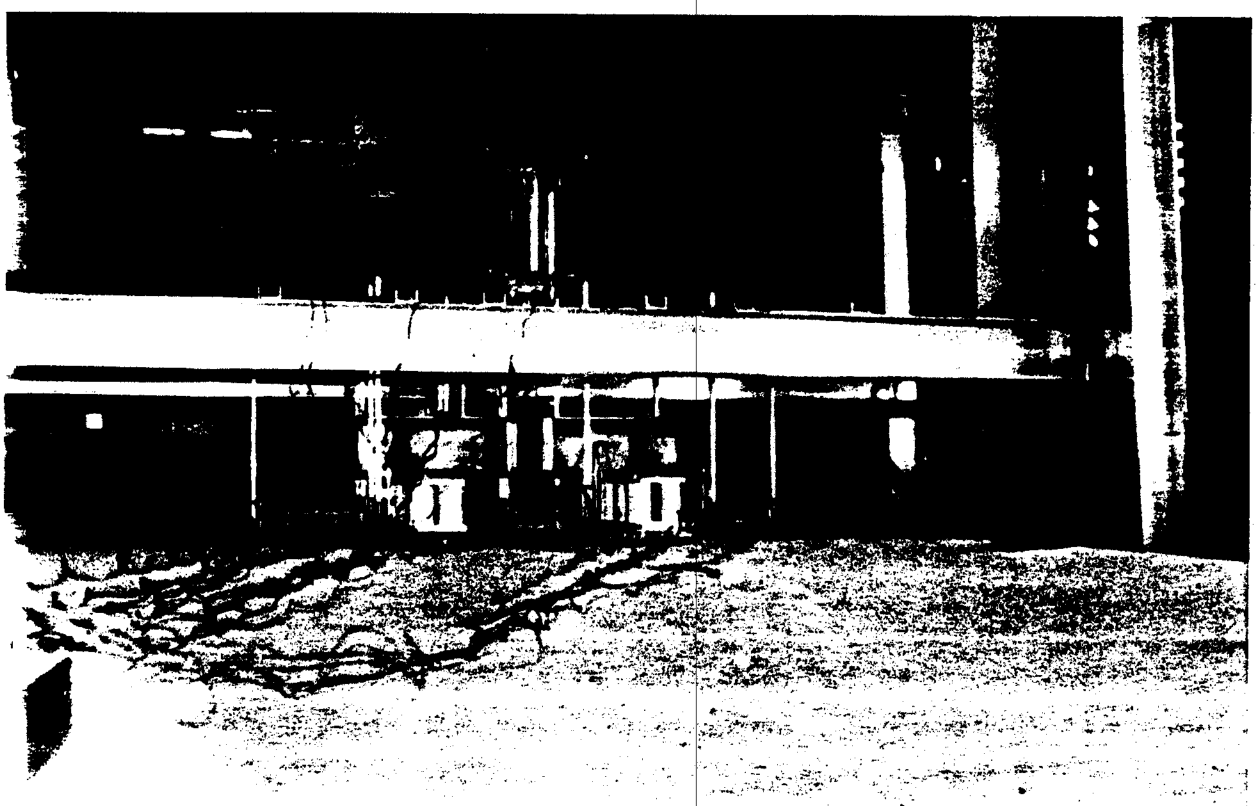

Figure 8 Load Assembly for Specimens Two and Three

Loads were applied statically using an hydraulic ran and left in place briefly prior to reading the instruments. Differential transformers (LVDT's) were used to measure vertical deflections and electric resistance strain gages were used to measure strains. LVDT and s rain gage readings were obtained and recorded on a HP 9820 data acquisition system.

Vertical deflections were measured using 15 LVDT's, arranged in a pattern so as to define a deflection basin. All VDTs, except for the one measuring the deflection of the load plate, were supported on wooden support beams for specimen #1 and aluminum support beams for specimens two and three. The central LVDT used to measure the deflection f the load plate was supported such that it included the vertical deflection f the test frame. Appendix A shows. the locations of the LVDT's for all tests and Appendix B gives complete load deflection plots for all tests.

Electrical resistance strain gages w re used at various locations in the tests, including the top and bottom surfaces of the deck, on the reinforcement, on the longitudinal girders, and on the bracing. Two inch long gages with high endurance lead wires were used on the concrete surfaces, 0.031" gage length general purpose miniature gages were used on the reinforcing steel and 0.23" universal general purpose strain gag s were used on the steel angle braces. Appendix C gives the locations of the strain gages for the various tests and Appendix D contains all of the 1 ad-strain plots.

CHAPTER 3 TEST 13EH VIOR

The general load-deflection response and failure modes of the specimens are described in this chapter. Detailed studies of the behavior and comparisons with analytical models will be done s a part of planned future studies. The general load-deflection response for all three specimens are shown in Figures 9, 10 and 11 as variations of tot 1 applied load with deflection at the center of the tire imprint formation. As stated earlier, this deflection includes the vertical deflection of the s eel framing. The maximum load attained during each test, the load at which a flexural yield pattern was well developed in the deck, and the maximum de lection attained beneath the load during each test, along with the above results converted to full scale, are given in Table 1. Each curve is labeled T-i where i represents the test number whose locations are shown in Figures 5, 6 and 7. Full scale loads and deflections were obtained by multiplying the test values by the scale factor and the square of the scale factor for deflection and load values, respectively. The scale factors used were those shown in Figure 1.

Most of the tests were continued to complete failure. However, seven of the test, as shown in Table 1., were stopped prior to failure. All of these except one were due to limitations of the test set-up rather than the deck and these loads raised to full scale were well beyond any reasonable highway loading. However, test T-2 on specimen 3 as stopped because of the development of a negative moment yield line over he full length of the specimen. It was felt that to continue this test would make further testing anywhere on that side of the specimen completely unrepresentative of an actual undamaged deck.

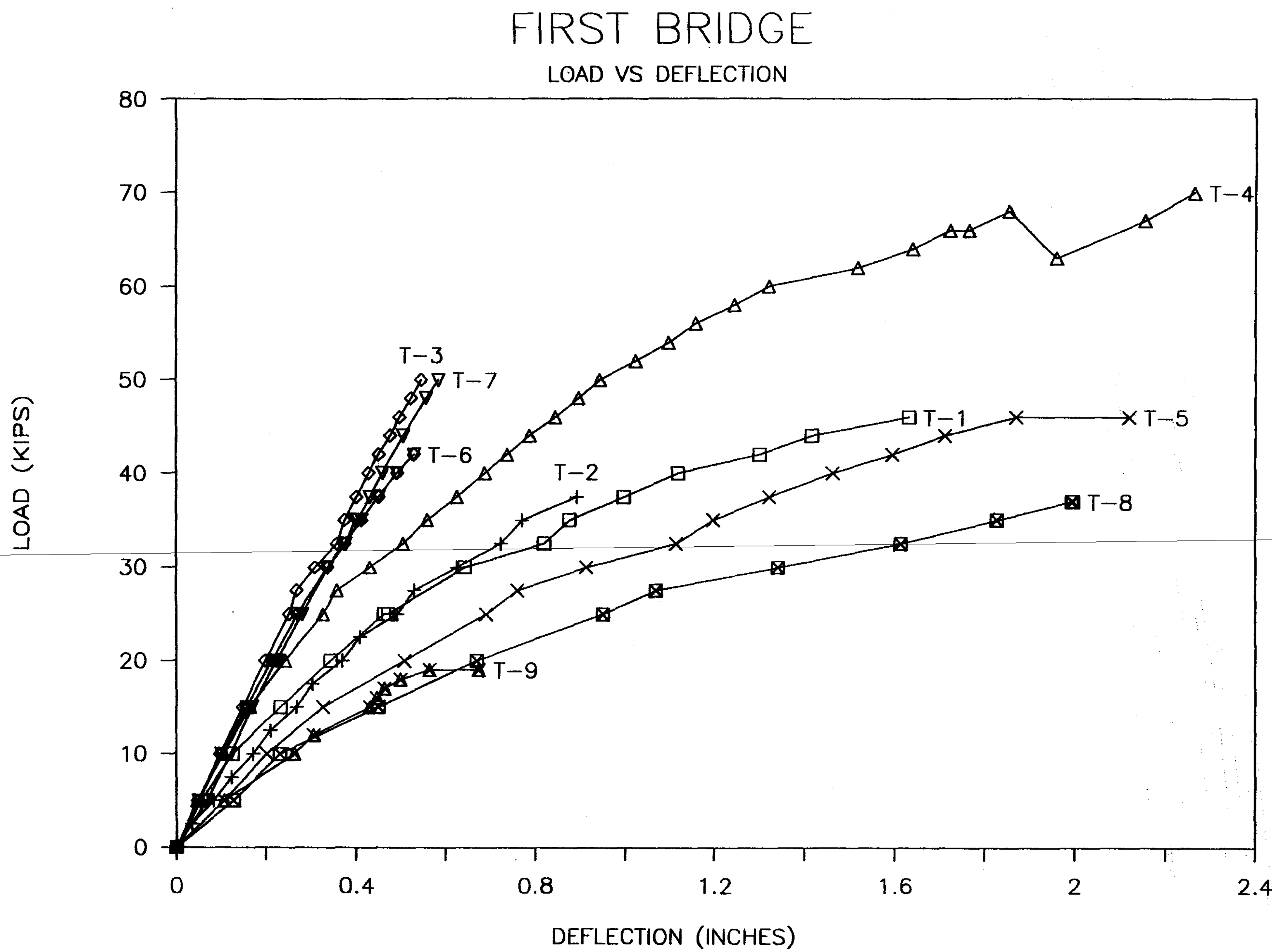

Figure 9 General Load-Deflection Curves for Specimen One

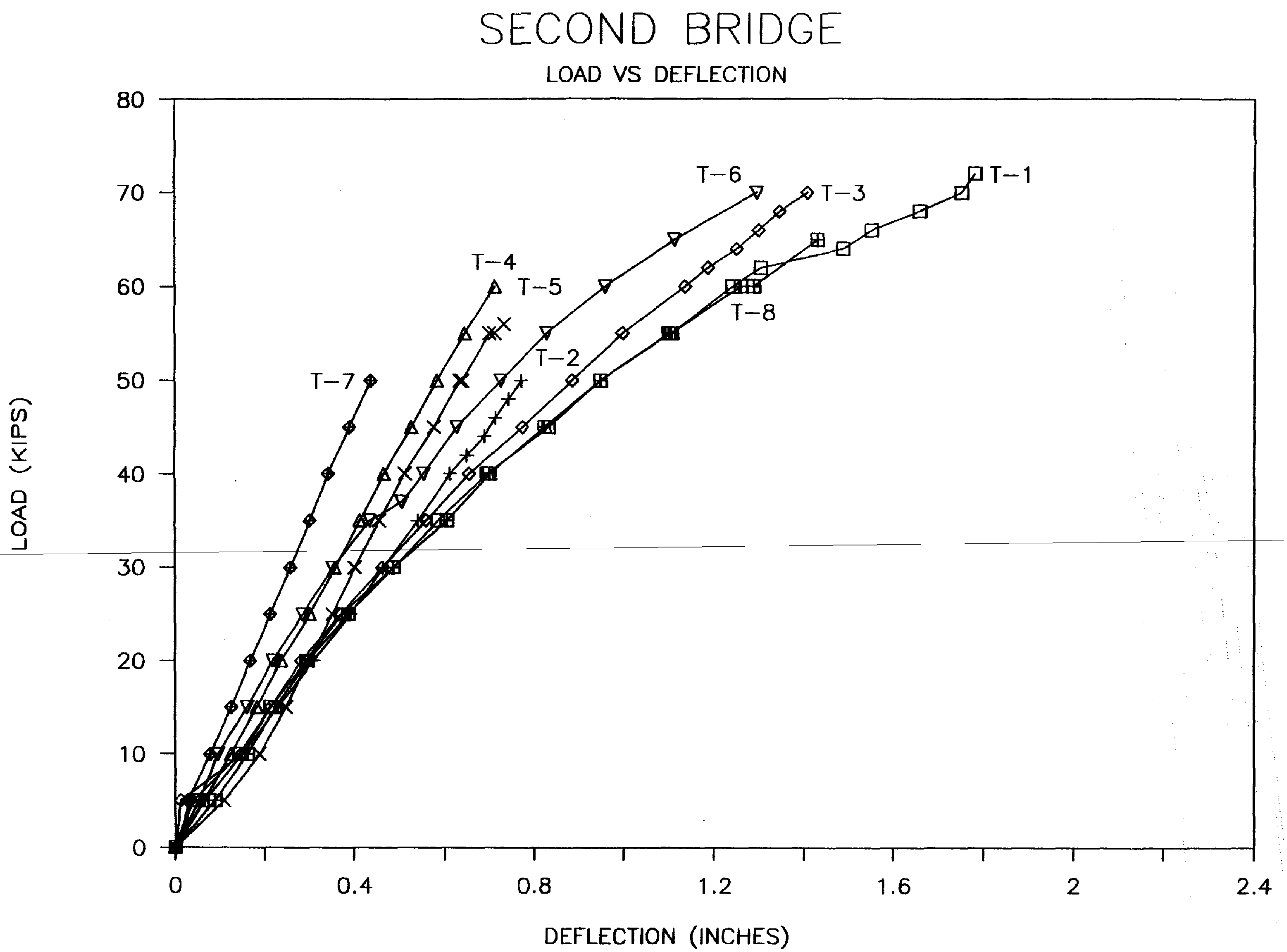

Figure 10 General Load-Deflection Curves for Specimen Two

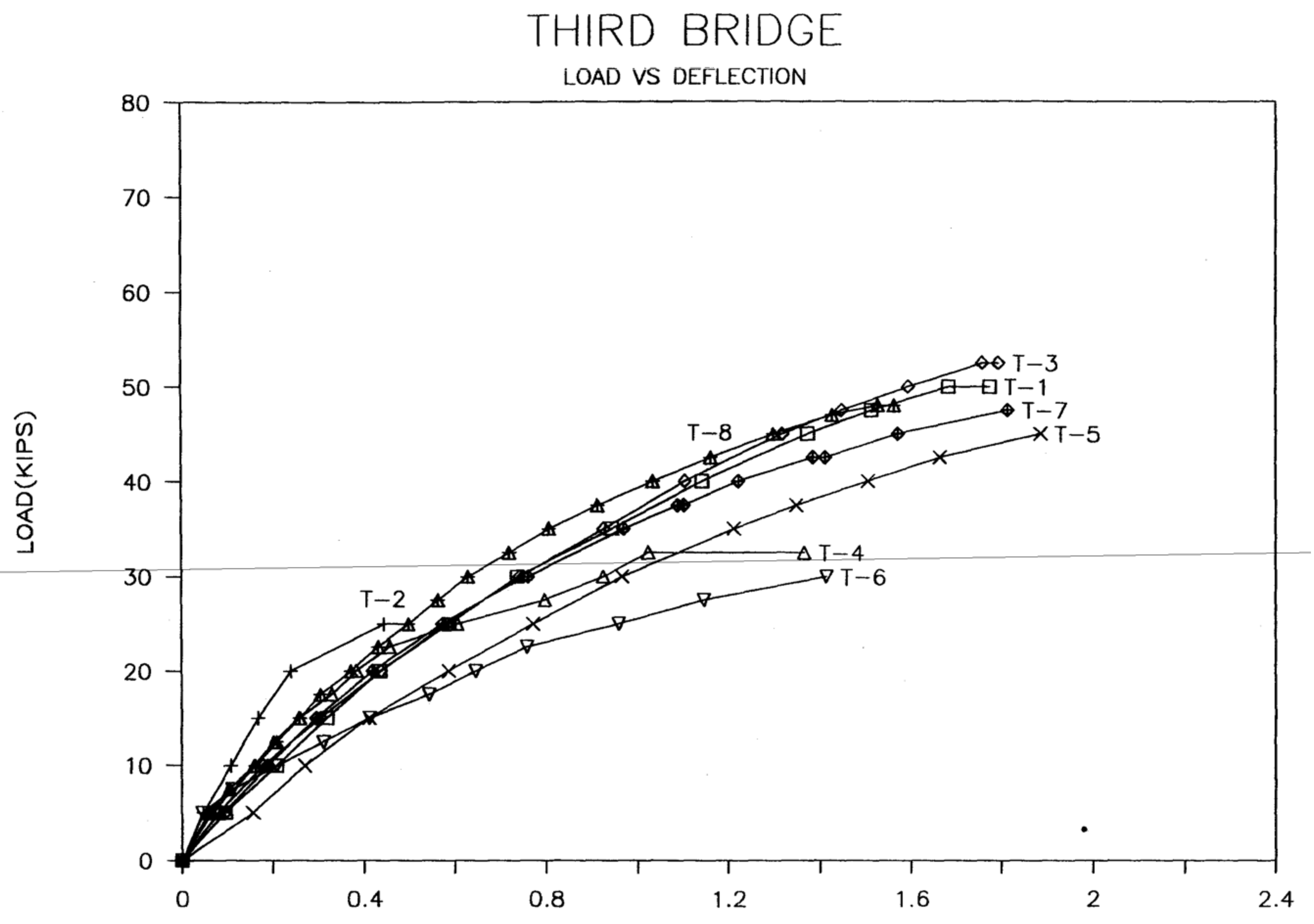

Figure 11 General Load-Deflection Curves for Specimen Three

Table 1 Summary of Maximum Loads and Deflections

Position	Load Pattern (Number of Imprints)	Specimen	Test	Test Result				Test Result Converted to Full Scale	
				Yield Load (kips)	Maximum Load (kips)	Failure?	Maximum Deflection (in.)	Maximum Load (kips)	Maximum Deflection (in.)
Interior (Mid-span)	Single	1	1	30	46	Yes	1.52	156	2.80
	Double	1	4	32.5	72	Yes	2.35	244	4.32
	Quadruple	2	1	40	70	No	1.78	330	3.86
	Quadruple	2	3	40	70	No	1.41	330	3.06
	Quadruple	3	1	35	52.5	Yes	1.78	331	4.47
	Quadruple	3	3	35	54.5	Yes	1.79	343	4.49
Interior (End)	Double	1	5	25	46	Yes	2.12	156	3.90
	Single	1	8	27.5	37.5	Yes	2.00	127	3.68
	Quadruple	2	6	35	70	Yes	1.30	330	2.82
	Quadruple	2	8	35	69	Yes	1.43	325	3.10
	Quadruple	3	5	30	45	Yes	1.89	283	4.74
	Quadruple	3	7	30	47.5	Yes	1.81	299	4.54
Free Edge	Single	1	2	25	37.5	Yes	1.83	127	3.37
	Quadruple	2	2	25	50	No	0.77	235	1.67
	Quadruple	3	8	32.5	49	Yes	1.56	309	3.92
Free Corner	Single	1	9	10	19.5	Yes	0.68	66	1.25
	Quadruple	2	5	25	58	Yes	0.73	273	1.58
	Quadruple	3	6	15	30	Yes	1.41	189	3.54
Parapet Edge	Single	1	3	46	50	No	0.68	169	1.25
	Single	1	7	25	50	No	0.57	169	1.05
	Quadruple	2	4	25	60	No	0.71	282	1.54
	Quadruple	3	2	20	25	No*	0.57	158	1.43
Parapet Corner	Single	1	6	32.5	44	Yes	0.58	149	1.07
	Quadruple	2	7	25	55	Yes	0.48	259	1.04
	Quadruple	3	4	27.5	35	Yes	1.37	220	3.44

* Test stopped due to development of yield line for full length of specimen.

3.1 Interior Tests

This section describes the behavior f the interior tests. Comparison of the maximum loads and yield loads in Table 1 indicate the reserve strength of the deck relative to the load associated with the flexural yield line mechanism. For the first specimen, in-plane forces developed in the slab were sufficient to cause welds in the bracing adjacent to the test position to fail for several of the tests. In the second and third specimens, the welds were strengthened, and weld failure occurred in only one case. It is difficult to say how much of the increased strength for specimen 2 was due to the effect of the bracing on the in-plane forces and ho much was due to the load pattern, but the reserve strength beyond yielding w s certainly considerable, even though the transverse span-to-thickness ratio for this specimen was 20, as opposed to the maximum of 15 in the 0ntari code.

Also, it should be noted that for all tests in which weld failures occurred, that while the load decreased when the weld failure occurred, continued loading was possible after the weld failure to an increased load.

Appendix E. shows the observed crack patterns for the various tests. The mode of failure for specimen 1 was clearly punching, involving the entire width of the panel between girders and an approximately equal distance along the length of the slab. For specimen 2, t ere was some tendency for the pattern to not be as circular and to involve a longer length, perhaps reflecting the proximity of the load plates o the steel girders. The basic ductility inherent in the failure mechanism for all interior tests was apparent in the no linearity of the load deflection relations and the large magnitude of the deflections, shown in Figures 9, 10 and 11.

3.2 Free Edge Within-San and Corner Tests

This section discusses the behavior f the tests on the side of the bridge without the parapet, either within the span or at the corners. For all specimens, as indicated in Table 1, even these tests, indicated considerable reserve capacity beyond the load at which the yield line pattern formed. For specimen 1, the failure load for the midspan edge was equal to the lowest failure load recorded for the interior tests, while the midspan edge for specimen 2 had still not failed at 50 kips. he reserve capacity of the free edge is evidently aided by transfer of load directly to the longitudinal girder, as indicated by the similarity of stiffness between the midspan edge test and the adjacent interior test in specimen 1, by the linearity and high stiffness of the midspan edge test in specimen 2, and the observation that the maximum deflection for both tests in specimen 2 occurred immediately to the inside of the girder.

3.3 Parapet Within-spar and Corner Tests

This section discusses the behavior o the tests on the side of the bridge with the parapet, either within the span or at the corners. Considering the behavior of the free edge, the r serve capacity of the parapet edge is not surprising. A major aspect of these test results was the strong interaction of the parapet with the slab. This was illustrated by load-deflection stiffnesses, which for both specimens were highest for the parapet edge tests, by the fact that for specimen 1 all three parapet edge tests involved the formation of wide inclined cracks over the en ire height of the parapet, that failure was not attained for either specimen one or two at midspan, even though comparable interior tests failed at loads lower or not much higher than the maximum applied, and from the observation in specimen 2 that failure in the corner test occurred only when the de k vertically separated from the parapet.

However, the development of the full length yield line for test T-2 on specimen three, which was described above, points out that some consideration of yield line theory should be given for he overhang condition. This aspect of the behavior will be investigated in future studies.

3.4 Comparisons to Highway Loads

The AASHTO axle load for a single axle with dual wheels is 32 kips, implying 16 kips on each dual tire pattern. Using an impact factor of 0.3, and a load factor of (2.2*1.3) implies a required ultimate wheel load of 59 kips. This is less than the maximum load (converted to full scale) for any of the single imprint tests, less than one half t e load for any of the dual imprint tests, and less than one fourth the load f r any of the four imprint (tandem) tests with four exceptions. All four of tie exceptions occur for the tandem loadings. And, as discussed subsequently, the assumption of two AASHTO axle loads in a single tandem is very conservative. Also, none of the exceptions occur in the interior tests; not even for he maximum S/T ratio of 22.

One of the exceptions occurred in the free edge test for specimen 2. and for this test the maximum load recorded was not based on a slab failure. Also, it should be noted that the corresponding test for specimen 3, with a larger B/T ratio carried a full scale tandem load of 306 kips implying a wheel load of 76 kips well above 59 kips. The o her three exceptions were in the overhangs for specimen #3 with the very hi h A/T and B/T ratios.

Evaluating the results in the above manner is very conservative, since the AASHTO design axle loads are spaced fourteen feet apart and thus do not realistically imply a tandem loading. The results could be evaluated in a somewhat different manner based on the heaviest commercial axle, which is rated at 23 kips. Applying a safety factor of 2.5 results in an ultimate axle load of 57.5 kips, which translates into 2&75 kips on one dual tire formation,,57.5 kips on two dual tire formations, and 115 kips total on an entire tandem assembly. All of the full scale maximum applied loads in Table 1 exceed these levels by a considerable margin, even those for the overhangs of specimen number three. Clearly the orthotropically reinforced slabs have a tremendous reserve load capacity compared to typical highway vehicle loads.

CHAPTER 4

SUMMARY AND RECOMMENDATIONS

Load tests on three bridge deck specimens with 0.3% orthotropic reinforcement top and bottom, supported on steel beams, produced the following general results

(1) Interior tests on all three specimens indicated large amounts of reserve strength beyond that associated with the formation of the flexural yield line pattern, even though they had transverse span-to-thickness ratios of approximately 18, 20, and 22, significantly in excess of the maximum of 15 allowed by the Ontario code.

(2) All interior tests carried to slab failure exhibited marked flexural yielding followed by a punching type failure, accompanied by large amounts of deformation.

(3) For all specimens, even tests on a free edge of the slab (over-hang without parapet) indicated considerable reserve strength beyond the load corresponding to the formation of the flexural yield pattern. The stiffness levels and linearity of response for these tests suggested significant transfer of load directly into the longitudinal girder.

(4) For specimens one and two, tests on the parapet over-hang were characterized by the strong interaction of both the parapet and the longitudinal girder with the slab. In several tests wide inclined cracks appeared in the parapet, and in one corner test, failure occurred by vertical separation of the slab from the parapet.

(5) Specimen three with the large A/T ratio of 32 developed a full length yield line, the entire length of the specimen, for the edge test on the parapet side. Thus, the possibility of a full length beam mechanism

should be considered in establishing he maximum over-hang-to-thickness ratio. However, the parapet still participated in strengthening the deck in the corner tests; for this specimen. Thus, it is likely that if the edge test had been carried to completion, the specimen would have had additional reserve strength beyond the pint at which the test was stopped. (6) Static load capacities for all tests, when converted to a full scale 8" deck thickness, gave more than an adequate factor-of-safety for typical highway legal tandem loads.

4.1 Research Application

Based on the observed behavior of the static tests, cyclic fatigue tests are now planned on a fourth specimen very similar to specimen two of the static tests. It is felt that these tests along with additional analytical studies can be used to establish guidelines on the limitations of the span-to-thickness and over-hang-to-thickness ratio which can be used in American practice with the Ontario orthotropic reinforcement procedure.

No direct application of this work is recommended in Florida, pending completion of the planned work in this are

REFERENCES

(1) American Association of State Highway and Transportation Officials, "Standard Specifications for Highway Bridges", American Association of State Highway and Transportation Officials, Washington D.C, 1984-1988.

(2) Beal, D., "Strength of Concrete Bridge Decks," New York State Department of Transportation, FHWA/NY/RR-81-89, Albany, New York, 1981.

(3) Batchelor, B., P. Csagoly, and B. Hewitt, "Investigation of the Fatigue Strength of Deck Slabs of Composite Steel/Concrete Bridges," Transportation Research Record 664, Washington, D.C., 1978.

(4) Batchelor, B., P. Csagoly, and B. Hewitt, "Load Carrying Capacity of Concrete Bridge Decks," Ontario Ministry of Transportation, SRR-85-03, Toronto, Canada, 1979.

(5) Christiansen, K. P., "Experimental Investigation of Rectangular Concrete Slabs with Horizontal Restraints," Material and Structures, Vol 16, No 93, May-June, 1982.

(6) Dorton, R. M. Holowka, and P. King, "The Conestoga River Bridge - Design and Testing," Canadian Journal of Civil Engineering, Vol 4, No 1, 1977.

(7) Fang, I-Kuang, and others "Behavior of Ontario-Type Bridge Deck on Steel Girders," Research Report 350-1, Center for Transportation Research, University of Texas, Austin, Texas, 1986.

(8) Ontario Ministry Of Transportation and Communications, "Ontario Highway Bridge Design Code", Ontario Ministry Of Transportation and Communications, Toronto, Canada, 1983.

(9) Kim, K. H., and others "Behavior of Ontario-Type Bridge Deck on Steel Girders," Research Report 350-4, Center for Transportation Research, University of Texas, Austin, Texas, 1988.

(10) Tsui, C. K., N. H. Burns, and R. E. Klinger, "Behavior of Ontario-Type Bridge Deck on Steel Girders : Negative Moment Region and Load Capacity", Research Report 350-4, Center for Transportation Research, University of Texas, Austin, Texas, 1986.

APPENDIX A LVDT

Locations For Tests

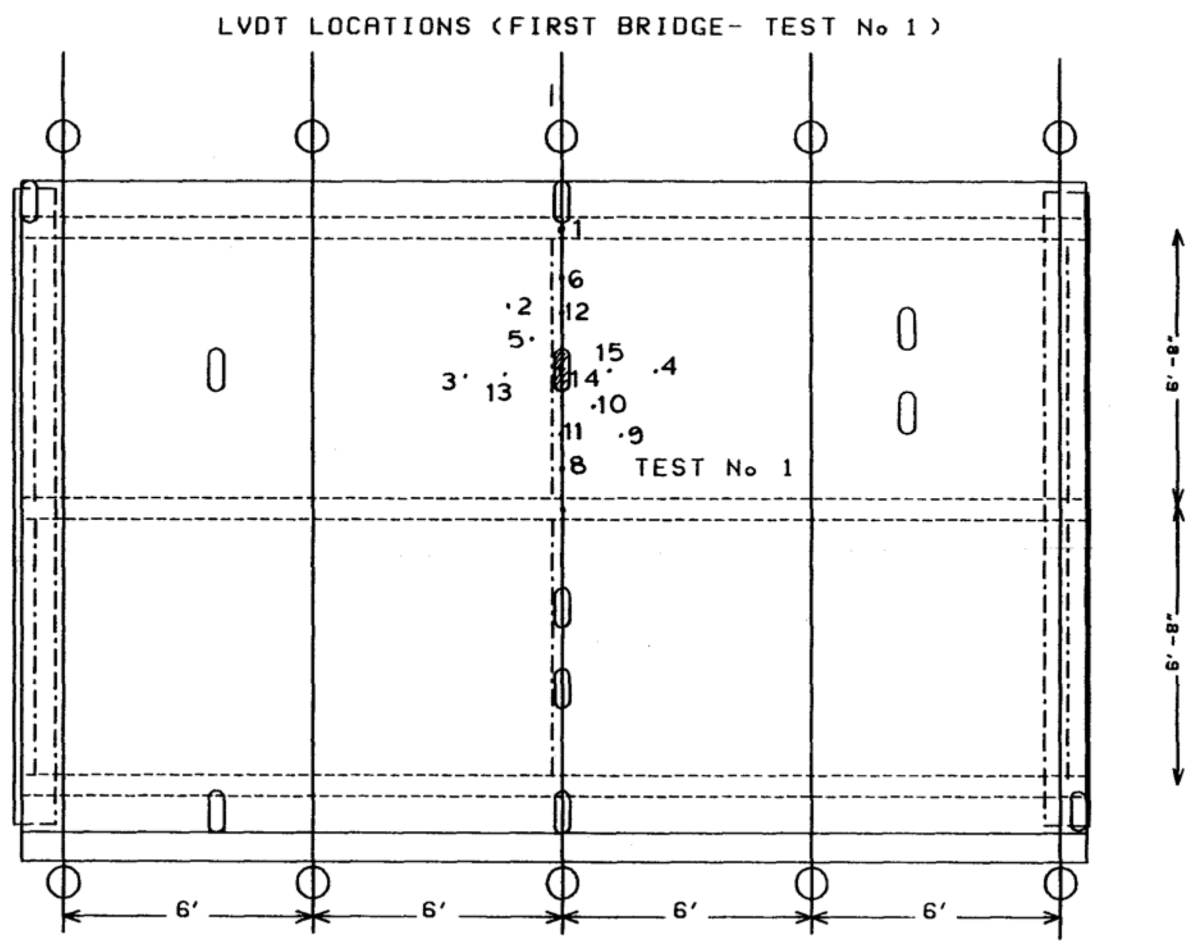

Figure A.1 LVDT Locations (First Bridge - Test No. 1)

LVDT LOCATIONS (FIRST BRIDGE- TEST No 2)

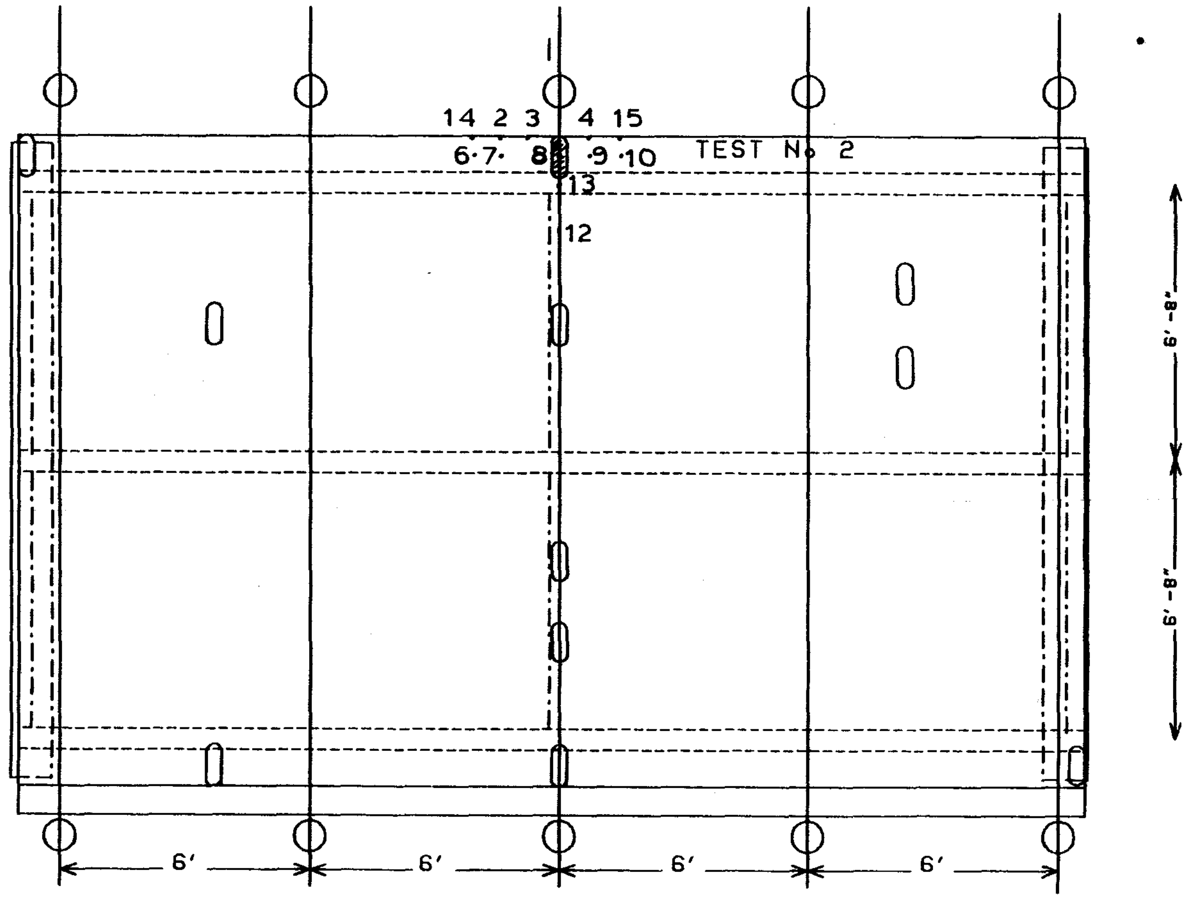

Figure A.2 LVDT Locations (First Bridge - Test No. 2)

LVDT LOCATIONS (FIRST BRIDGE- TEST No 3)

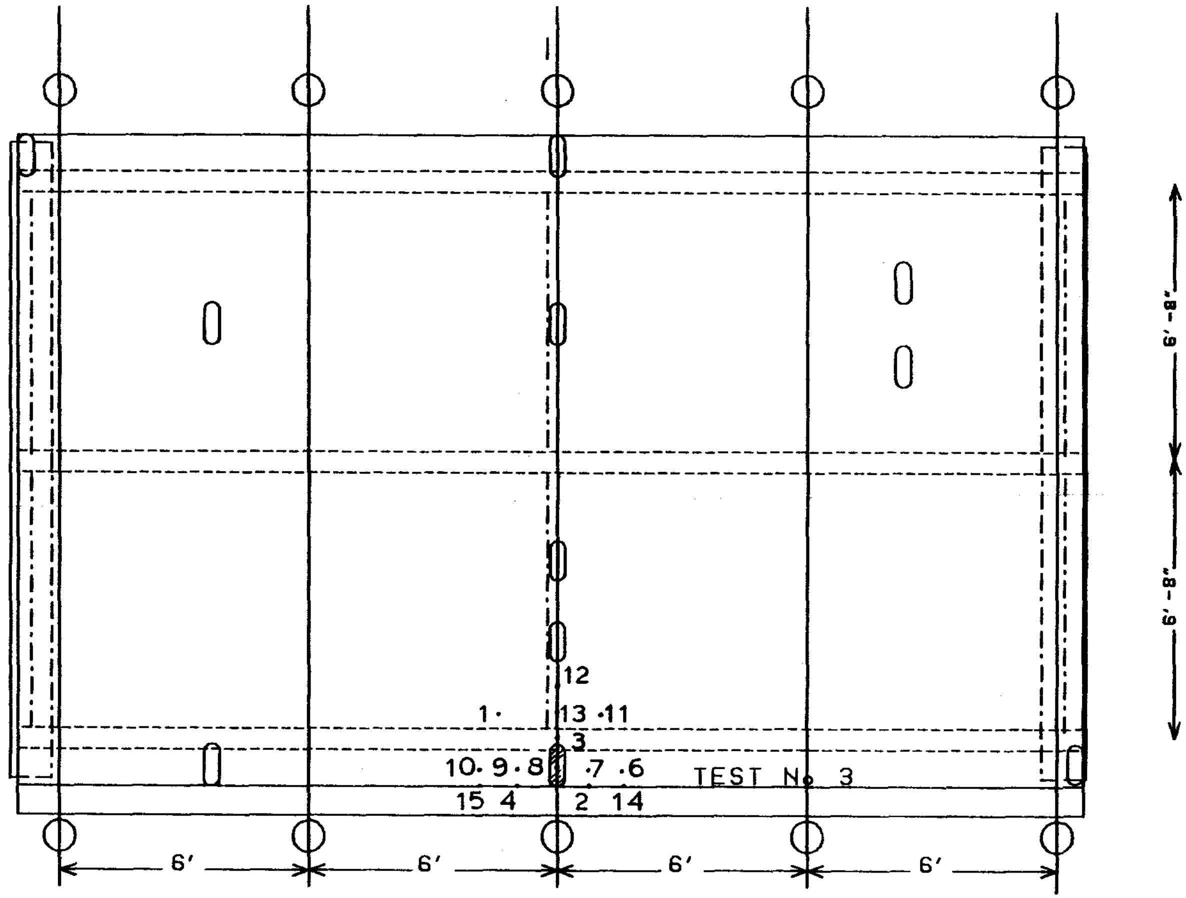

Figure A.3 LVDT Locations (First Bridge - Test No. 3)

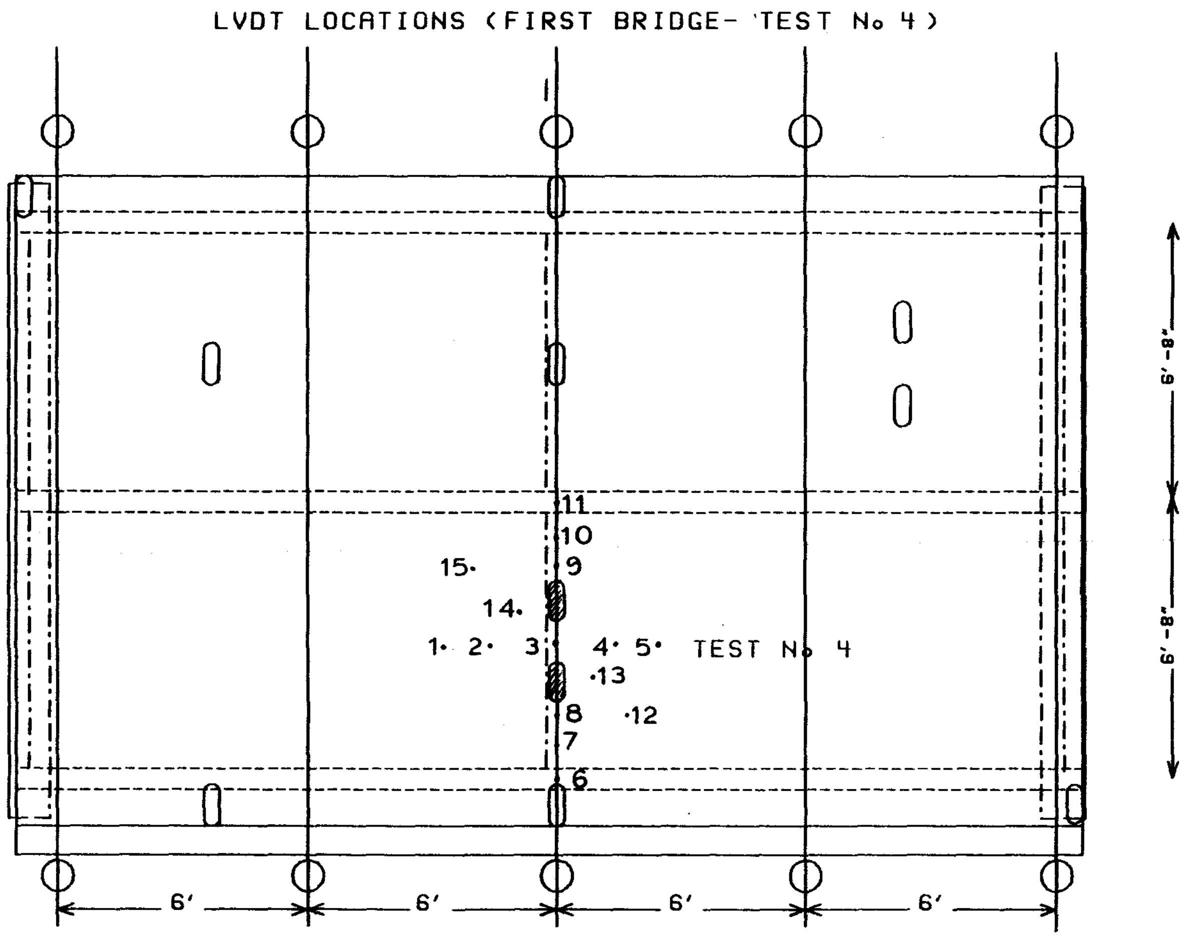

Figure A.4 LVDT Locations (First Bridge - Test No. 4)

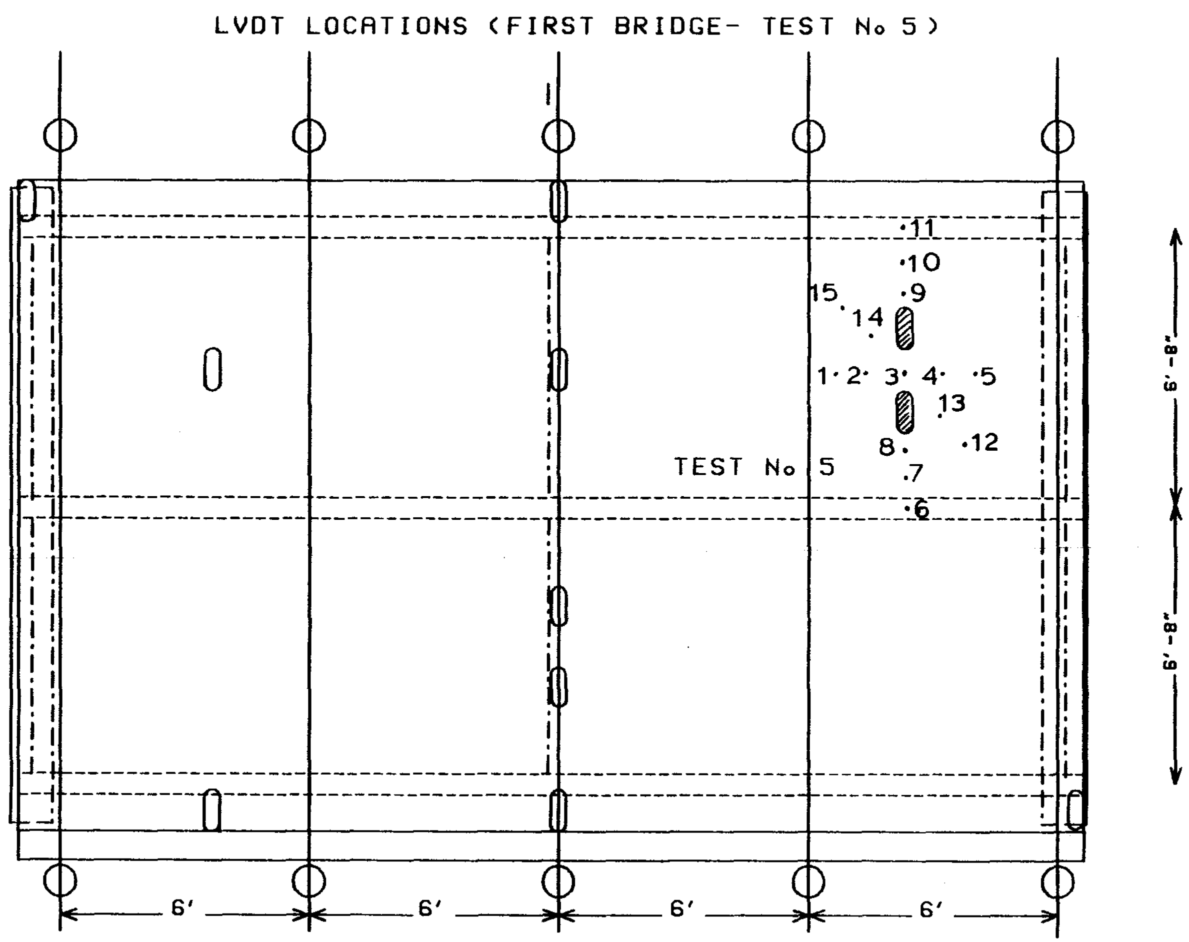

Figure A.5 LVDT Locations (First Bridge - Test No. 5)

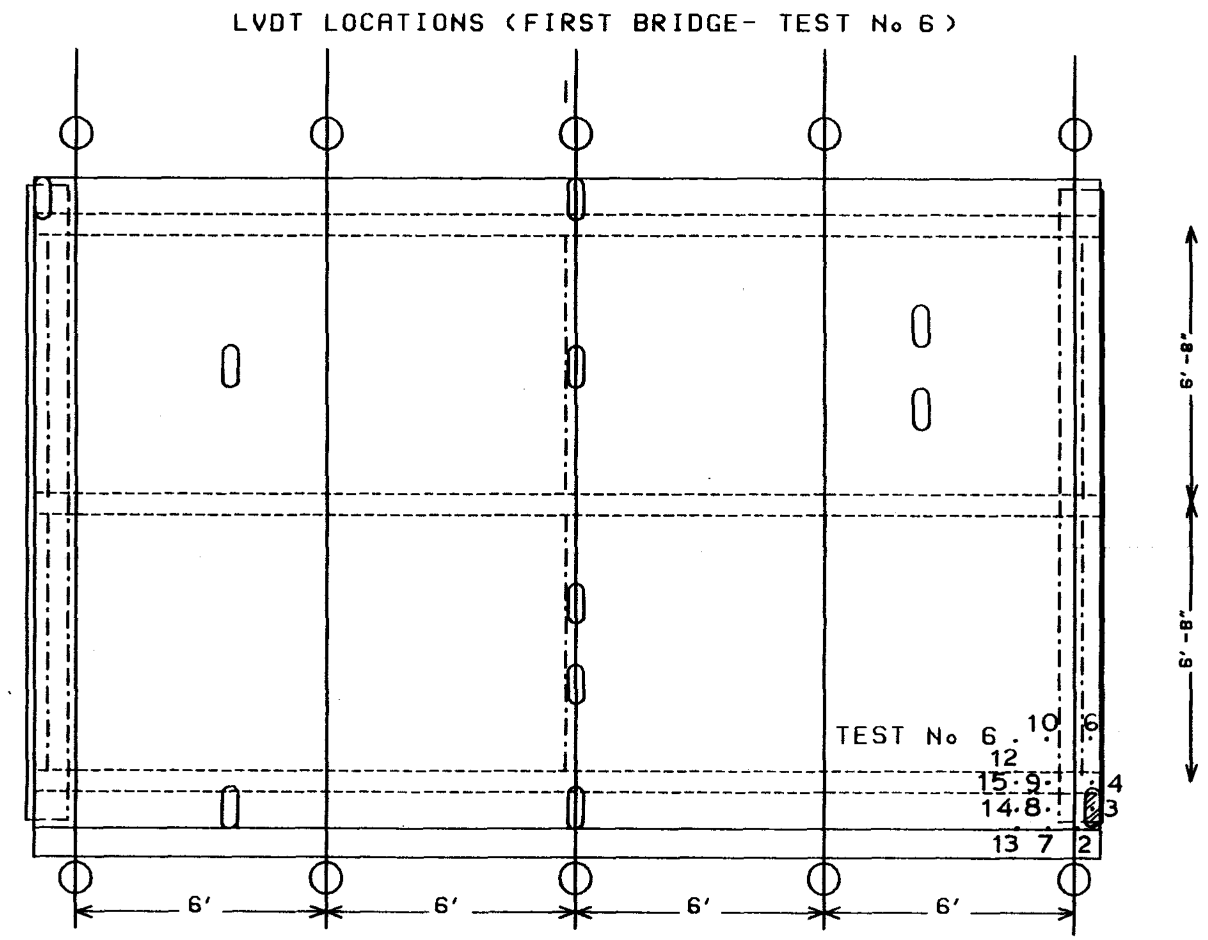

Figure A.6 LVDT Locations (First Bridge - Test No. 6)

LVDT LOCATIONS (FIRST BRIDGE- TEST No 7)

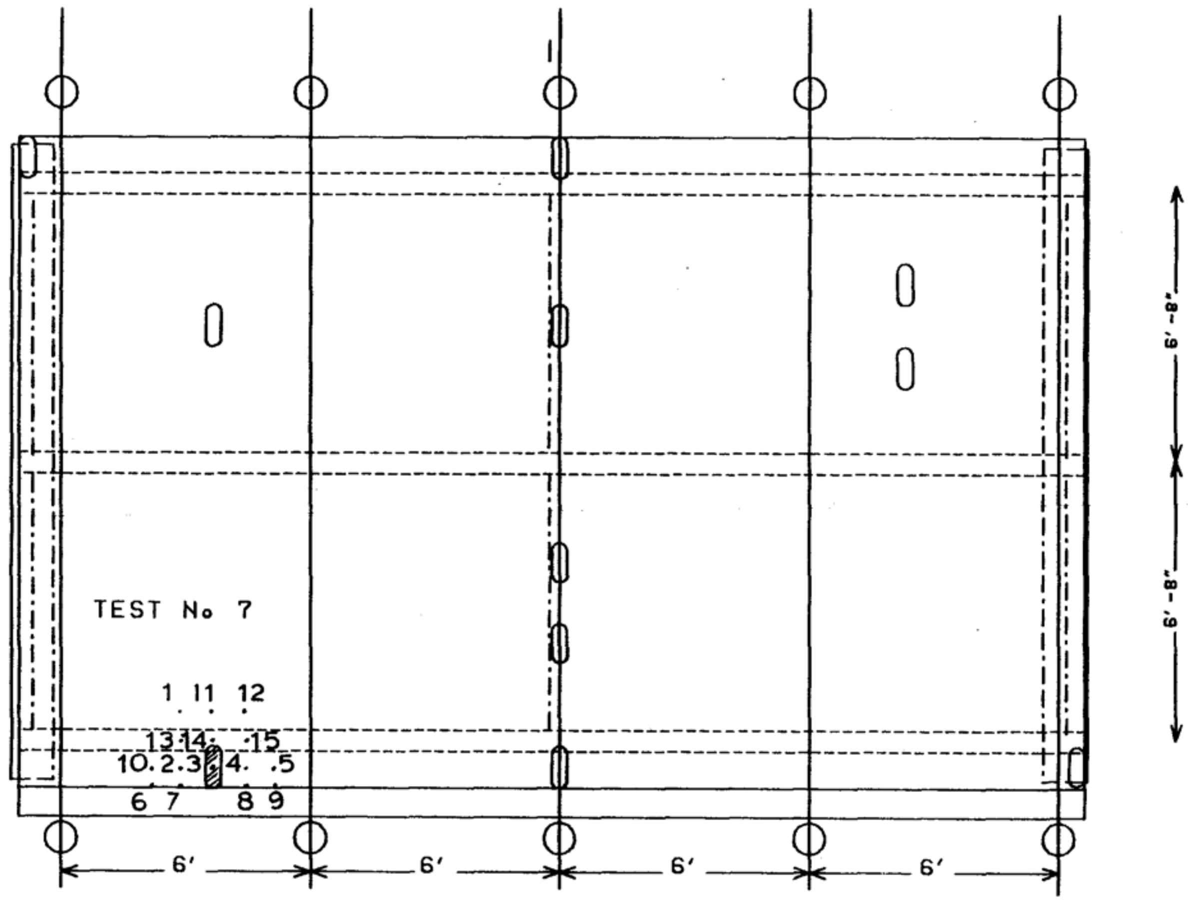

Figure A.7 LVDT Locations (First Bridge - Test No. 7)

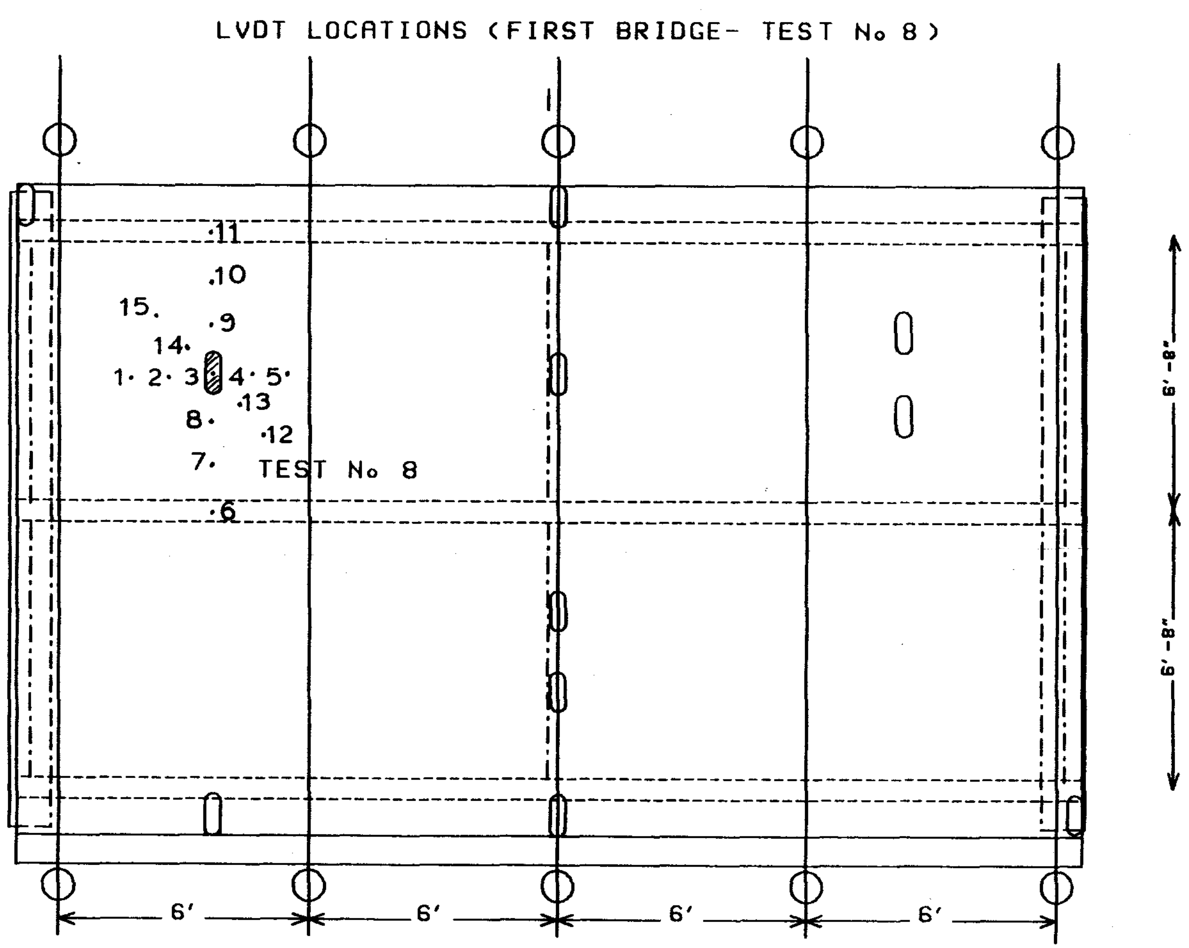

Figure A.8 LVDT Locations (First Bridge - Test No. 8)

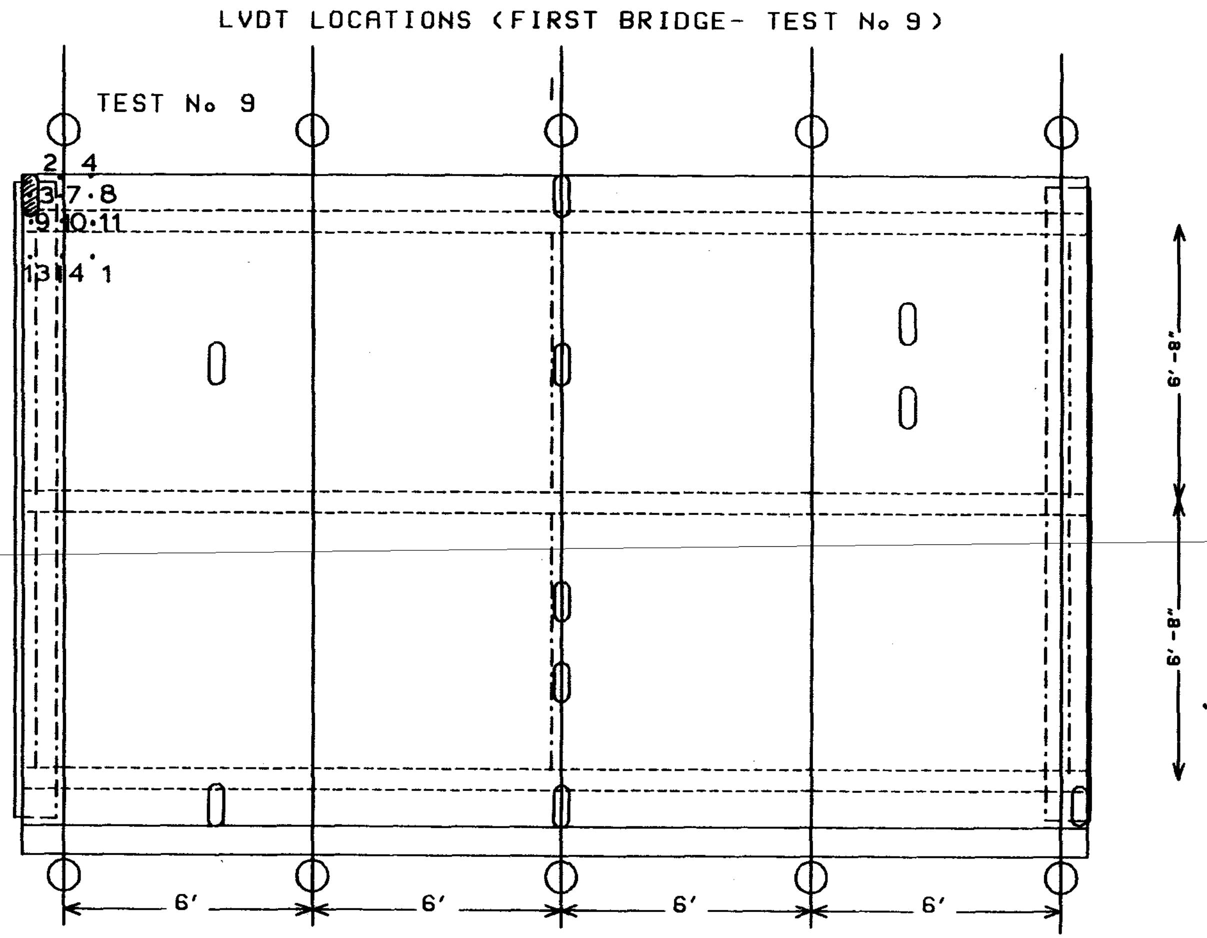

Figure A.9 LVDT Locations (First Bridge - Test No. 9)

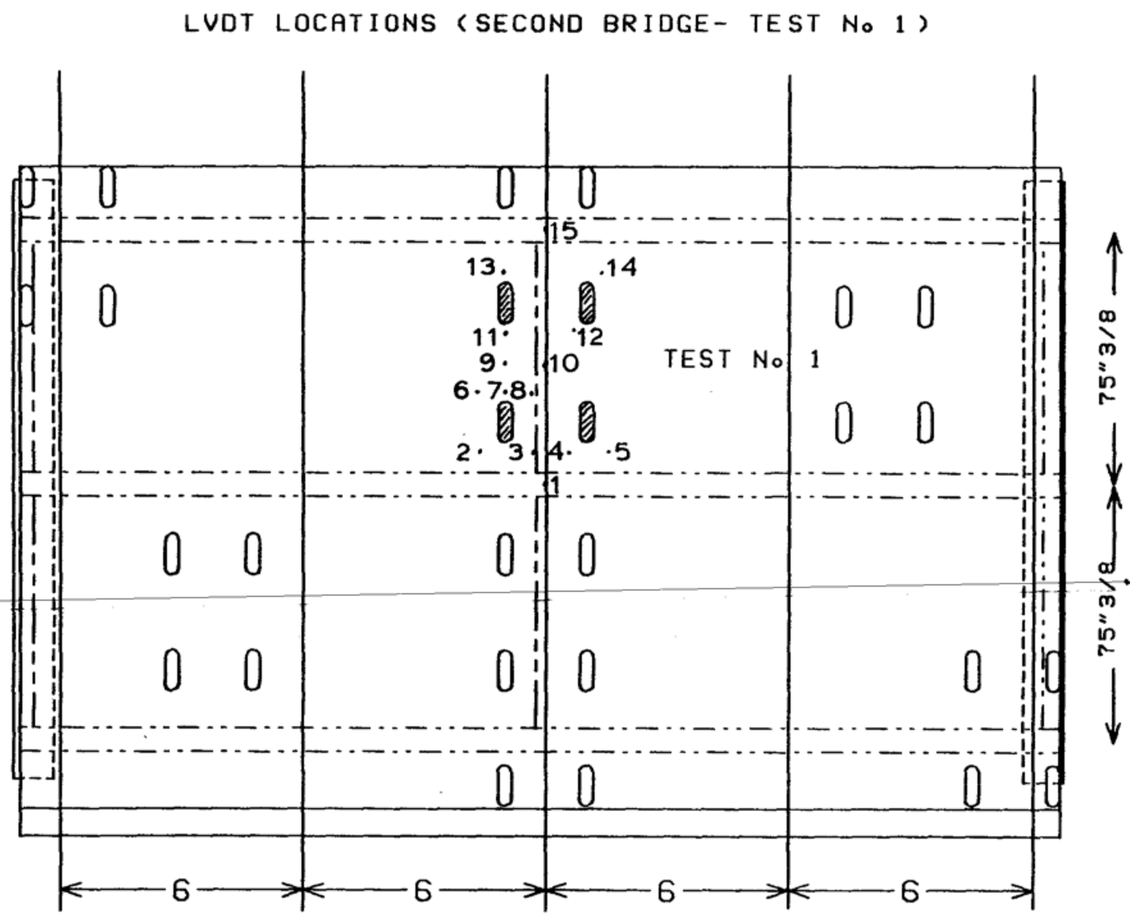

Figure A.10 LVDT Locations (Second Bridge - Test No. 1)

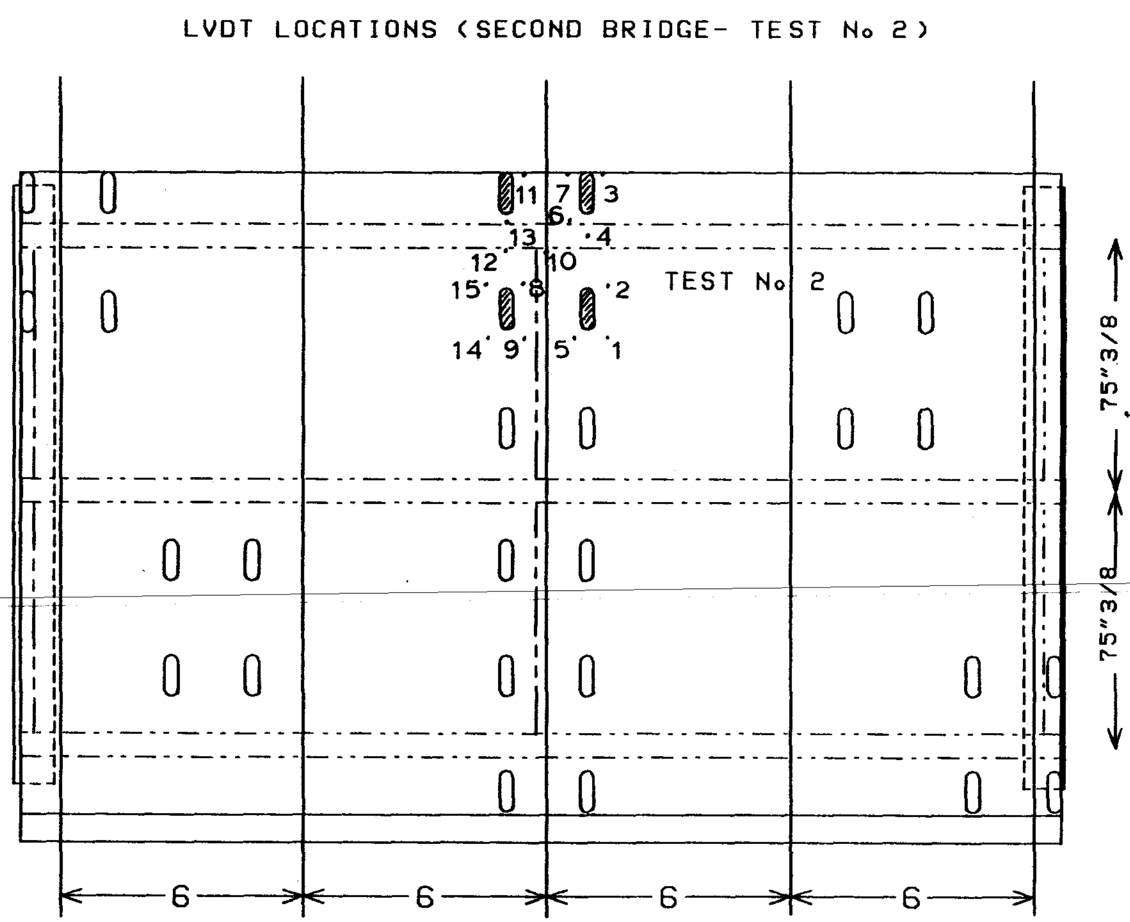

Figure A.11 LVDT Locations (Second Bridge - Test No. 2)

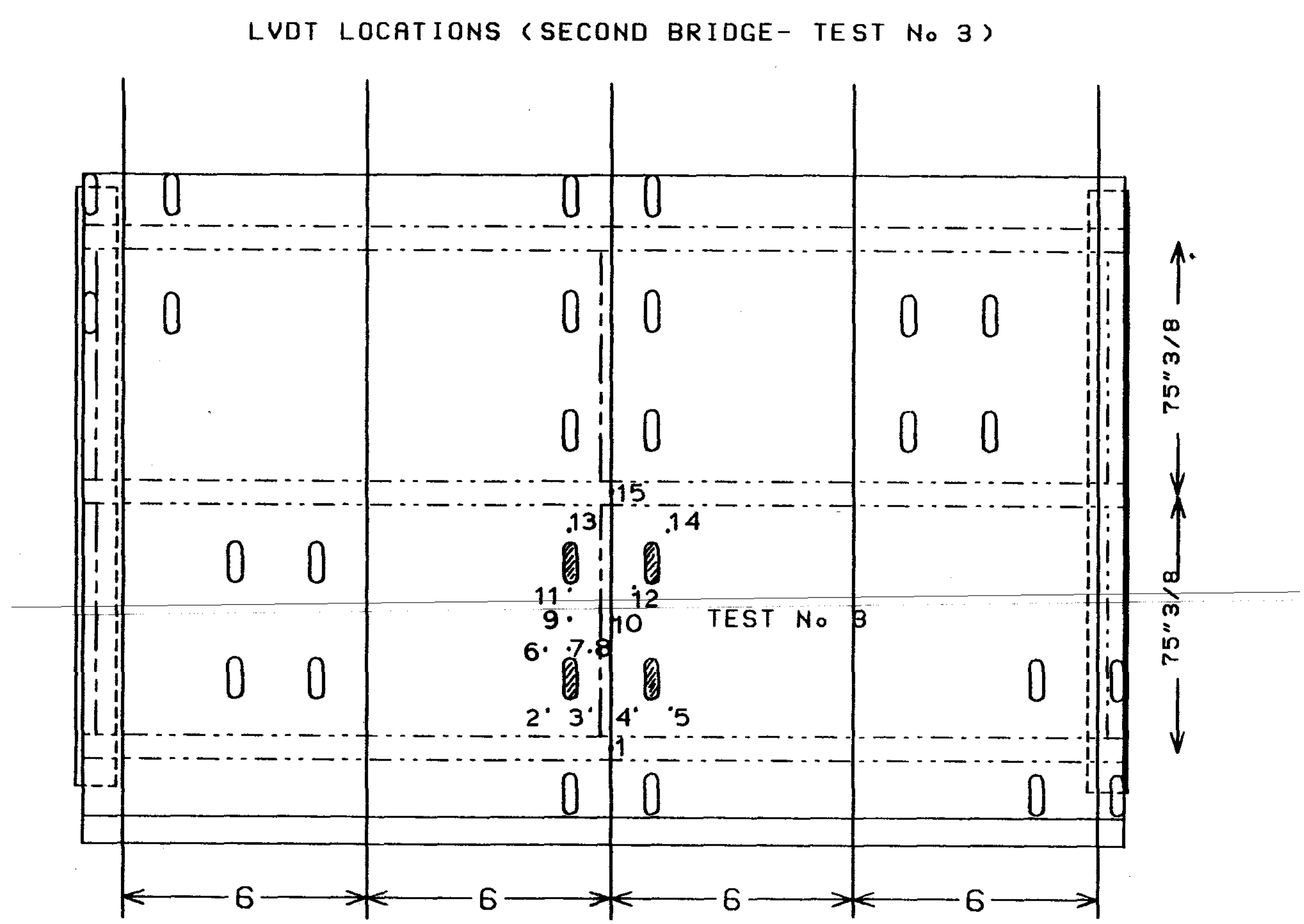

Figure A.12 LVDT Locations (Second Bridge - Test No. 3)

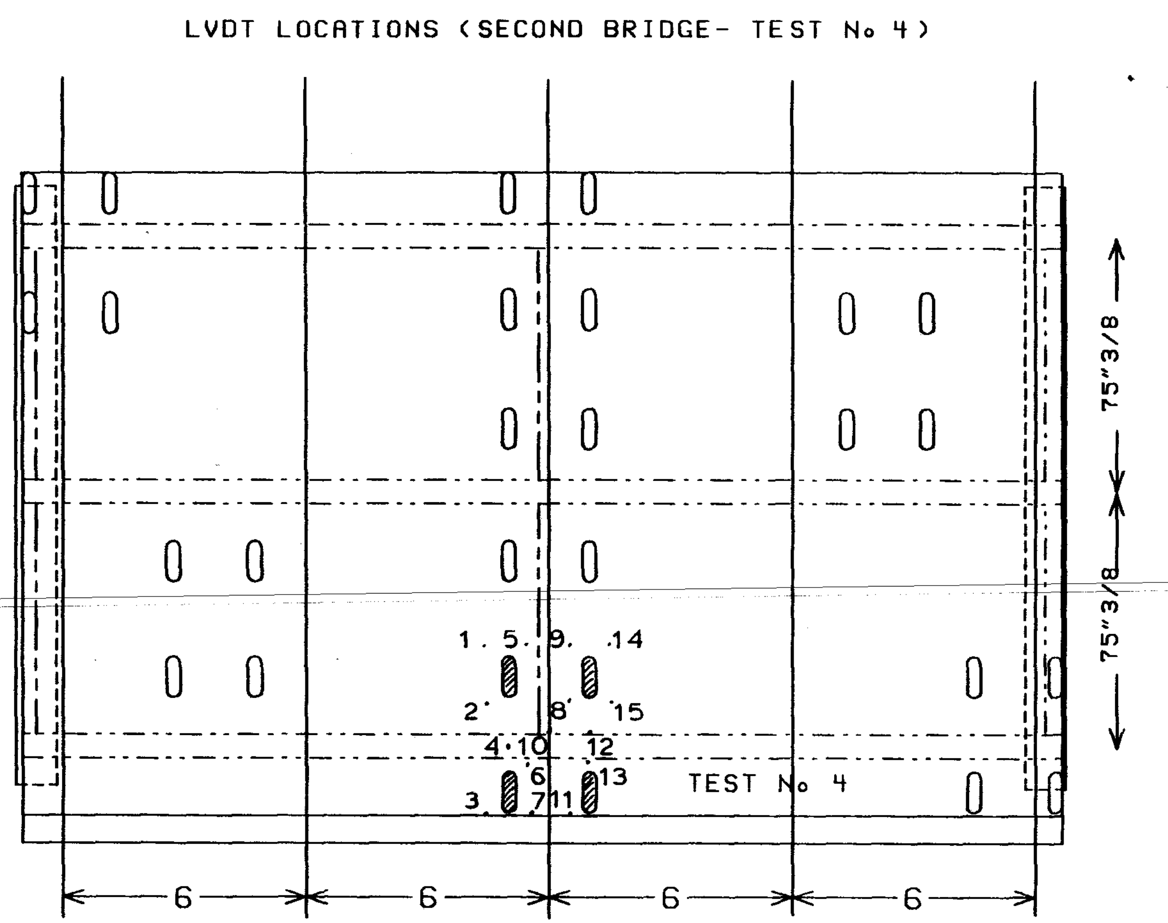

Figure A.13 LVDT Locations (Second Bridge - Test No. 4)

LVDT LOCATIONS (SECOND BRIDGE- TEST No 5)

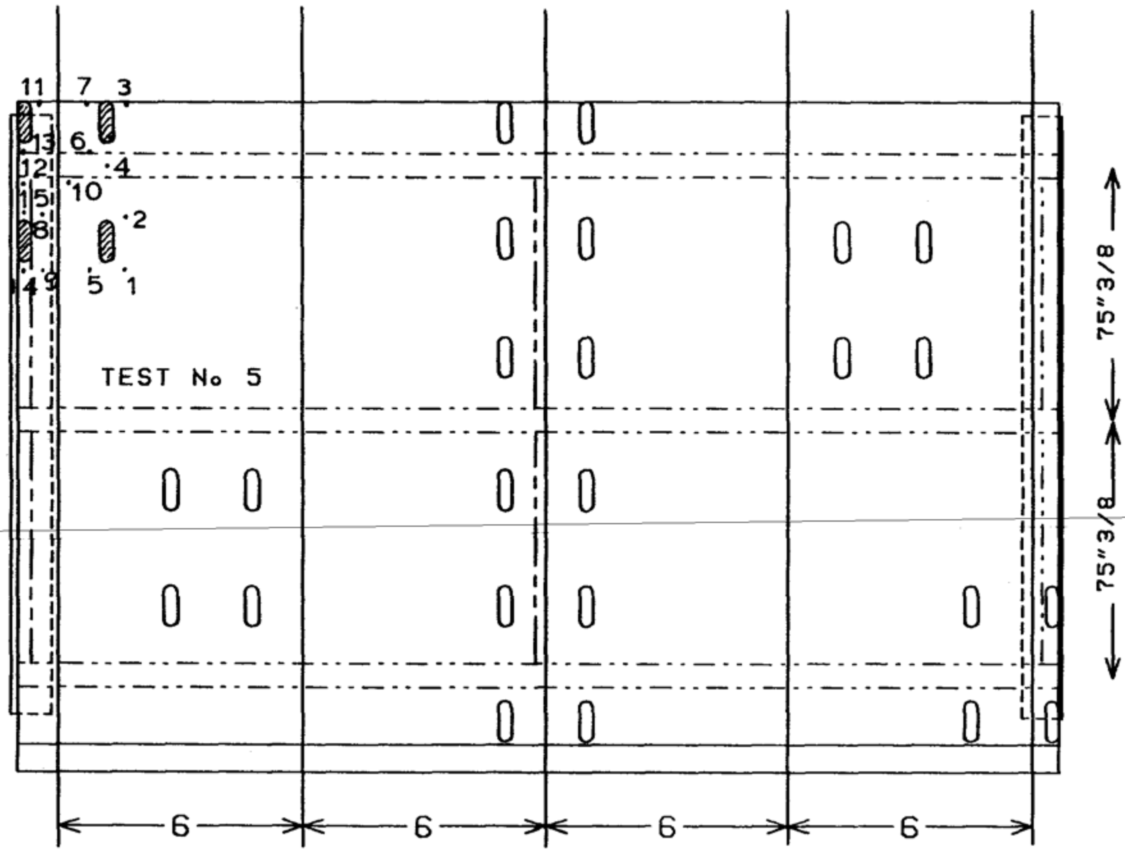

Figure A.14 LVDT Locations (Second Bridge - Test No. 5)

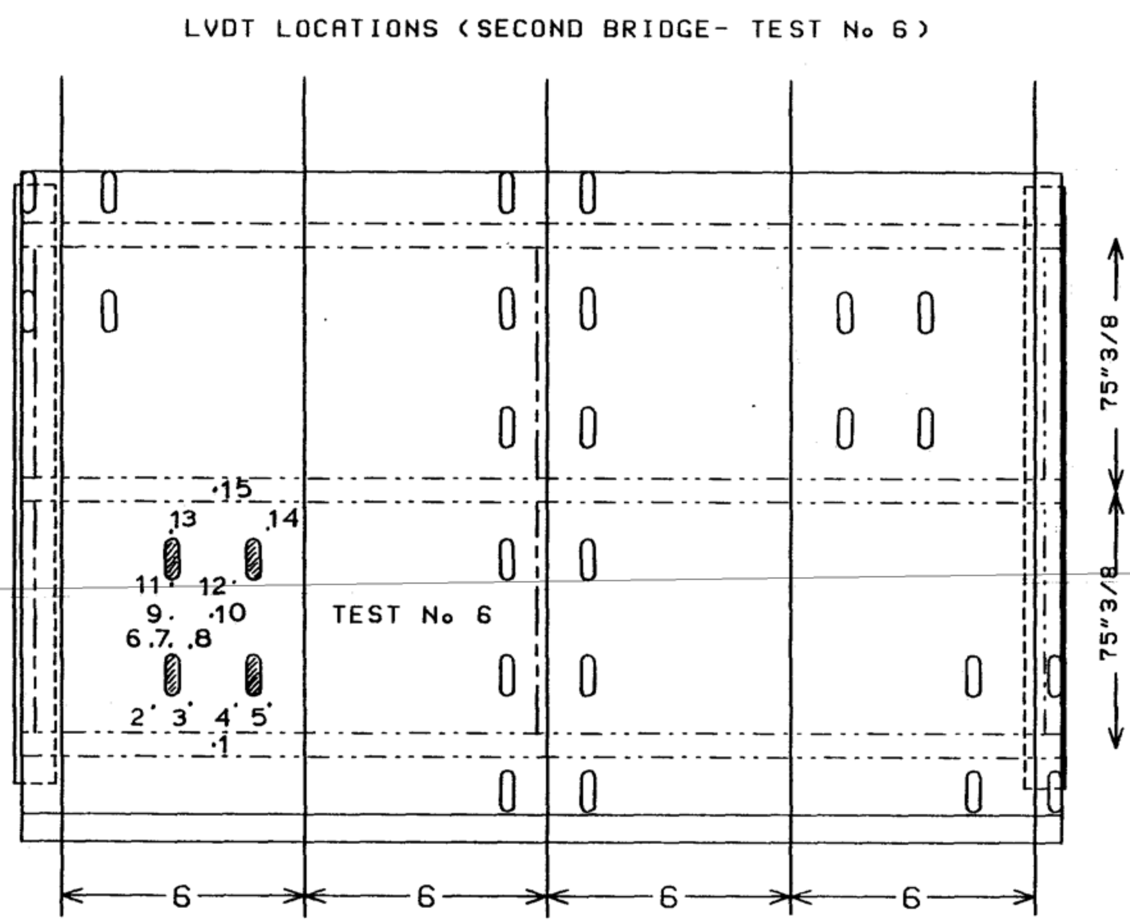

Figure A.15 LVDT Locations (Second Bridge - Test No. 6)

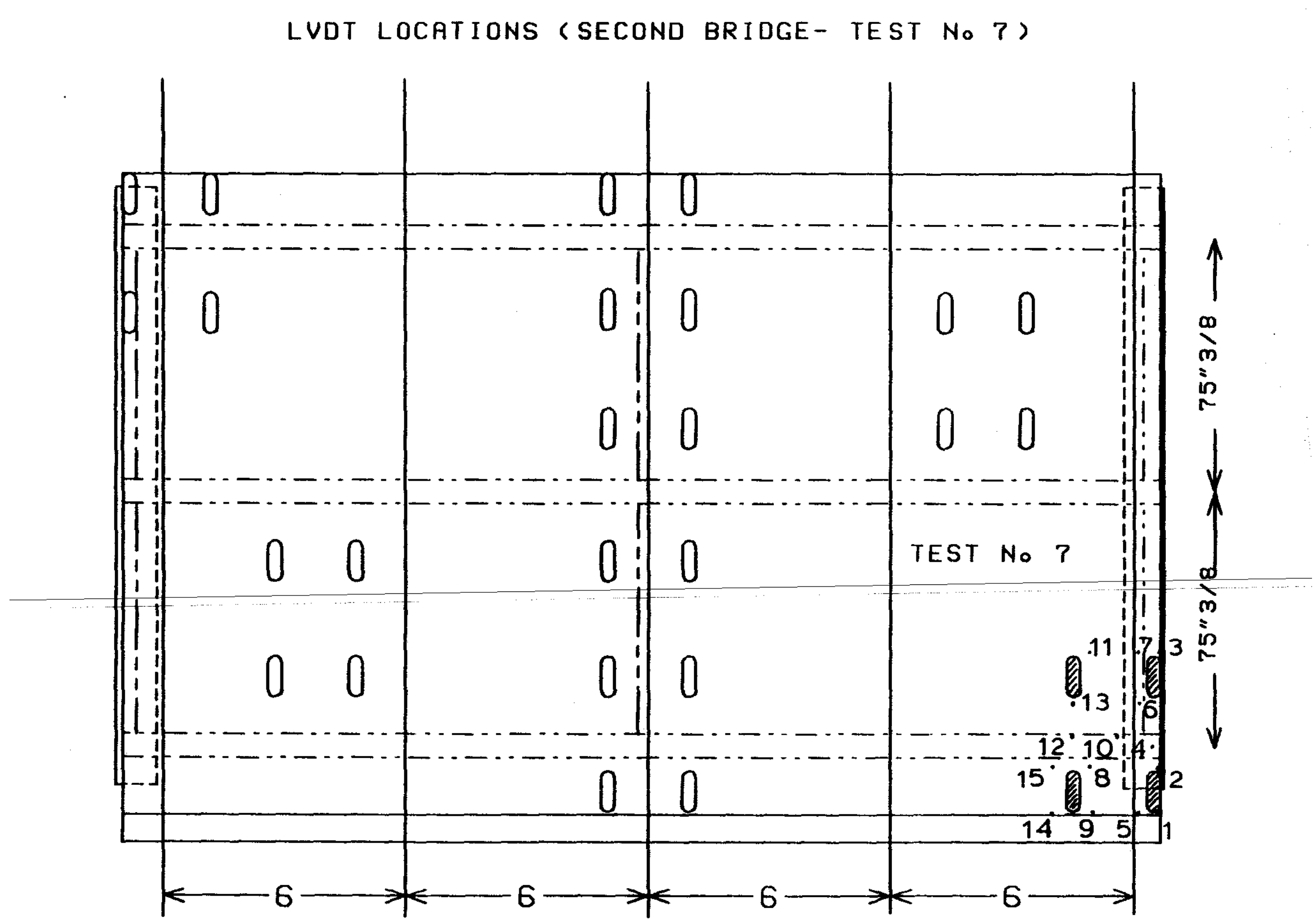

Figure A.16 LVDT Locations (Second Bridge - Test No. 7)

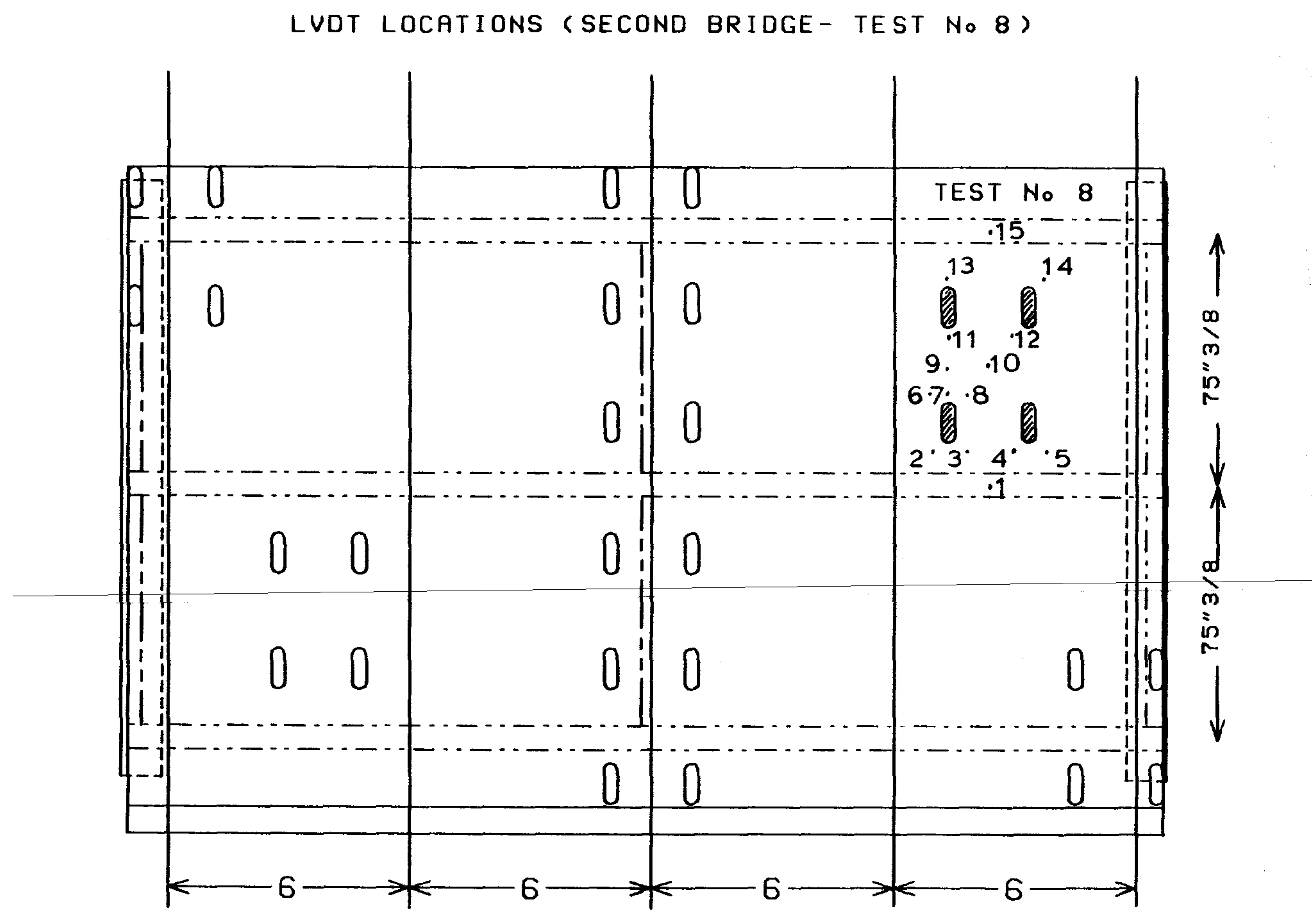

Figure A.17 LVDT Locations (Second Bridge - Test No. 8)

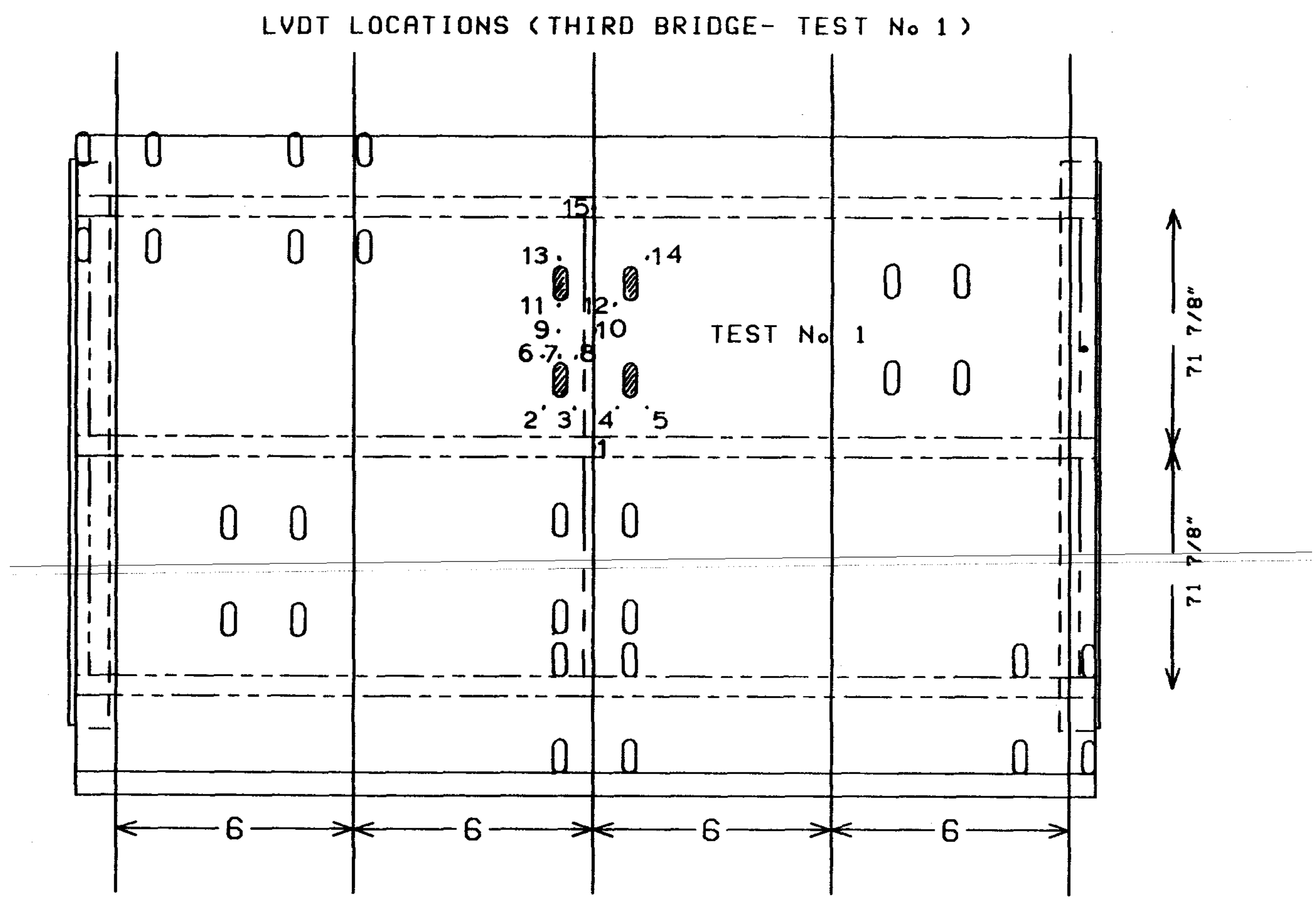

Figure A.18 LVDT Locations (Third Bridge - Test No. 1)

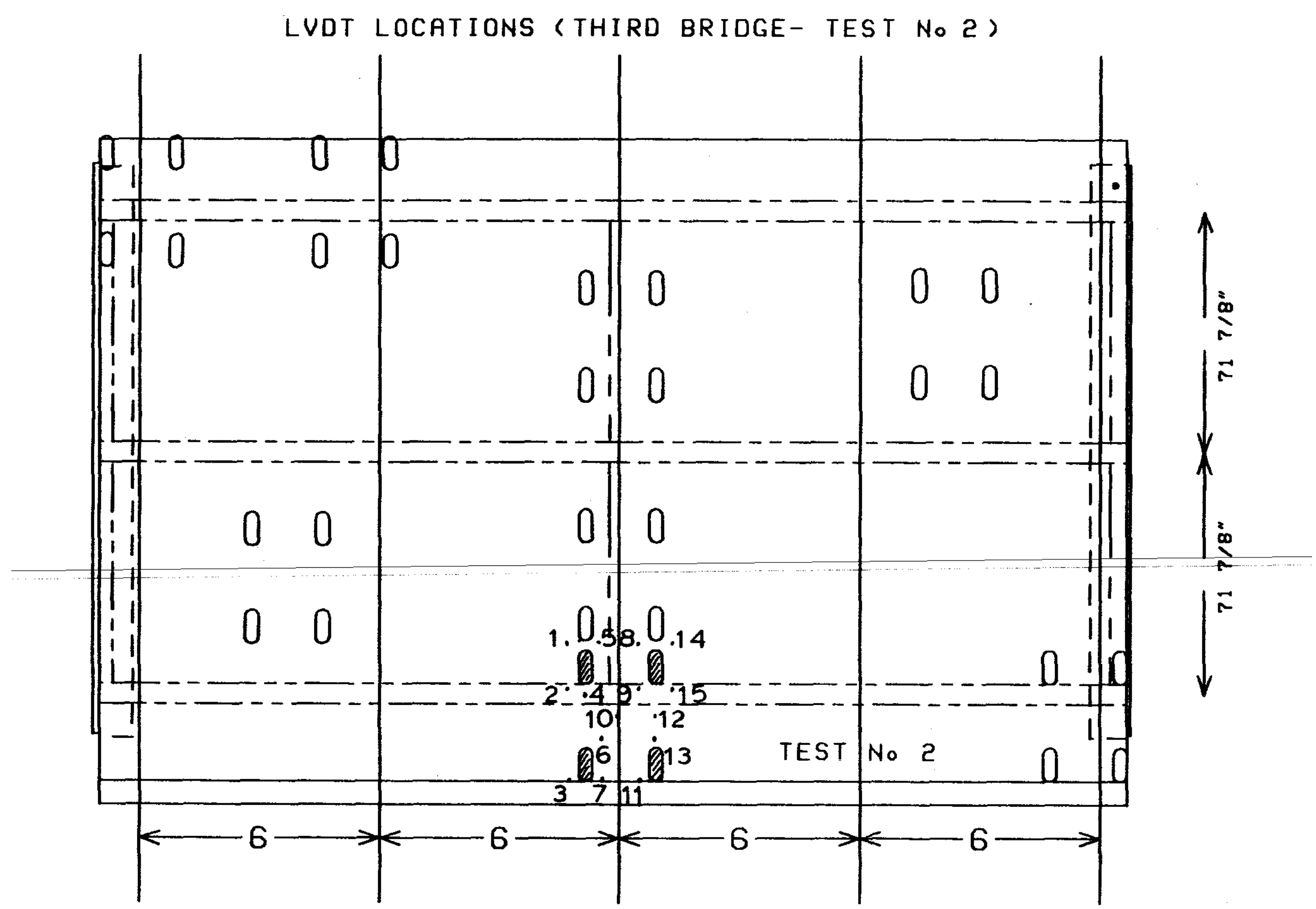

Figure A.19 LVDT Locations (Third Bridge - Test No. 2)

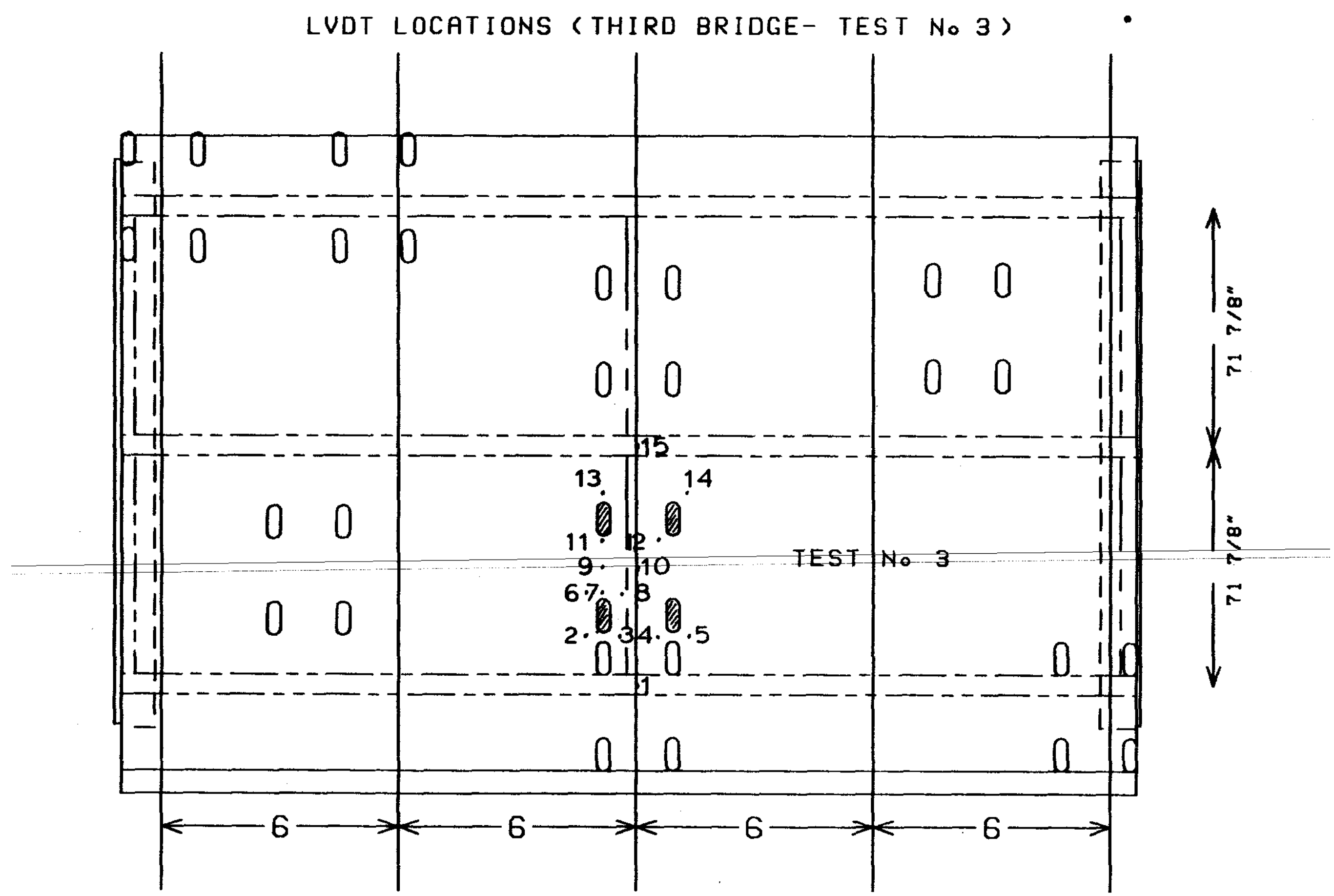

Figure A.20 LVDT Locations (Third Bridge - Test No. 3)

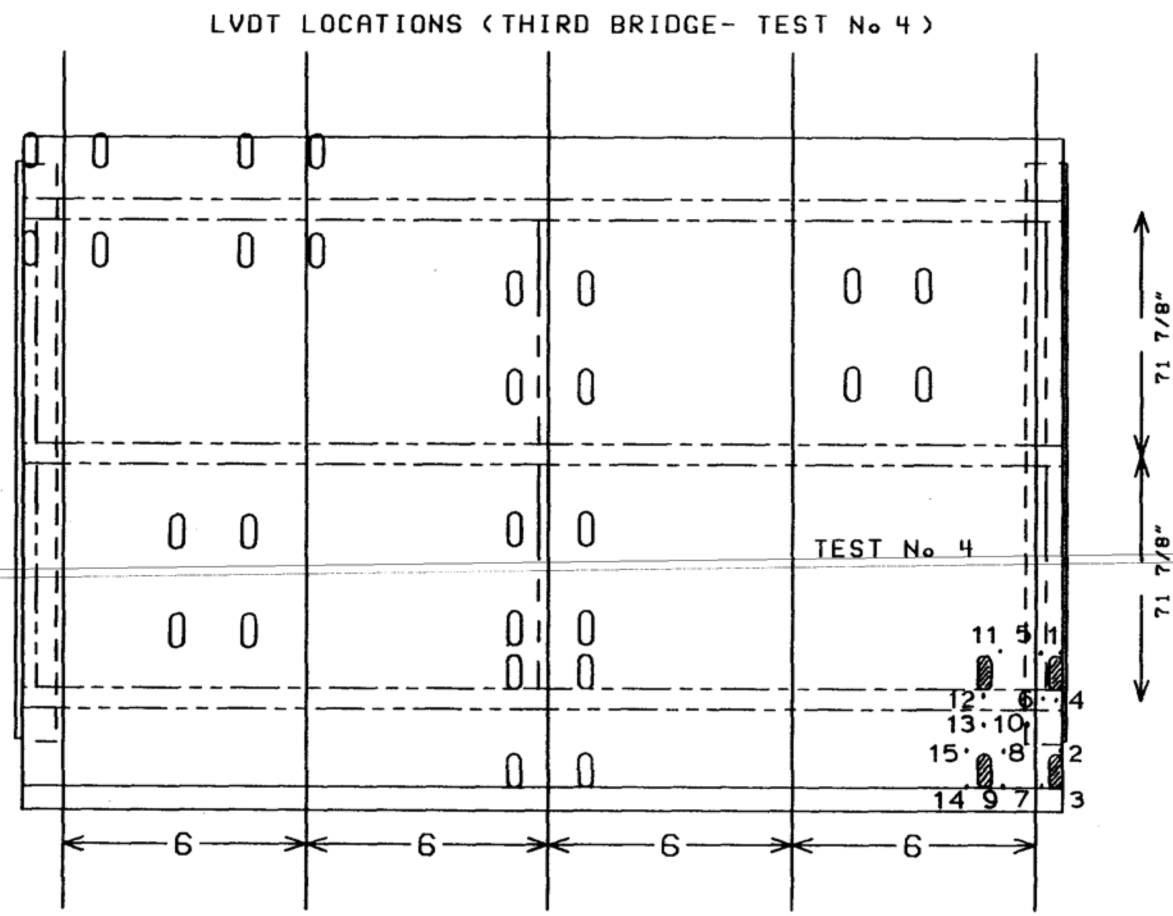

Figure A.21 LVDT Locations (Third Bridge - Test No. 4)

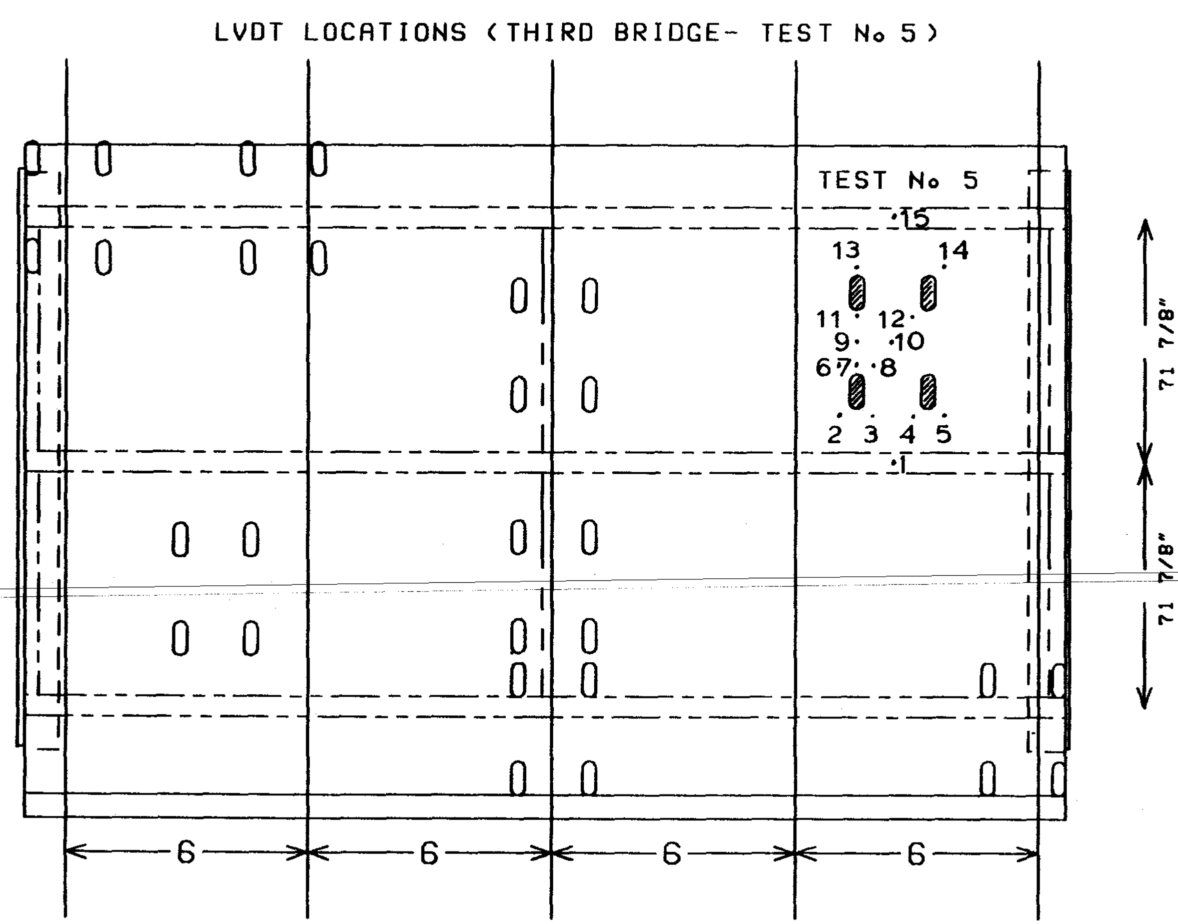

Figure A.22 LVDT Locations (Third Bridge - Test No. 5)

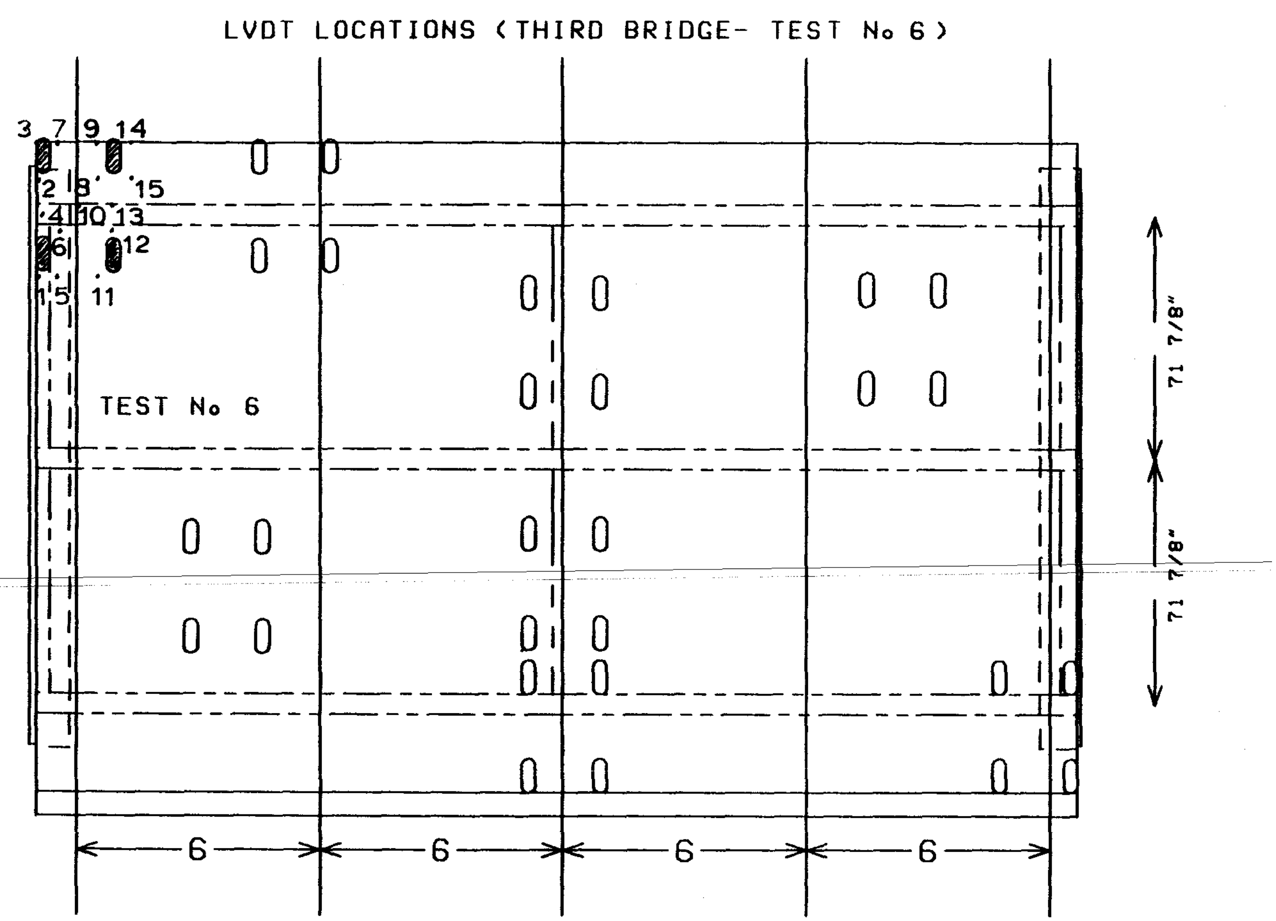

Figure A.23 LVDT Locations (Third Bridge - Test No. 6)

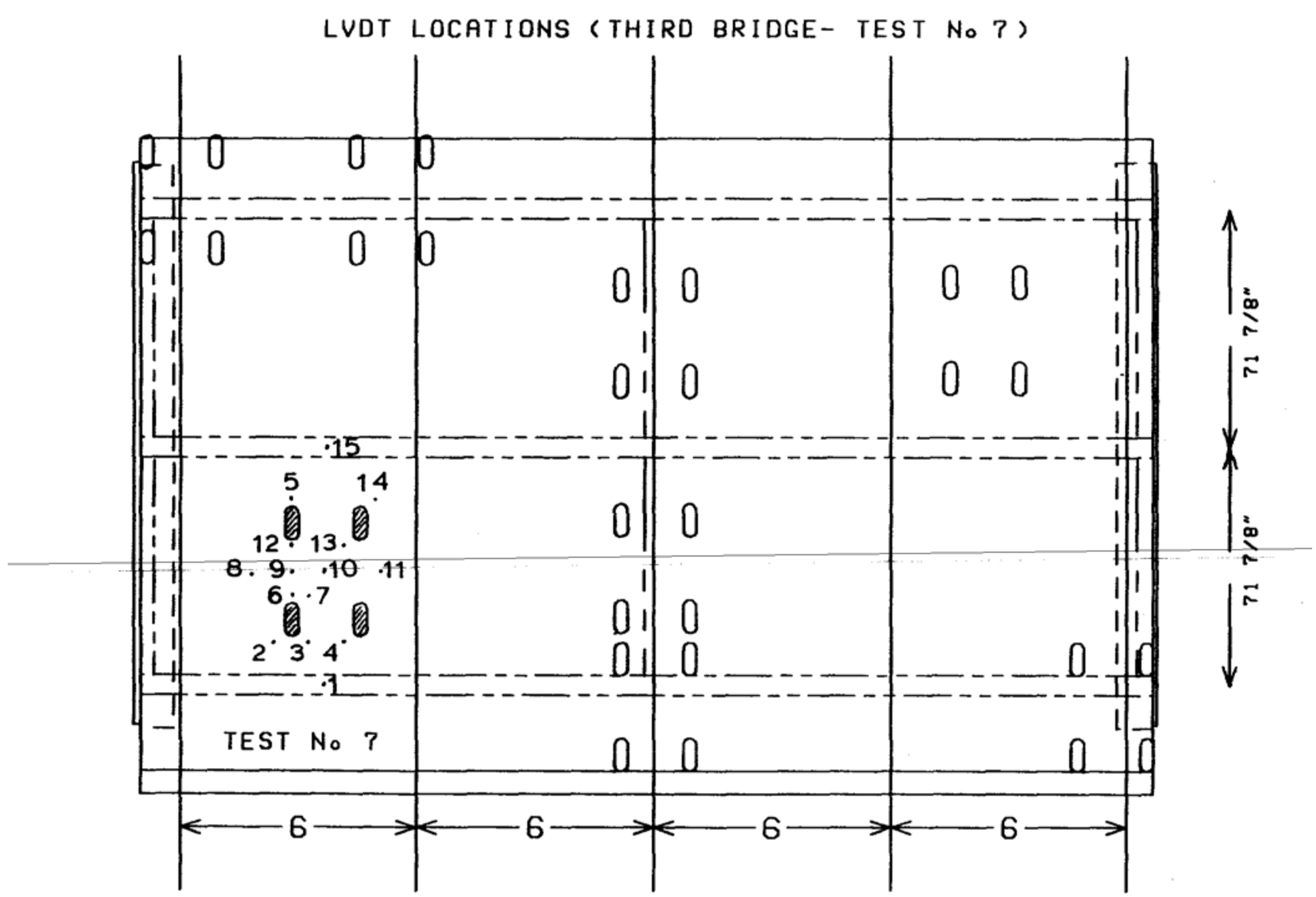

Figure A.24 LVDT Locations (Third Bridge - Test No. 7)

LVDT LOCATIONS (THIRD BRIDGE- TEST No 8)

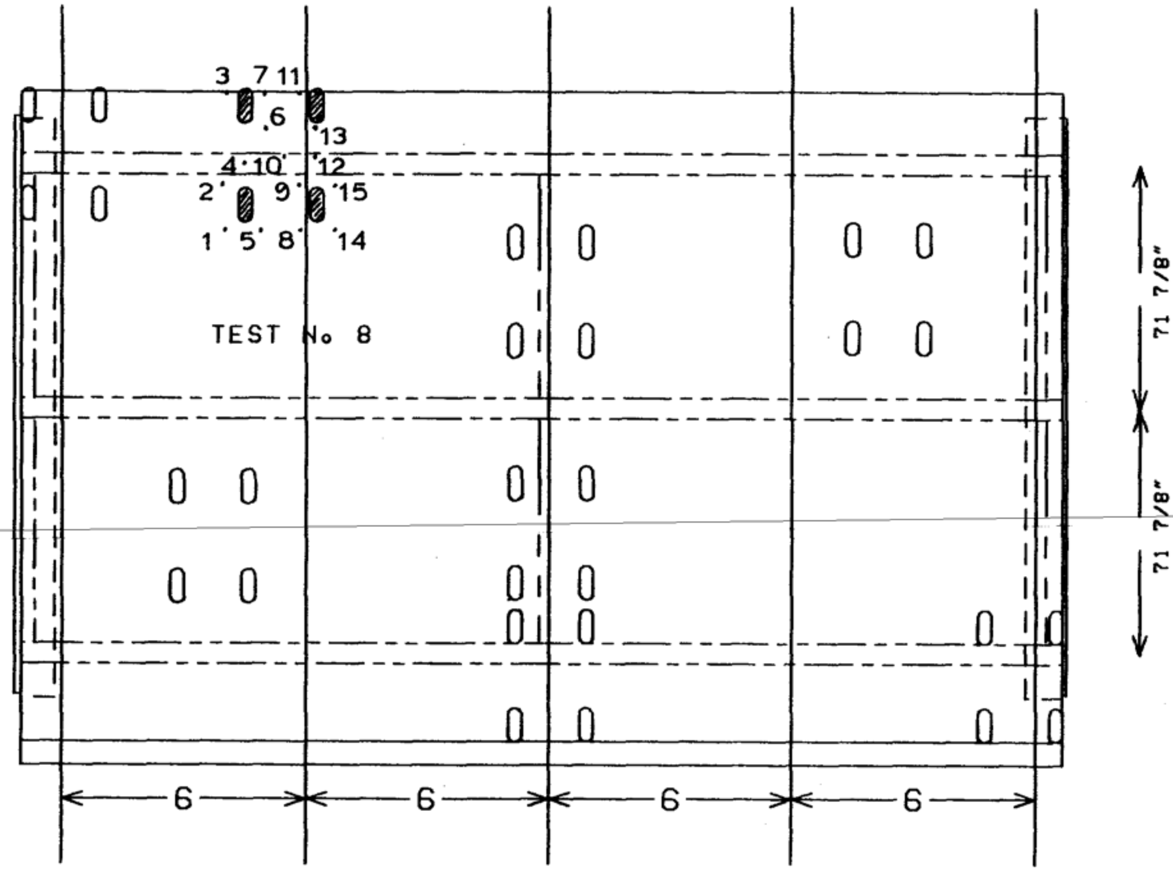

Figure A.25 LVDT Locations (Third Bridge - Test No. 8)

APPENDI B

Complete Load Deflection Plots

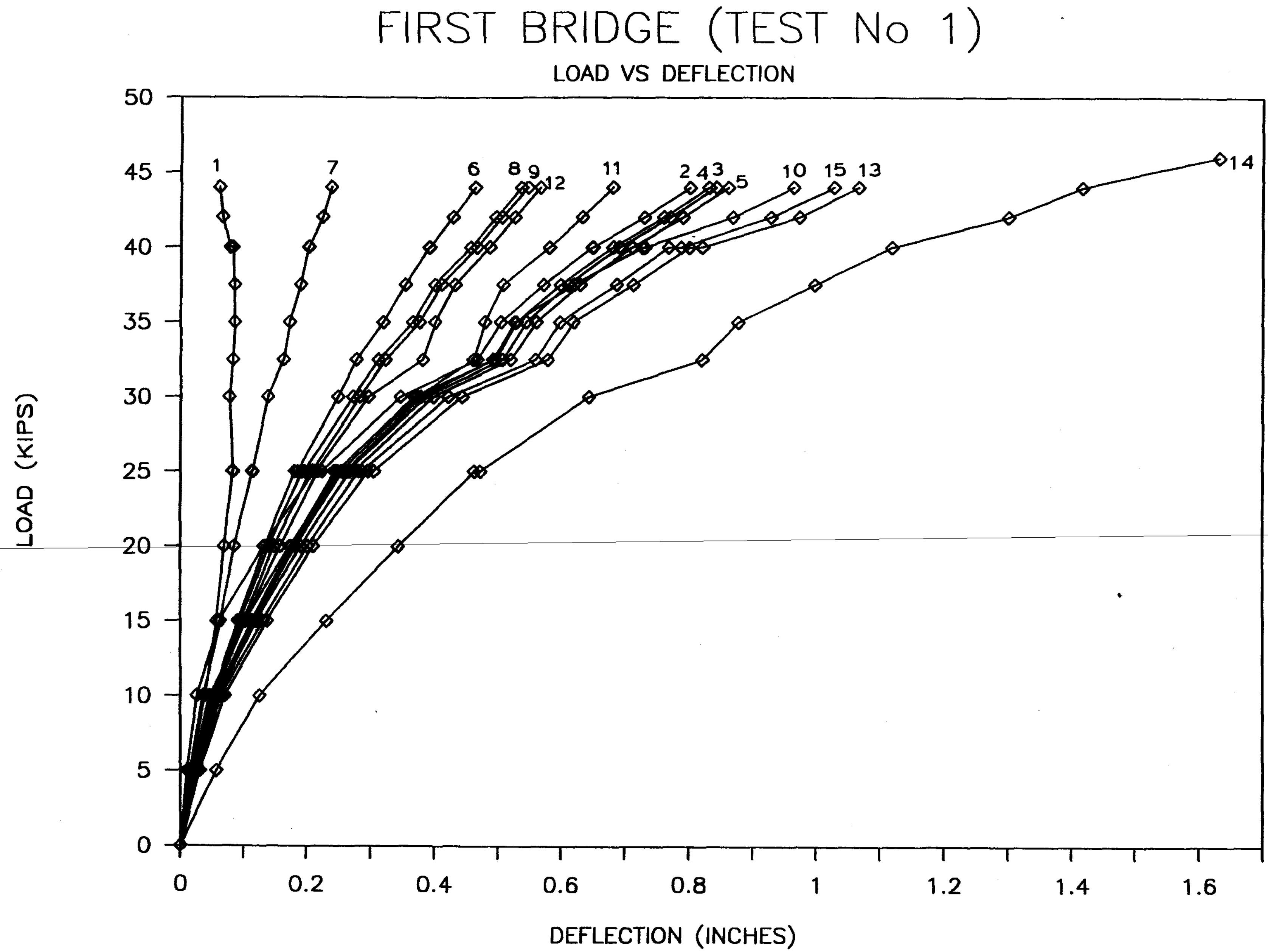

Figure B.1 Load-Deflection Curves (First Bridge - Test No. 1)

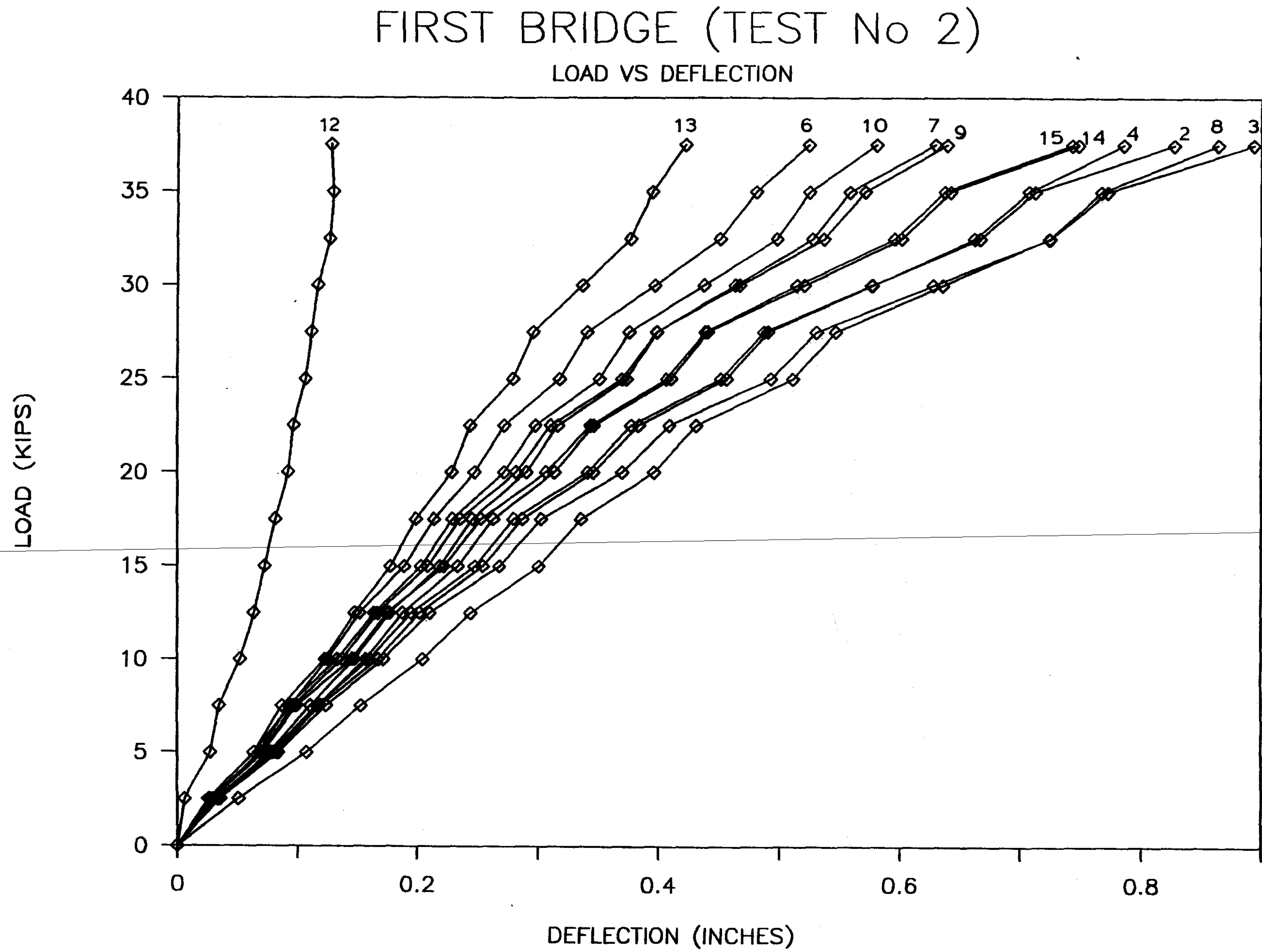

Figure B.2 Load-Deflection Curves (First Bridge - Test No. 2)

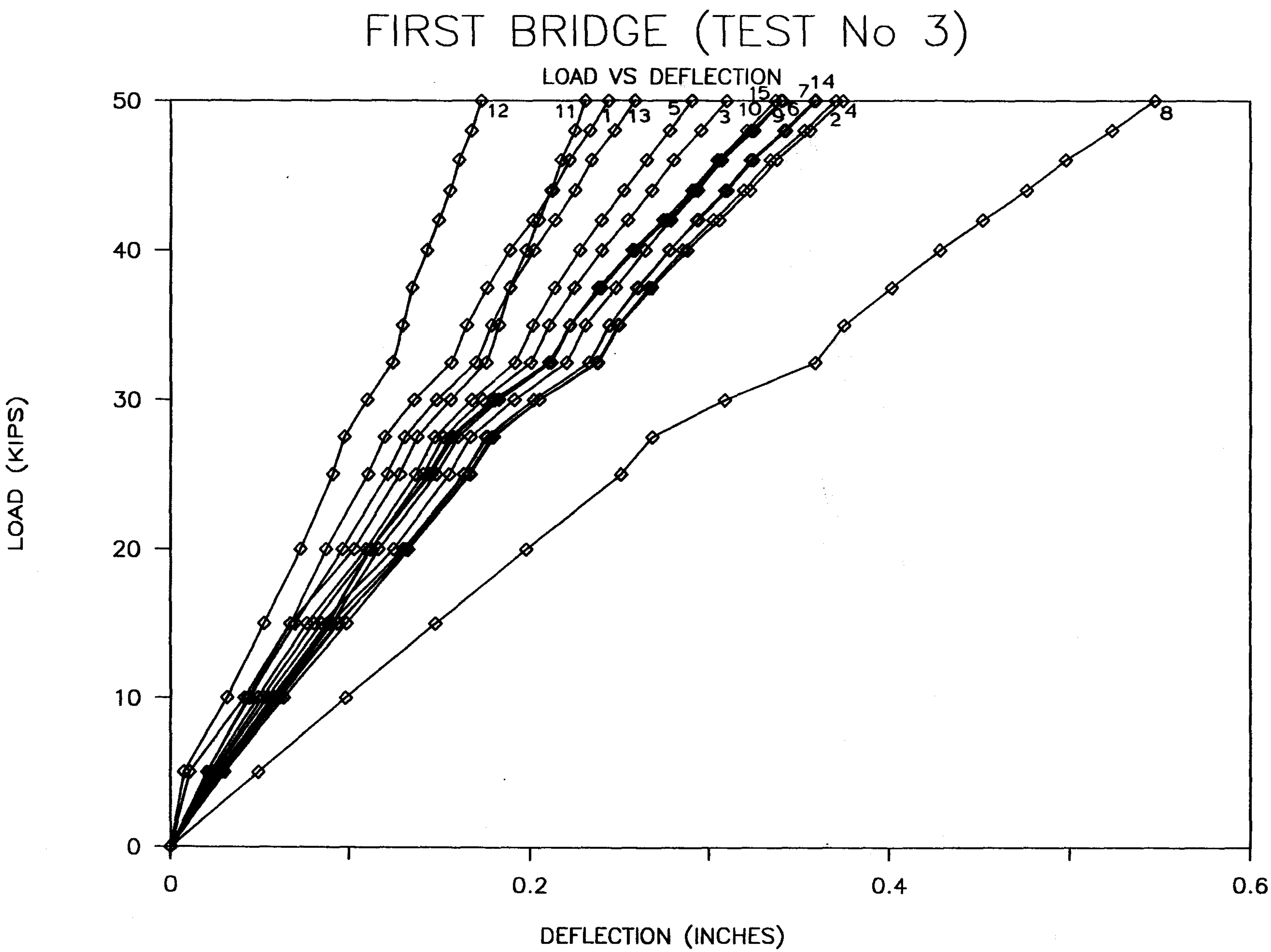

Figure B.3 Load-Deflection Curves (First Bridge - Test No. 3)

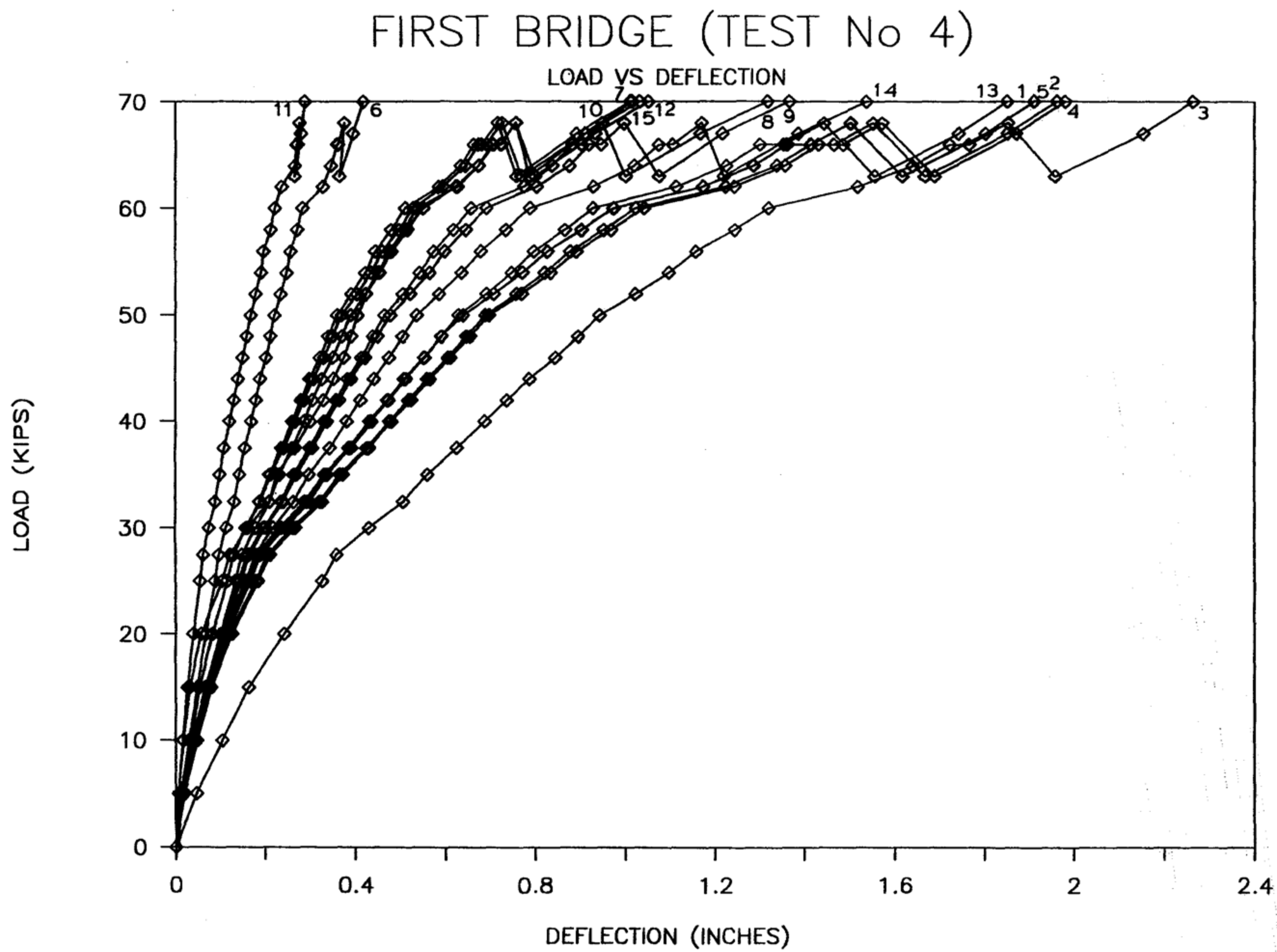

Figure B.4 Load-Deflection Curves (First Bridge - Test No. 4)

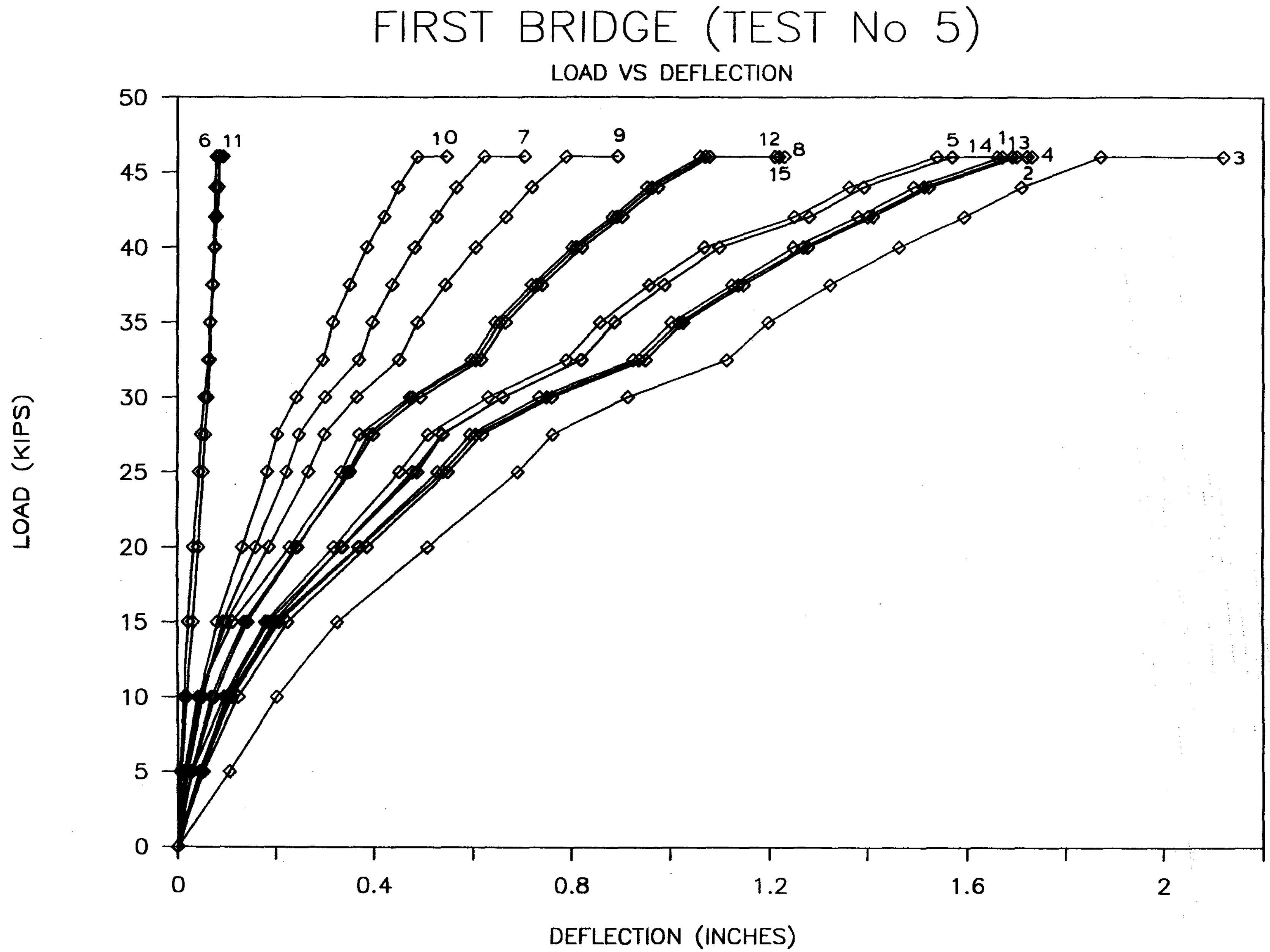

Figure B.5 Load-Deflection Curves (First Bridge - Test No. 5)

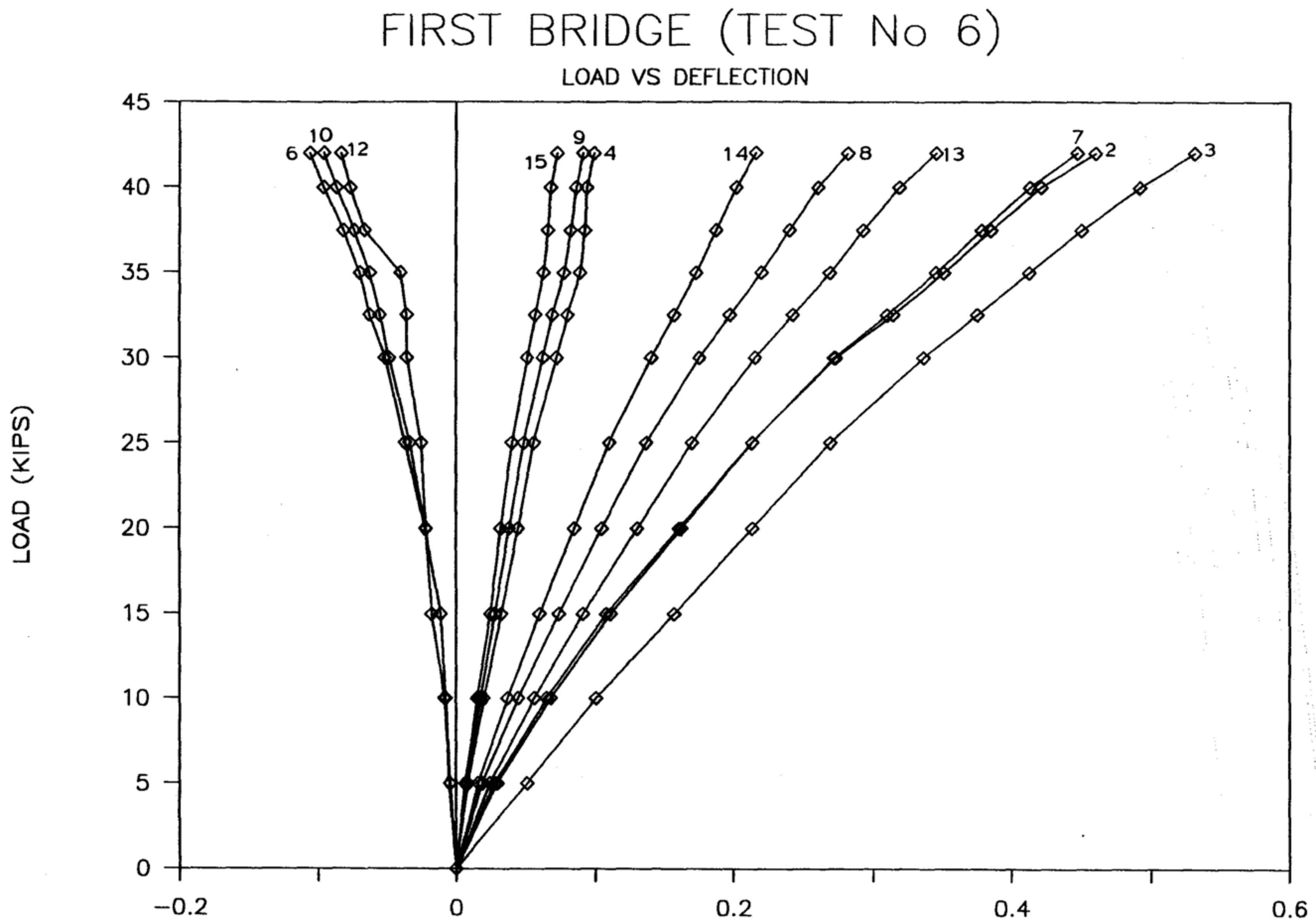

Figure B.6 Load-Deflection Curves (First Bridge - Test No. 6)

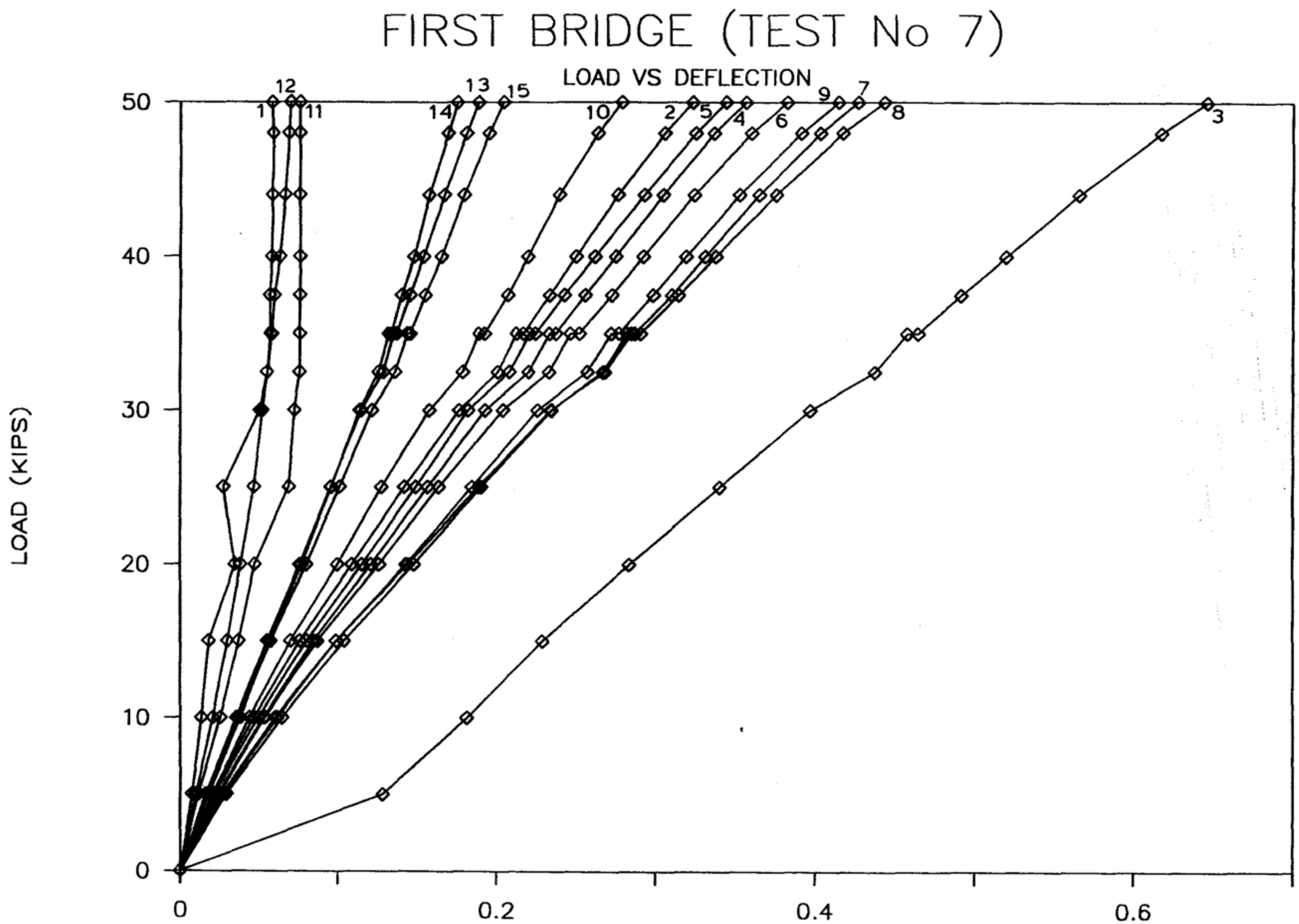

Figure B.7 Load-Deflection Curves (First Bridge - Test No. 7)

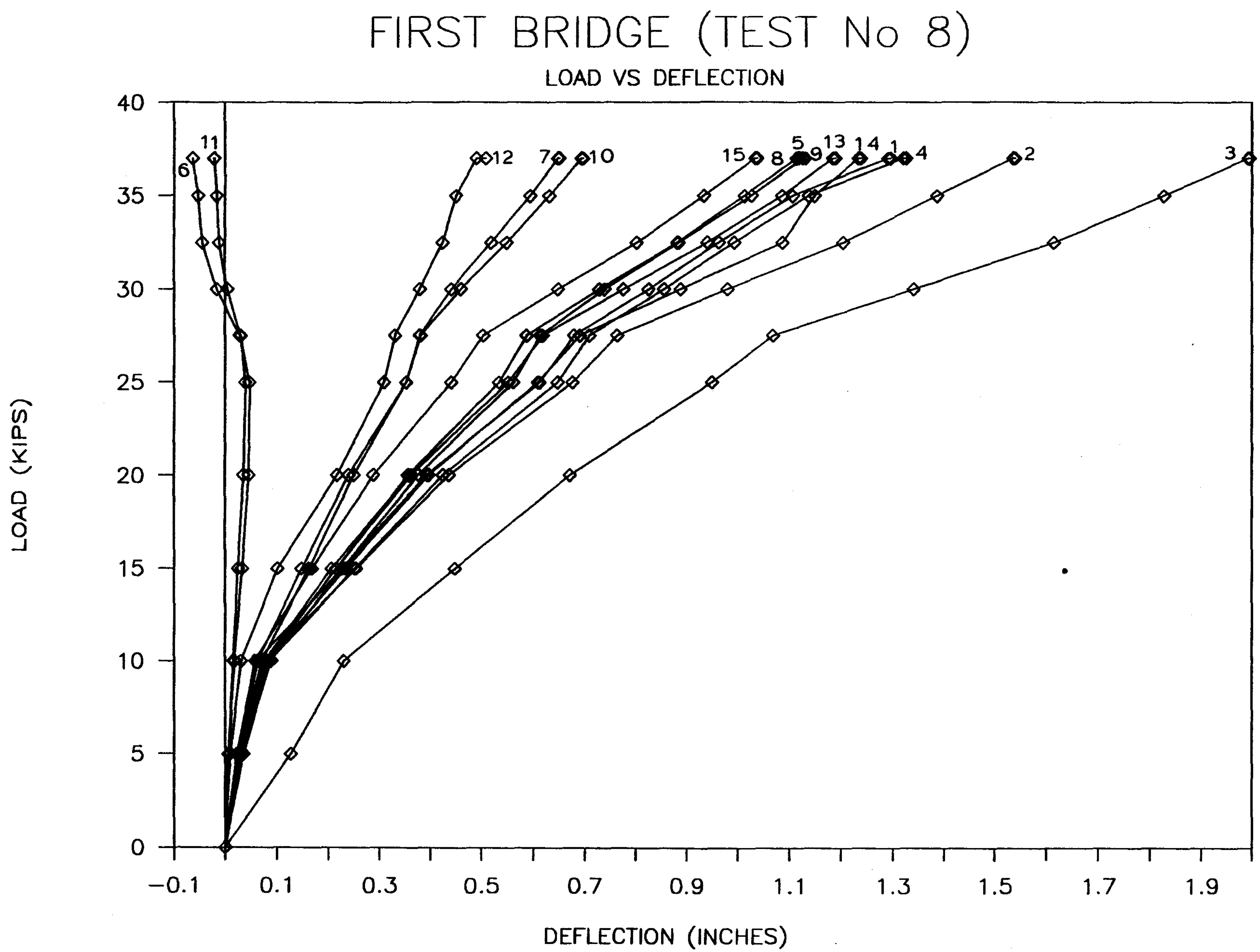

Figure B.8 Load-Deflection Curves (First Bridge - Test No. 8)

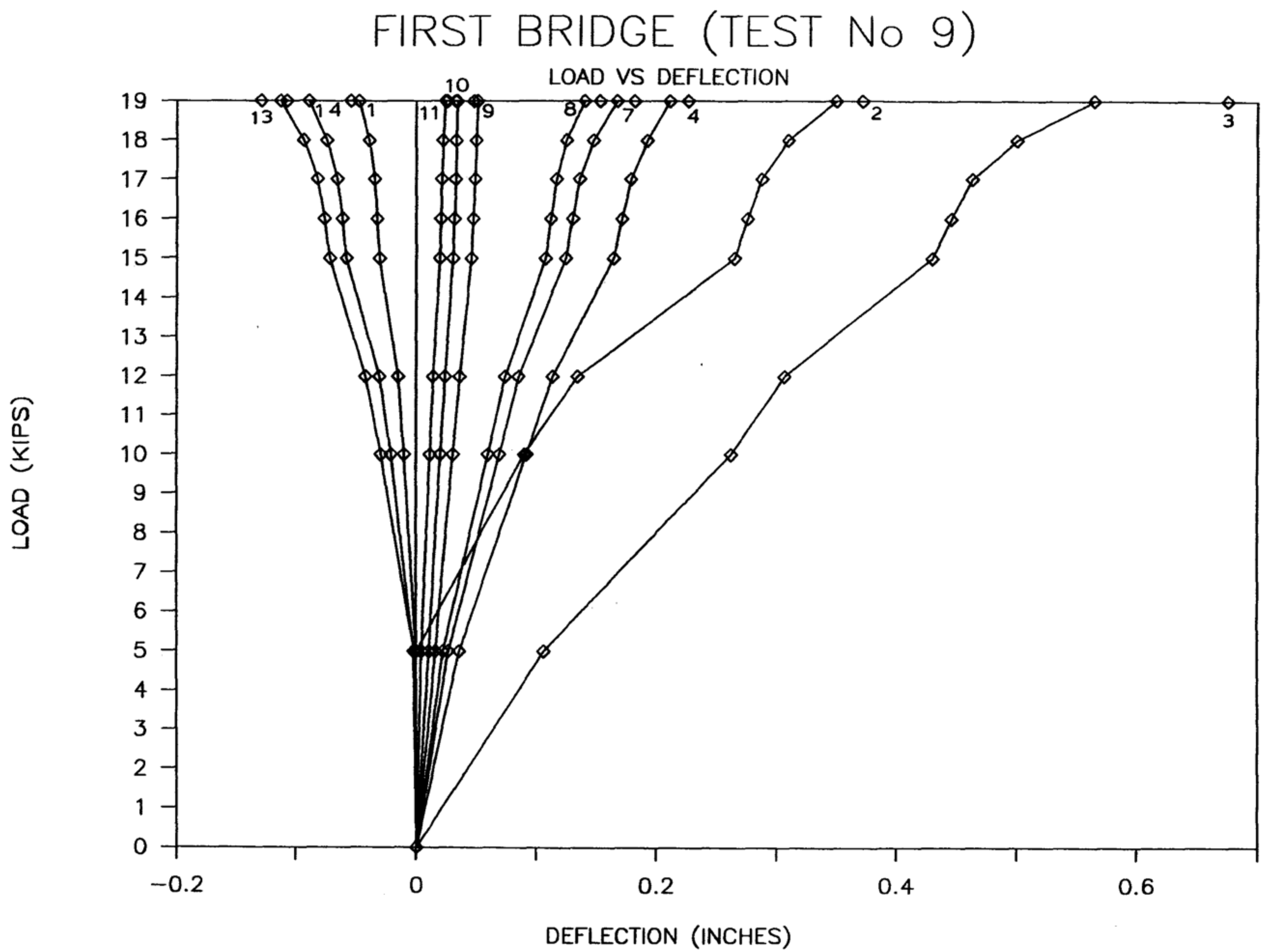

Figure B.9 Load-Deflection Curves (First Bridge - Test No. 9)

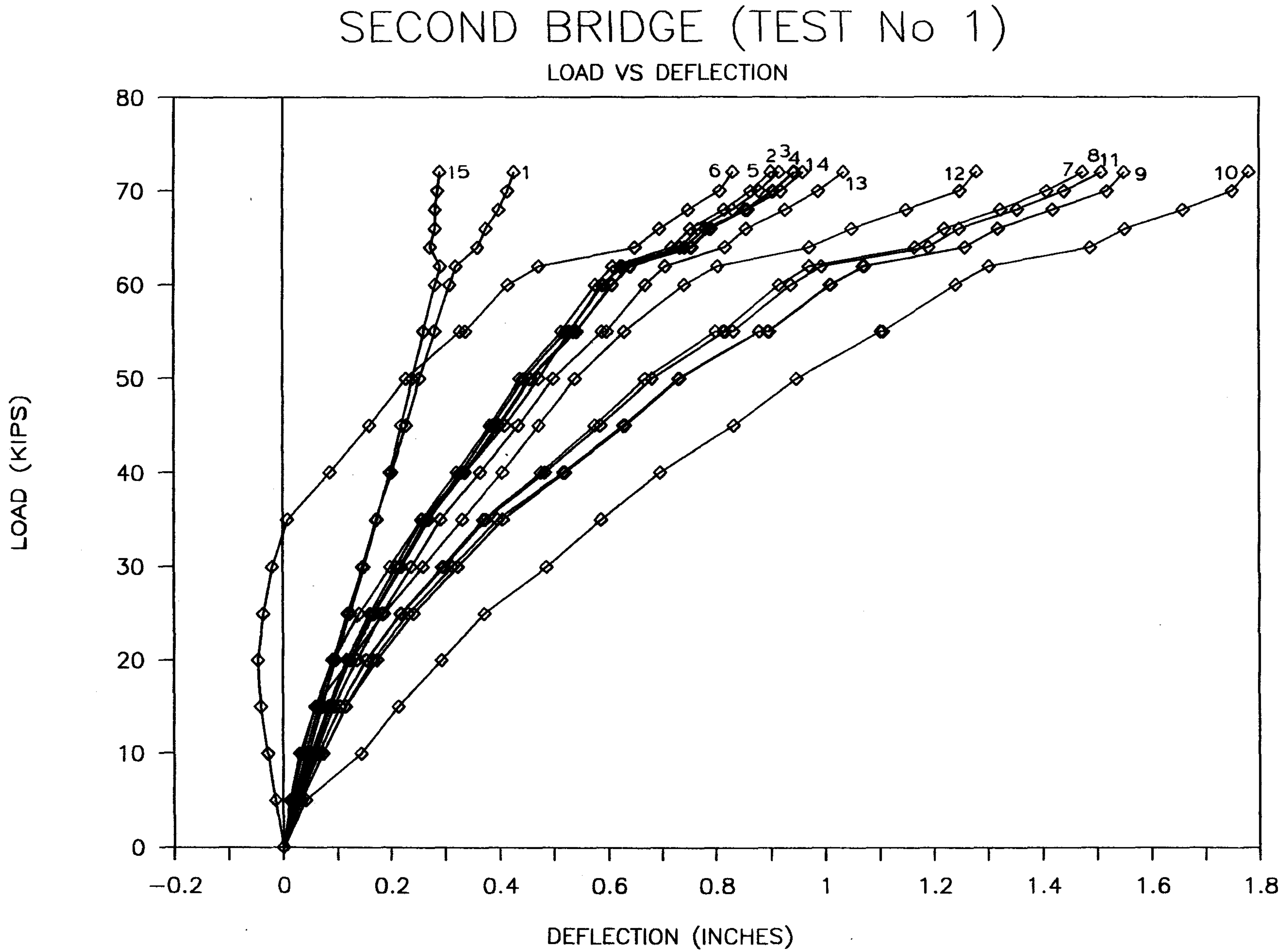

Figure B.10 Load-Deflection Curves (Second Bridge - Test No. 1)

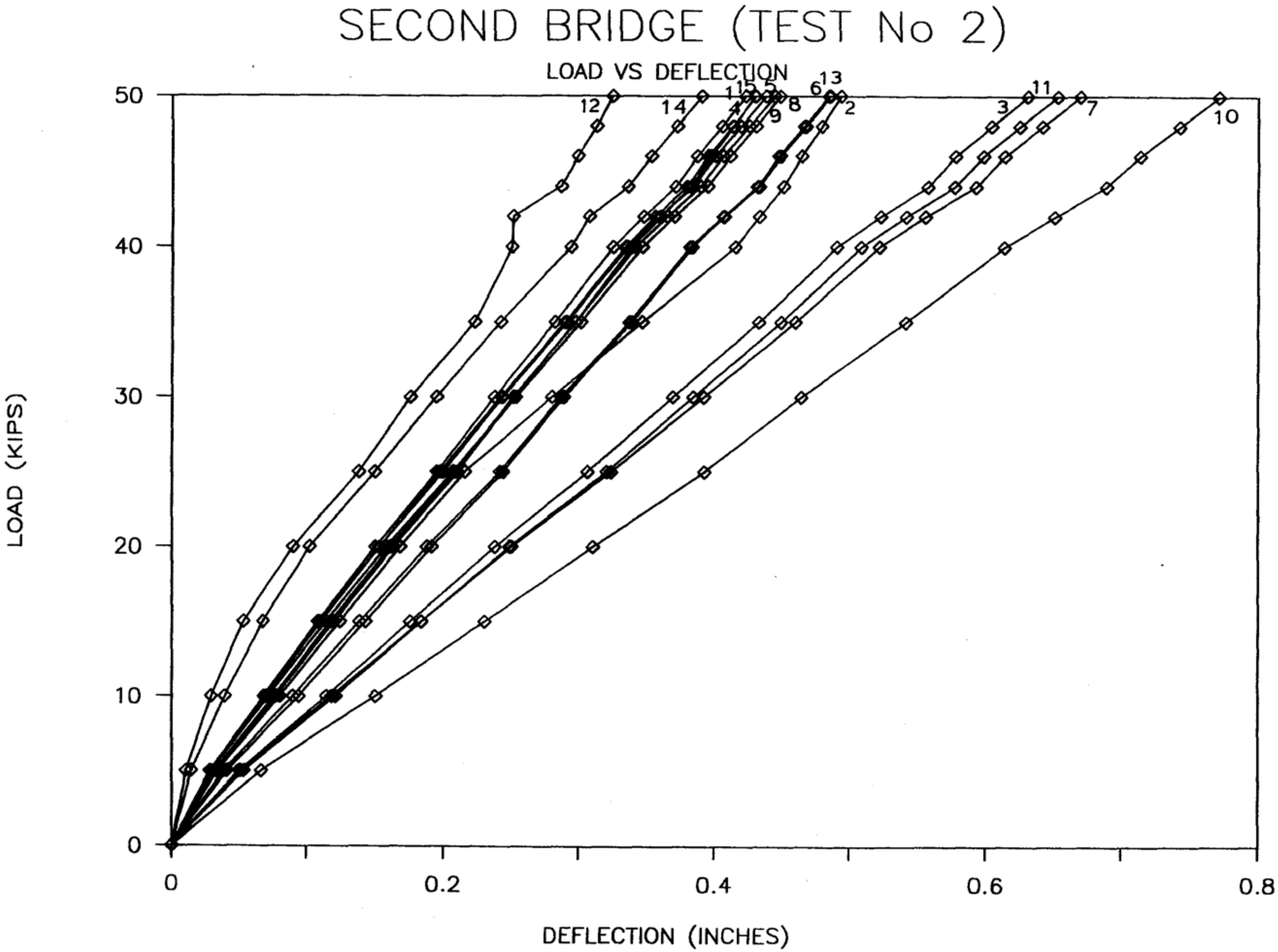

Figure B.11 Load-Deflection Curves (Second Bridge - Test No. 2)

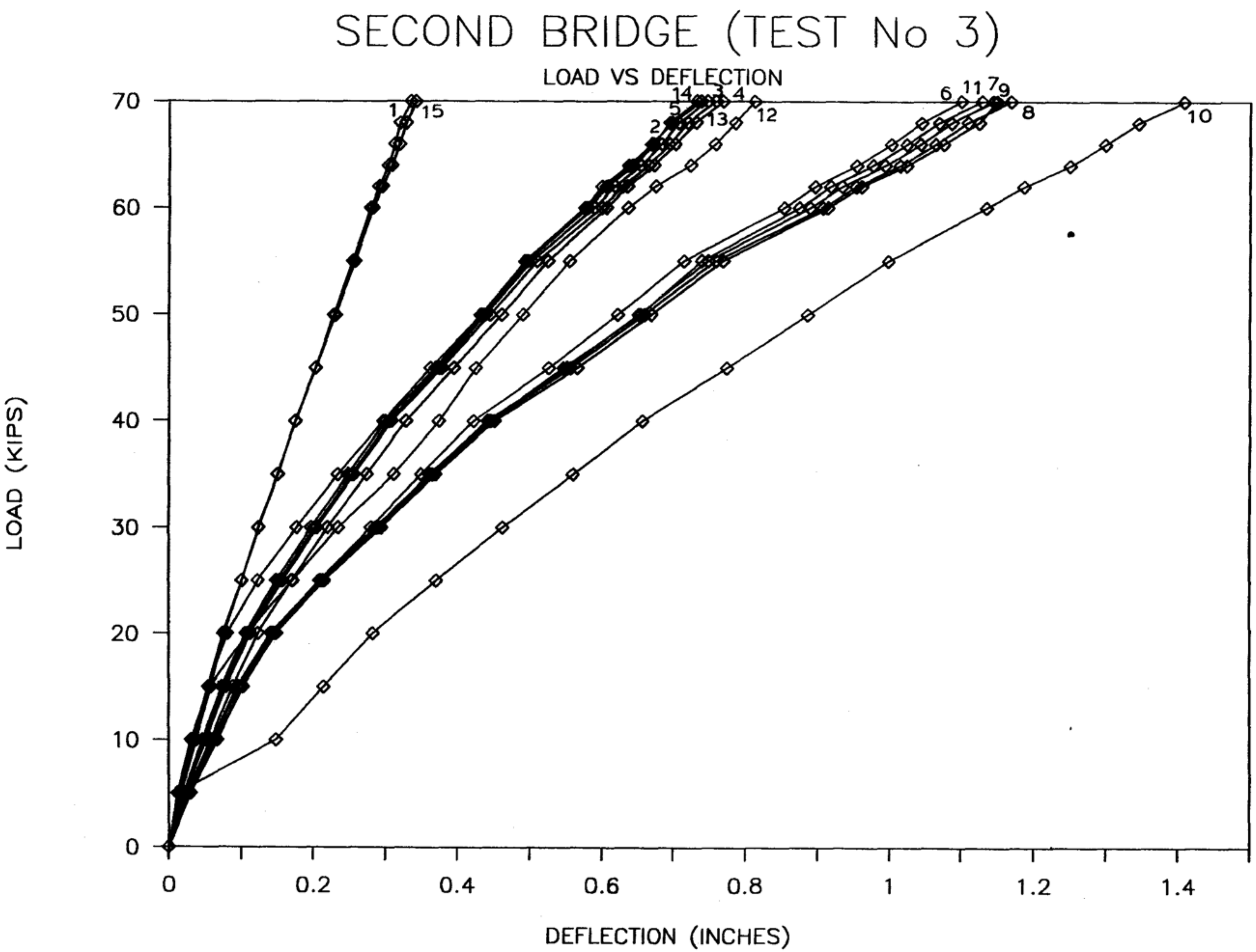

Figure B.12 Load-Deflection Curves (Second Bridge - Test No. 3)

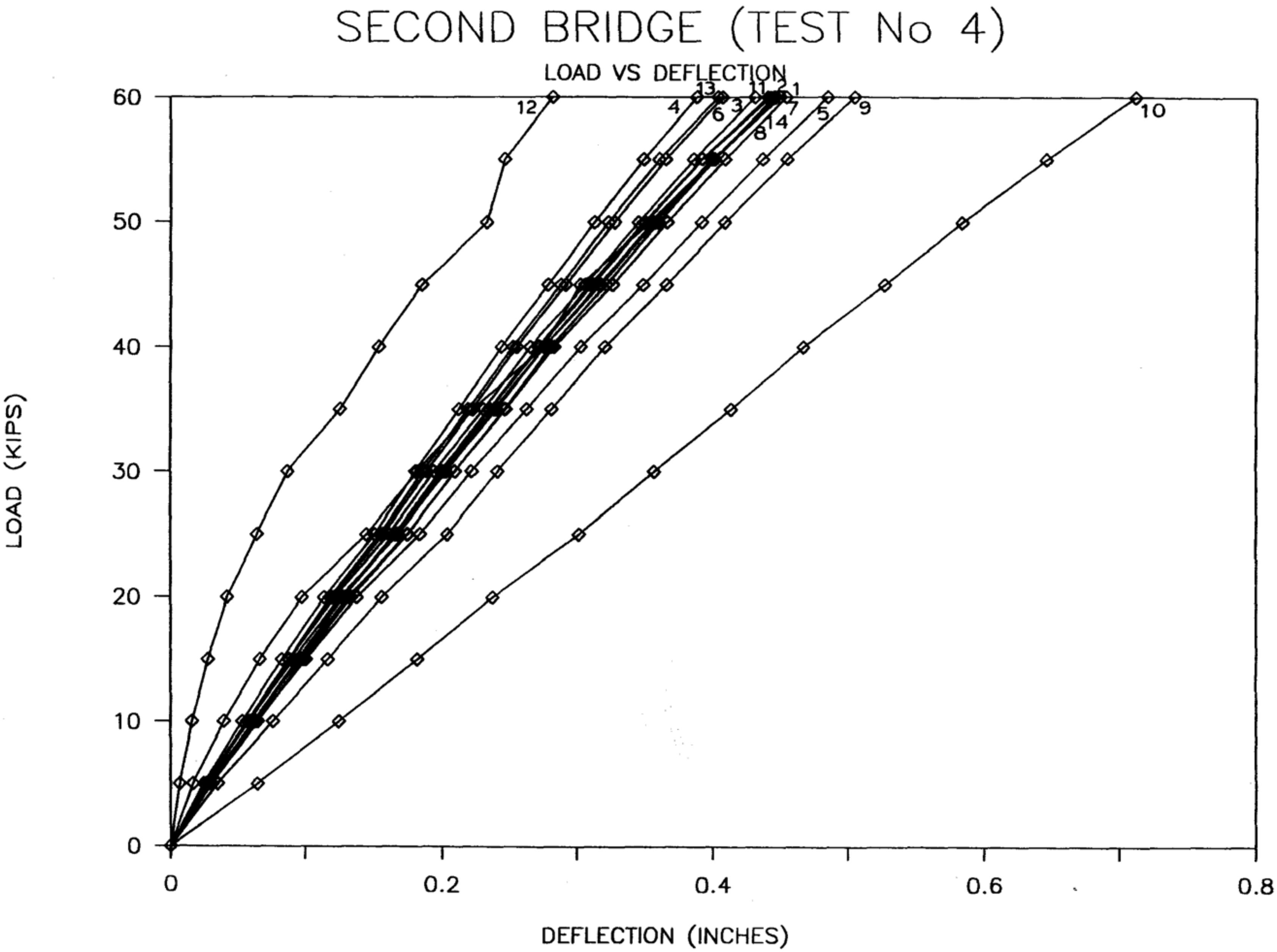

Figure B.13 Load-Deflection Curves (Second Bridge - Test No. 4)

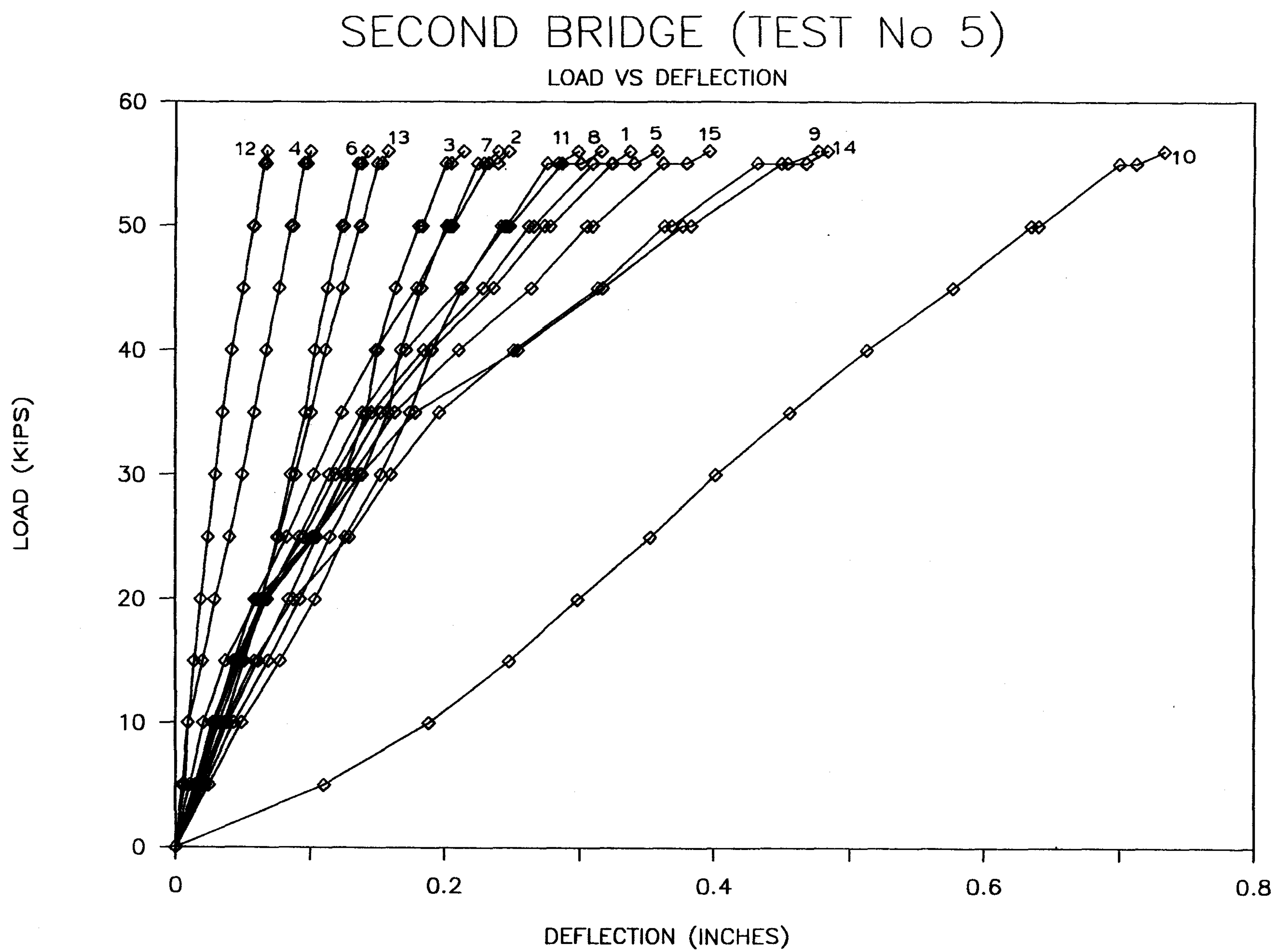

Figure B.14 Load-Deflection Curves (Second Bridge - Test No. 5)

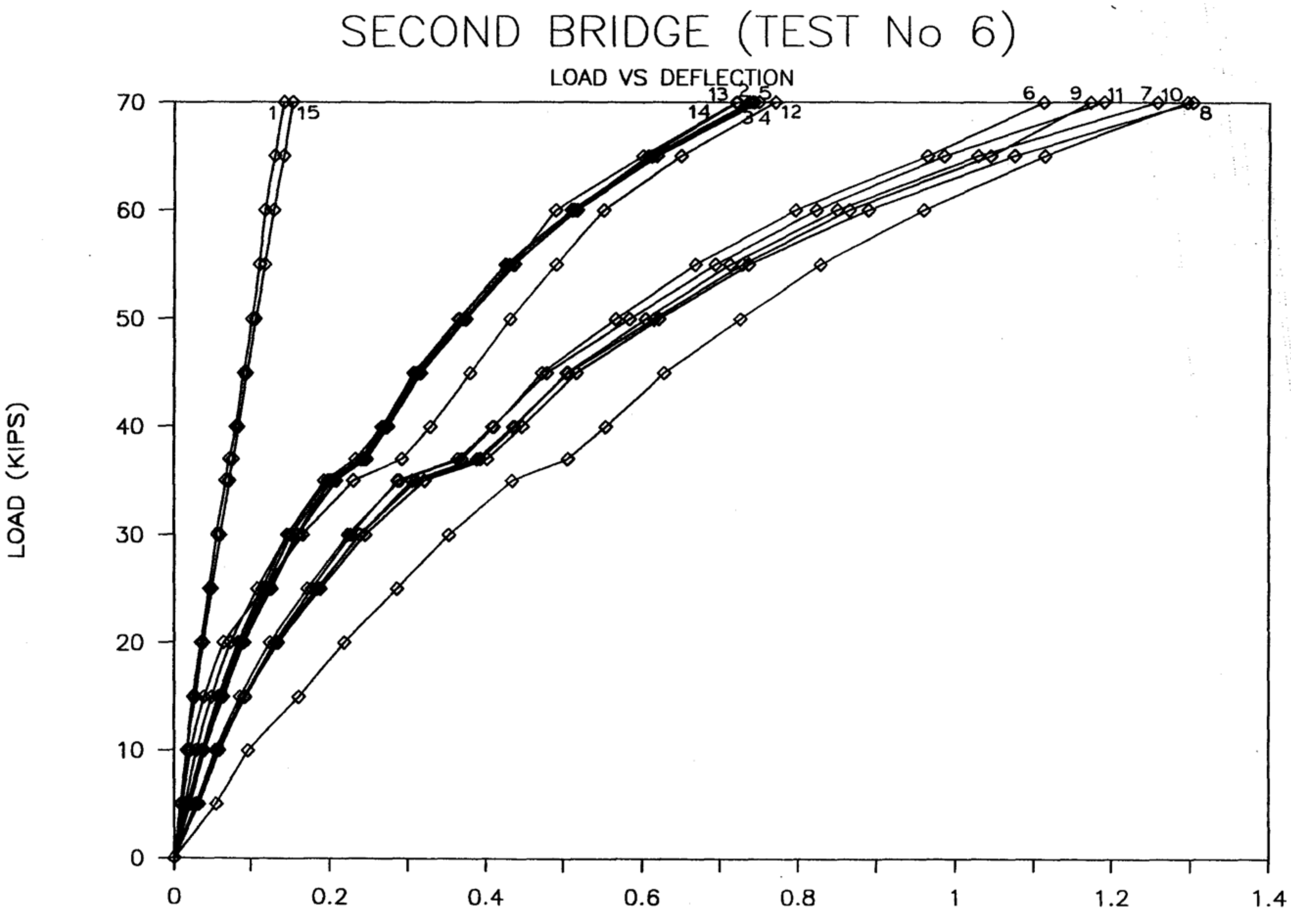

Figure B.15 Load-Deflection Curves (Second Bridge - Test No. 6)

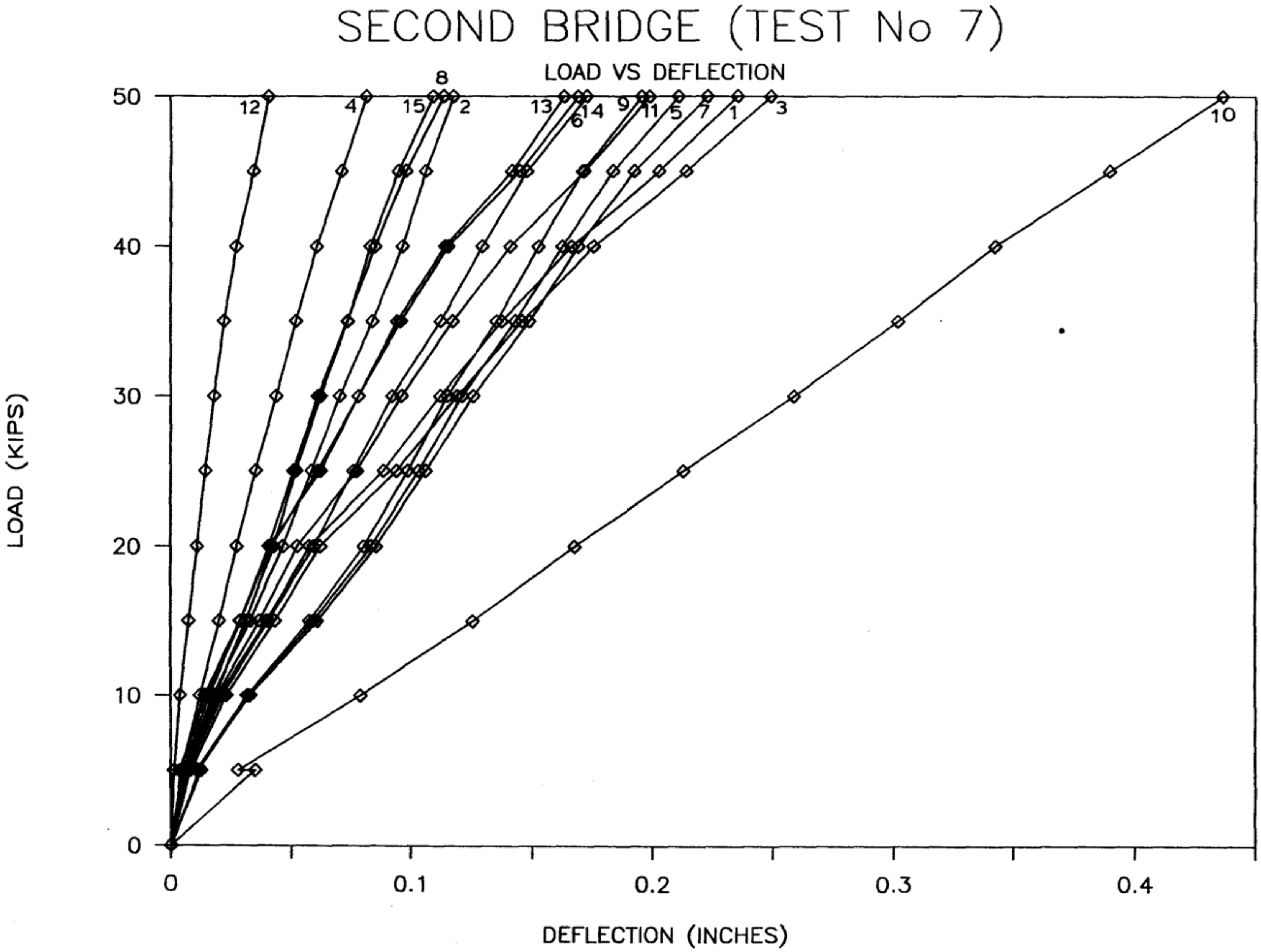

Figure B.16 Load-Deflection Curves (Second Bridge - Test No. 7)

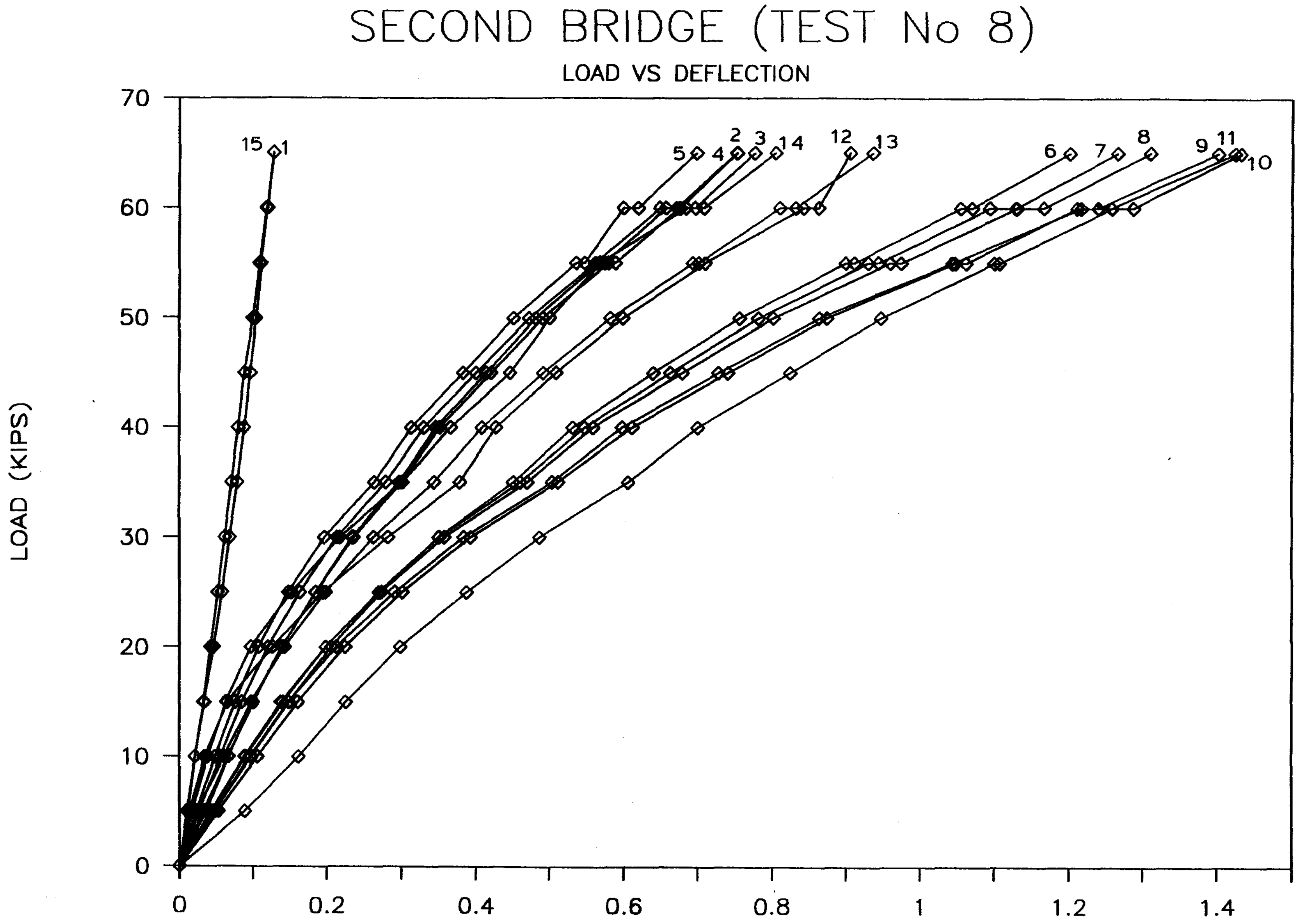

Figure B.17 Load-Deflection Curves (Second Bridge - Test No. 8)

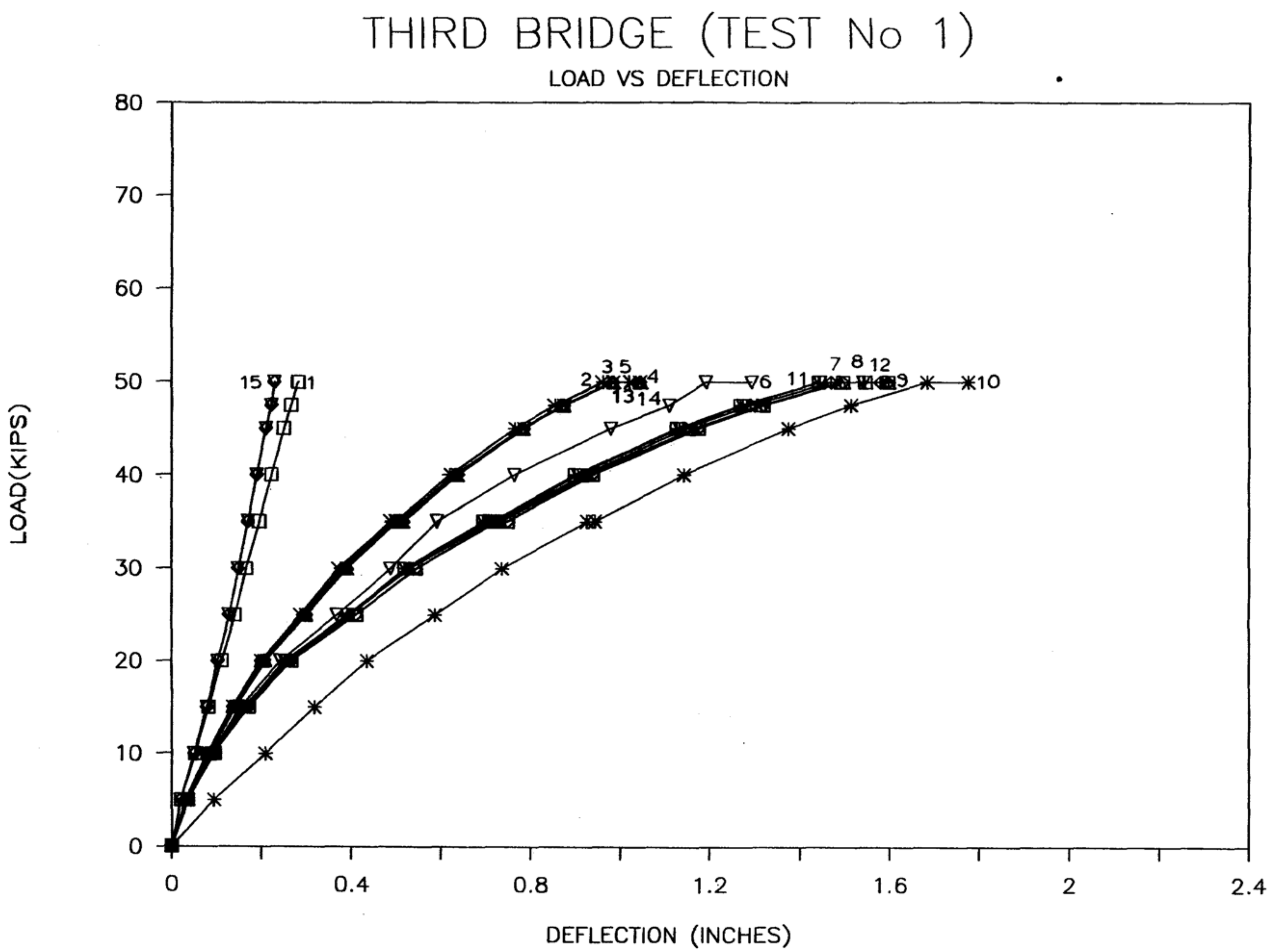

Figure B.18 Load-Deflection Curves (Third Bridge - Test No. 1)

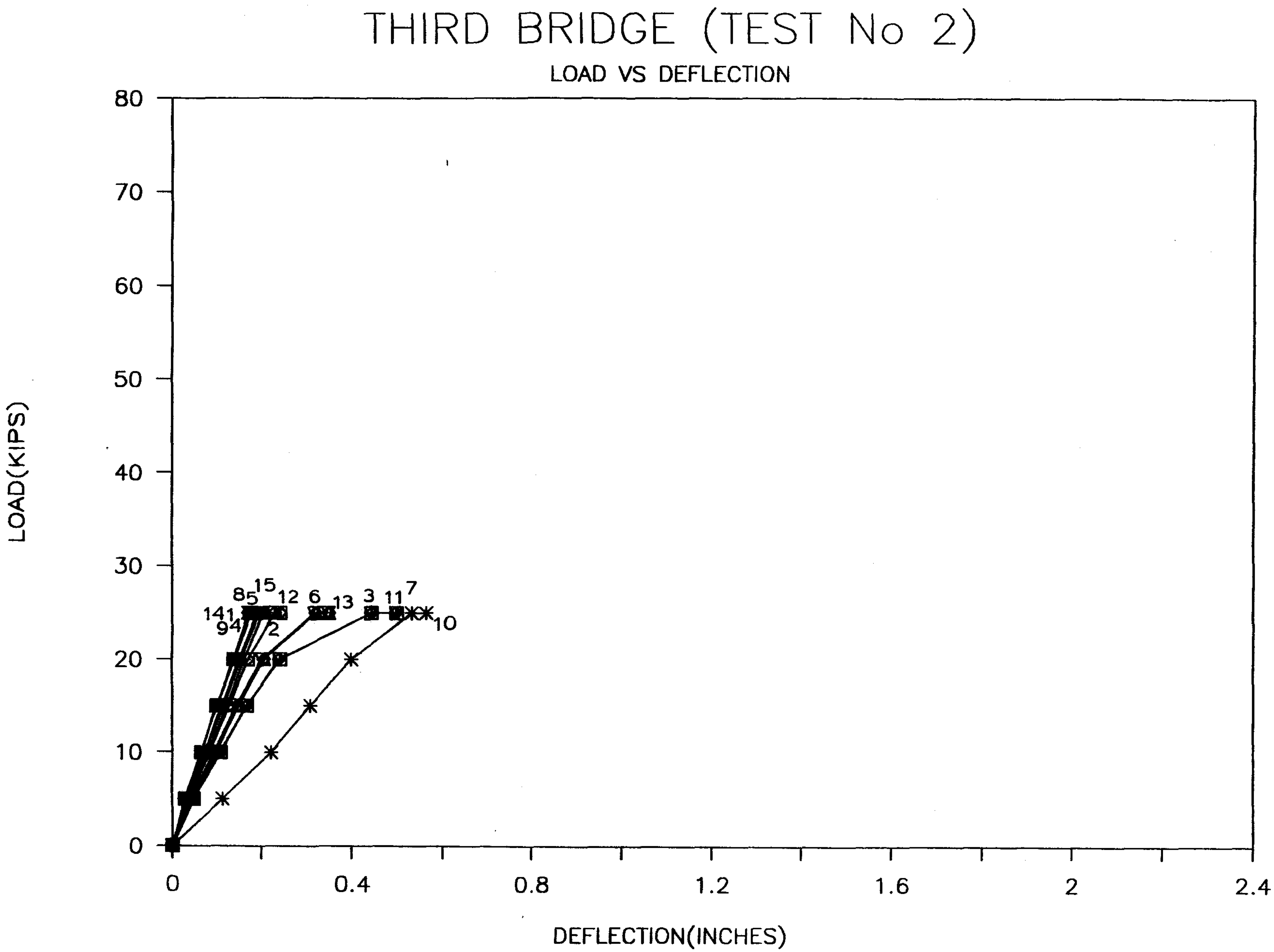

Figure B.19 Load-Deflection Curves (Third Bridge - Test No. 2)

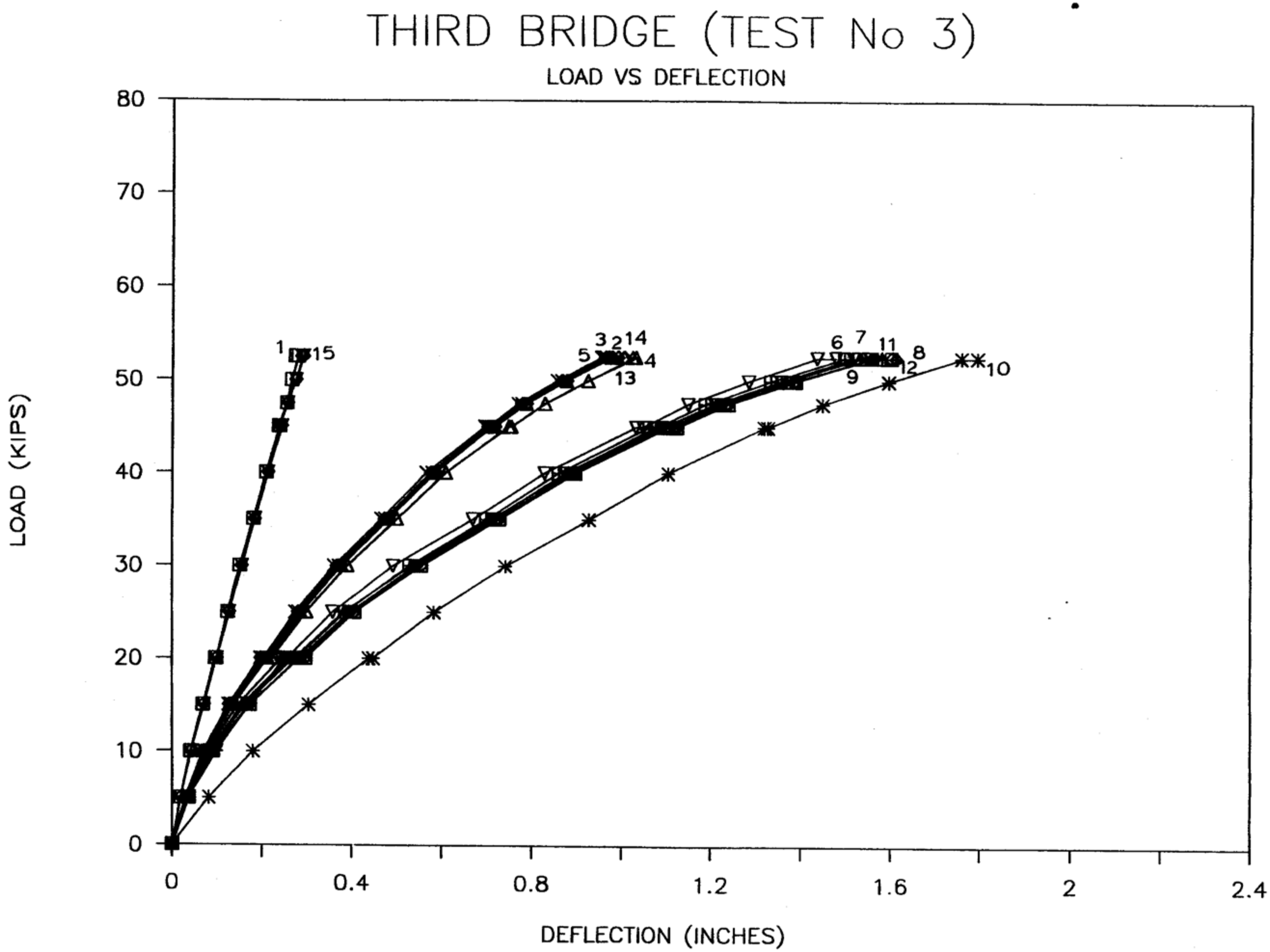

Figure B.20 Load-Deflection Curves (Third Bridge - Test No. 3)

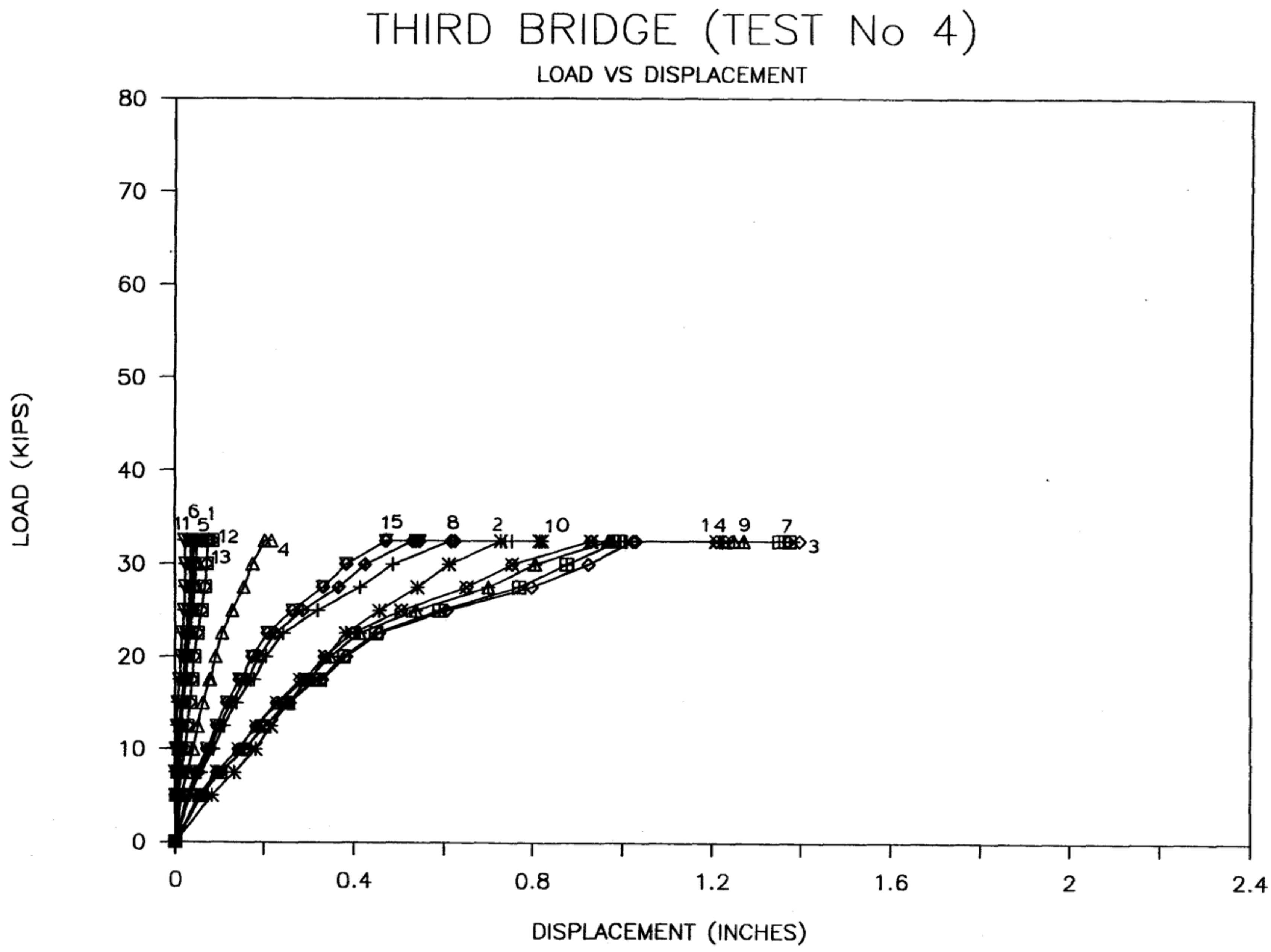

Figure B.21 Load-Deflection Curves (Third Bridge - Test No. 4)

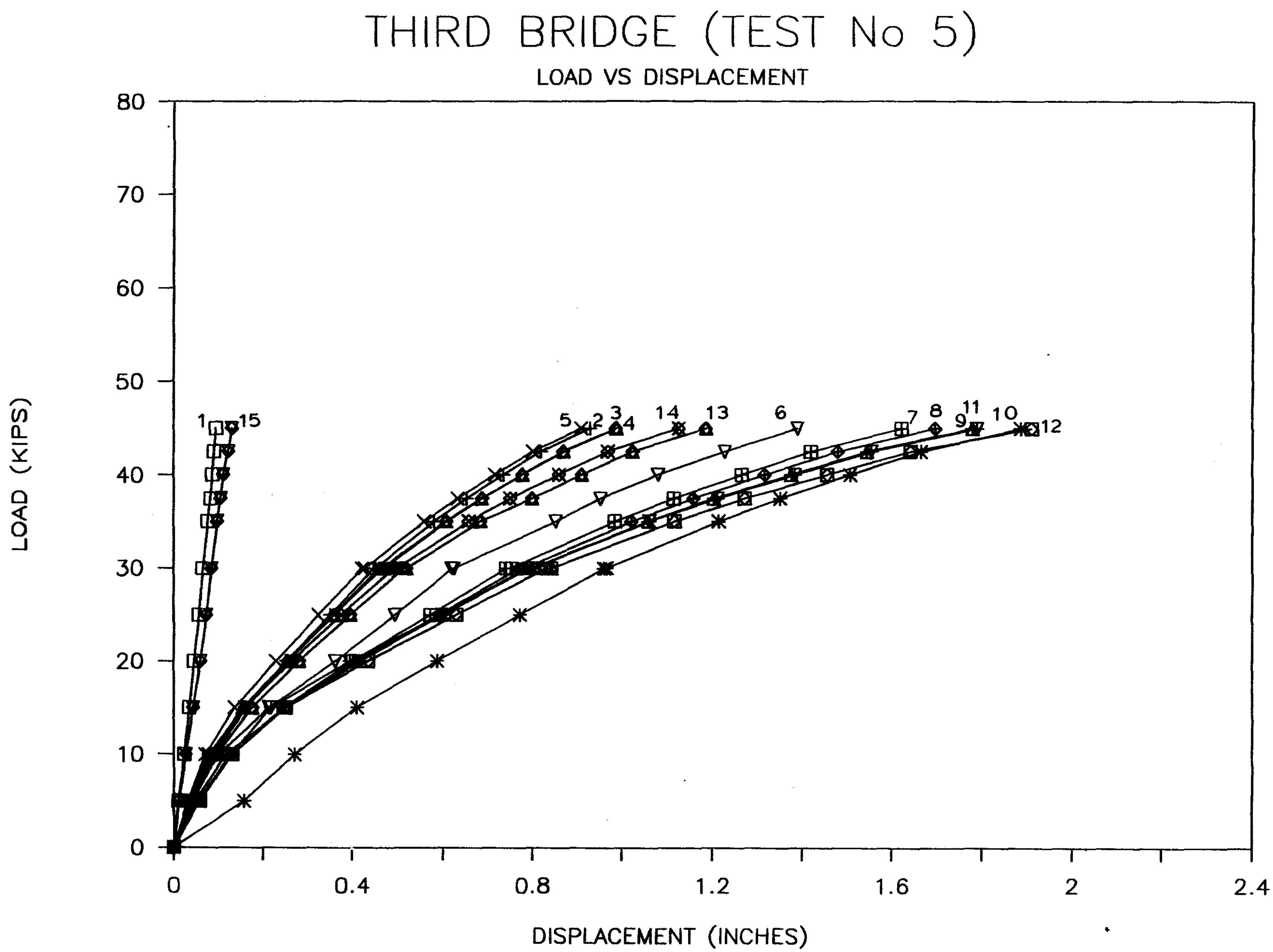

Figure B.22 Load-Deflection Curves (Third Bridge - Test No. 5)

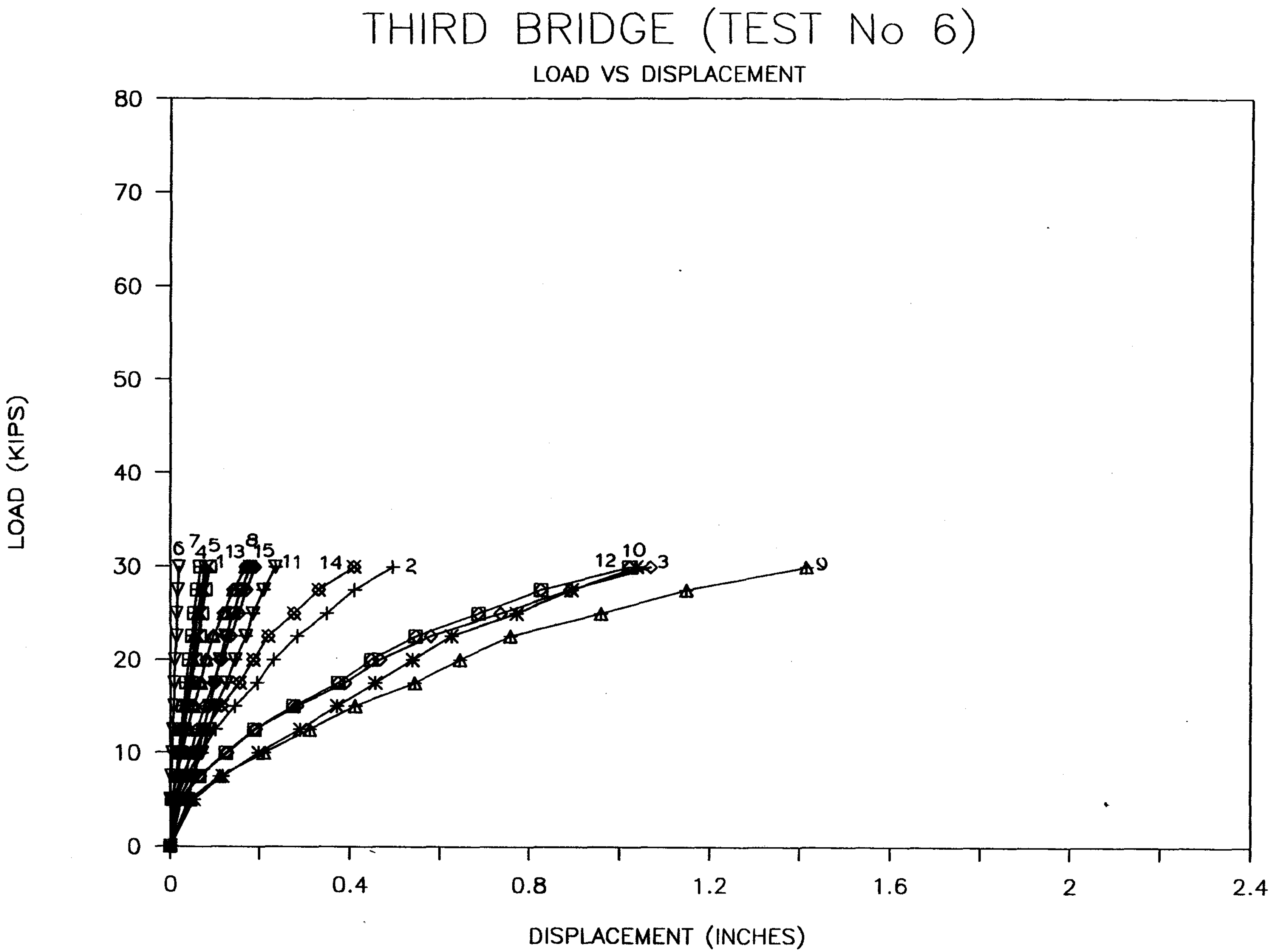

Figure B.23 Load-Deflection Curves (Third Bridge - Test No. 6)

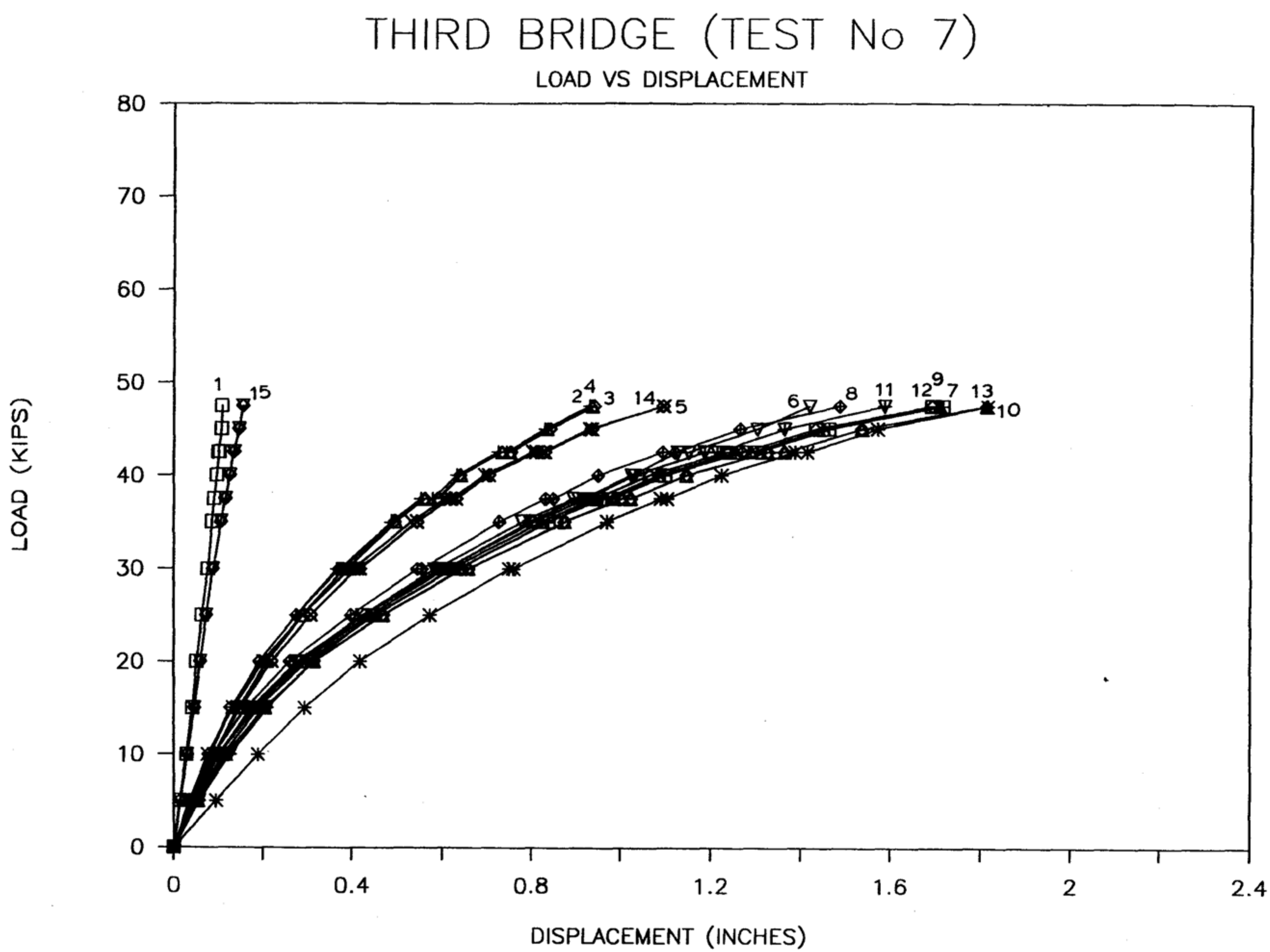

Figure B.24 Load-Deflection Curves (Third Bridge - Test No. 7)

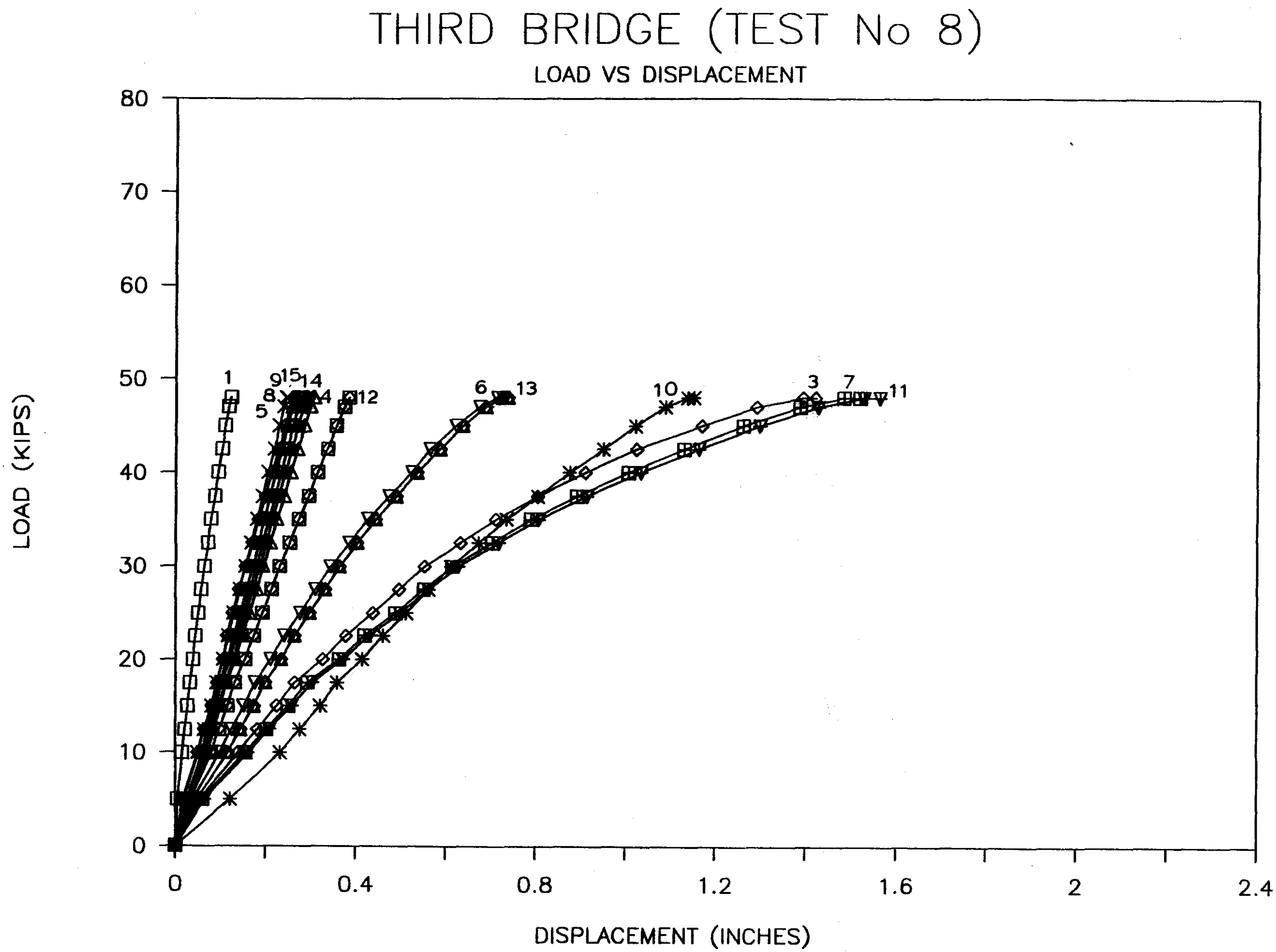

Figure B.25 Load-Deflection Curves (Third Bridge - Test No. 8)

APPENDIX C

Strain Gage Locations For Tests

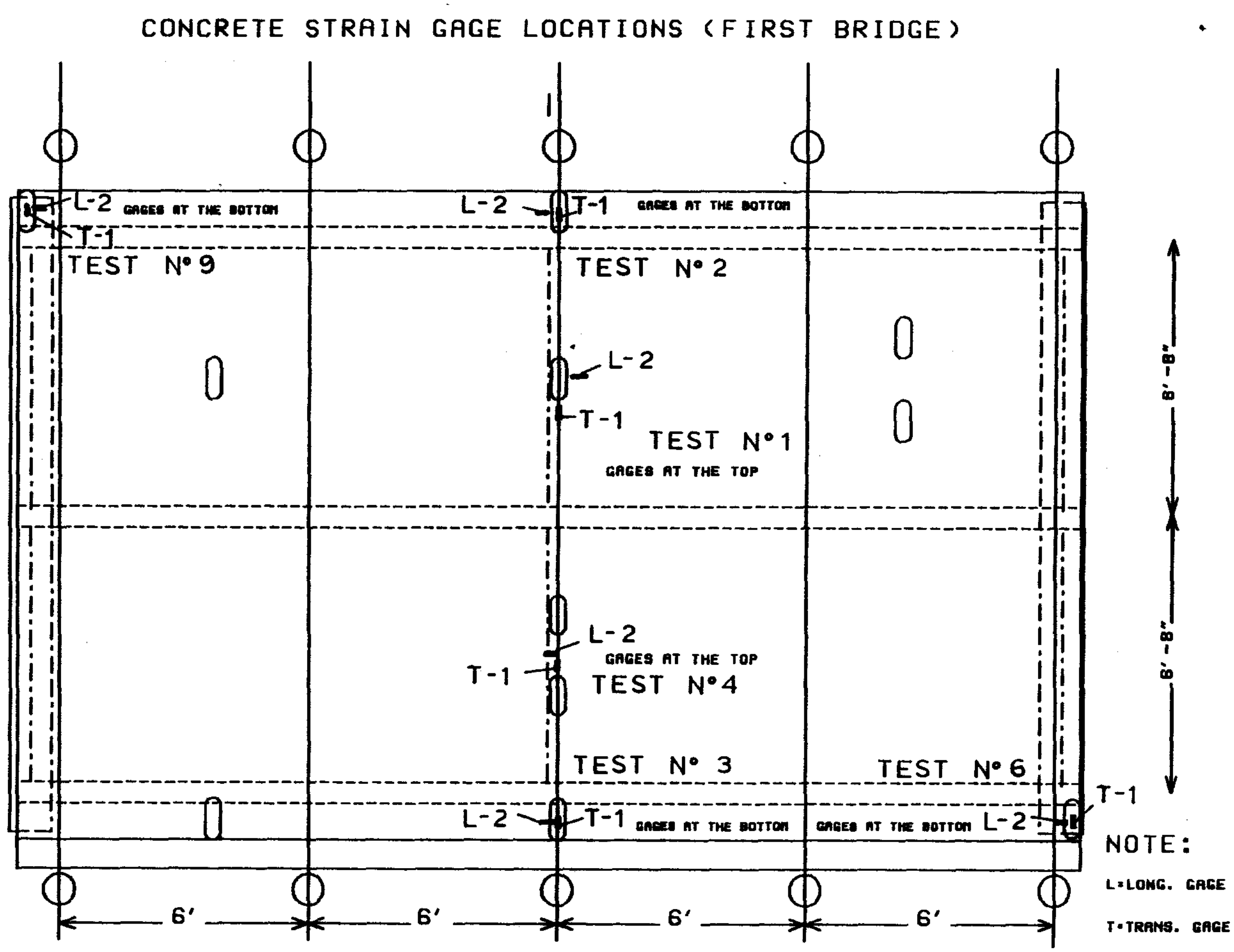

Figure C.1 Concrete Strain Gage Locations (First Bridge)

CONCRETE STRAIN GAGE LOCATIONS (SECOND BRIDGE)

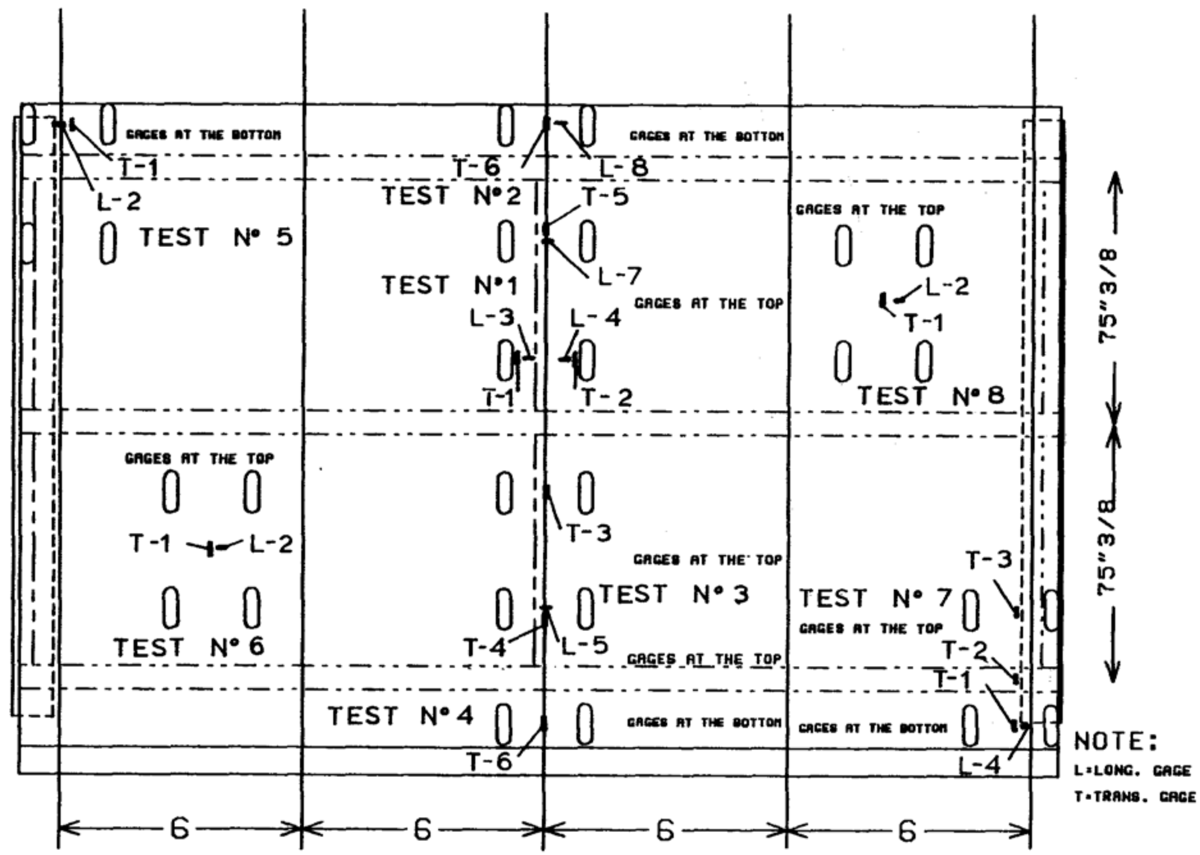

Figure C.3 Concrete Strain Gage Locations (Second Bridge)

REINFORCEMENT STEEL STRAIN GAGE LOCATIONS (SECOND BRIDGE)

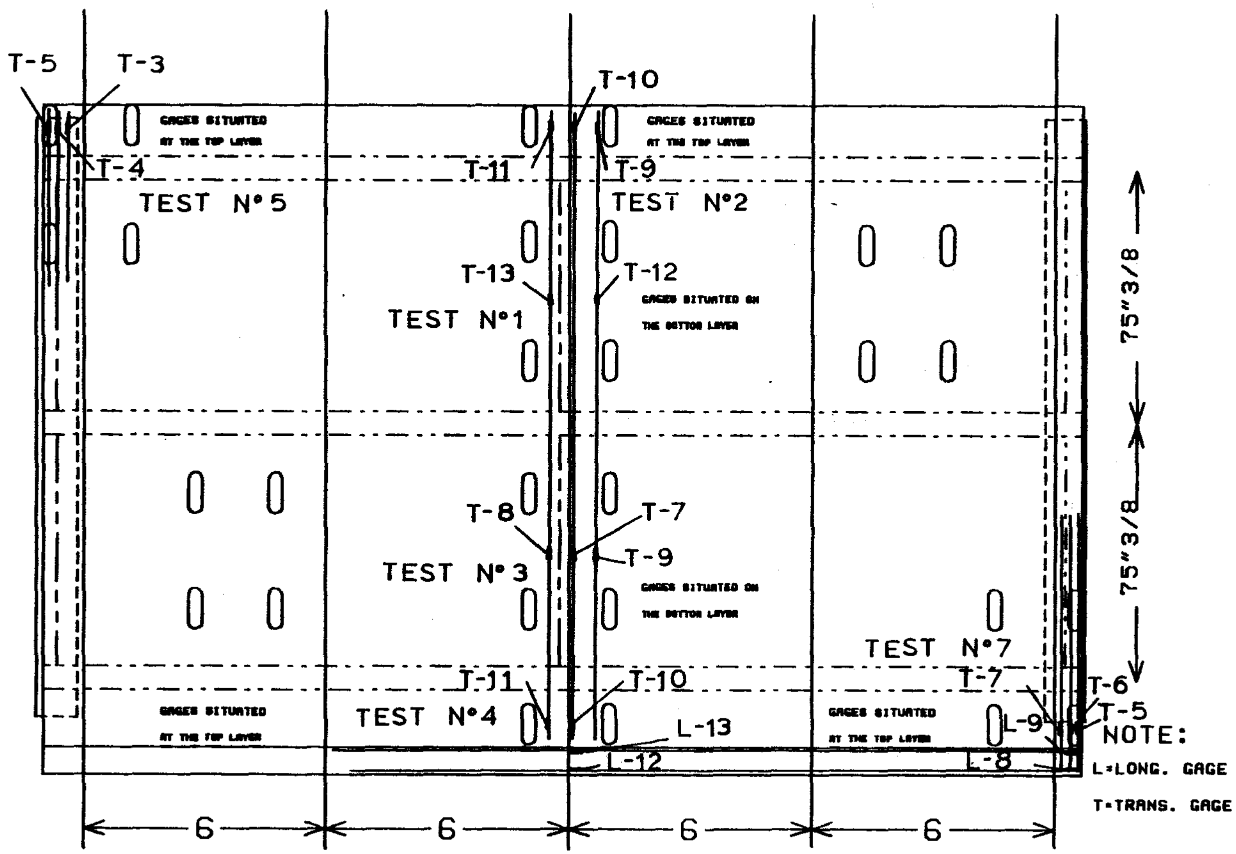

Figure C.4 Reinforcement Steel Strain Gage Locations (Second Bridge)

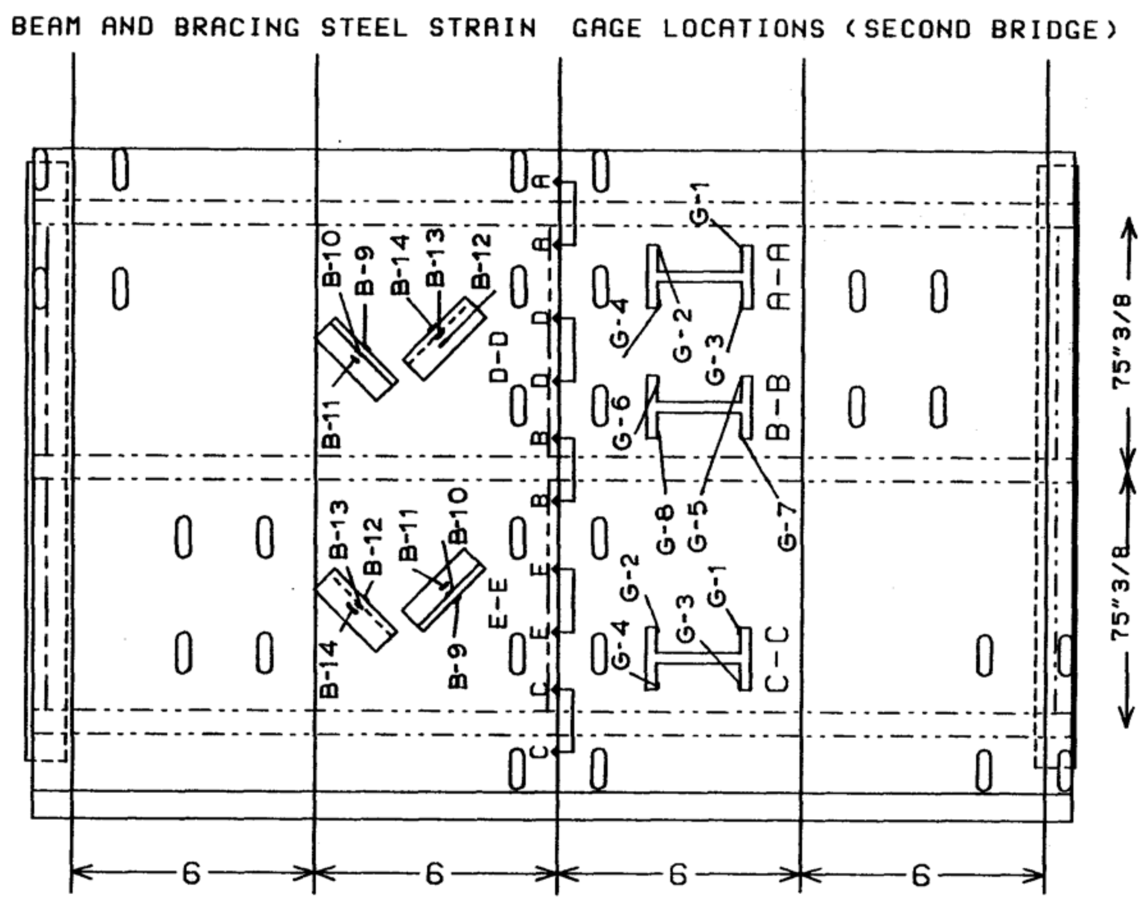

Figure C.5 Beam and Bracing Steel Strain Gage Locations (Second Bridge)

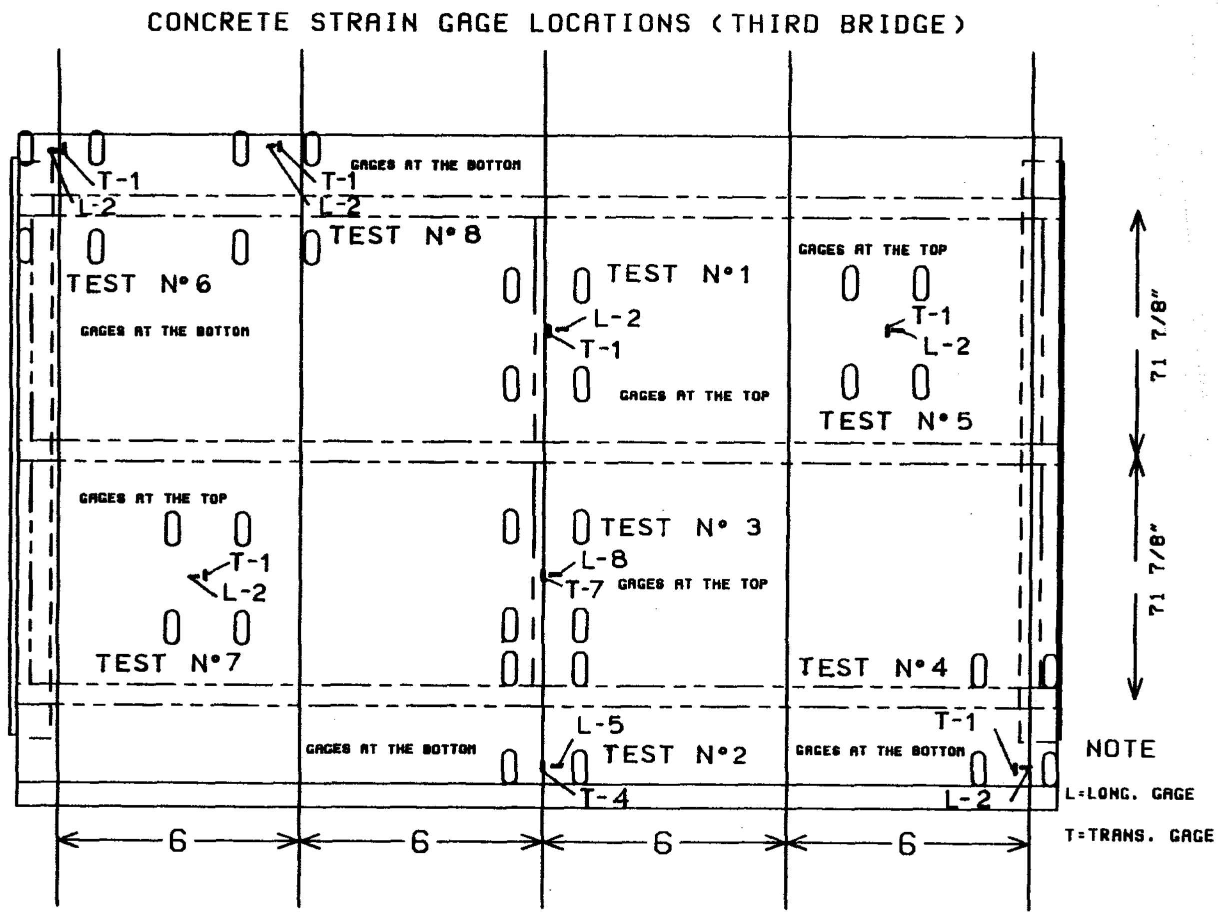

Figure C.6 Concrete Strain Gage Locations (Third Bridge)

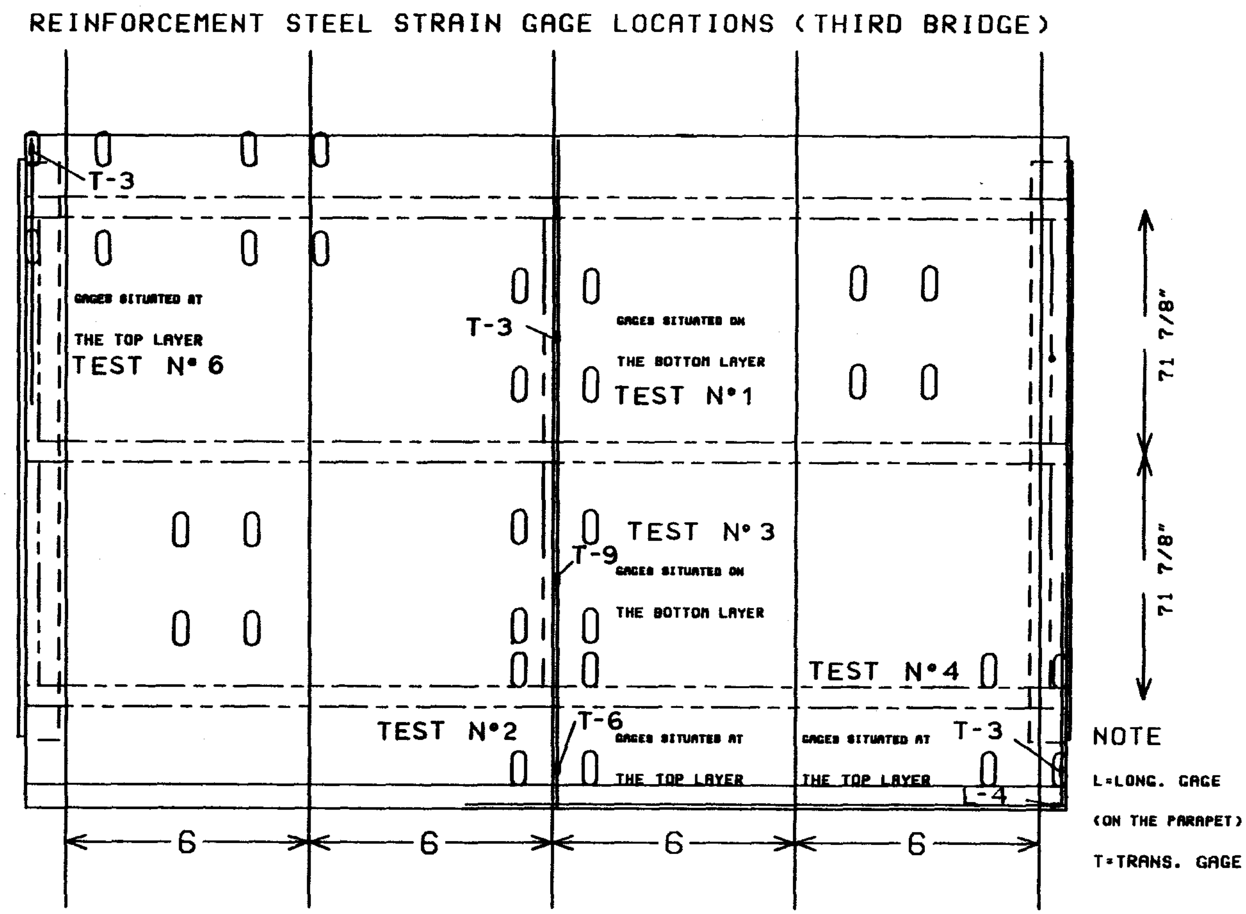

Figure C.7 Reinforcement Steel Strain Gage Locations (Third Bridge)

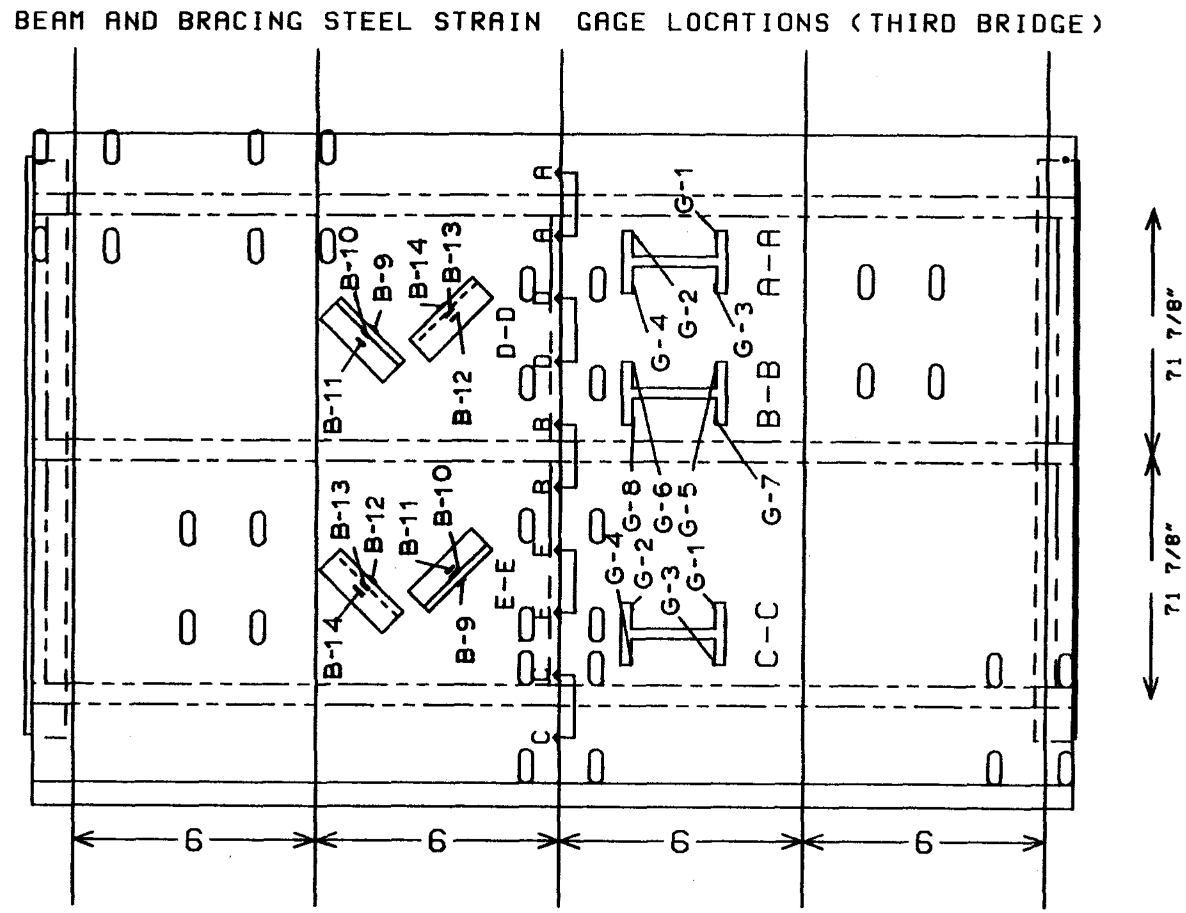

Figure C.8 Beam and Bracing Steel Strain Gage Locations (Third Bridge)

APPENDIX D

Strain Gage Plots

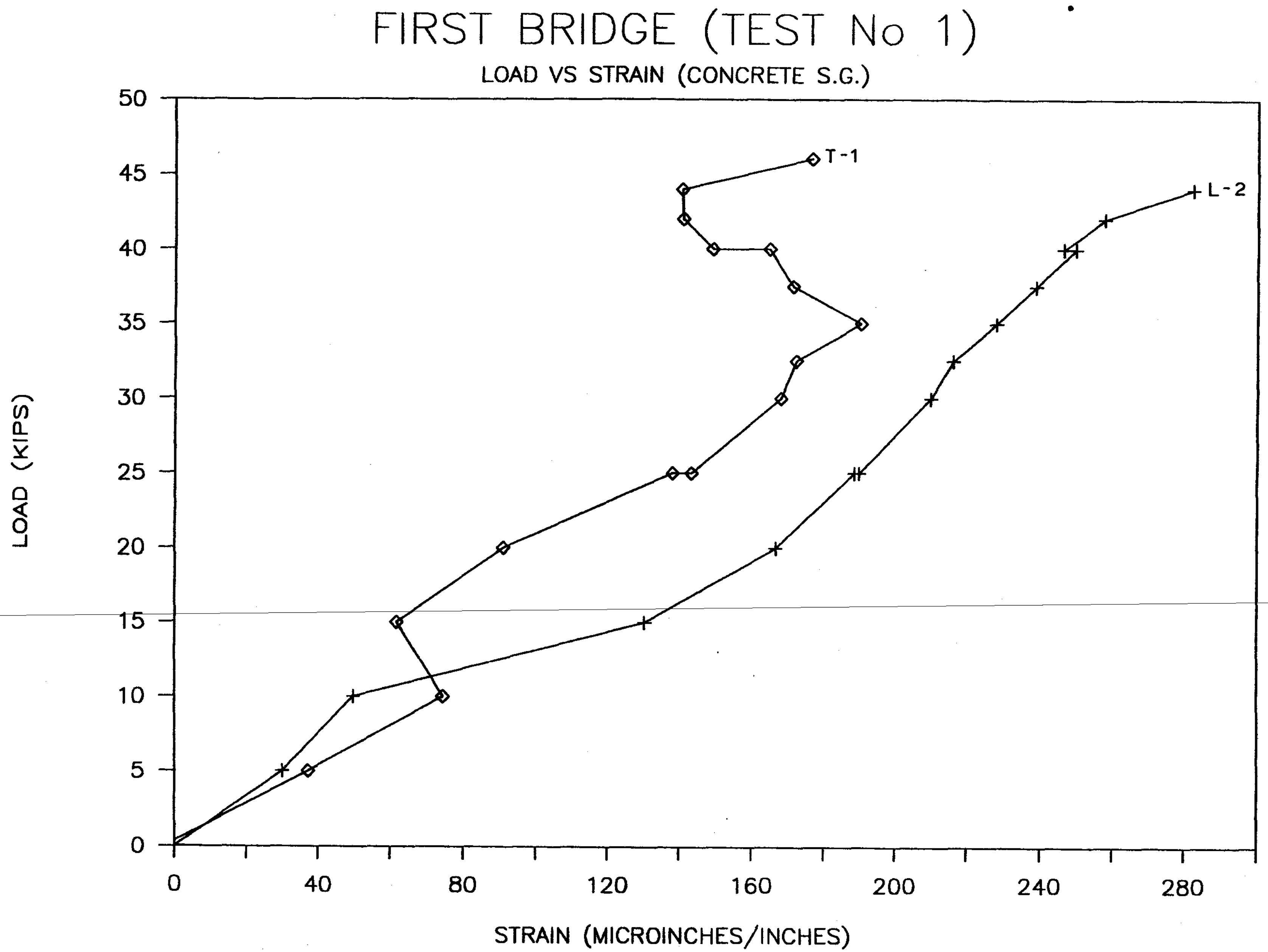

Figure D.1 Load-Strain Curves (First Bridge, Test No. 1, Concrete S.G.)

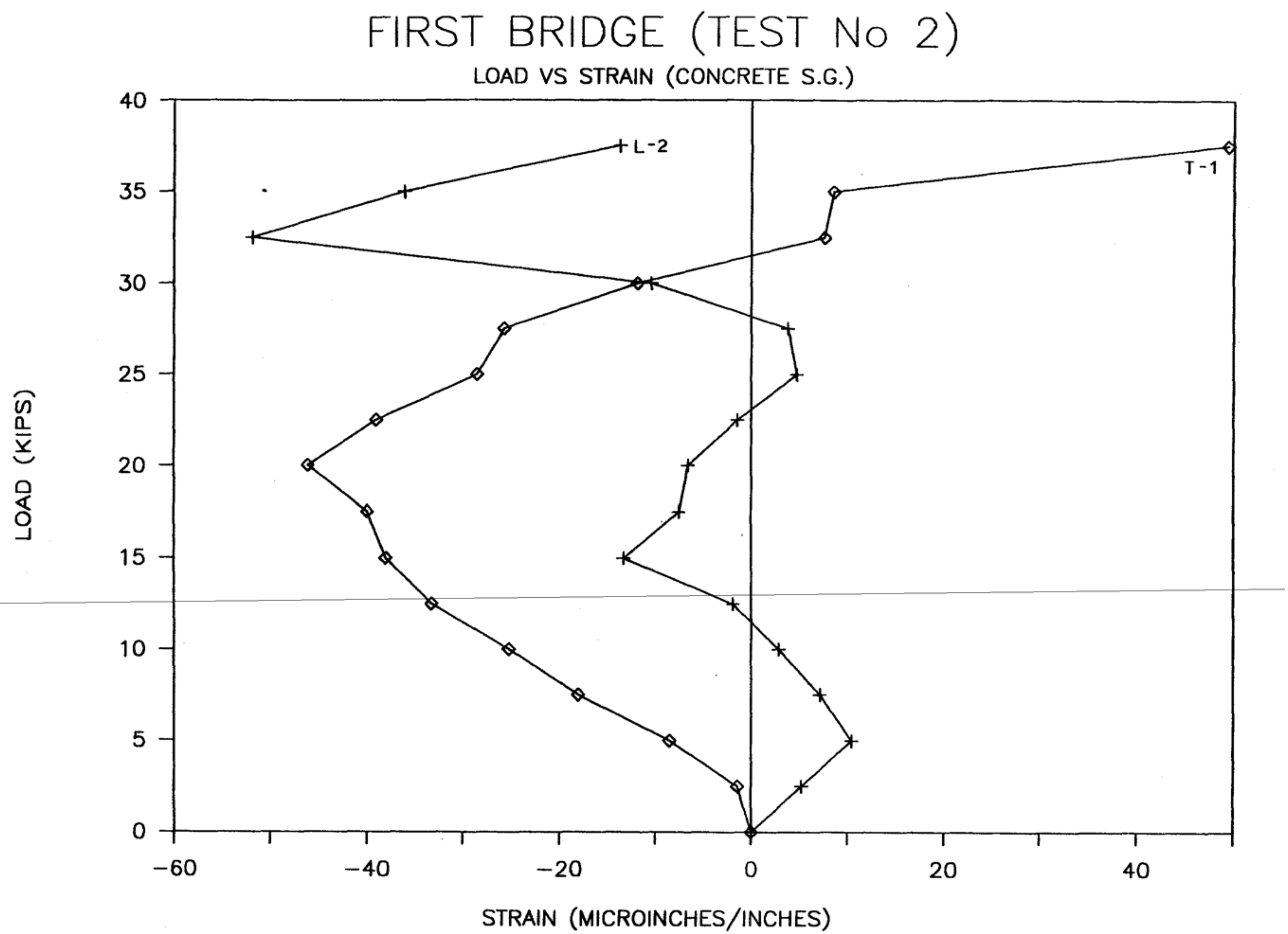

Figure D.2 Load-Strain Curves (First Bridge, Test No. 2, Concrete S.G.)

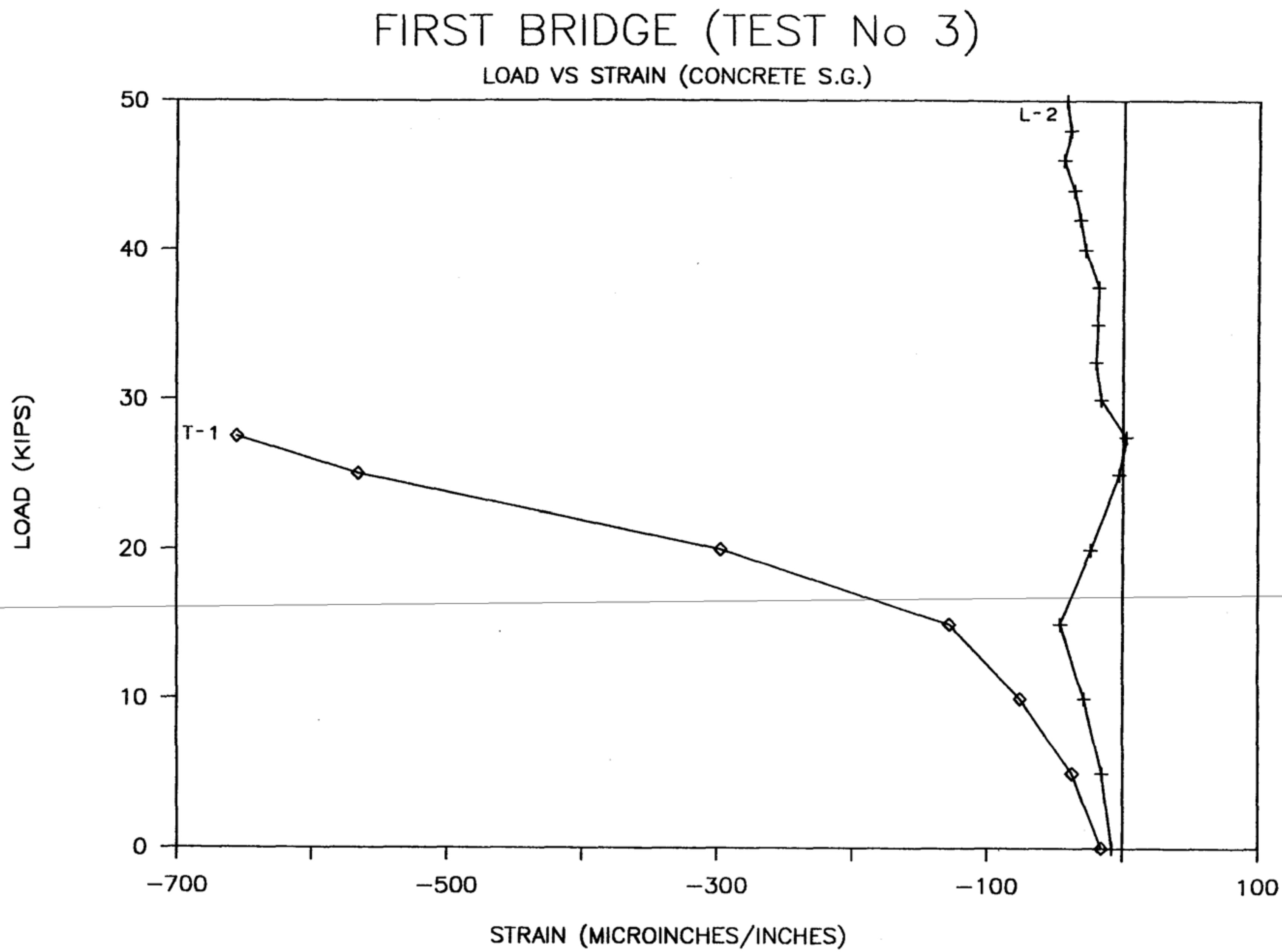

Figure D.3 Load-Strain Curves (First Bridge, Test No. 3, Concrete S.G.)

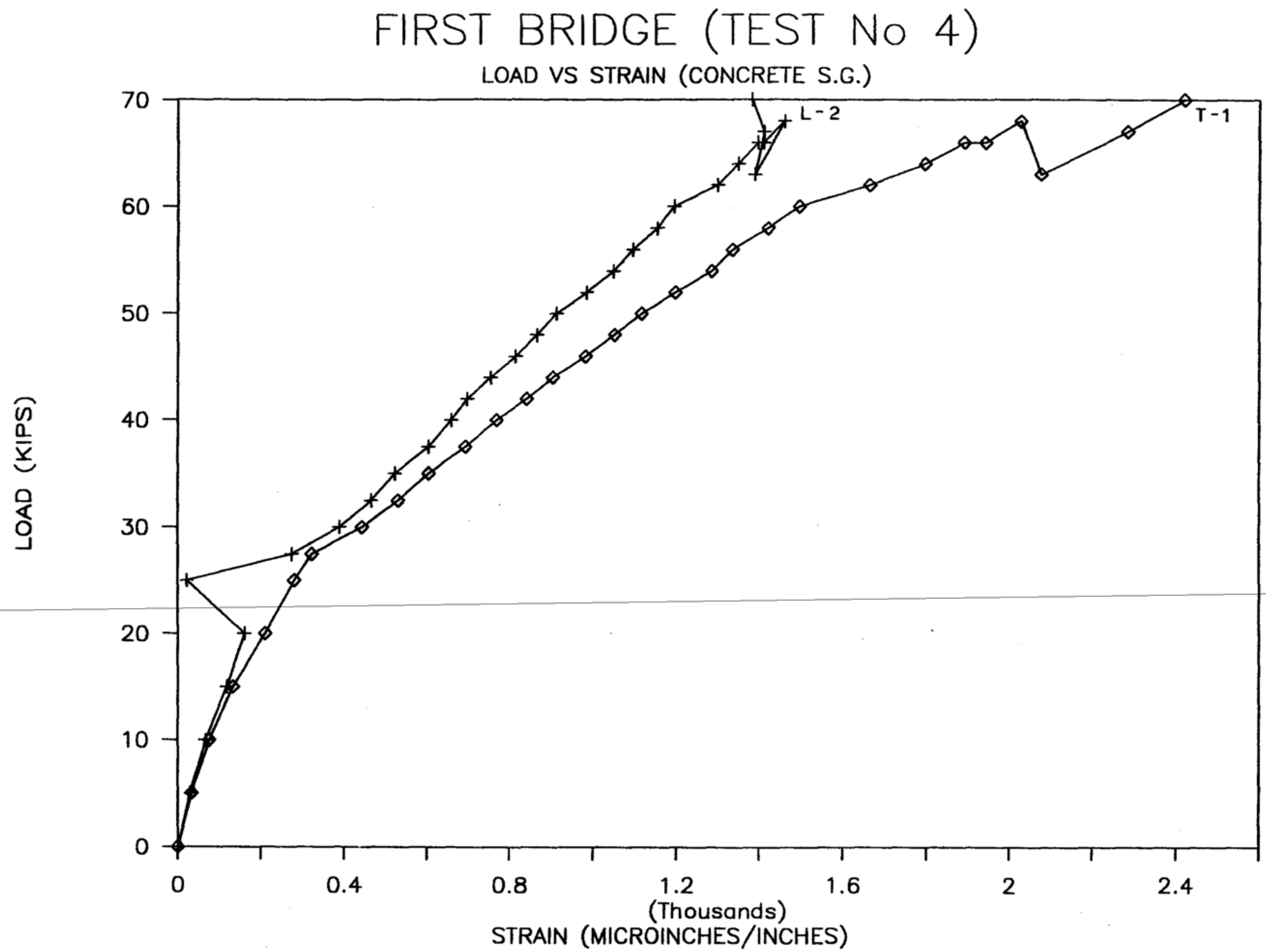

Figure D.4 Load-Strain Curves (First Bridge, Test No. 4, Concrete S.G.)

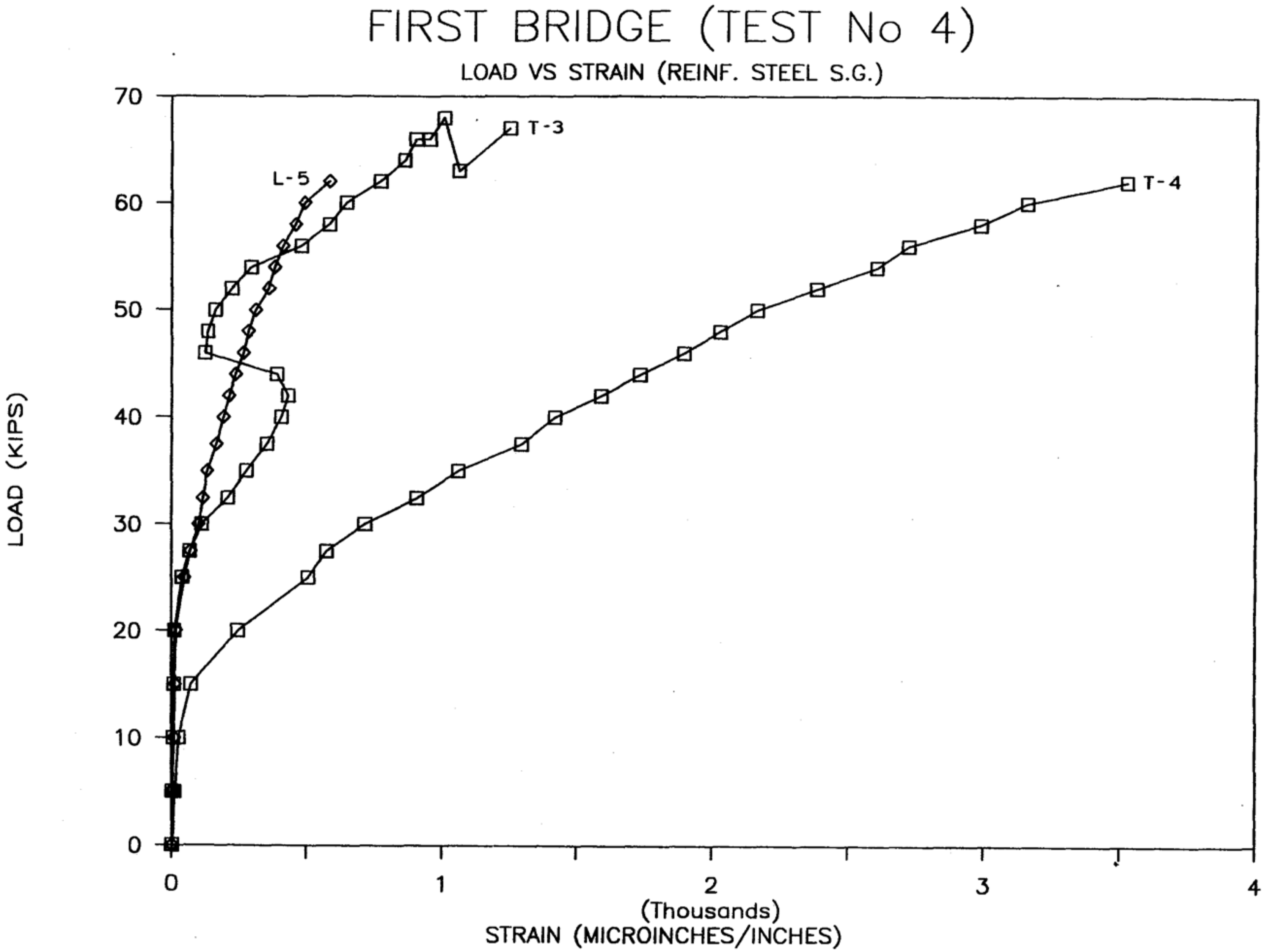

Figure D.5 Load-Strain Curves (First Bridge, Test No. 4, Reinforced Steel S.G.)

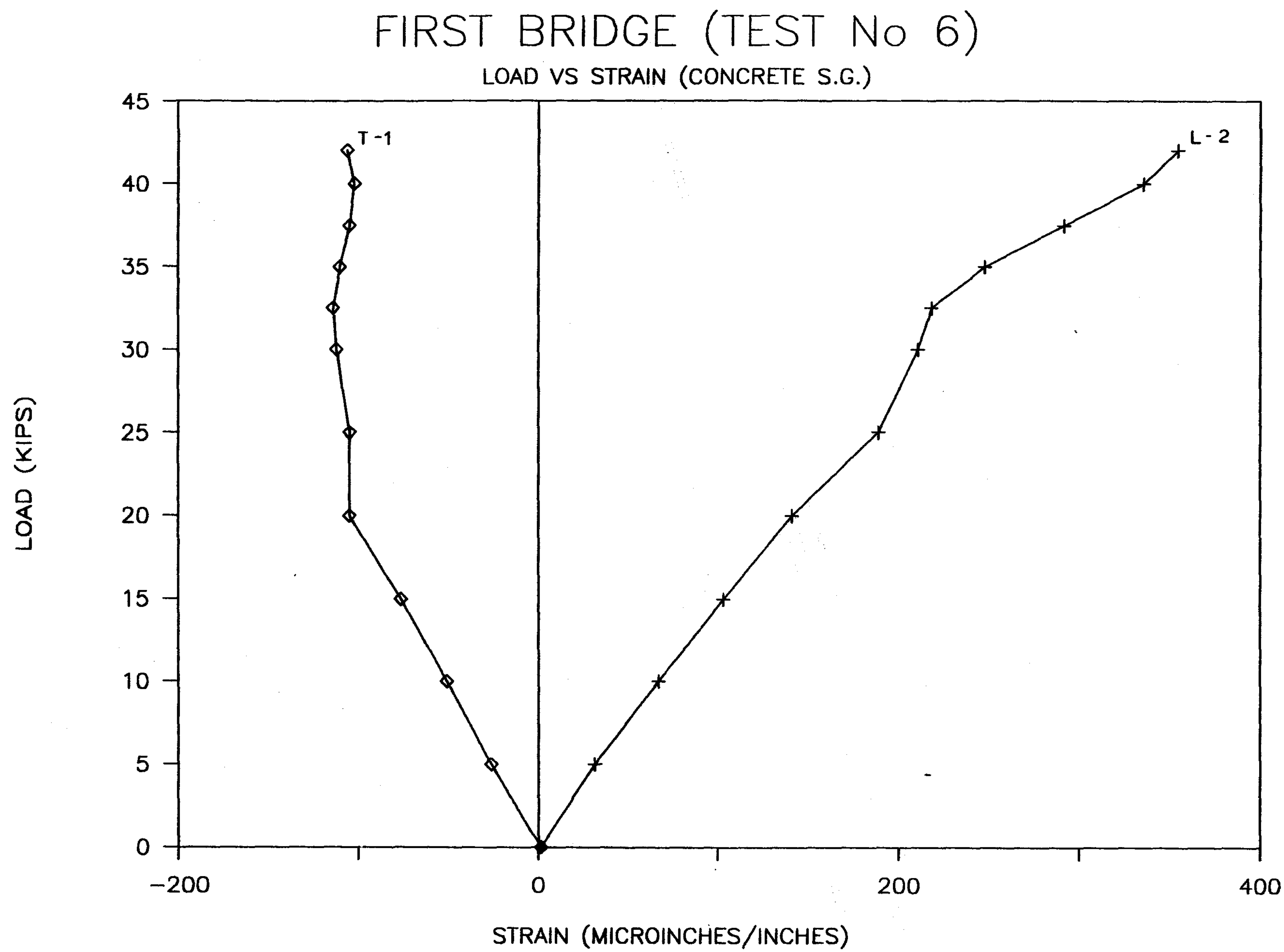

Figure D.6 Load-Strain Curves (First Bridge, Test No. 6, Concrete S.G.)

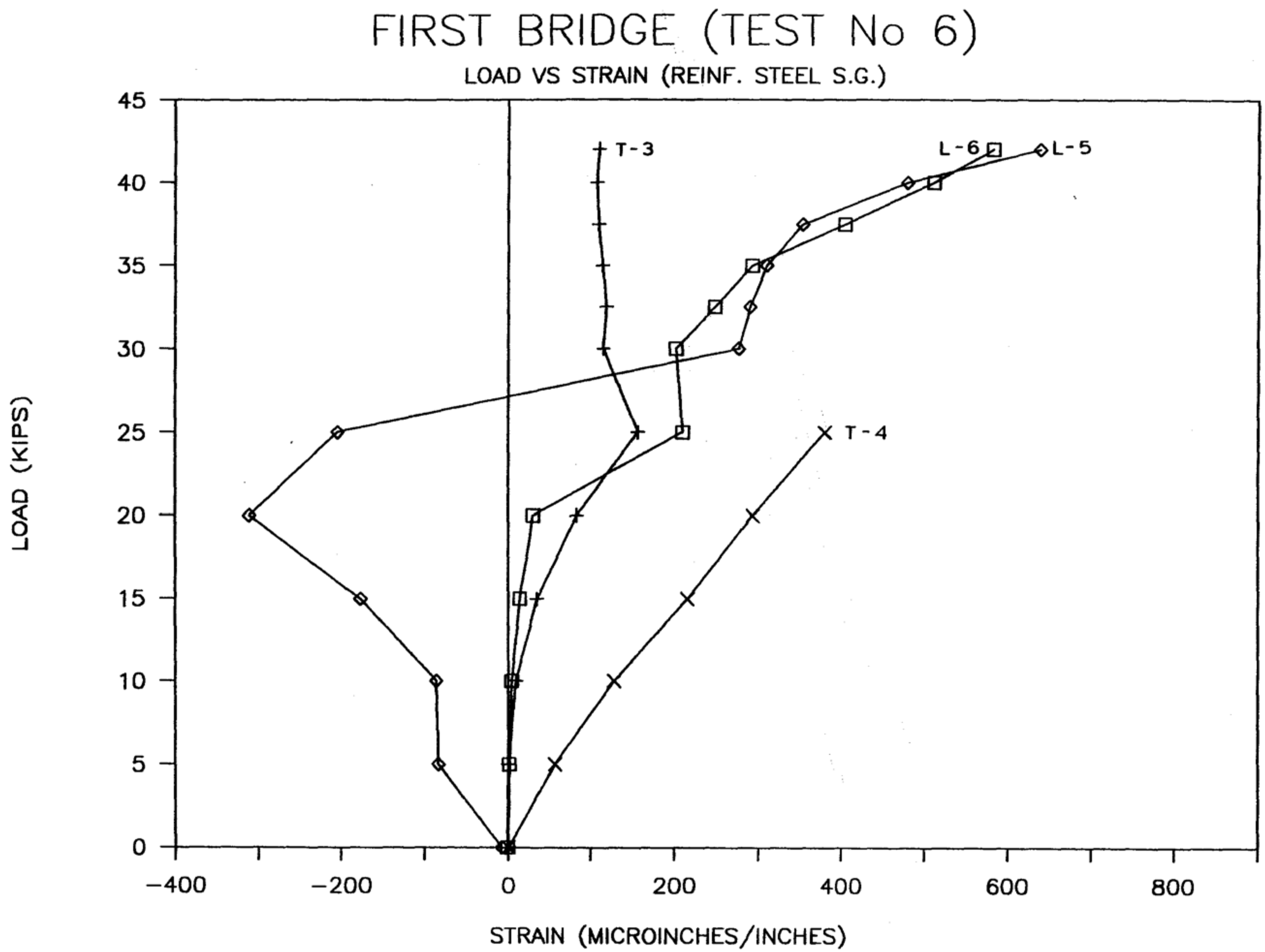

Figure D.7 Load-Strain Curves (First Bridge, Test No. 6, Reinforced Steel S.G.)

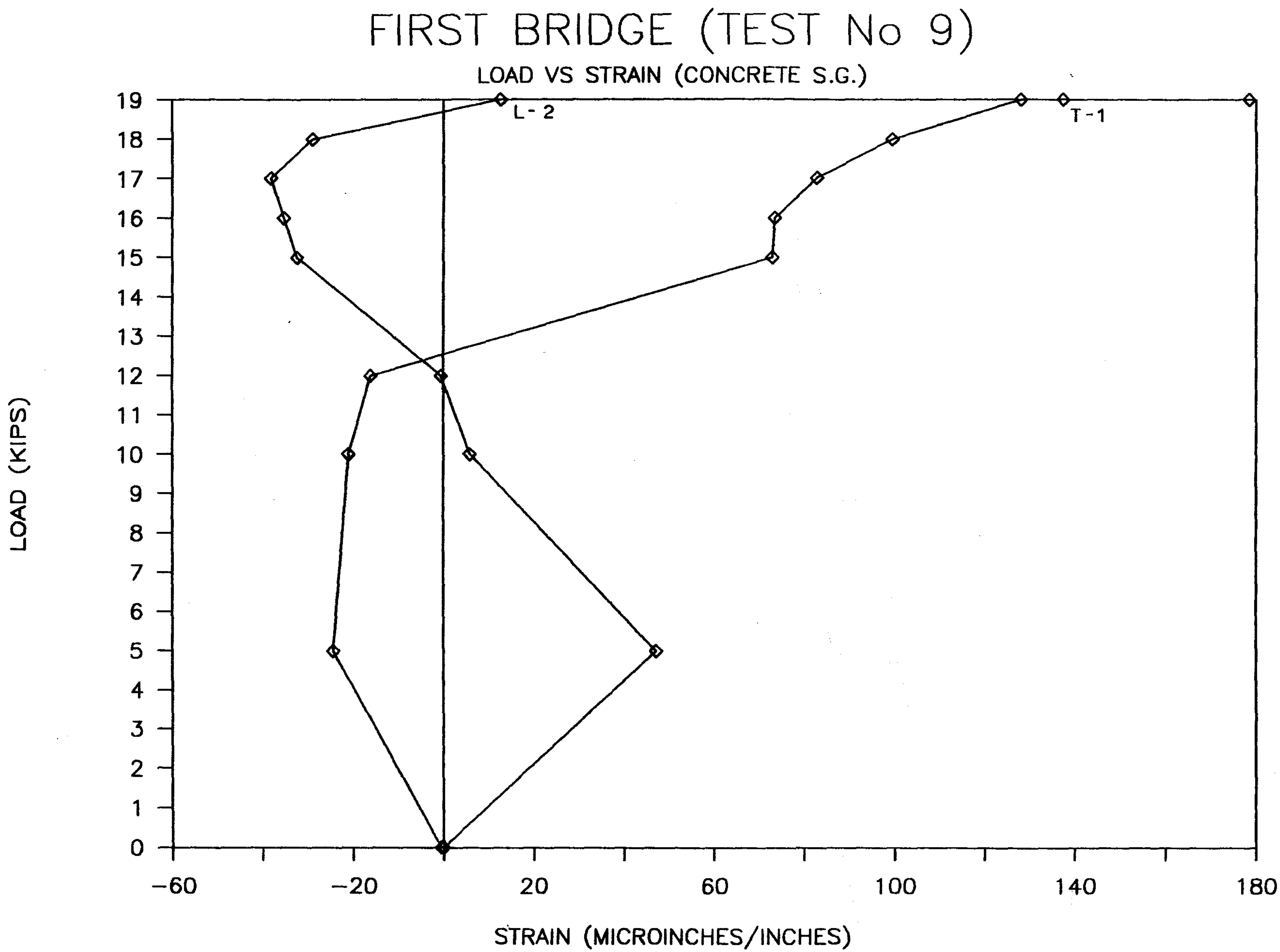

Figure D.8 Load-Strain Curves (First Bridge, Test No. 9, Concrete S.G.)

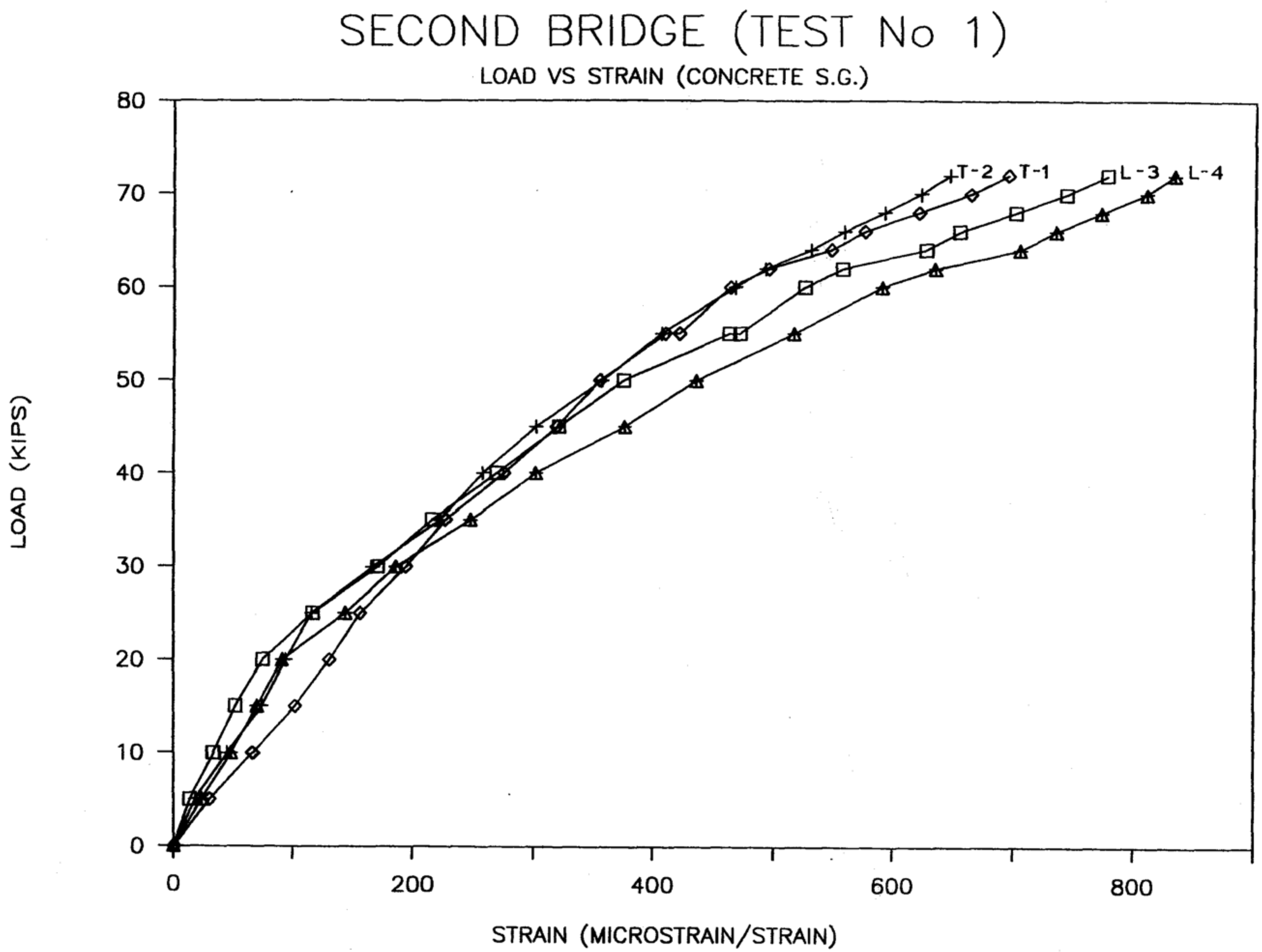

Figure D.9 Load-Strain Curves (Second Bridge, Test No. 1, Concrete S.G.)

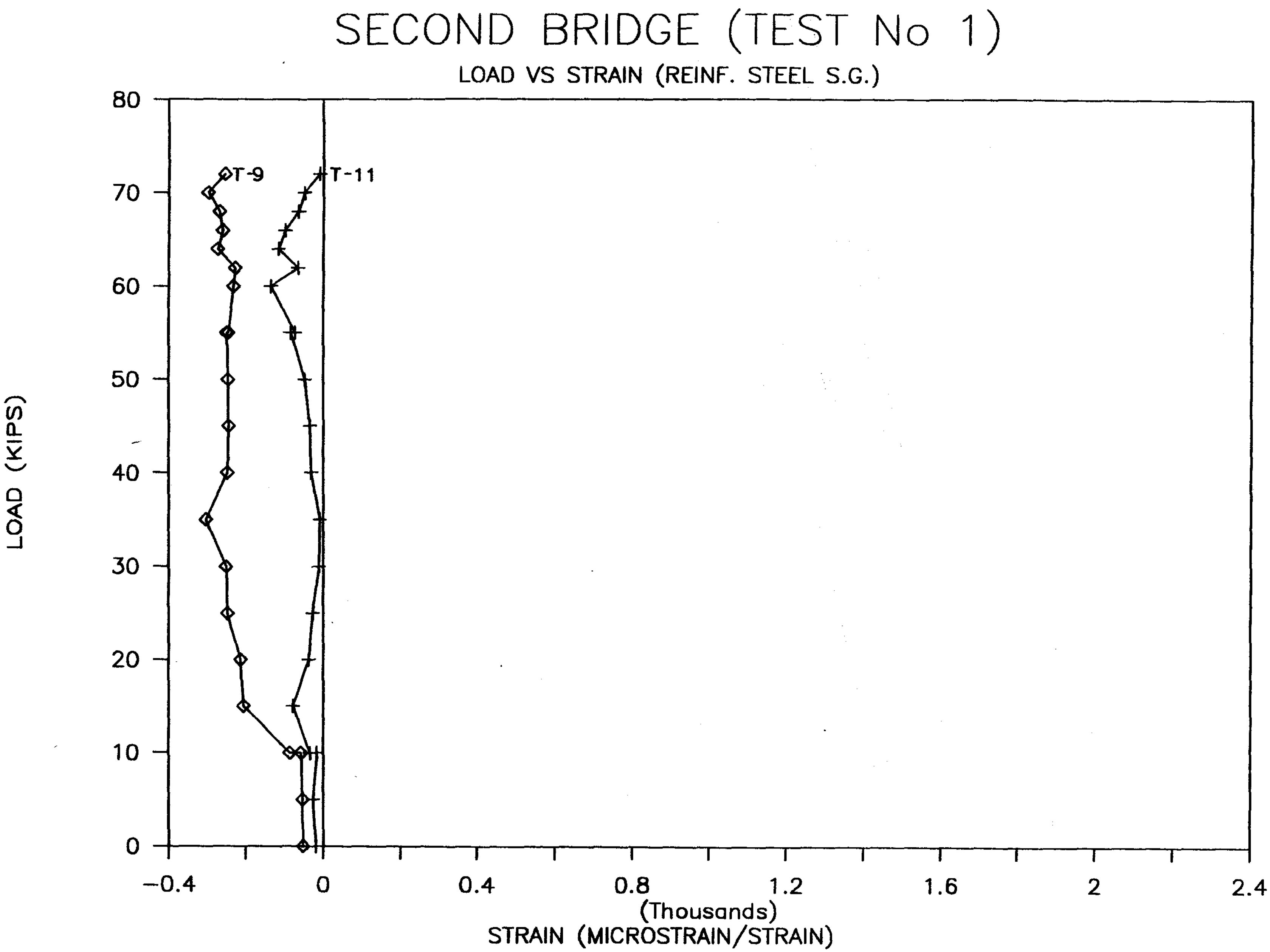

Figure D.10 Load-Strain Curves (Second Bridge, Test No. 1, Reinforced Steel S.G.)

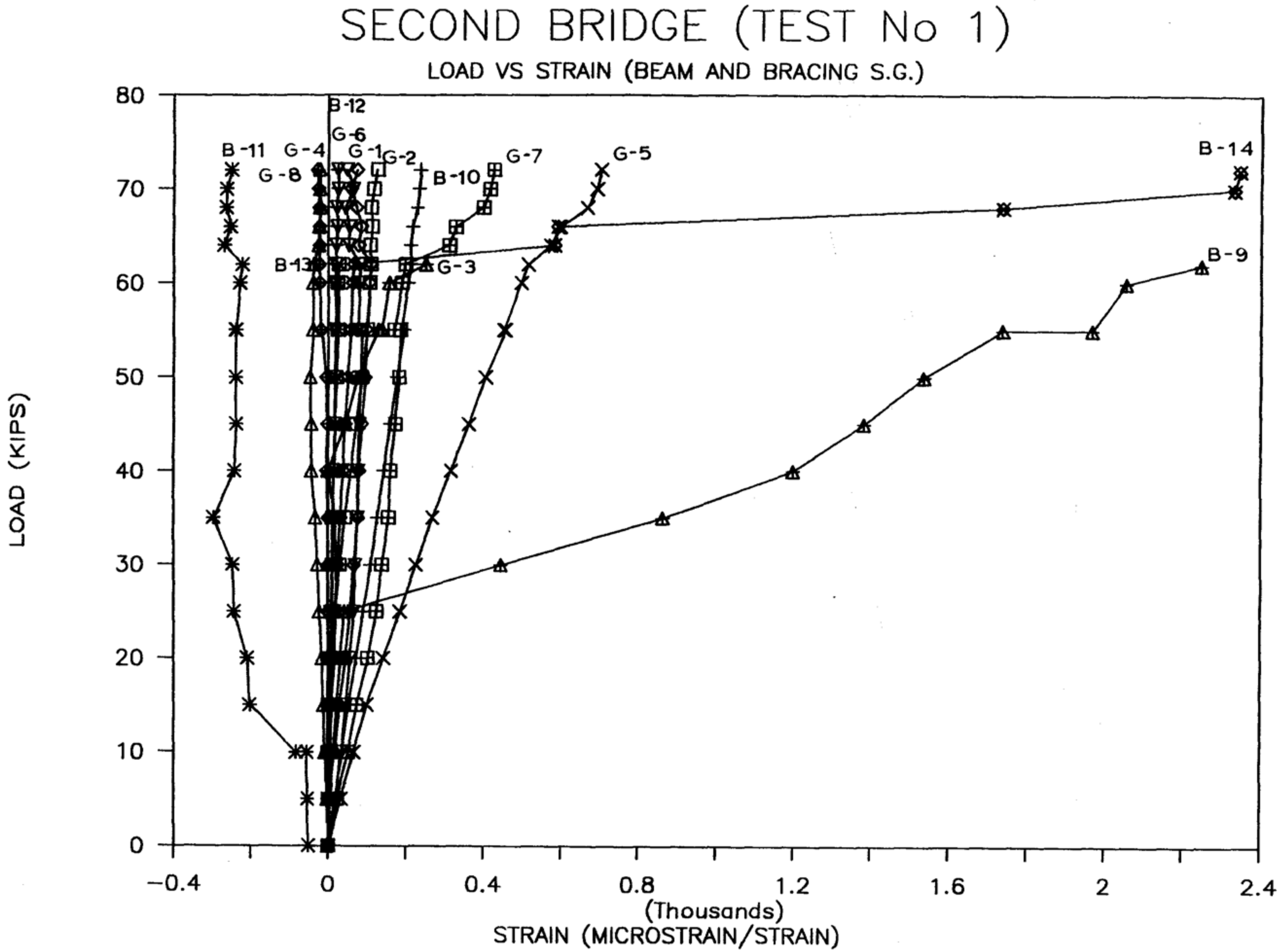

Figure D.11 Load-Strain Curves (Second Bridge, Test No. 1, Beam and Bracing S.G.)

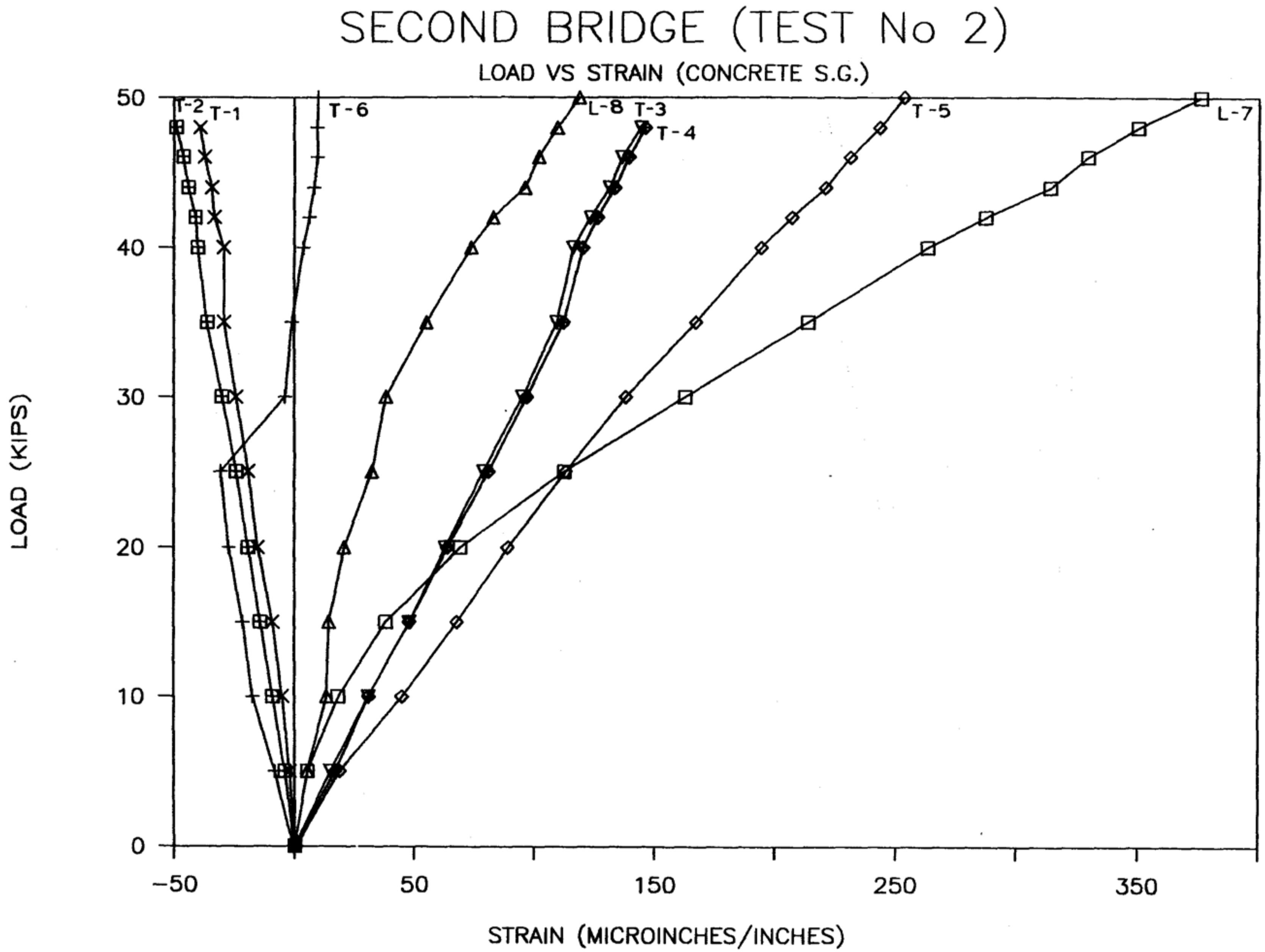

Figure D.12 Load-Strain Curves (Second Bridge, Test No. 2, Concrete S.G.)

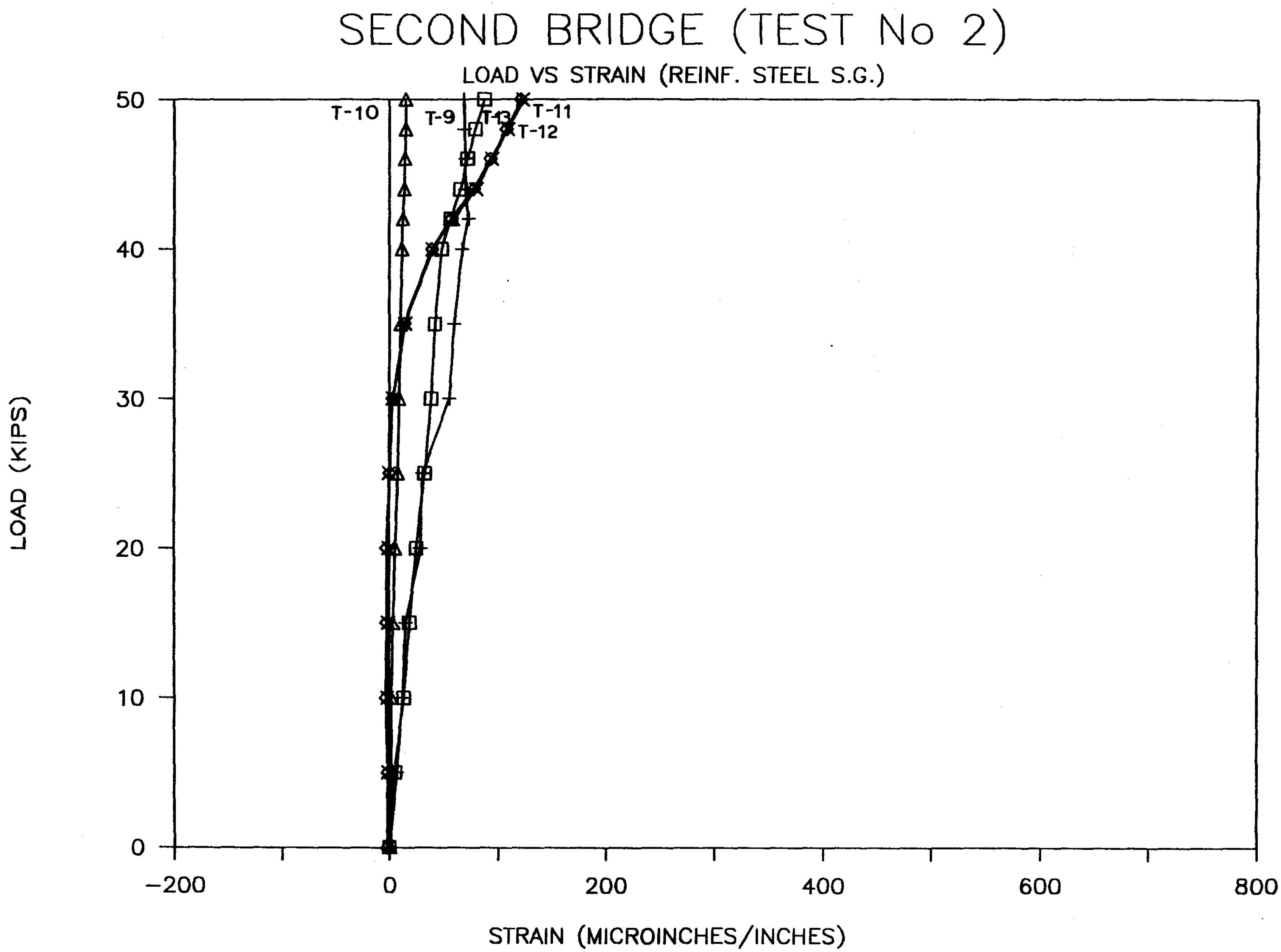

Figure D.13 Load-Strain Curves (Second Bridge, Test No. 2, Reinforced Steel S.G.)

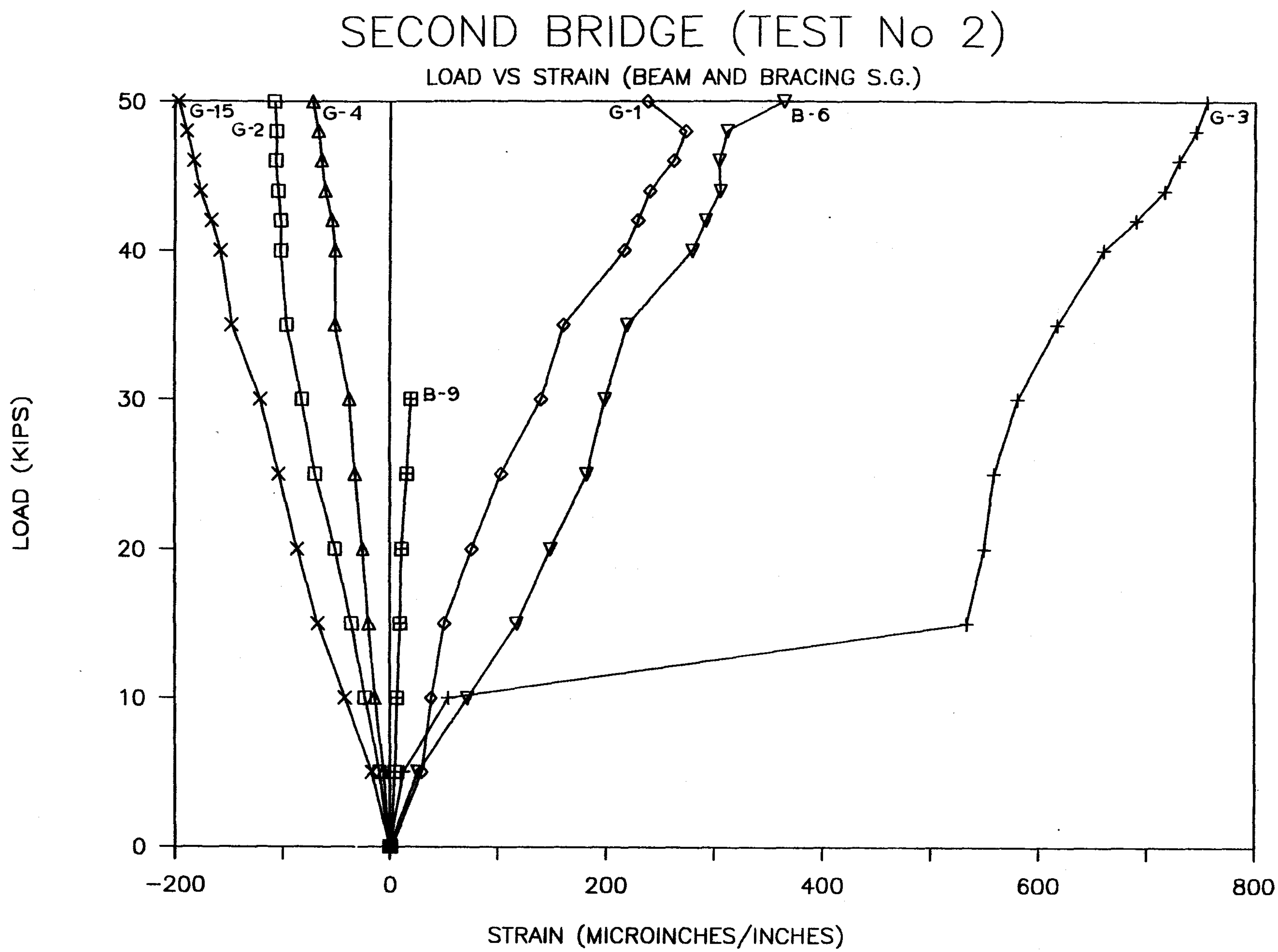

Figure D.14 Load-Strain Curves (Second Bridge, Test No. 2, Beam and Bracing S.G.)

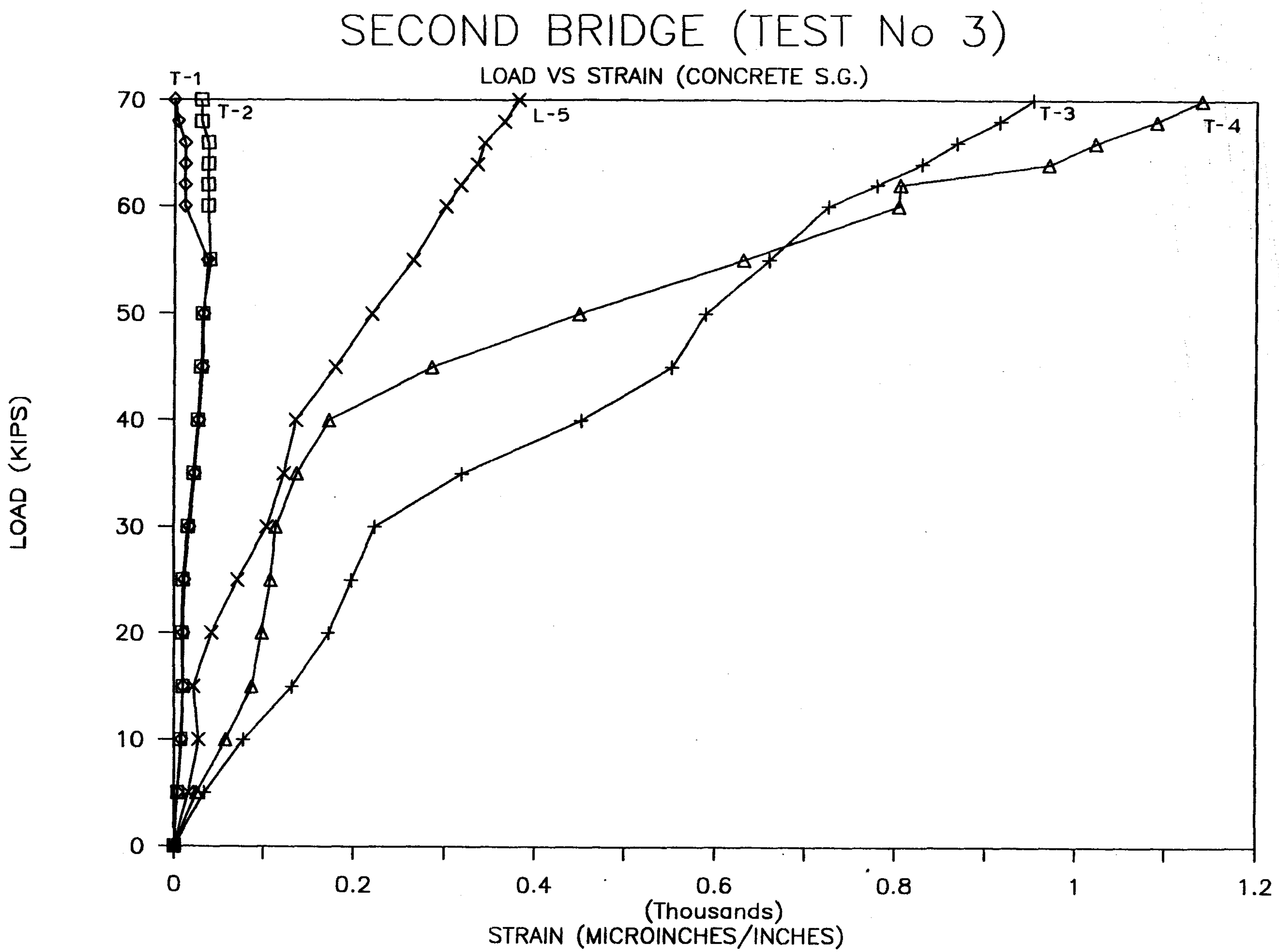

Figure D.15 Load-Strain Curves (Second Bridge, Test No. 3, Concrete S.G.)

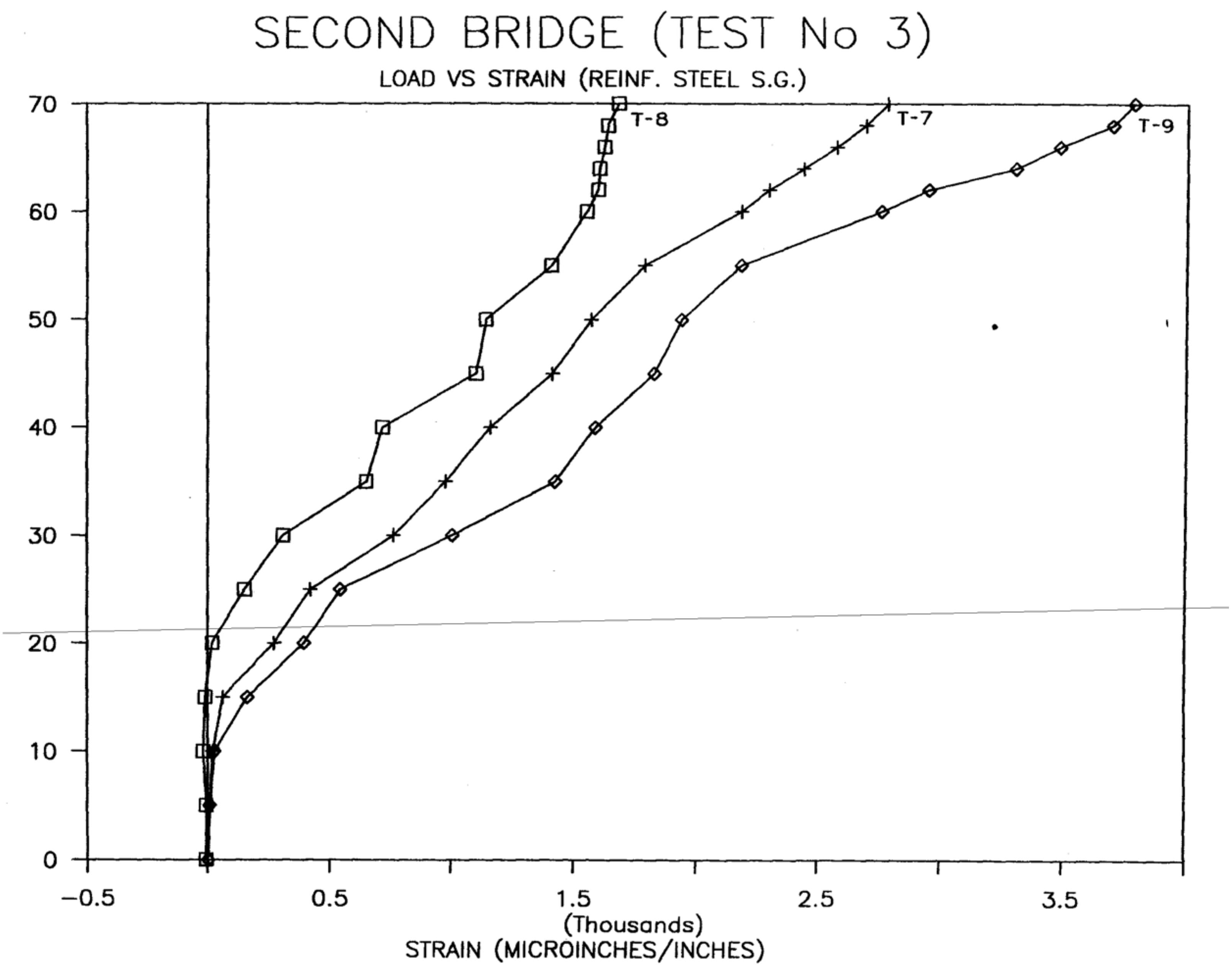

Figure D.16 Load-Strain Curves (Second Bridge, Test No. 3, Reinforced Steel S.G.)

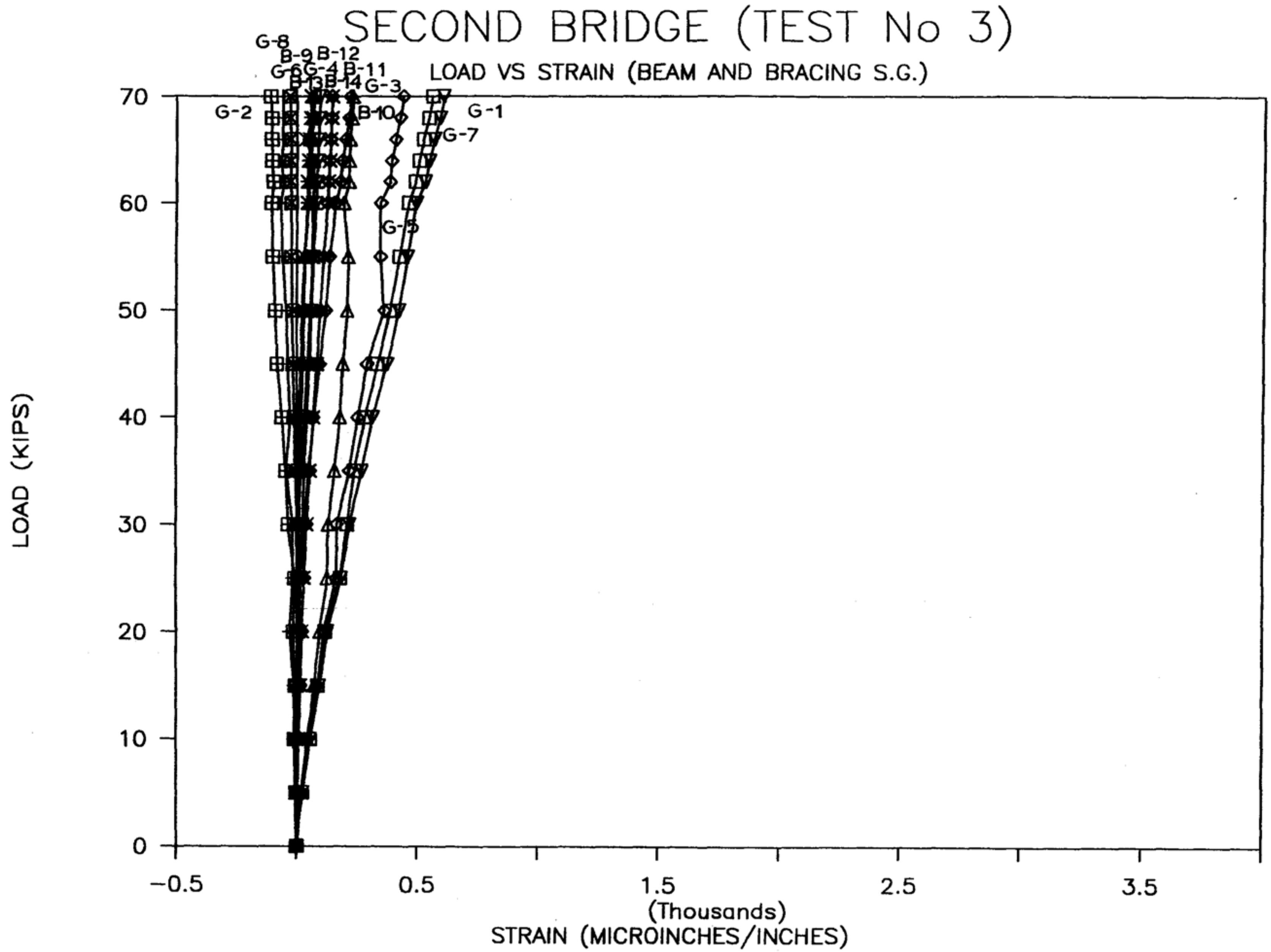

Figure D.17 Load-Strain Curves (Second Bridge, Test No. 3, Beam and Bracing S.G.)

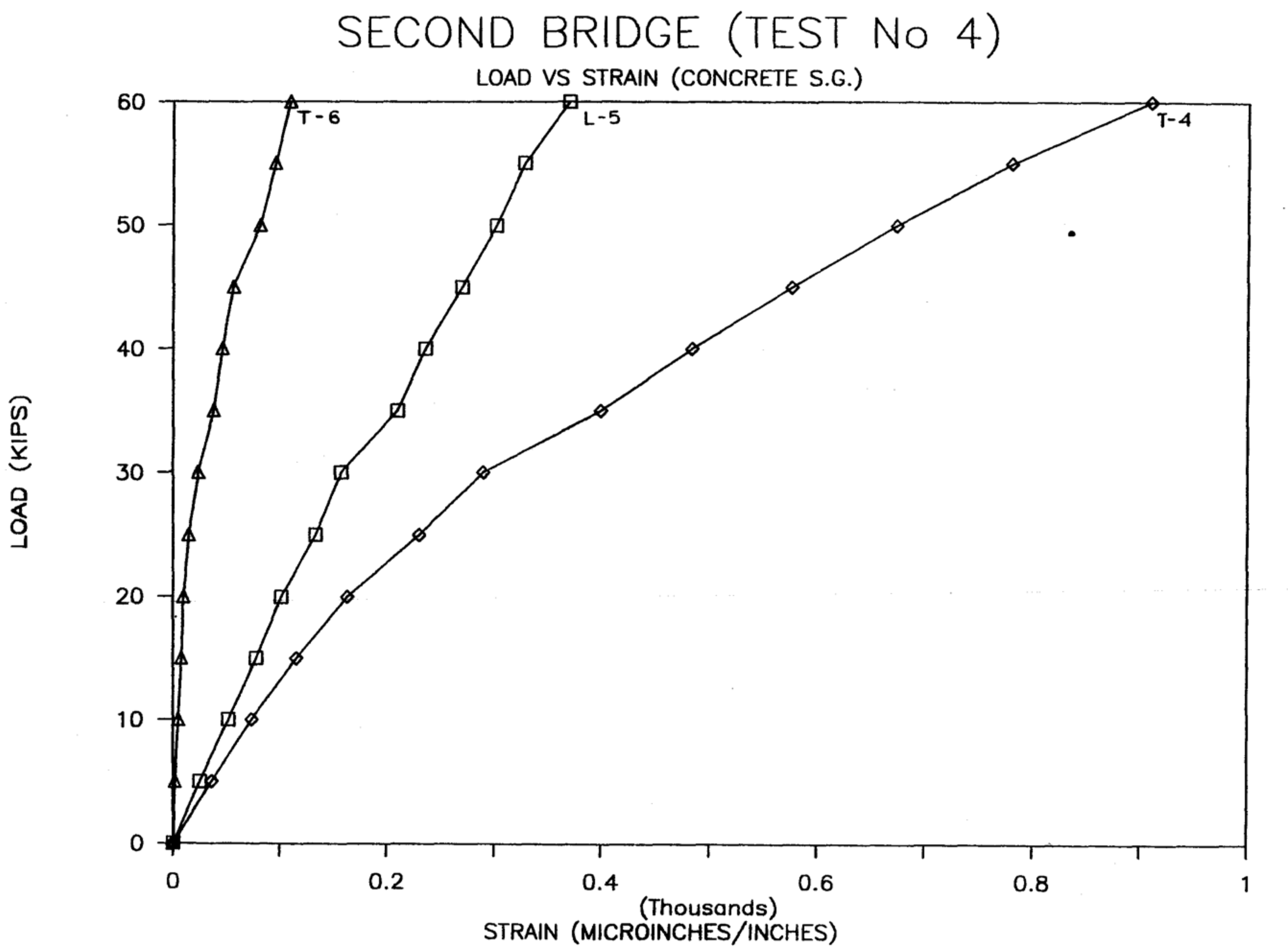

Figure D.18 Load-Strain Curves (Second Bridge, Test No. 4, Concrete S.G.)

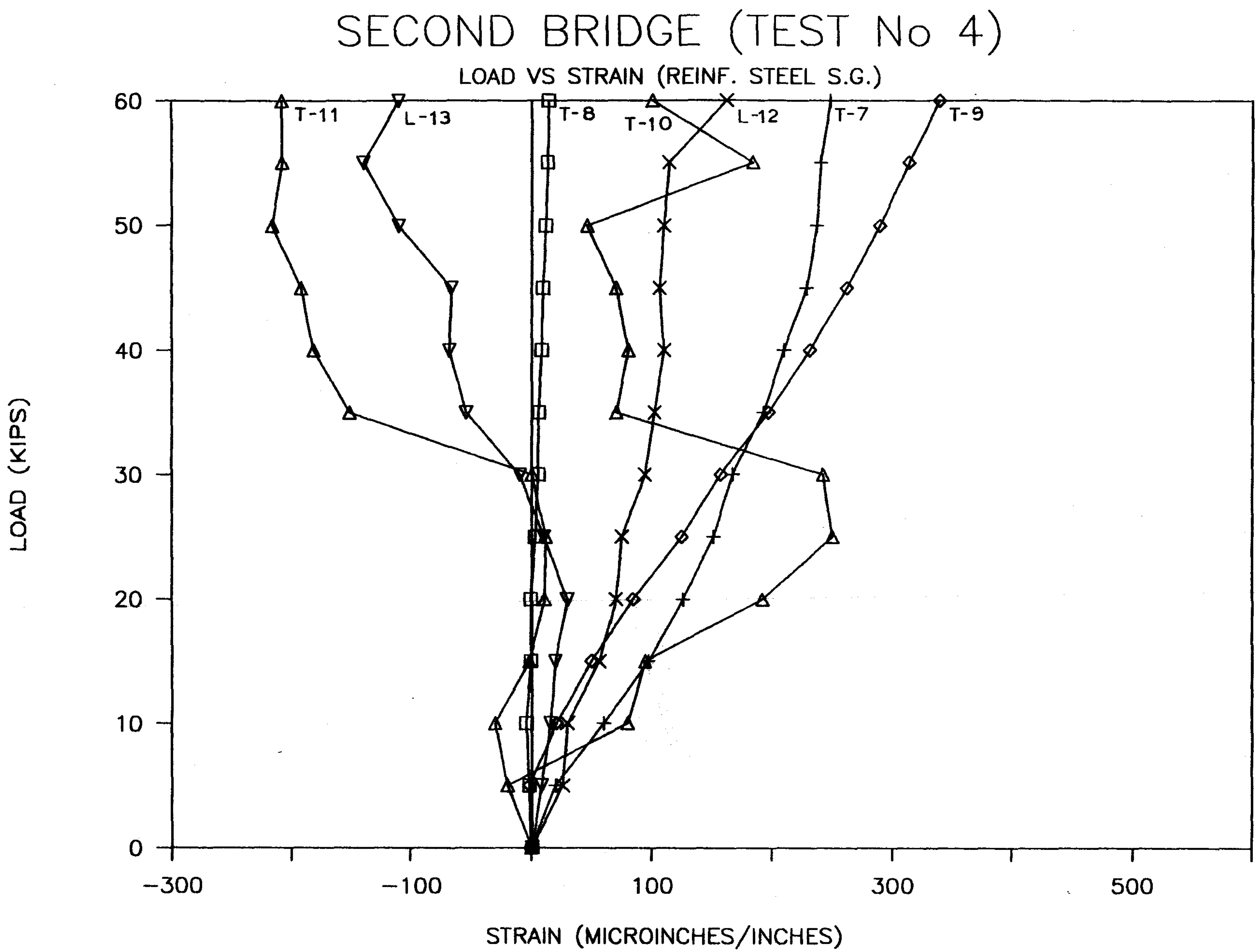

Figure D.19 Load-Strain Curves (Second Bridge, Test No. 4, Reinforced Steel S.G.)

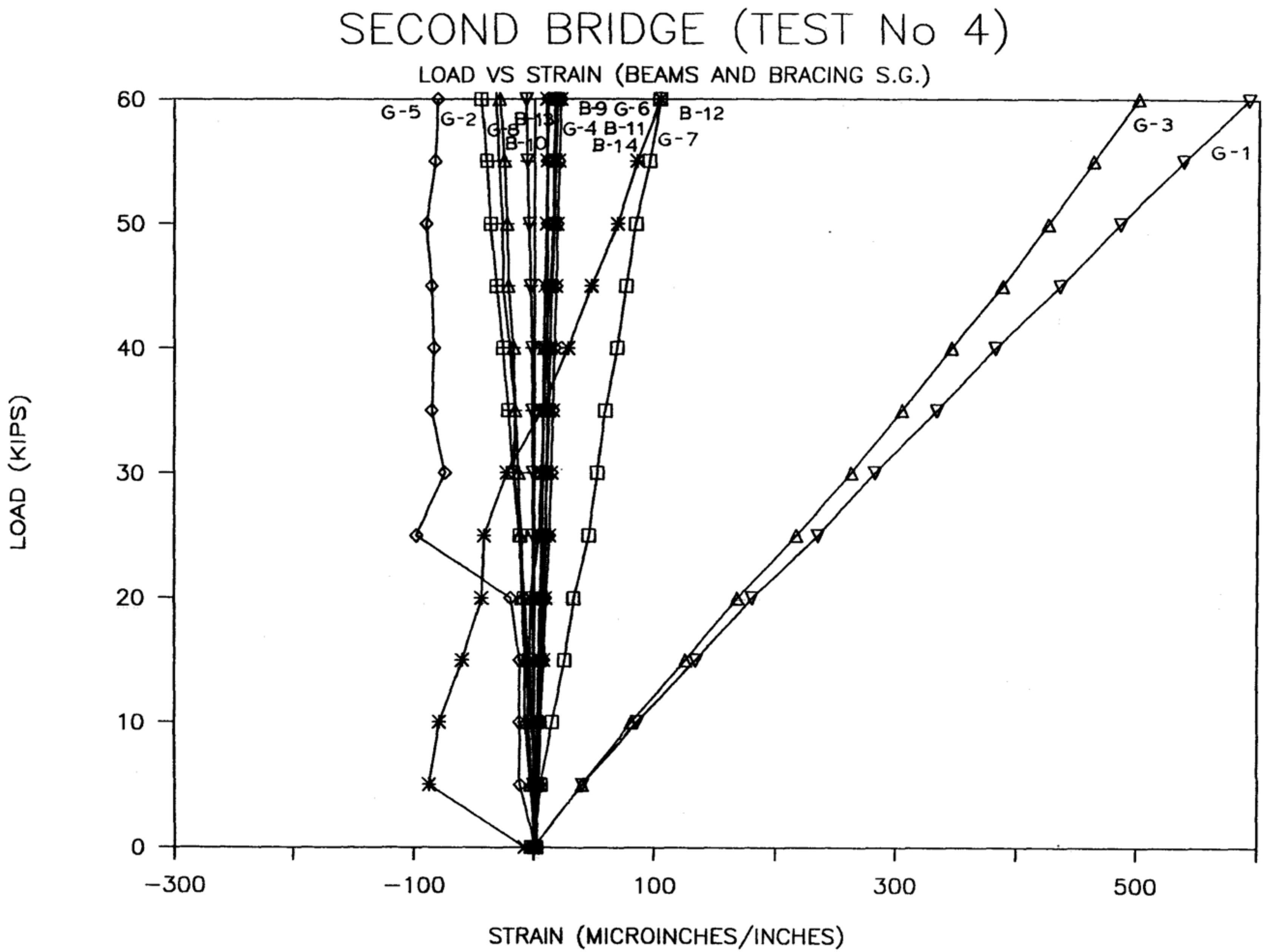

Figure D.20 Load-Strain Curves (Second Bridge, Test No. 4, Beams and Bracing S.G.)

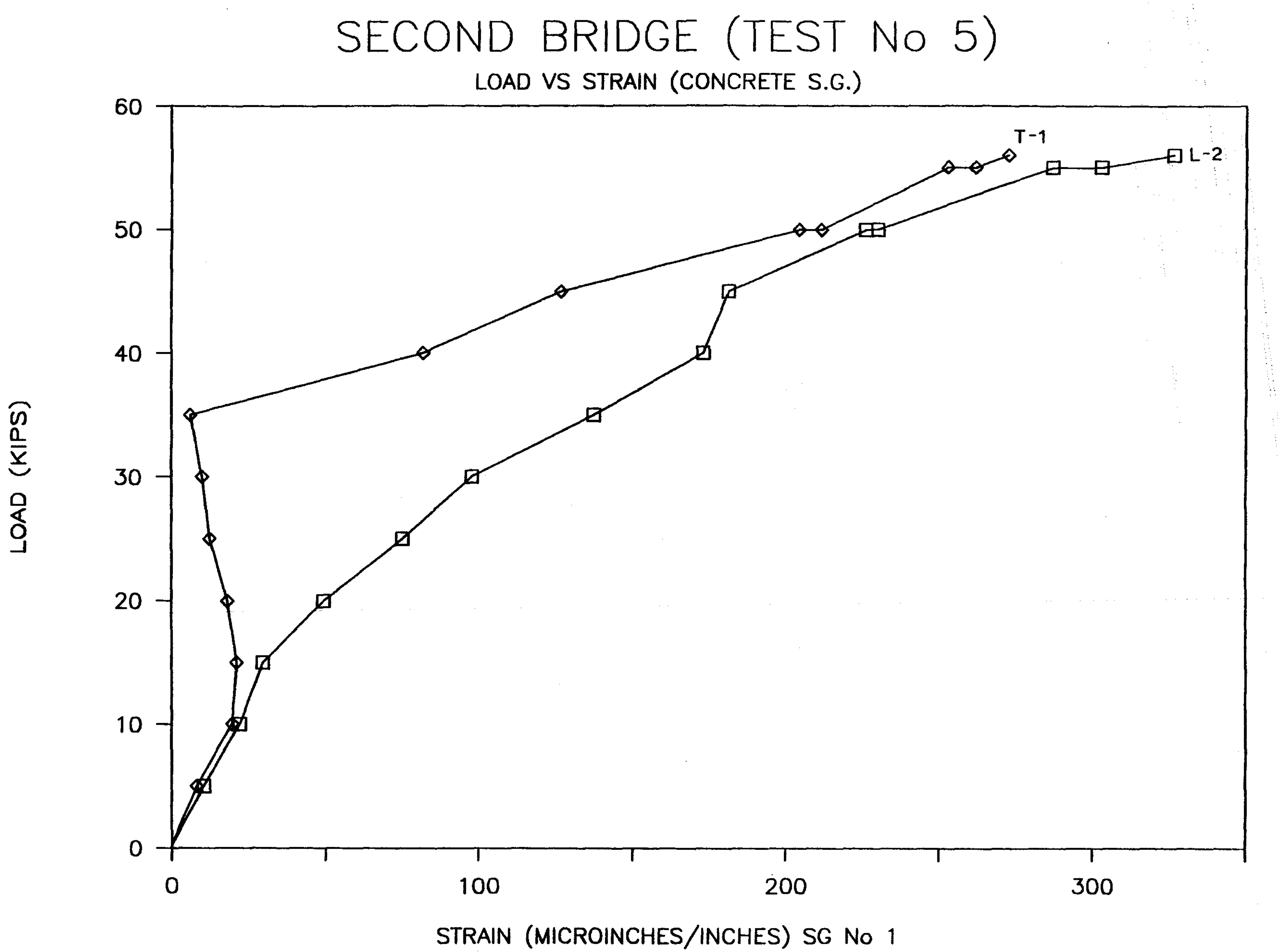

Figure D.21 Load-Strain Curves (Second Bridge, Test No. 5, Concrete S.G.)

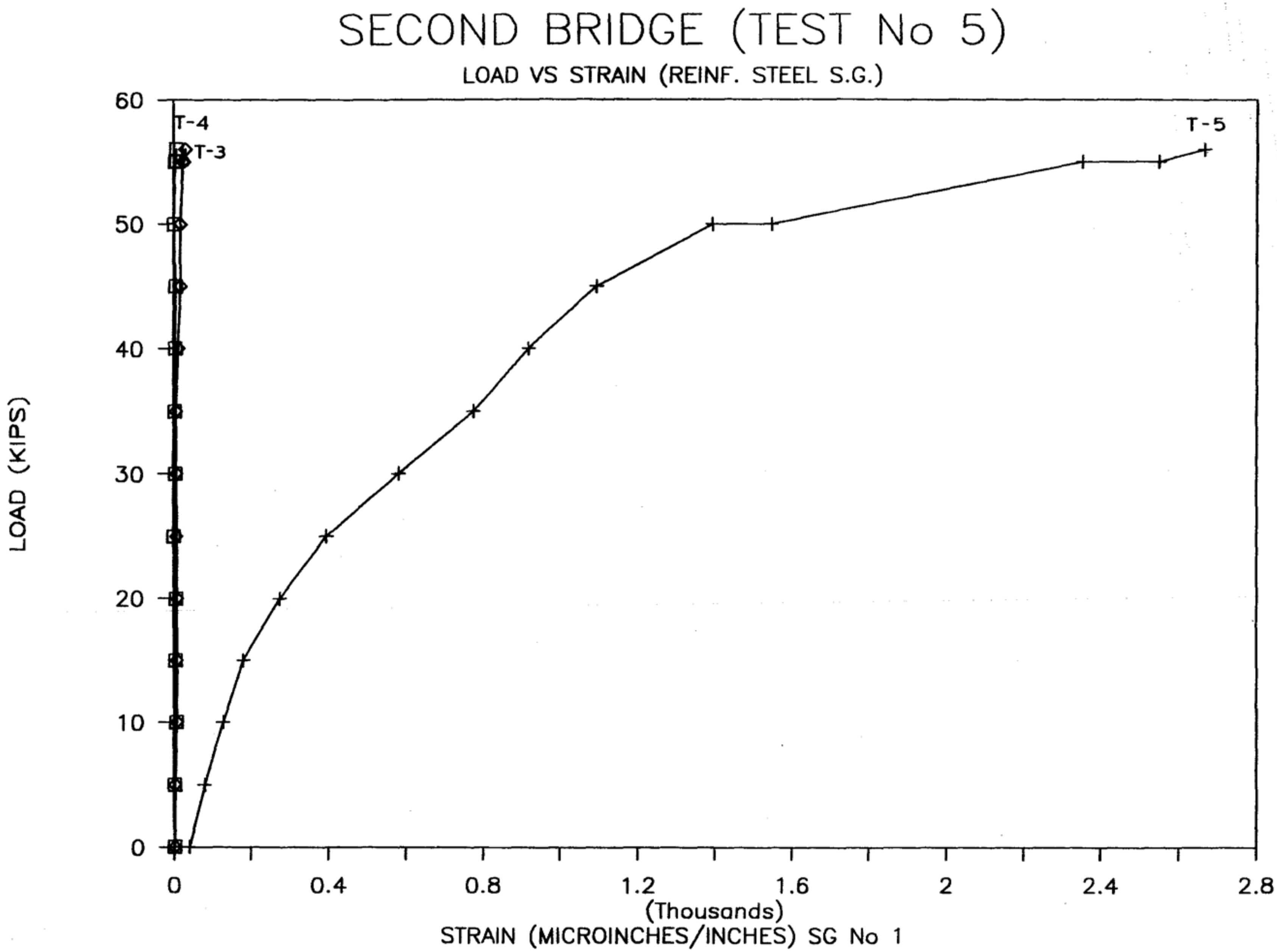

Figure D.22 Load-Strain Curves (Second Bridge, Test No. 5, Reinforced Steel S.G.)

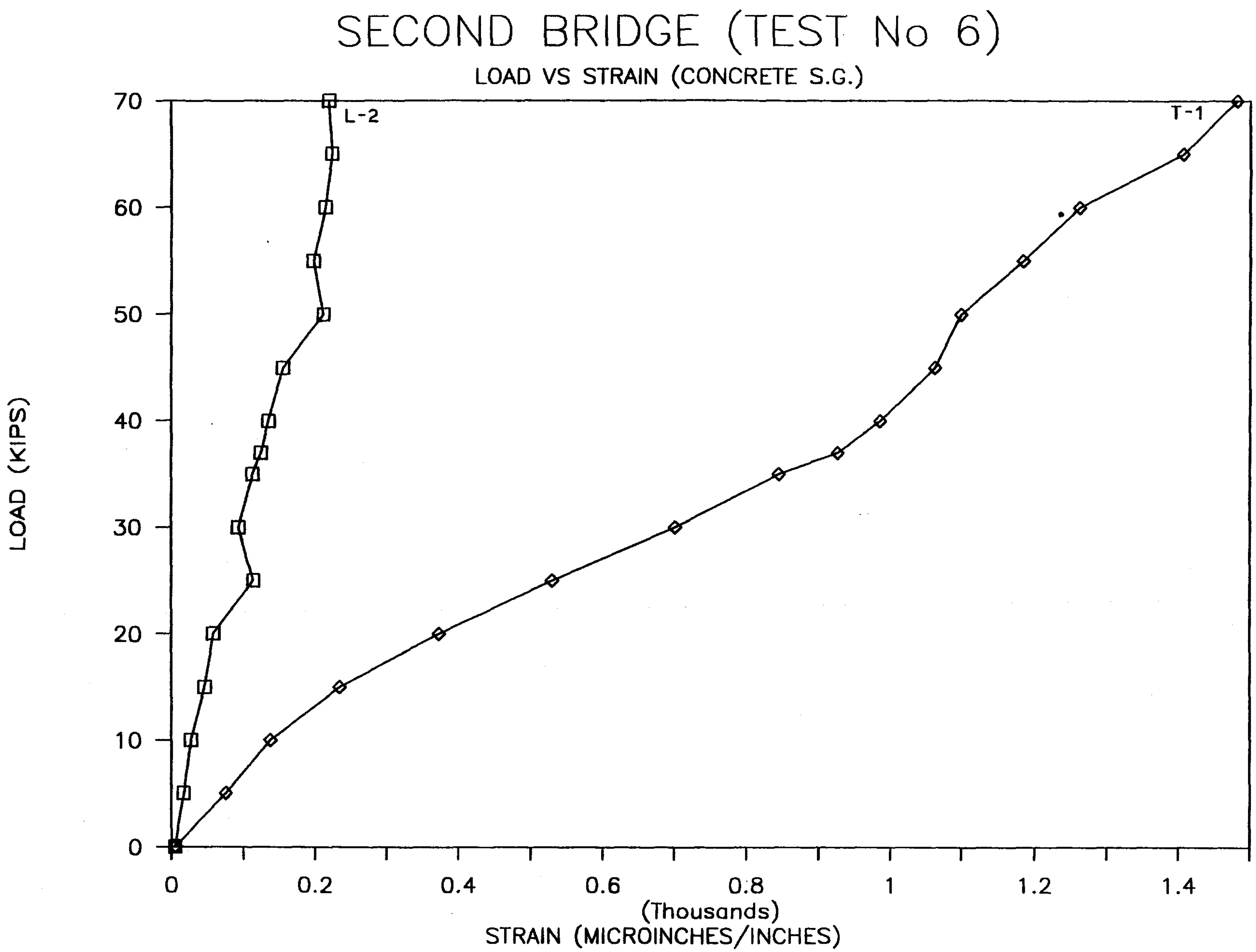

Figure D.23 Load-Strain Curves (Second Bridge, Test No. 6, Concrete S.G.)

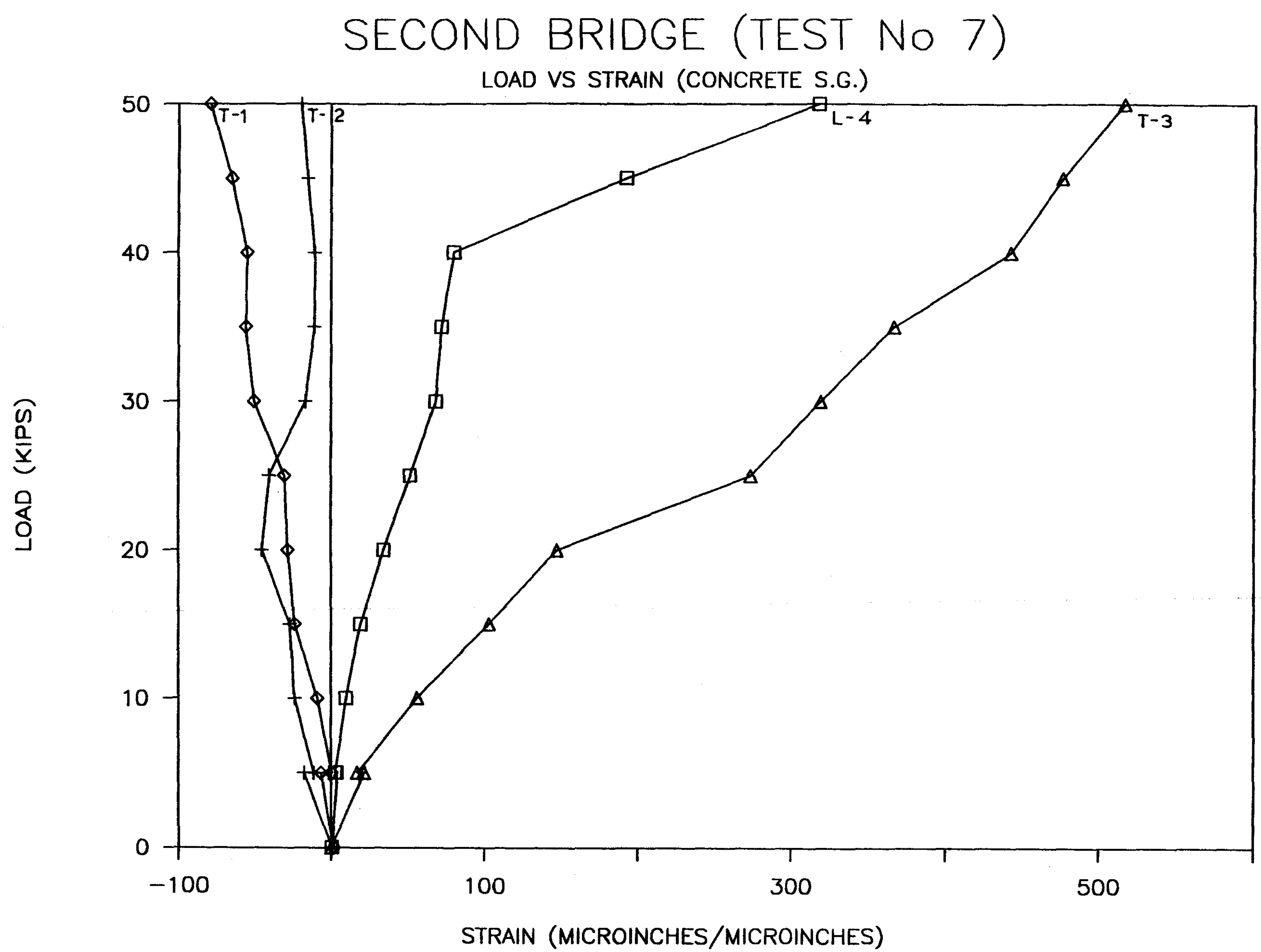

Figure D.24 Load-Strain Curves (Second Bridge, Test No. 7, Concrete S.G.)

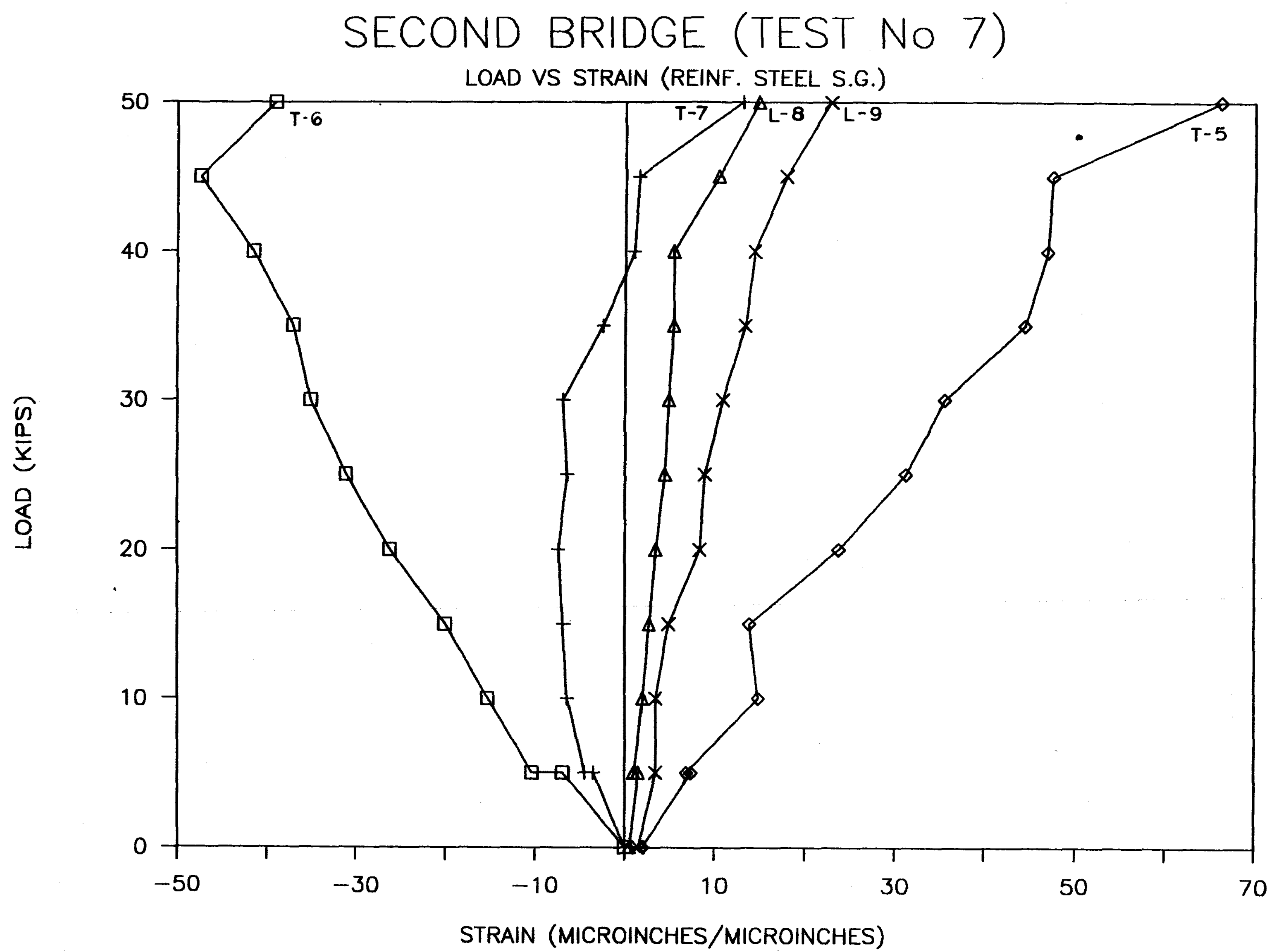

Figure D.25 Load-Strain Curves (Second Bridge, Test No. 7, Reinforced Steel S.G.)

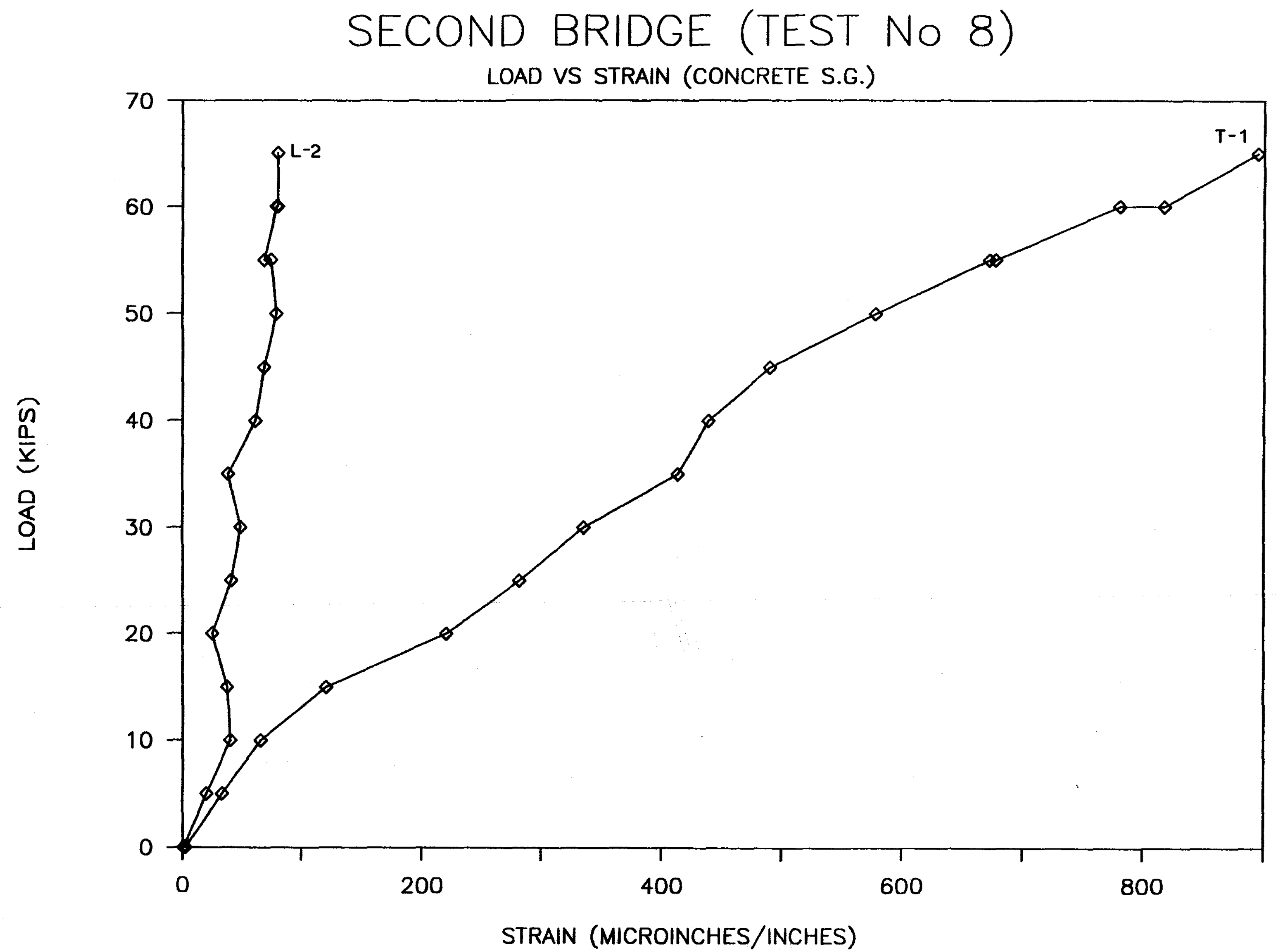

Figure D.26 Load-Strain Curves (Second Bridge, Test No. 8, Concrete S.G.)

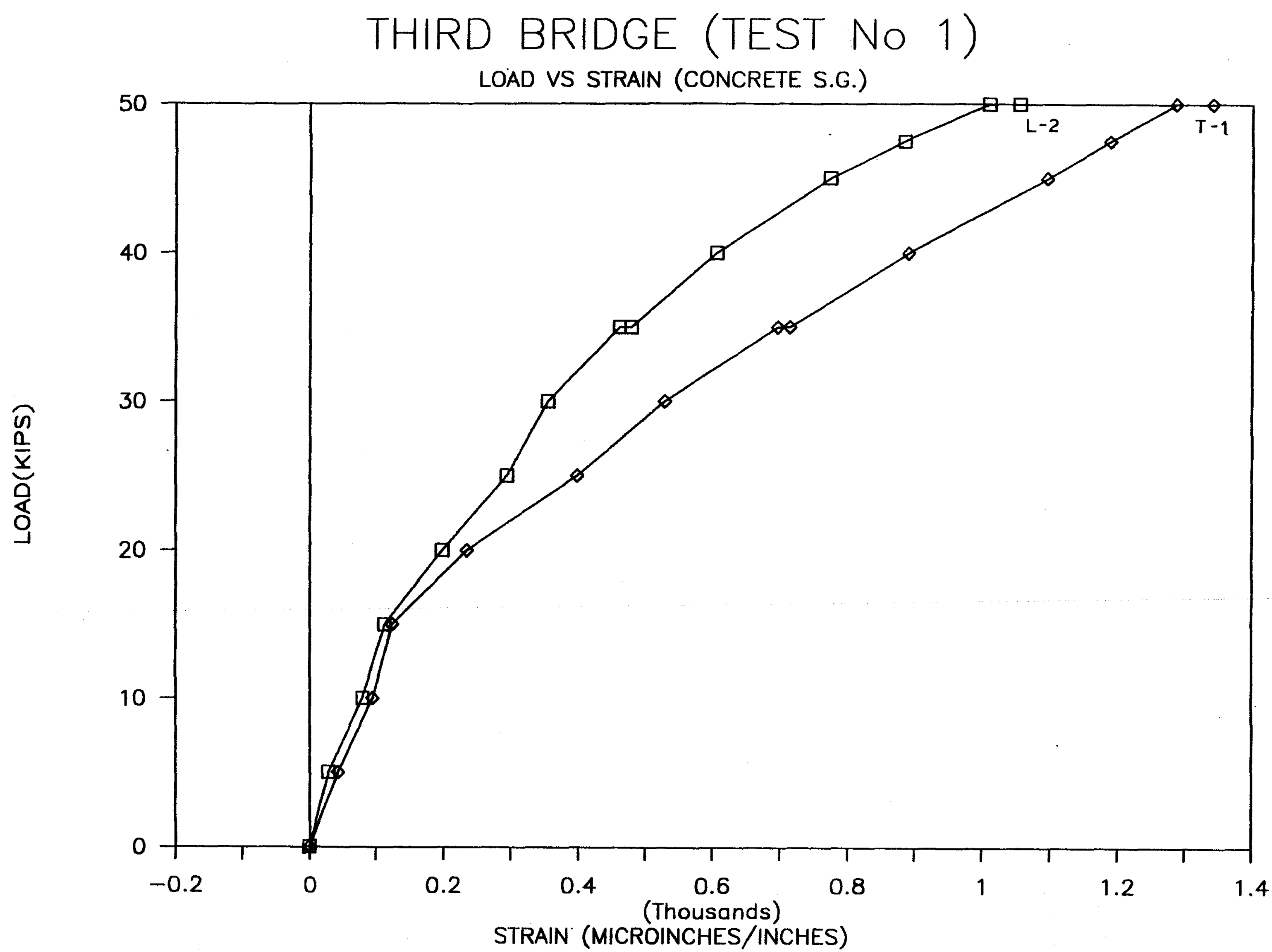

Figure D.27 Load-Strain Curves (Third Bridge, Test No. 1, Concrete S.G.)

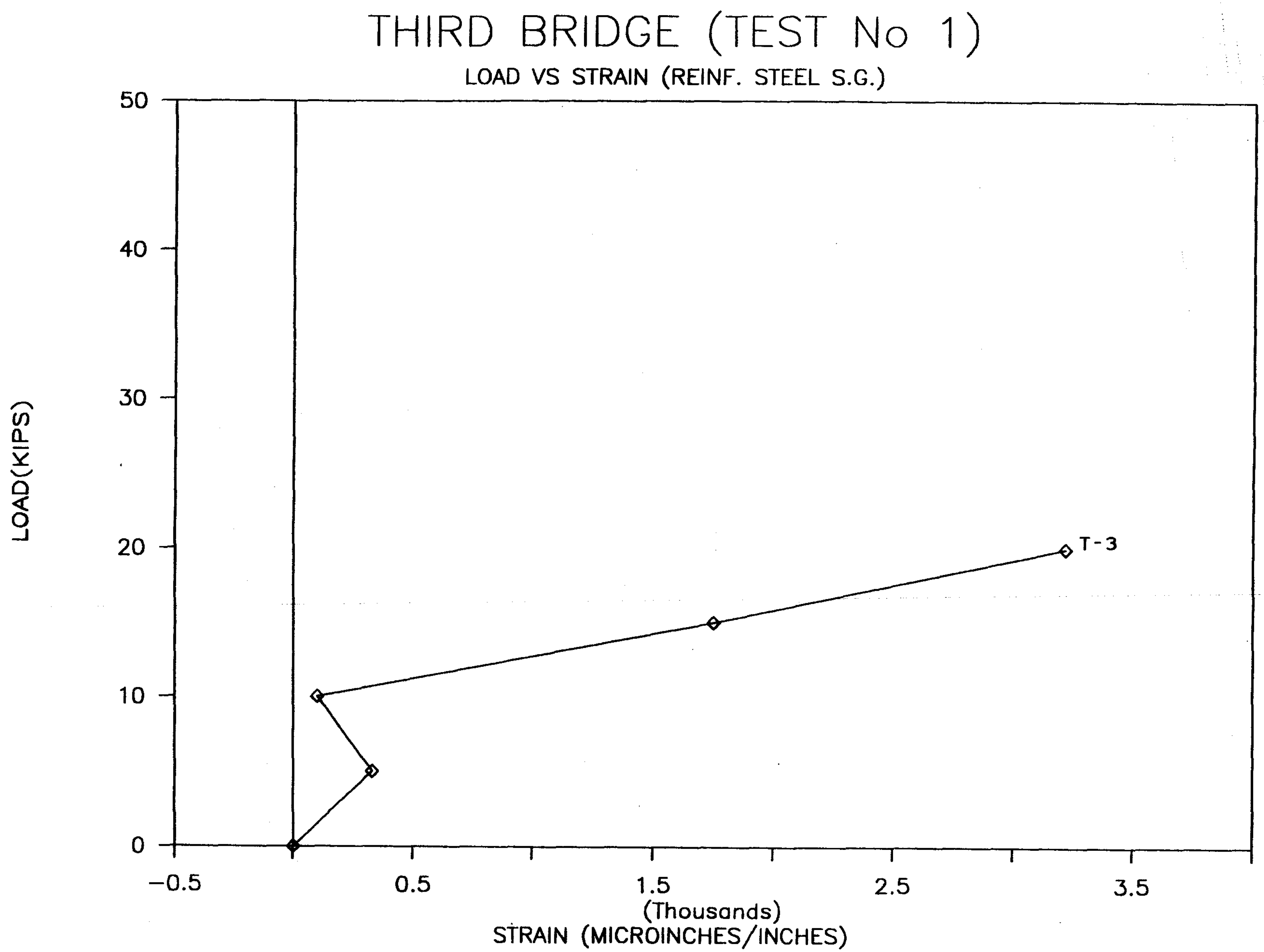

Figure D.28 Load-Strain Curves (Third Bridge, Test No. 1, Reinforced Steel S.G.)

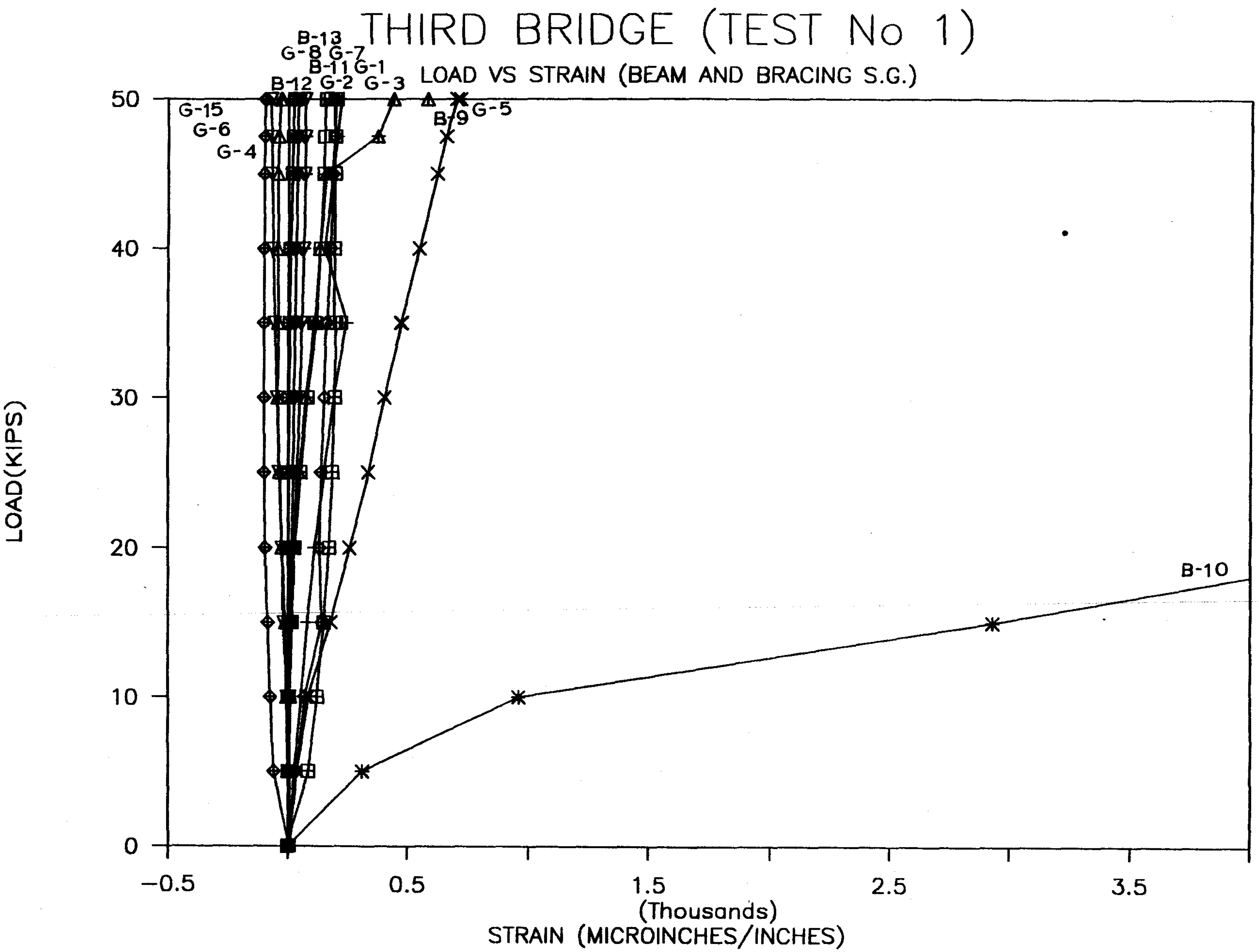

Figure D.29 Load-Strain Curves (Third Bridge, Test No. 1, Beam and Bracing S.G.)

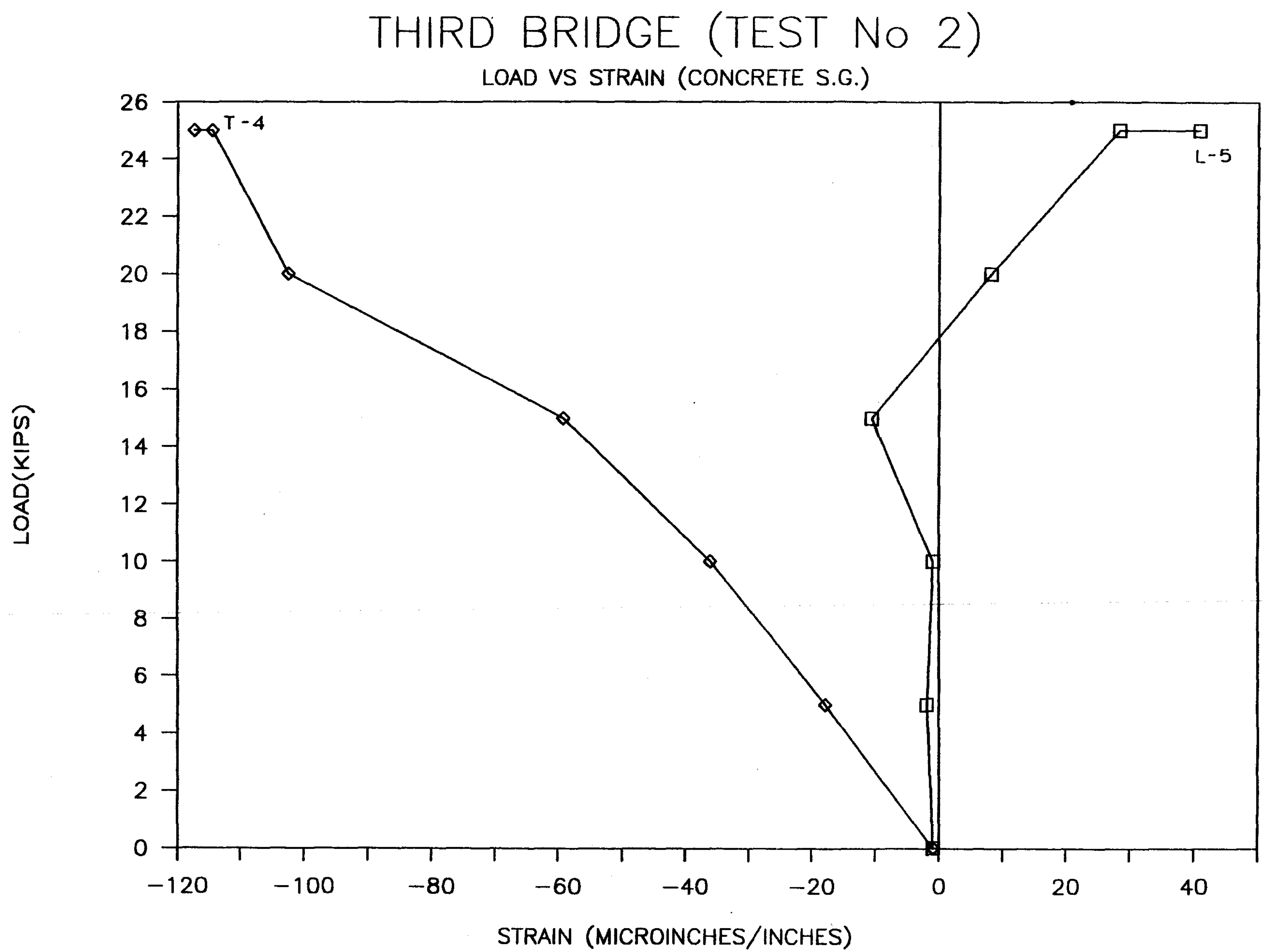

Figure D.30 Load-Strain Curves (Third Bridge, Test No. 2, Concrete S.G.)

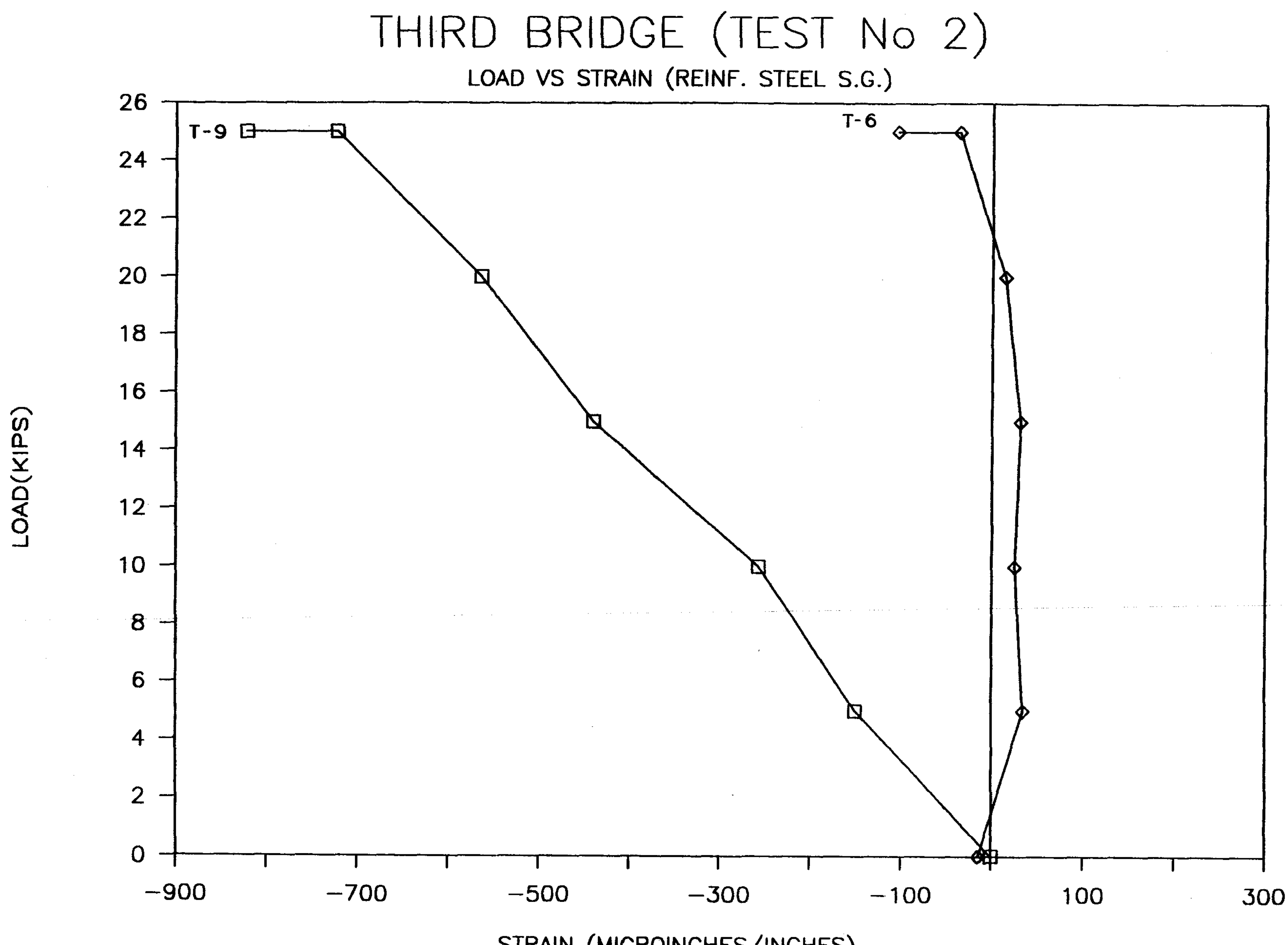

Figure D.31 Load-Strain Curves (Third Bridge, Test No. 2, Reinforced Steel S.G.)

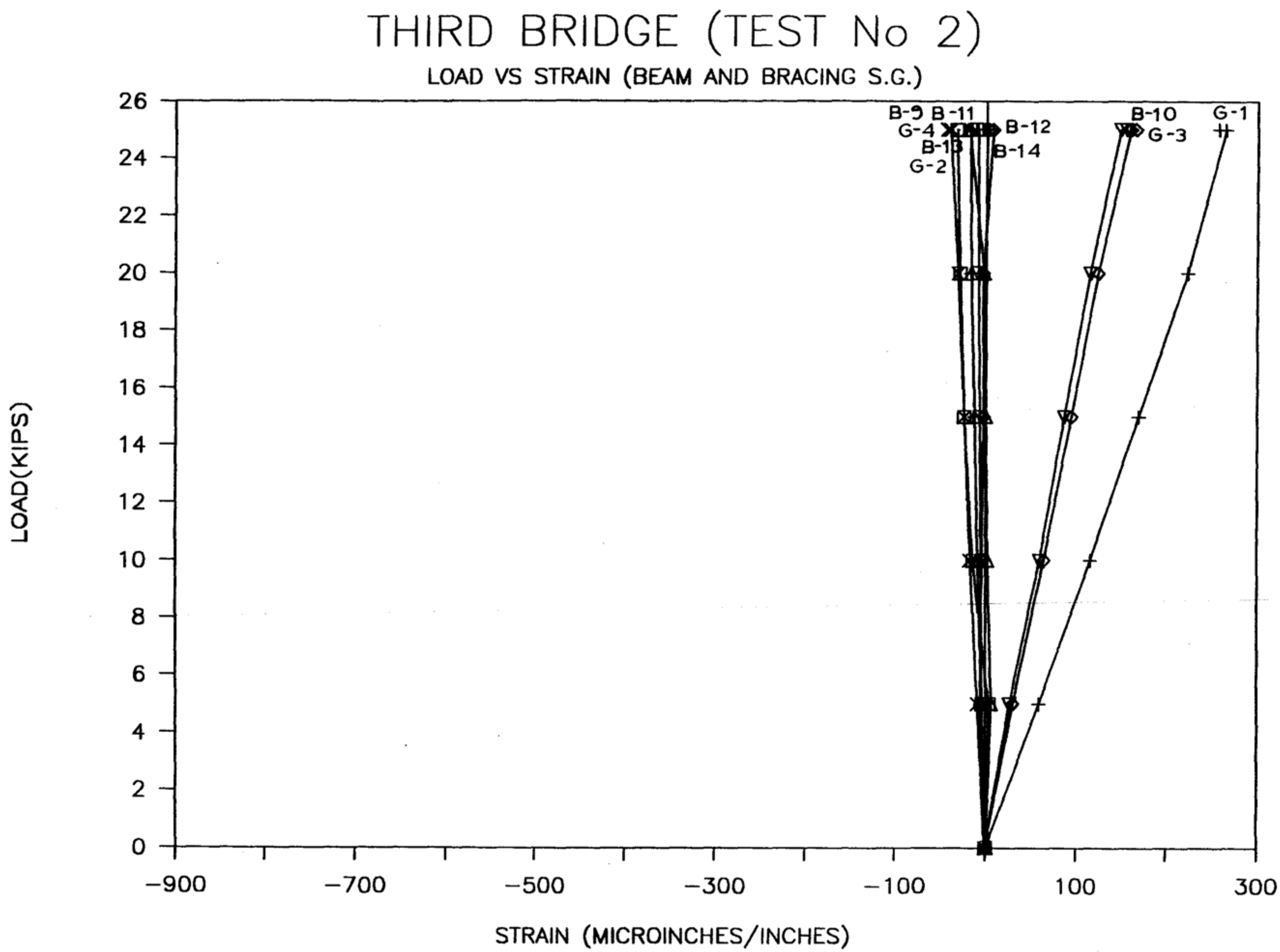

Figure D.32 Load-Strain Curves (Third Bridge, Test No. 2, Beam and Bracing S.G.)

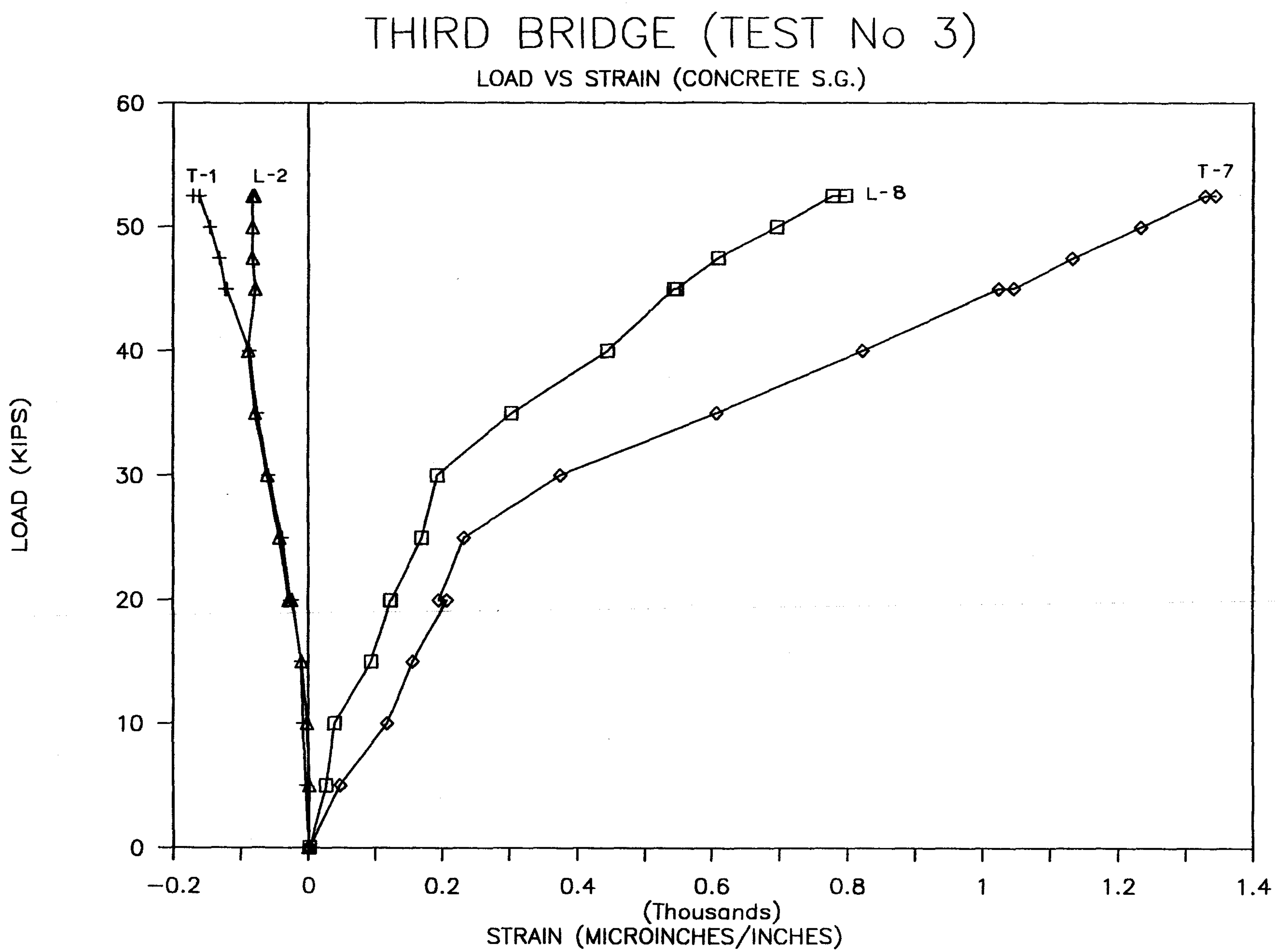

Figure D.33 Load-Strain Curves (Third Bridge, Test No. 3, Concrete S.G.)

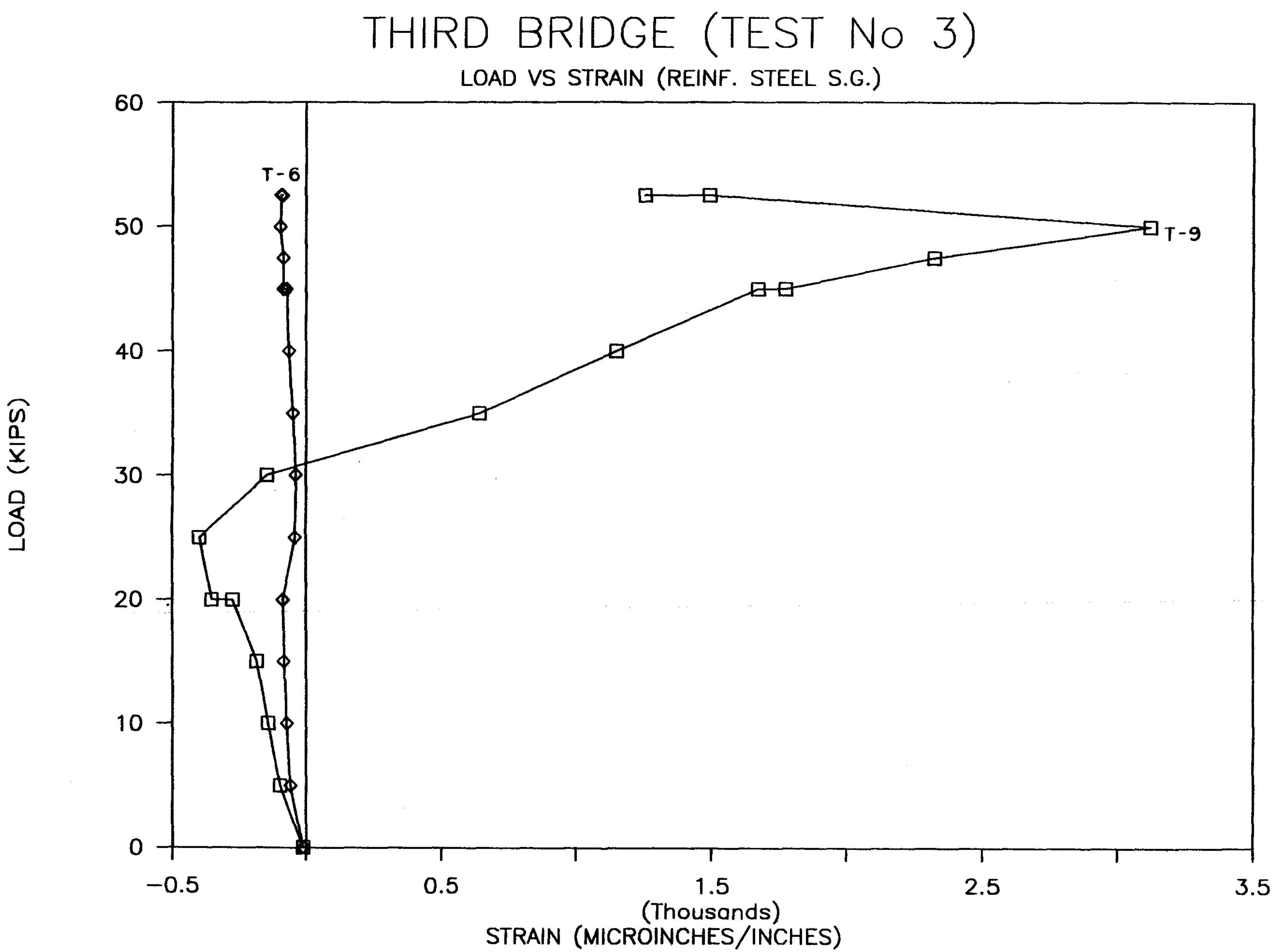

Figure D.34 Load-Strain Curves (Third Bridge, Test No. 3, Reinforced Steel S.G.)

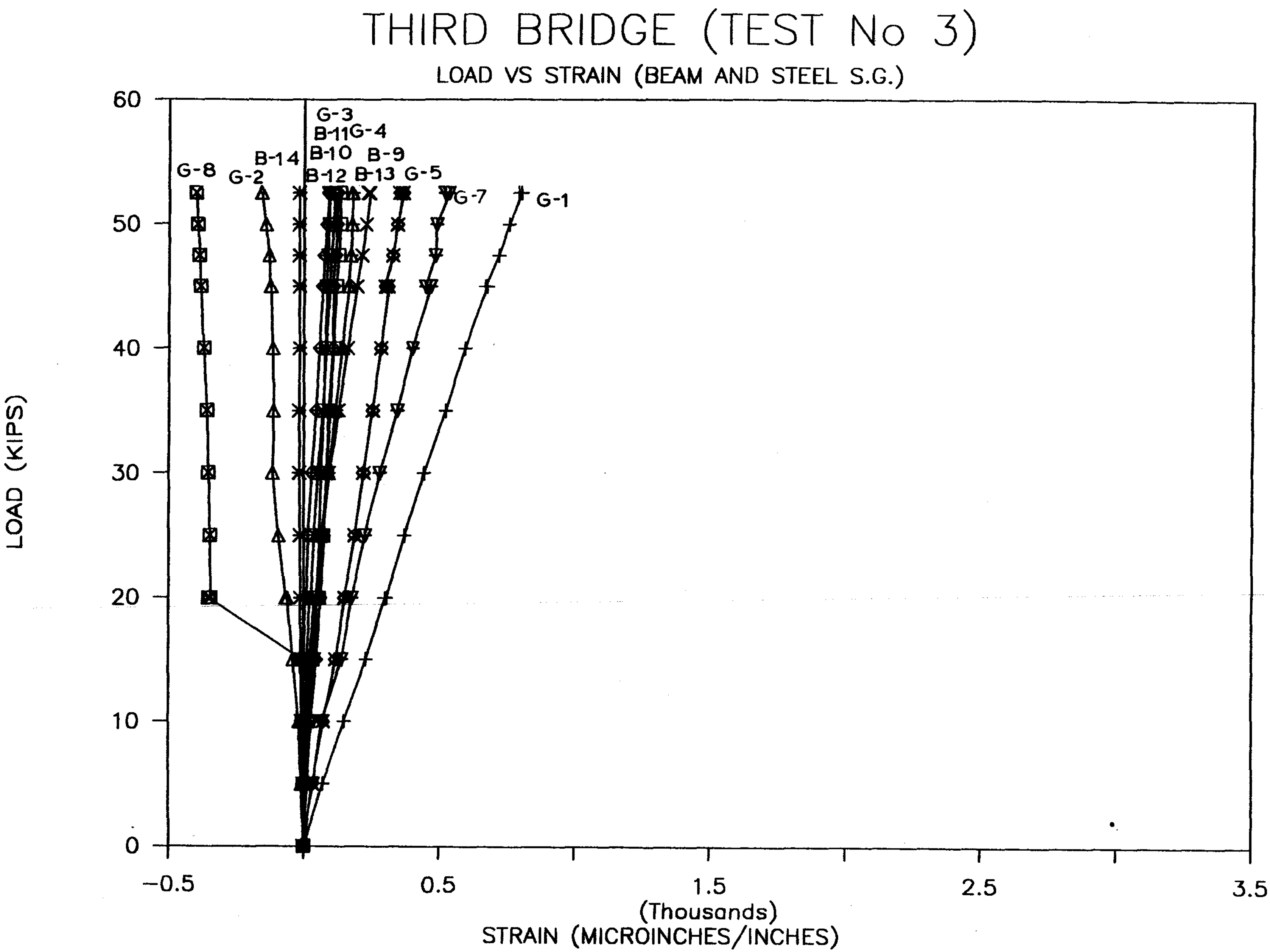

Figure D.35 Load-Strain Curves (Third Bridge, Test No. 3, Beam and Steel S.G.)

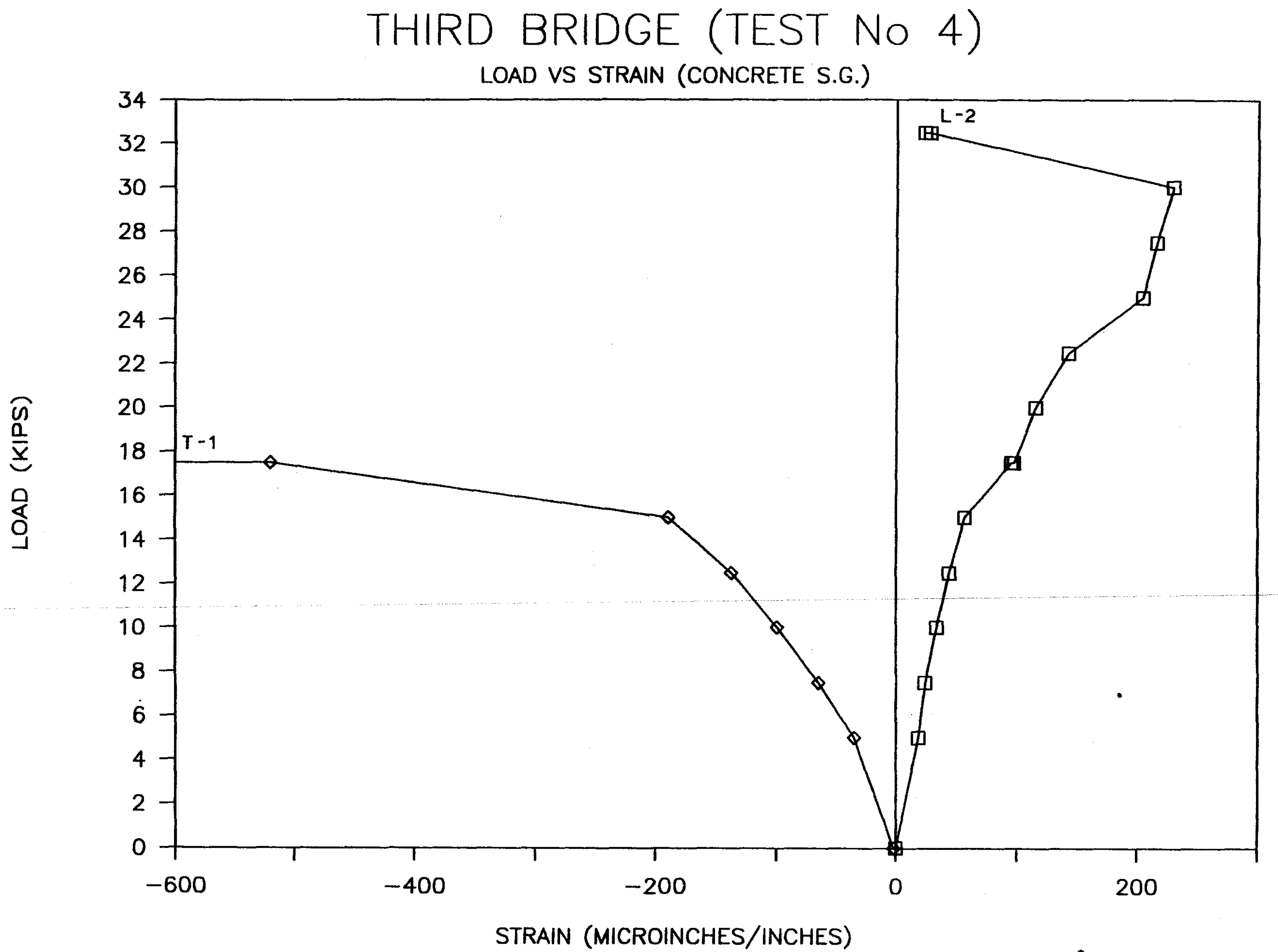

Figure D.36 Load-Strain Curves (Third Bridge, Test No. 4, Concrete S.G.)

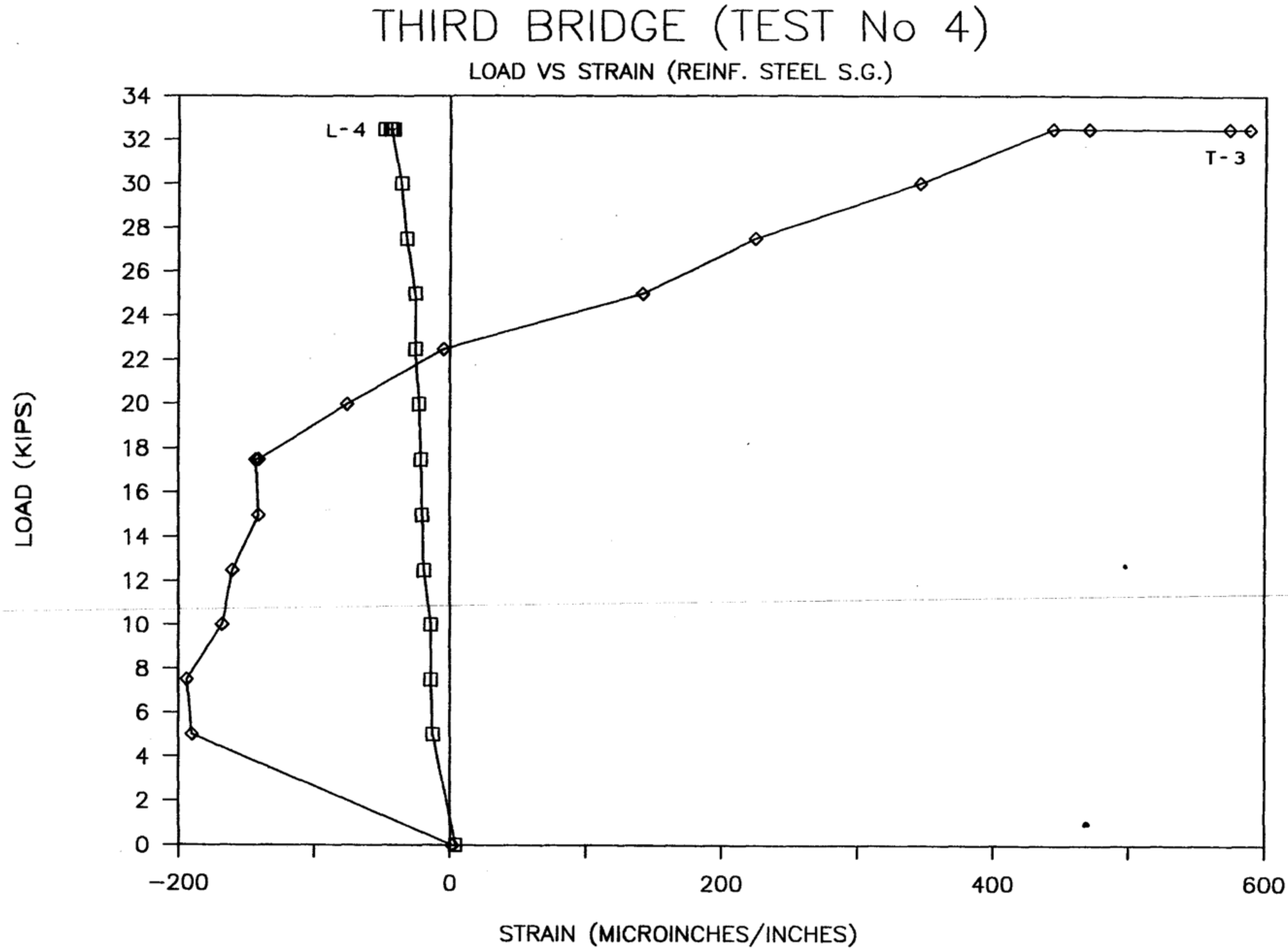

Figure D.37 Load-Strain Curves (Third Bridge, Test No. 4, Reinforced Steel S.G.)

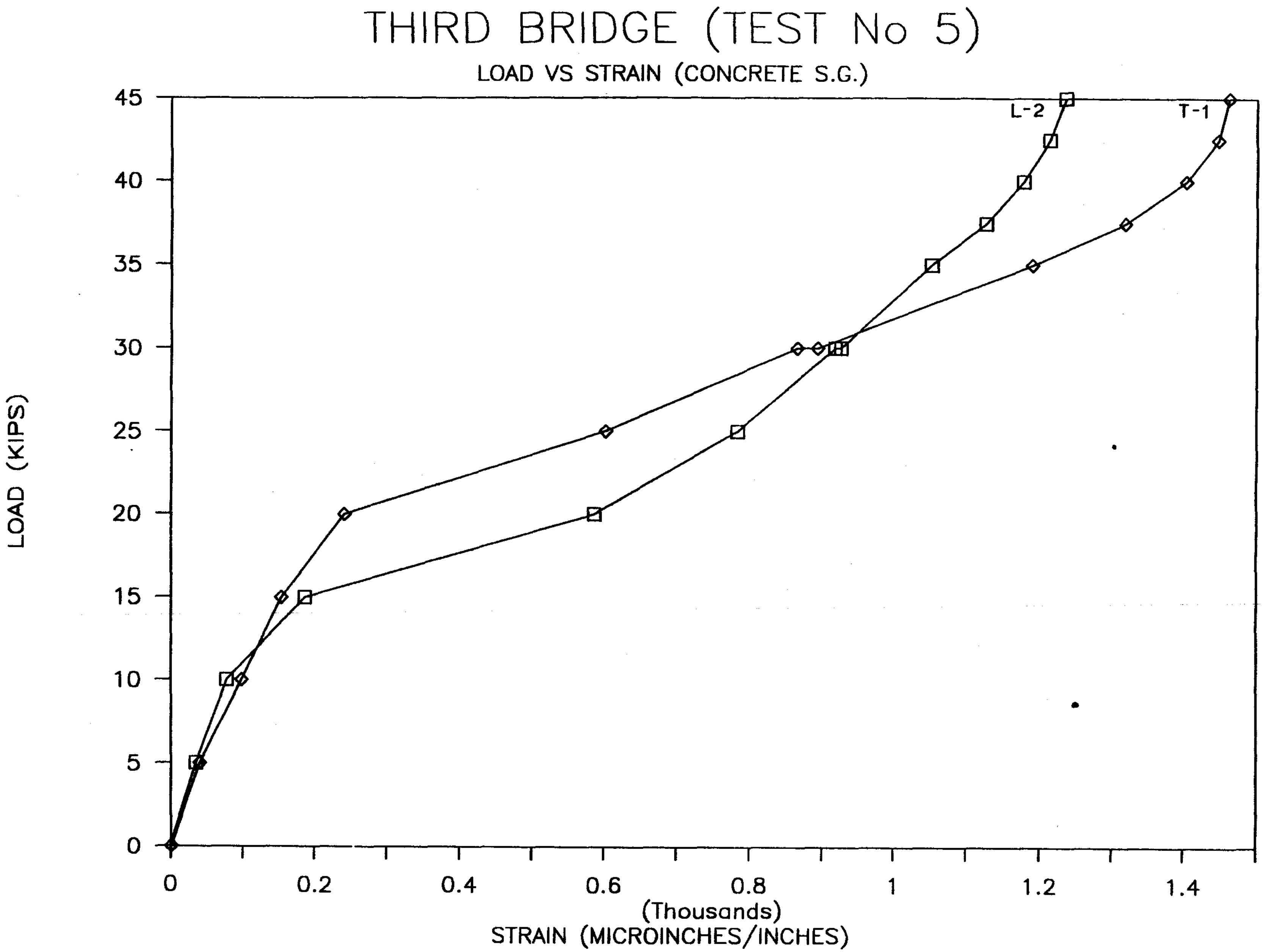

Figure D.38 Load-Strain Curves (Third Bridge, Test No. 5, Concrete S.G.)

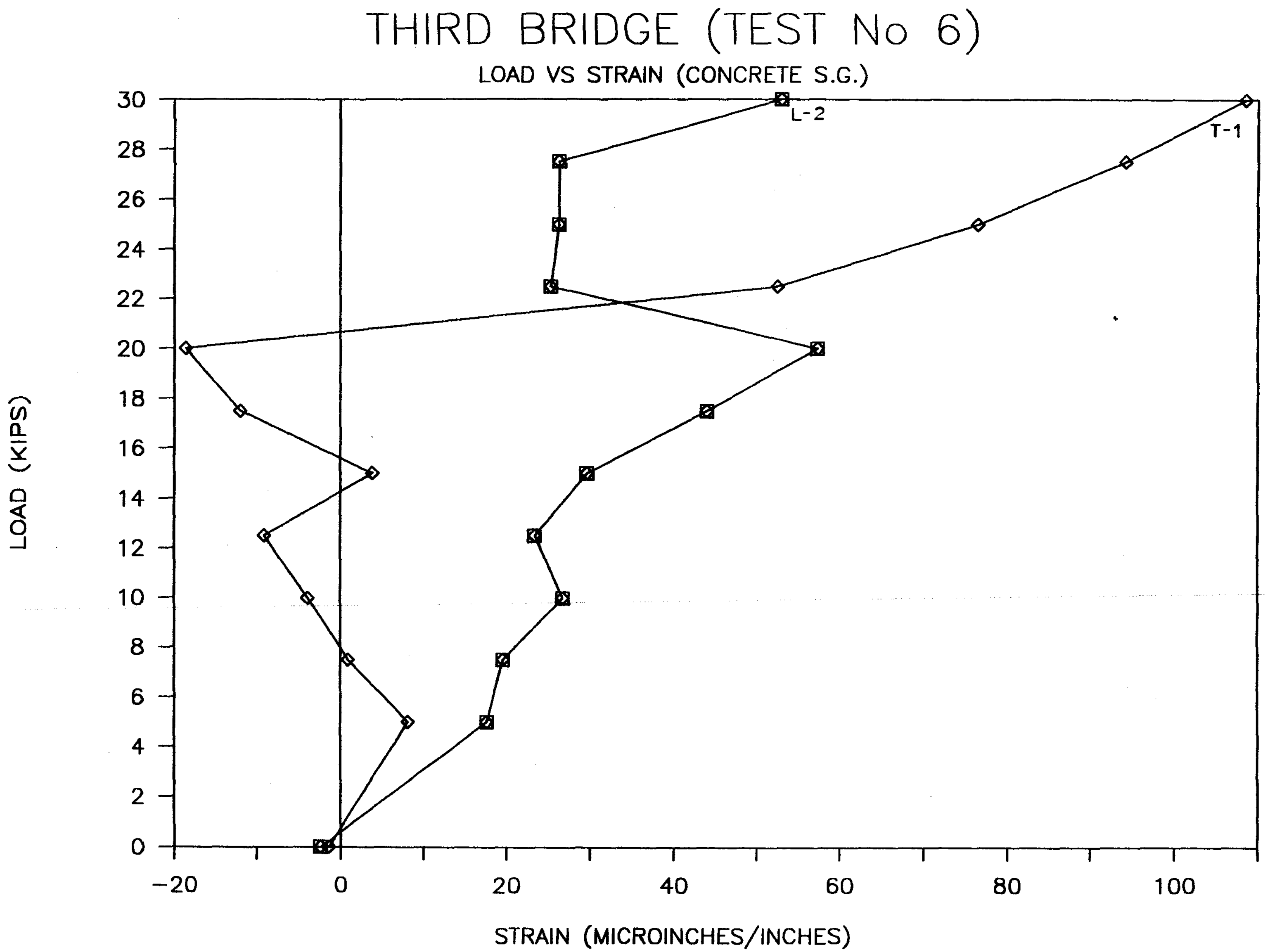

Figure D.39 Load-Strain Curves (Third Bridge, Test No. 6, Concrete S.G.)

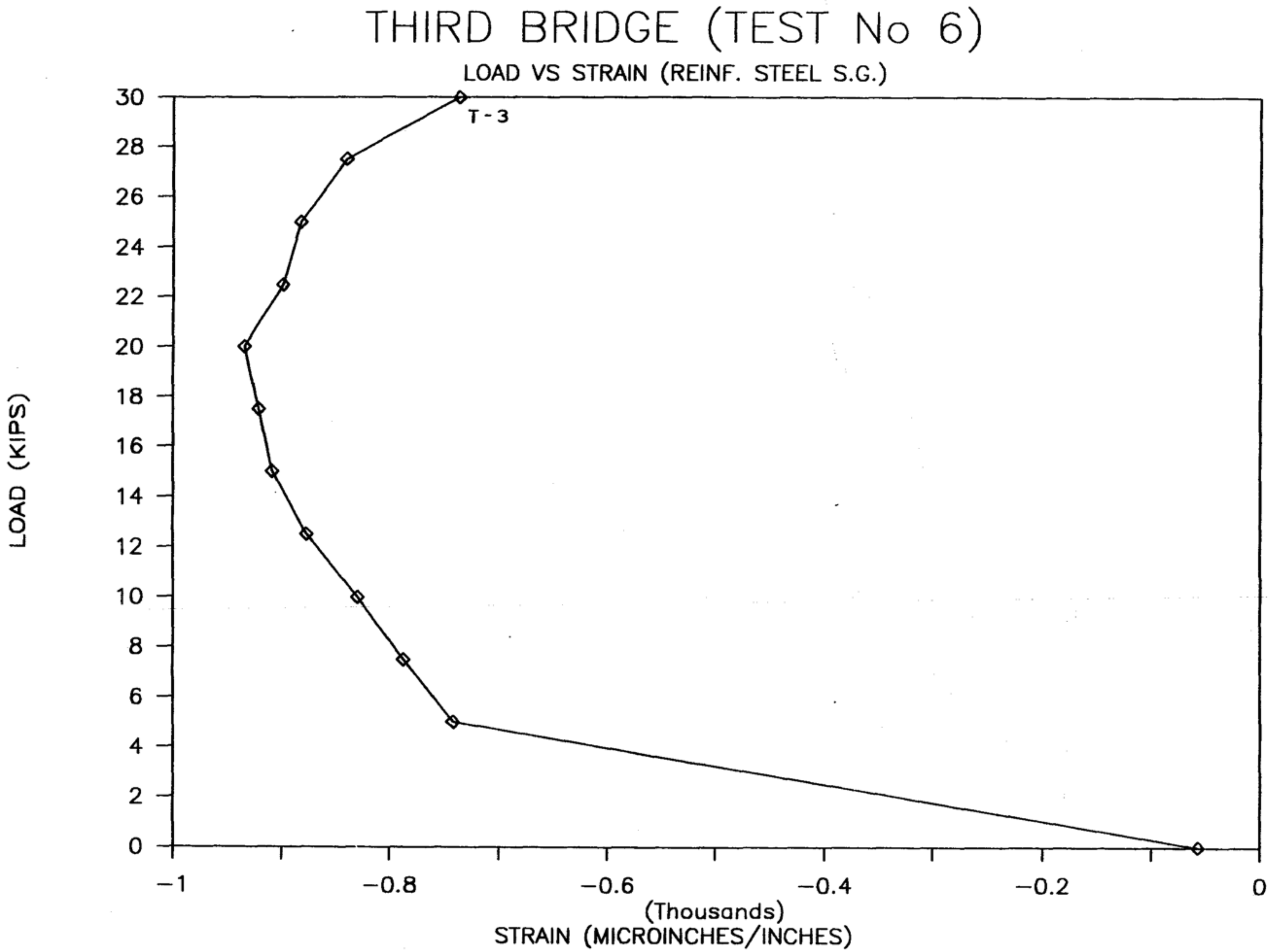

Figure D.40 Load-Strain Curves (Third Bridge, Test No. 6, Reinforced Steel S.G.)

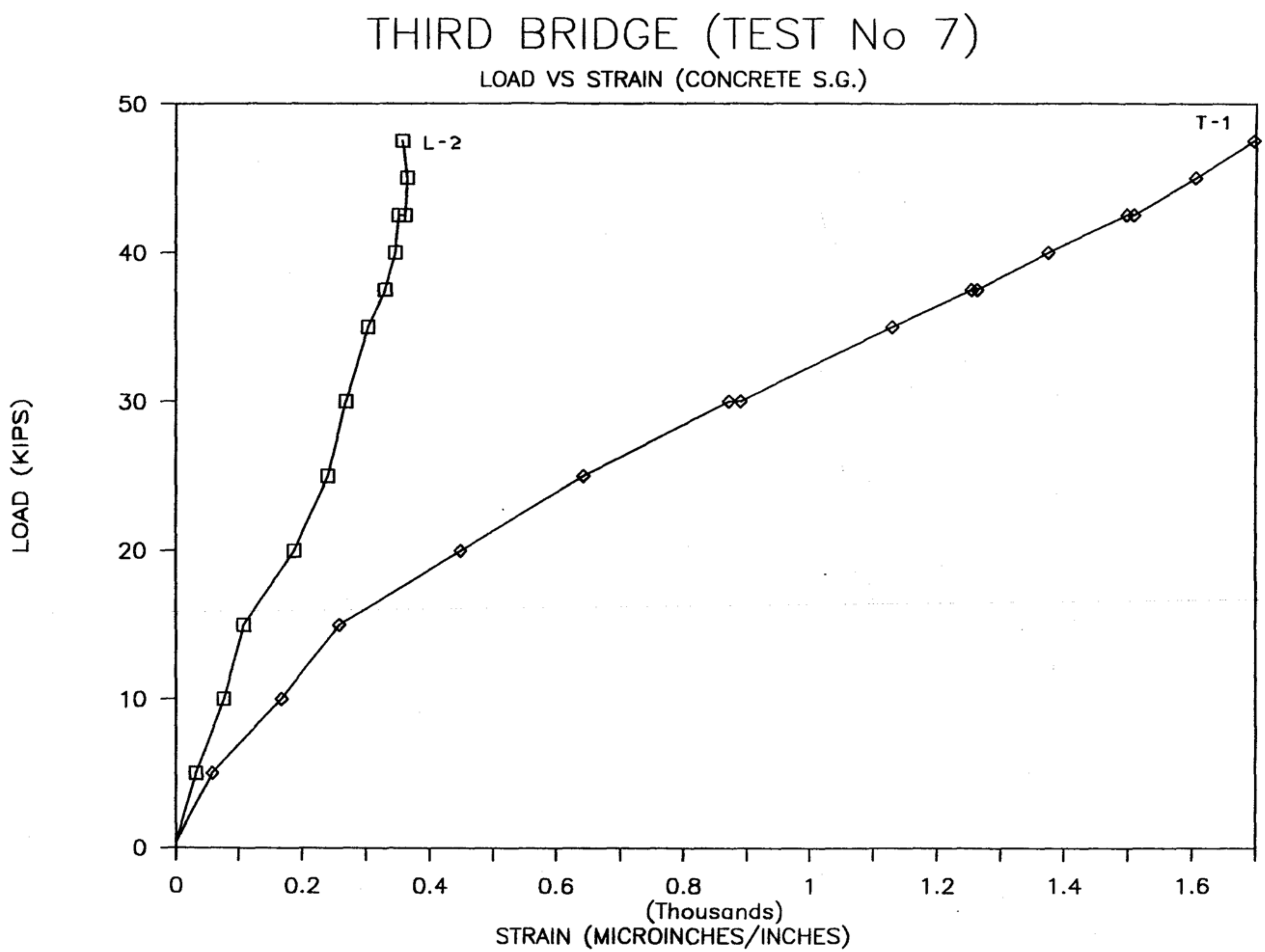

Figure D.41 Load-Strain Curves (Third Bridge, Test No. 7, Concrete S.G.)

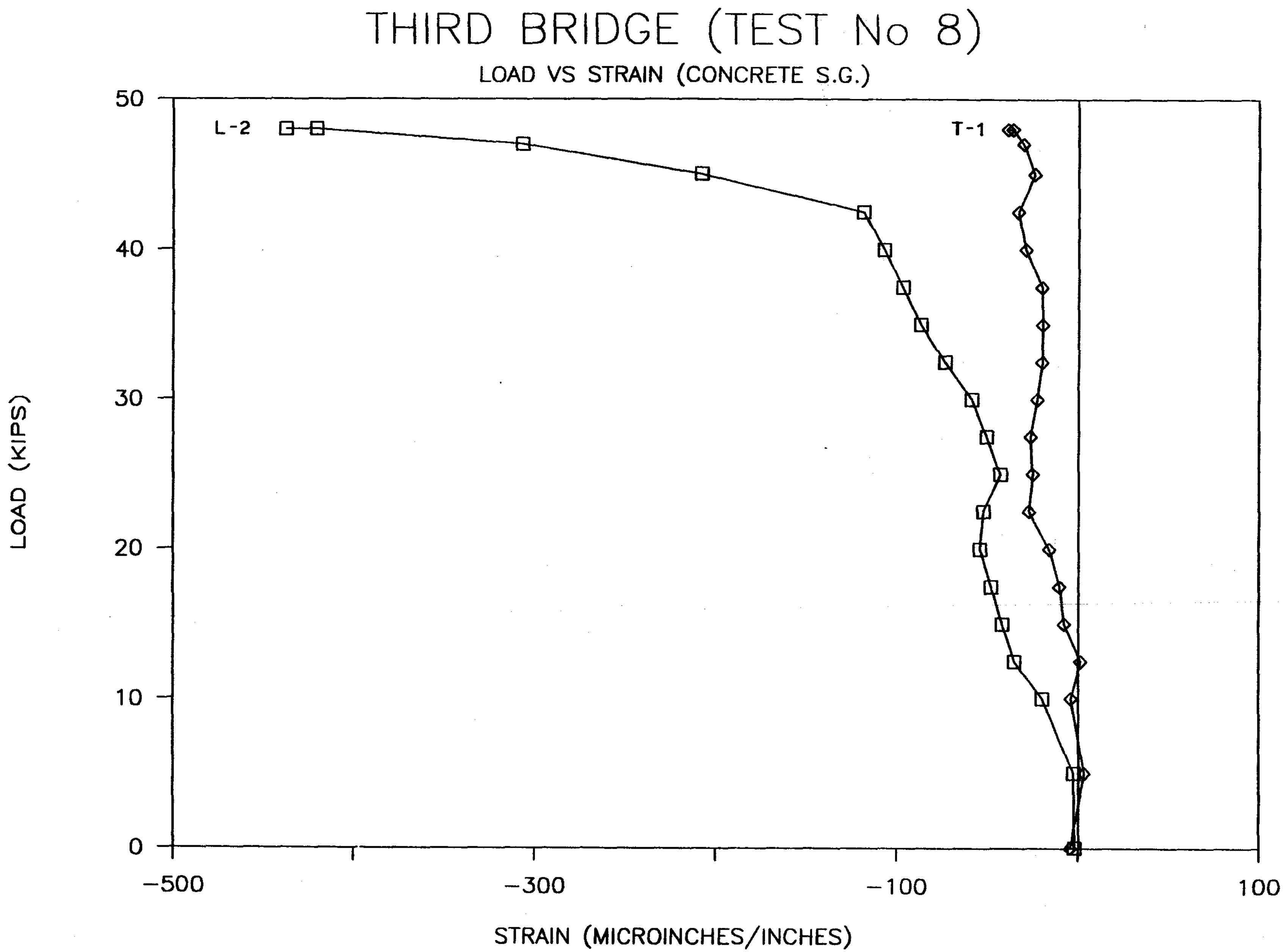

Figure D.42 Load-Strain Curves (Third Bridge, Test No. 8, Concrete S.G.)

APPENDIX E

Crack Patterns Observed

CRACK PATTERN (FIRST BRIDGE- TEST No 1)

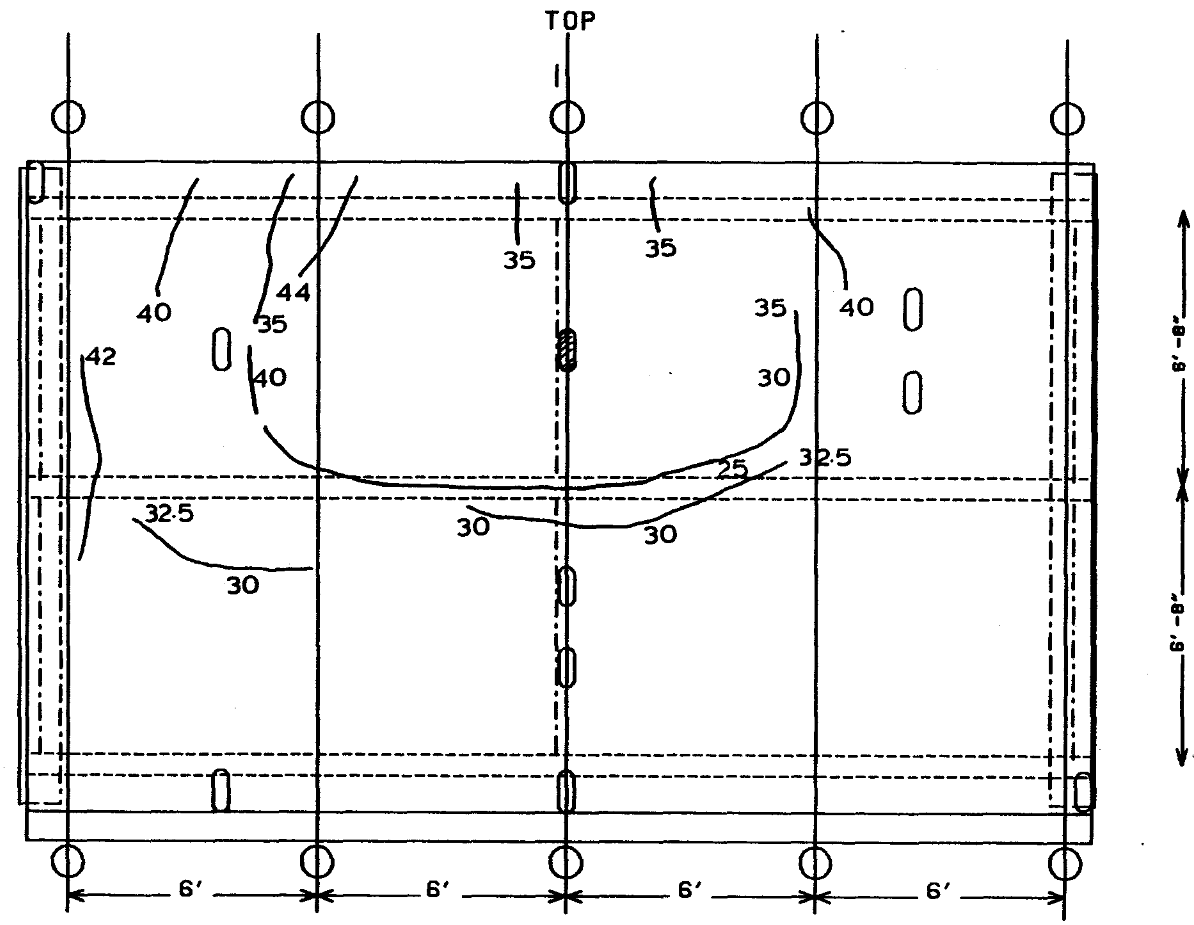

Figure E.1 Top Cracking Pattern (First Bridge - Test No. 1)

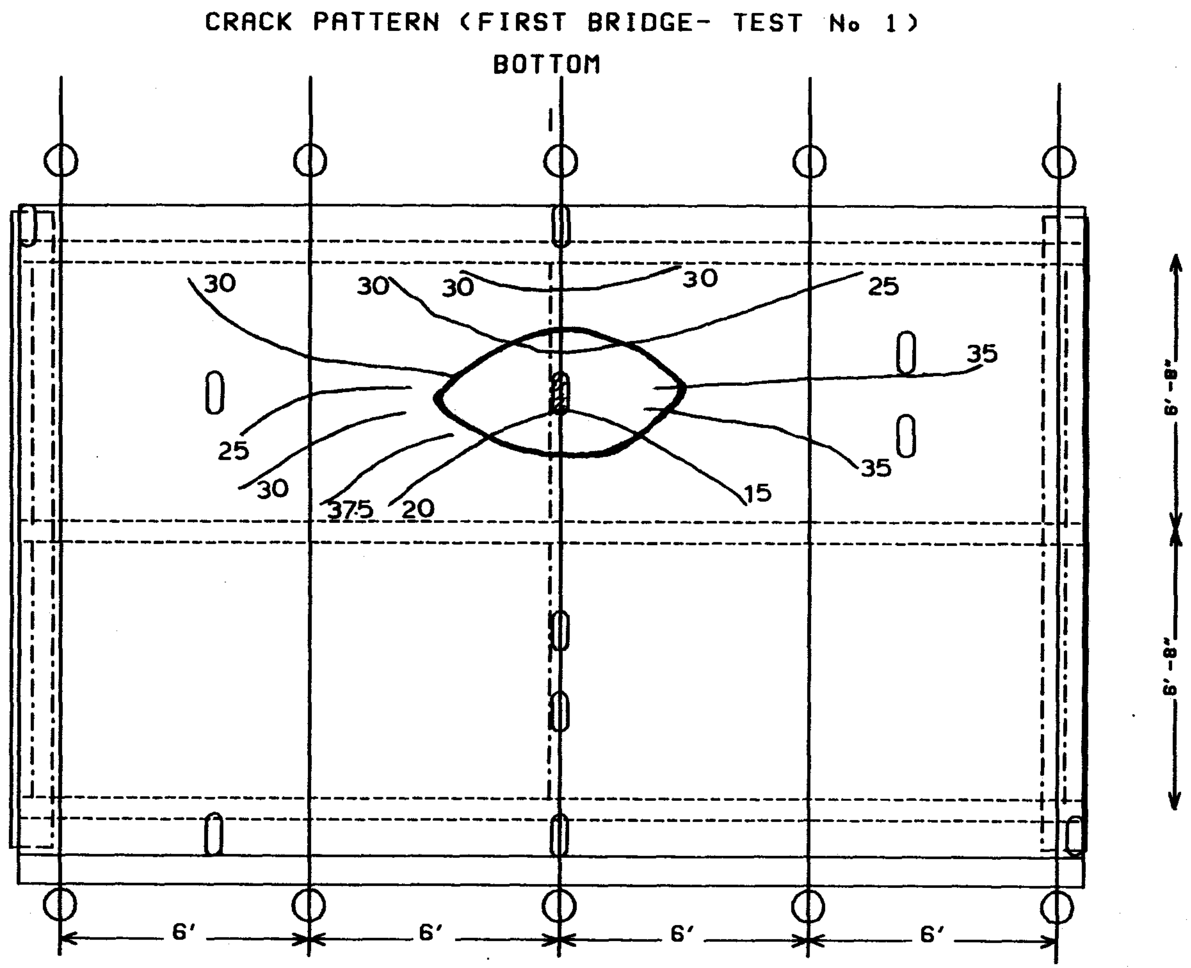

Figure E.2 Bottom Cracking Pattern (First Bridge - Test No. 1)

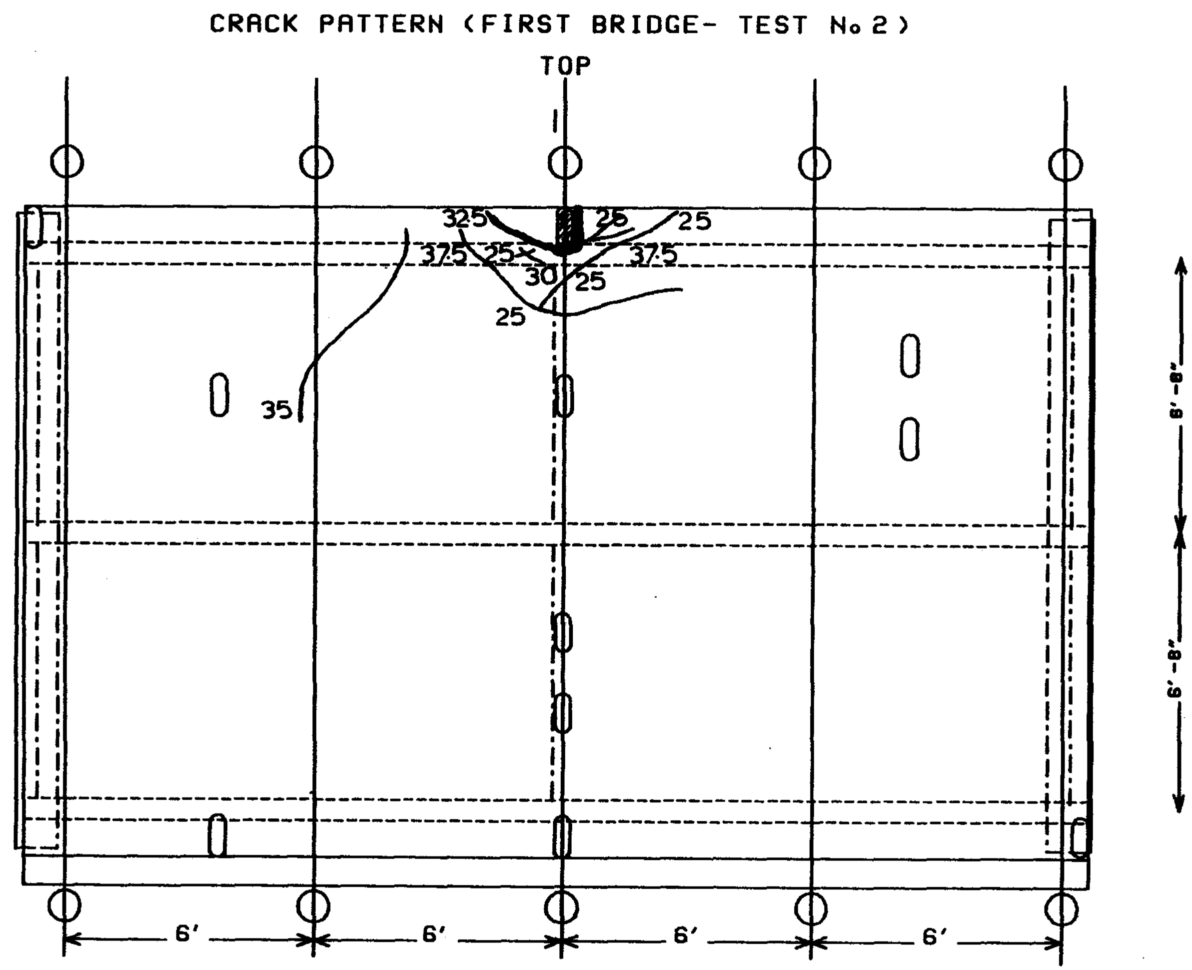

Figure E.3 Top Cracking Pattern (First Bridge - Test No. 2)

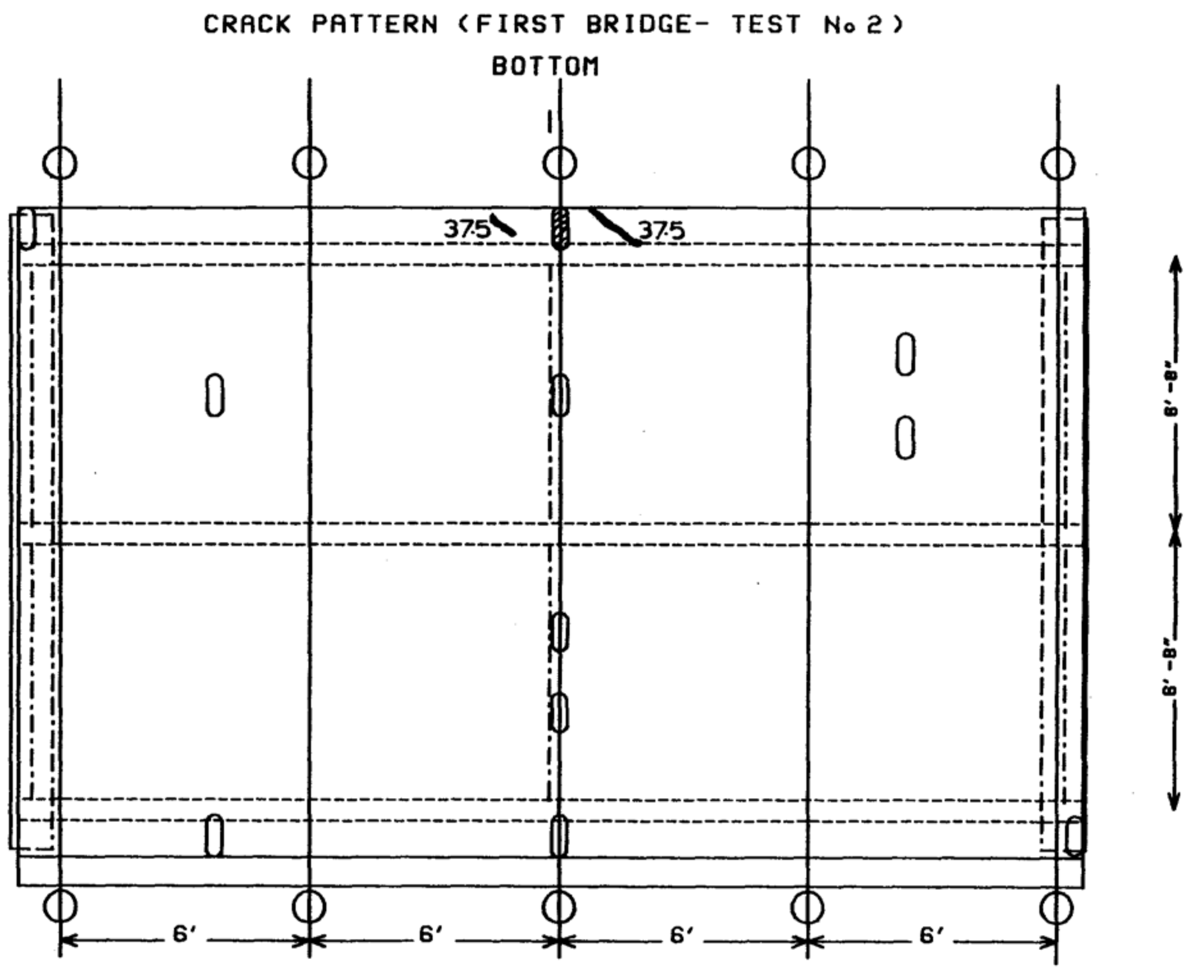

Figure E.4 Bottom Cracking Pattern (First Bridge - Test No. 2)

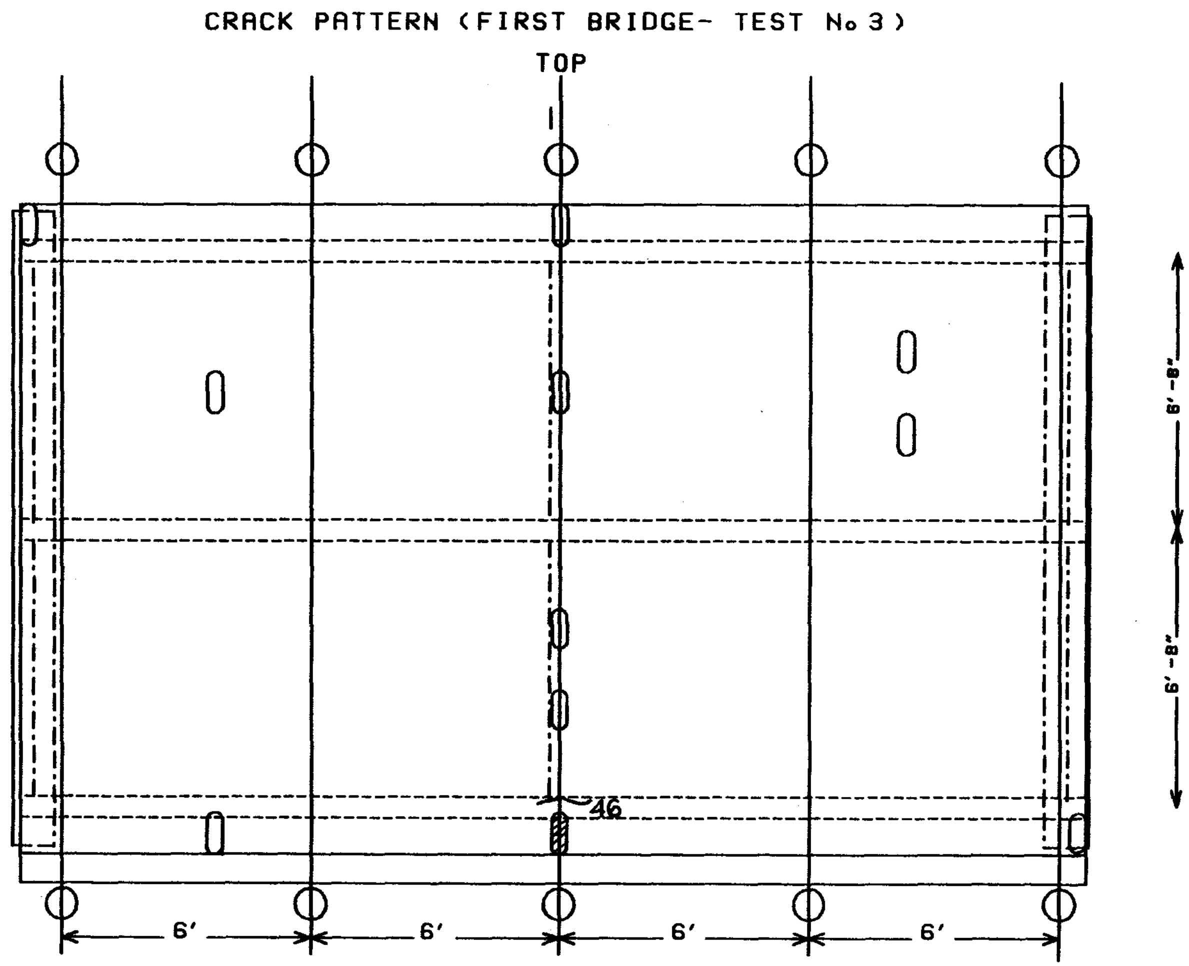

Figure E.5 Top Cracking Pattern (First Bridge - Test No. 3)

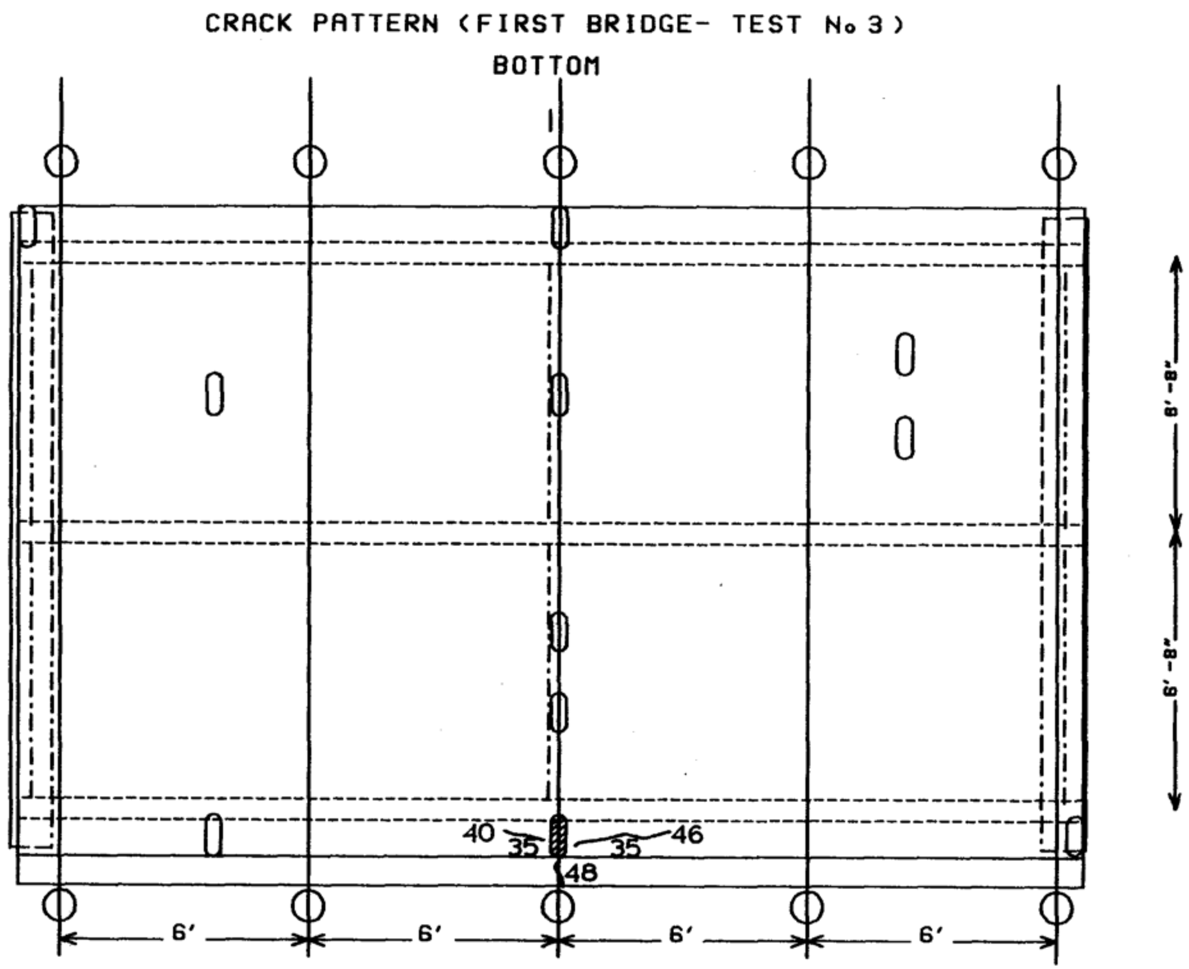

Figure E.6 Bottom Cracking Pattern (First Bridge - Test No. 3)

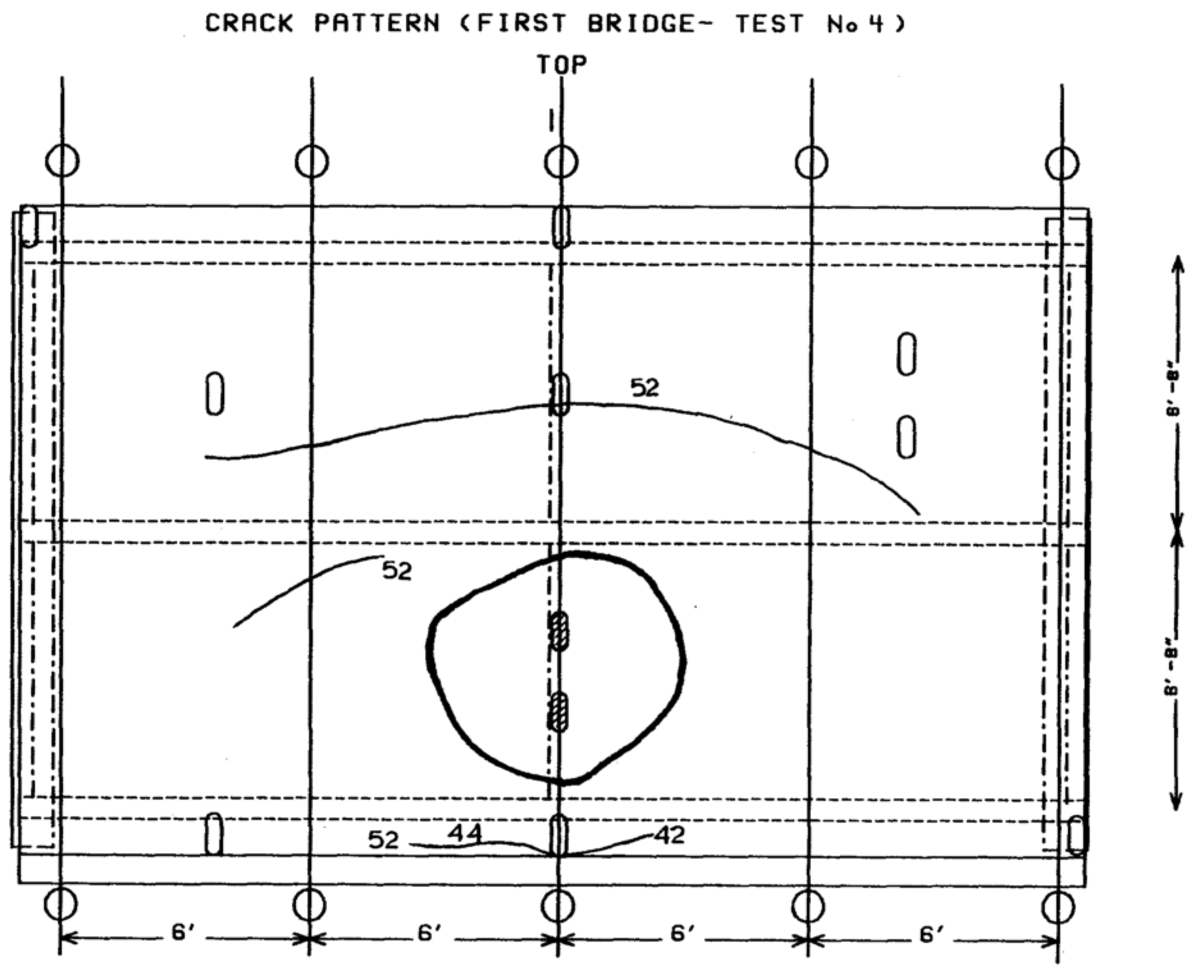

Figure E.7 Top Cracking Pattern (First Bridge - Test No. 4)

CRACK PATTERN (FIRST BRIDGE- TEST No 4)
BOTTOM

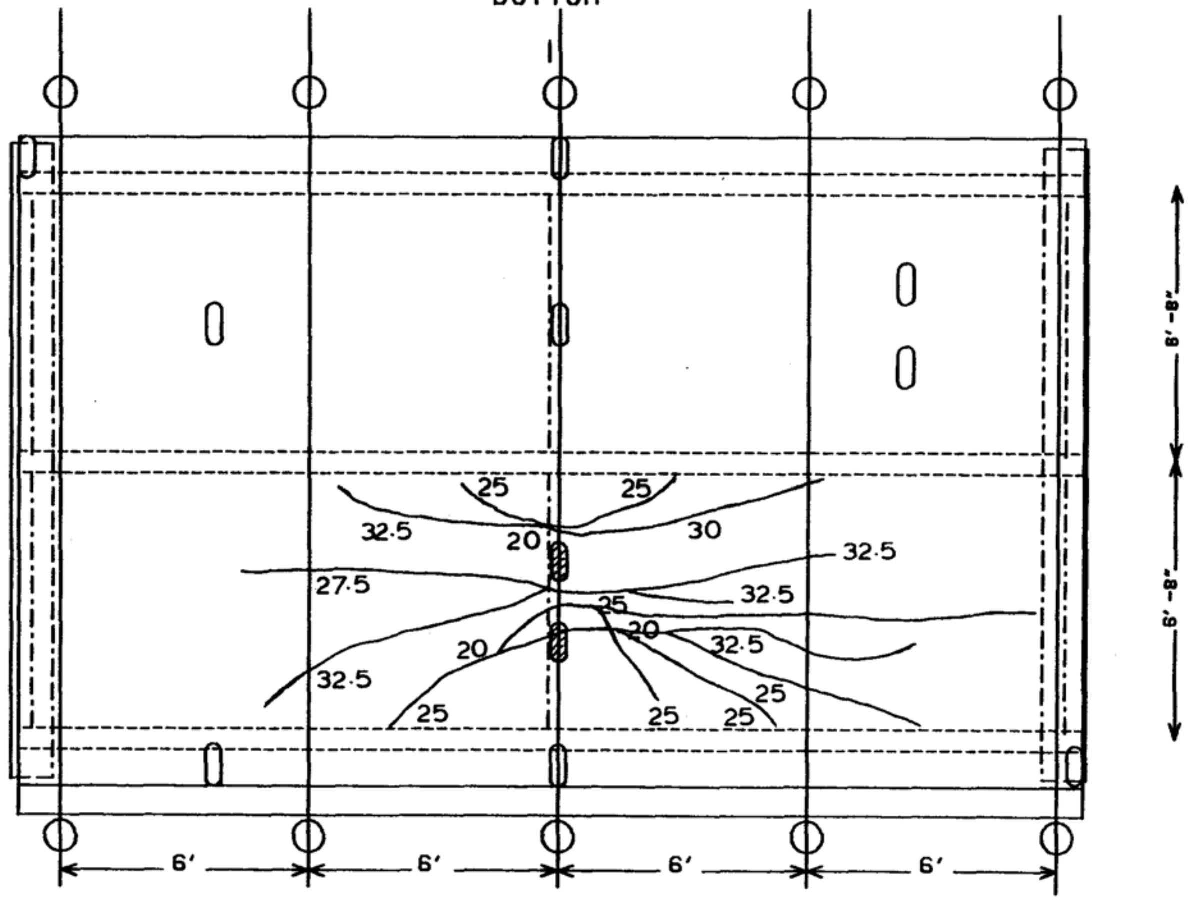

Figure E.8 Bottom Cracking Pattern (First Bridge - Test No. 4)

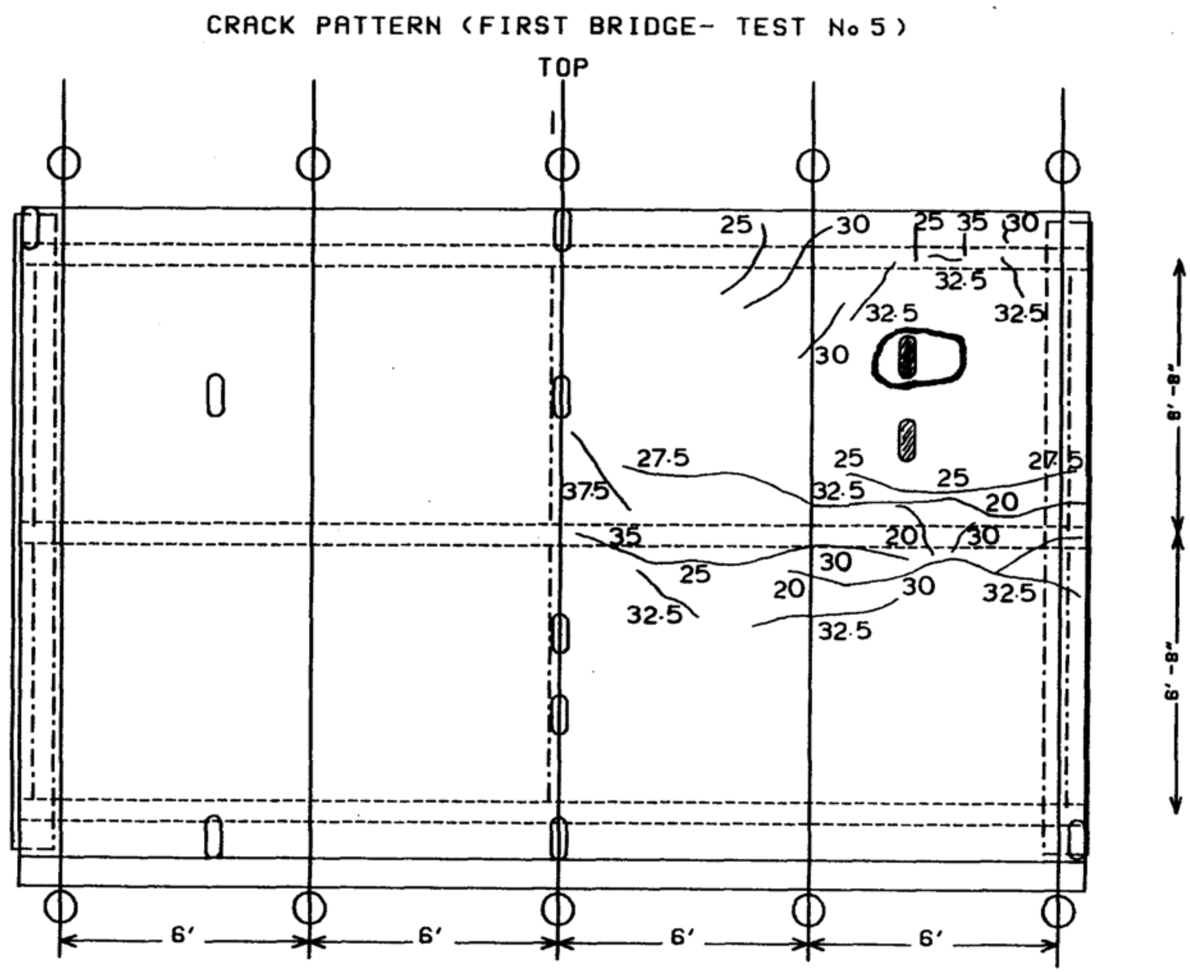

Figure E.9 Top Cracking Pattern (First Bridge - Test No. 5)

CRACK PATTERN (FIRST BRIDGE- TEST No 5)

BOTTOM

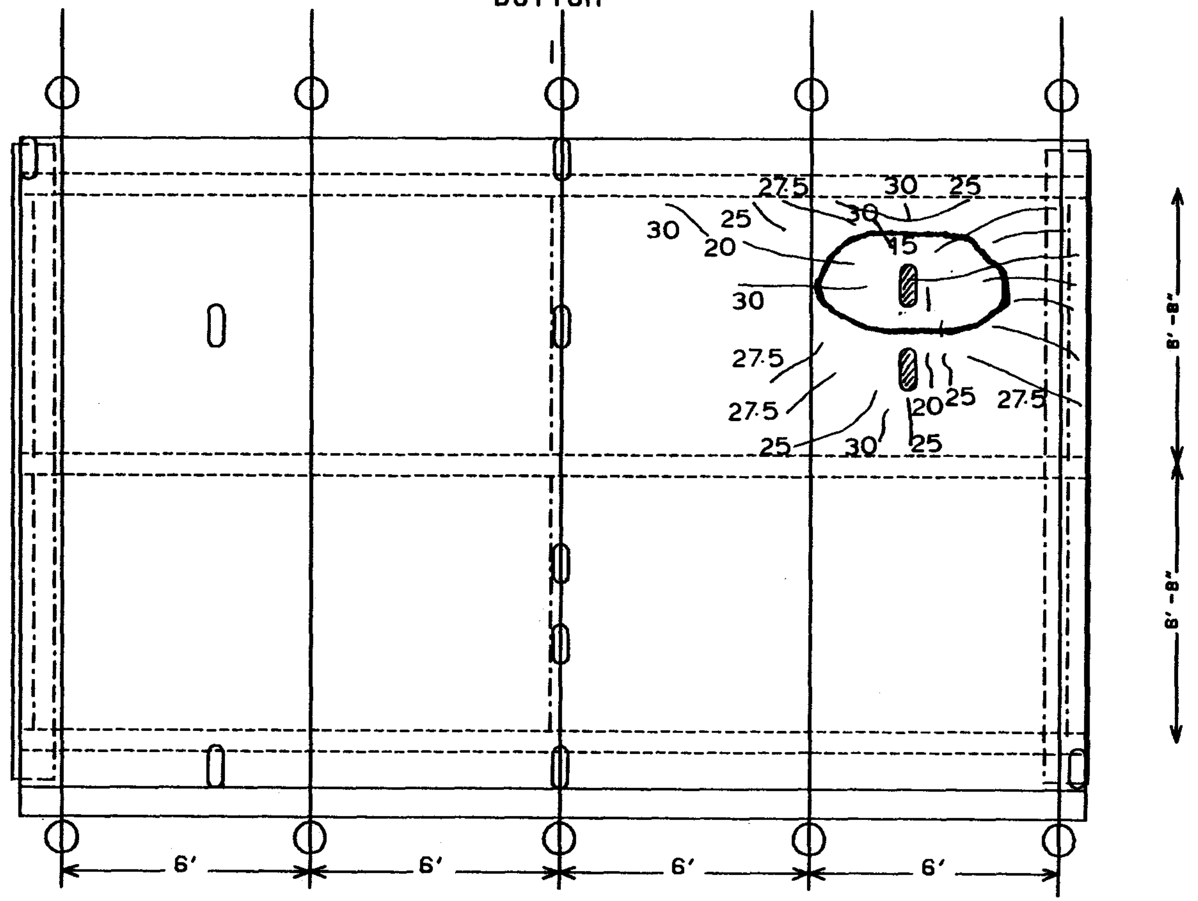

Figure E.10 Bottom Cracking Pattern (First Bridge - Test No. 5)

CRACK PATTERN (FIRST BRIDGE- TEST No 6)

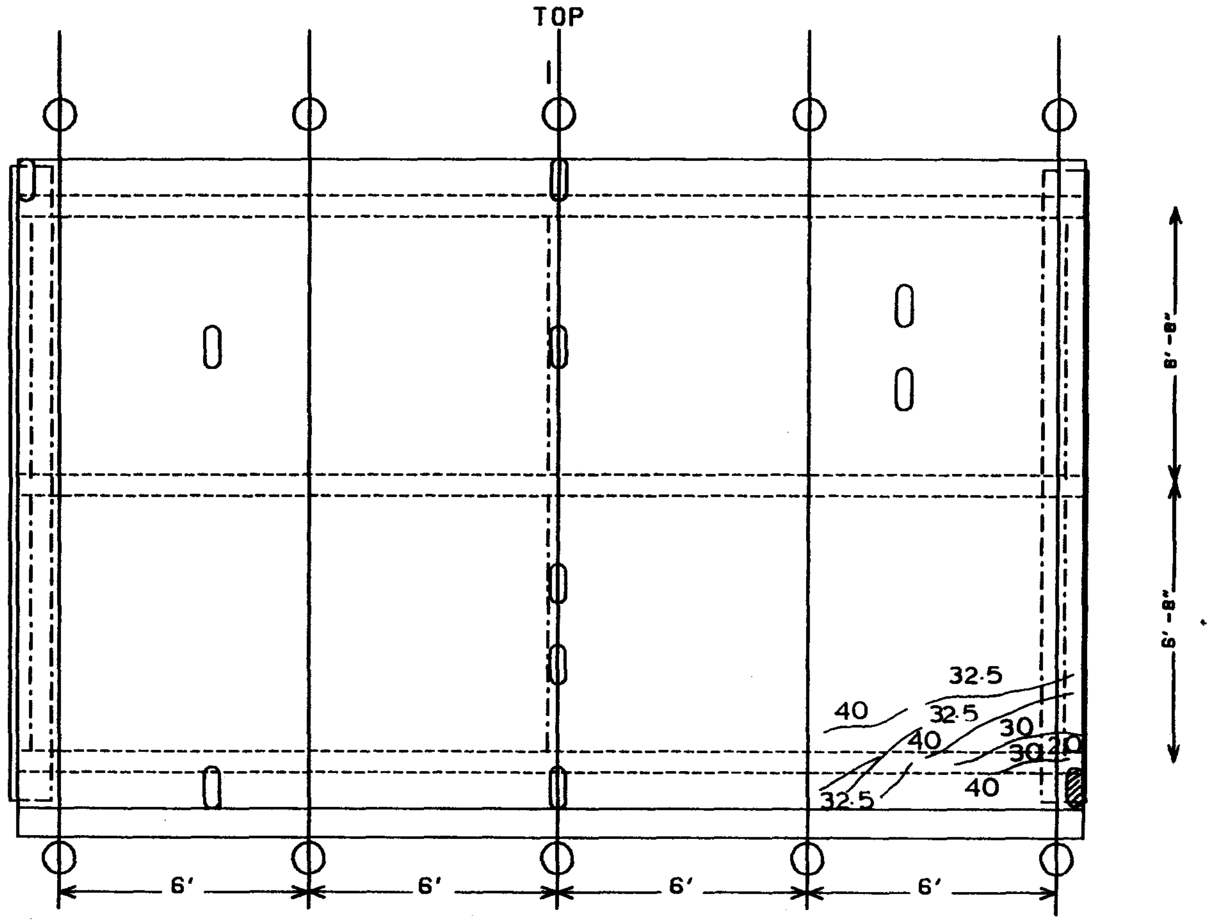

Figure E.11 Top Cracking Pattern (First Bridge - Test No. 6)

CRACK PATTERN (FIRST BRIDGE- TEST No 6)
BOTTOM

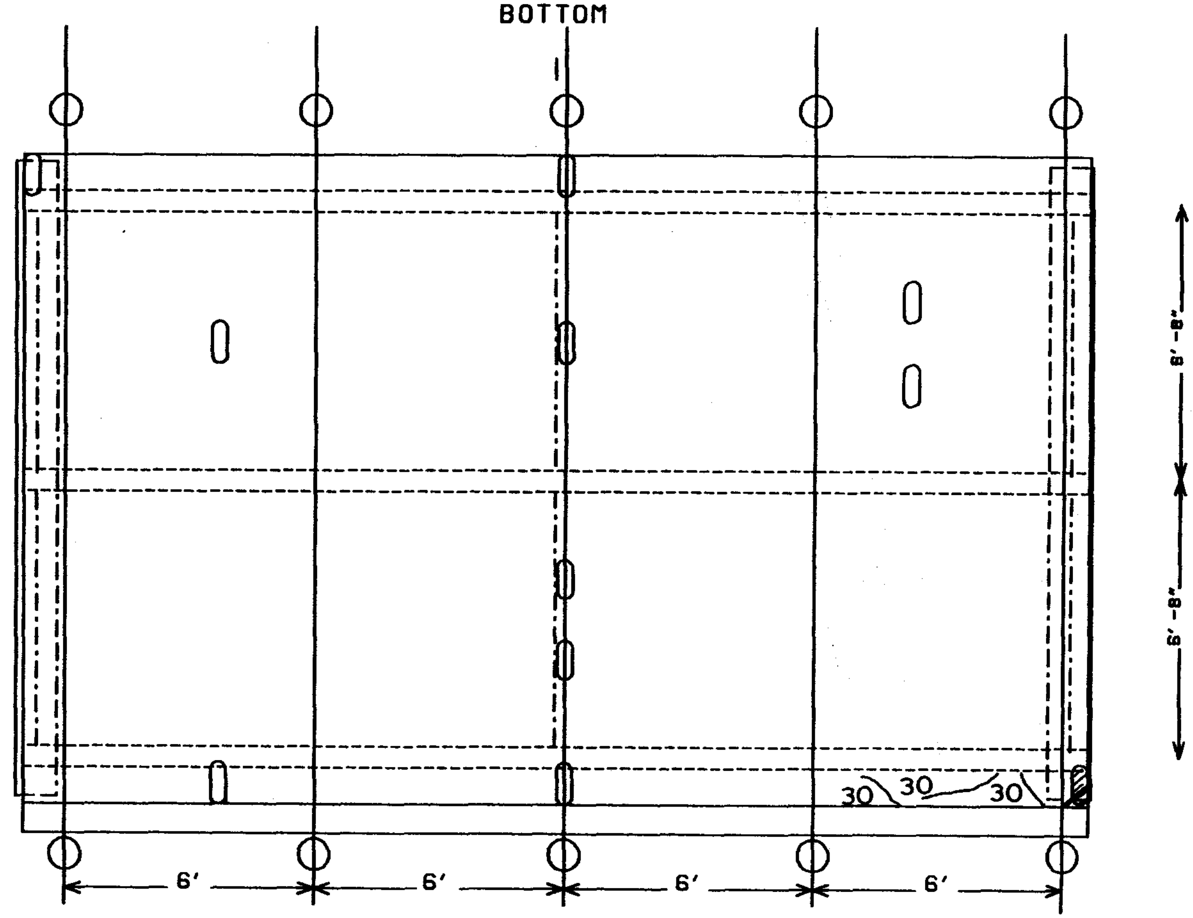

Figure E.12 Bottom Cracking Pattern (First Bridge - Test No. 6)

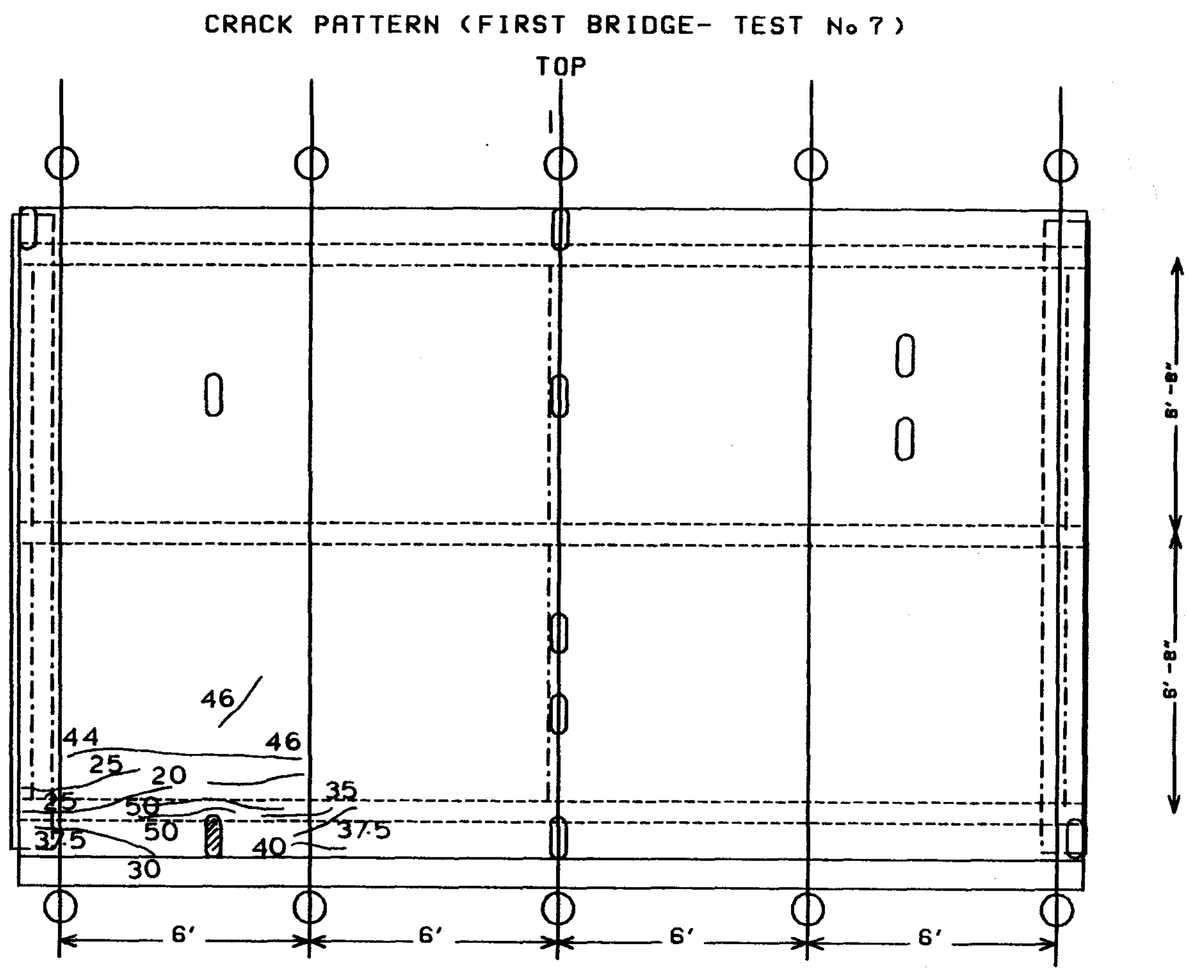

Figure E.13 Top Cracking Pattern (First Bridge - Test No. 7)

CRACK PATTERN (FIRST BRIDGE- TEST No 7)

BOTTOM

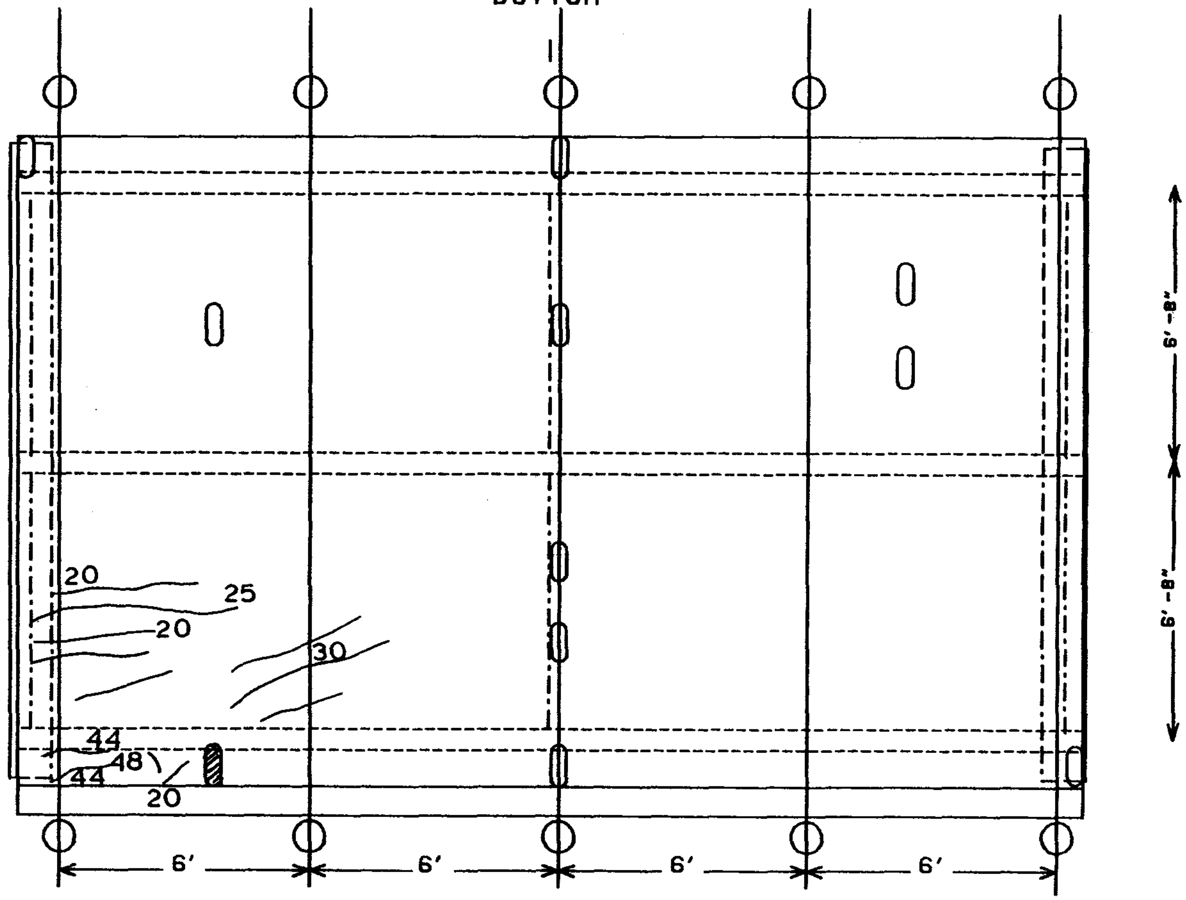

Figure E.14 Bottom Cracking Pattern (First Bridge - Test No. 7)

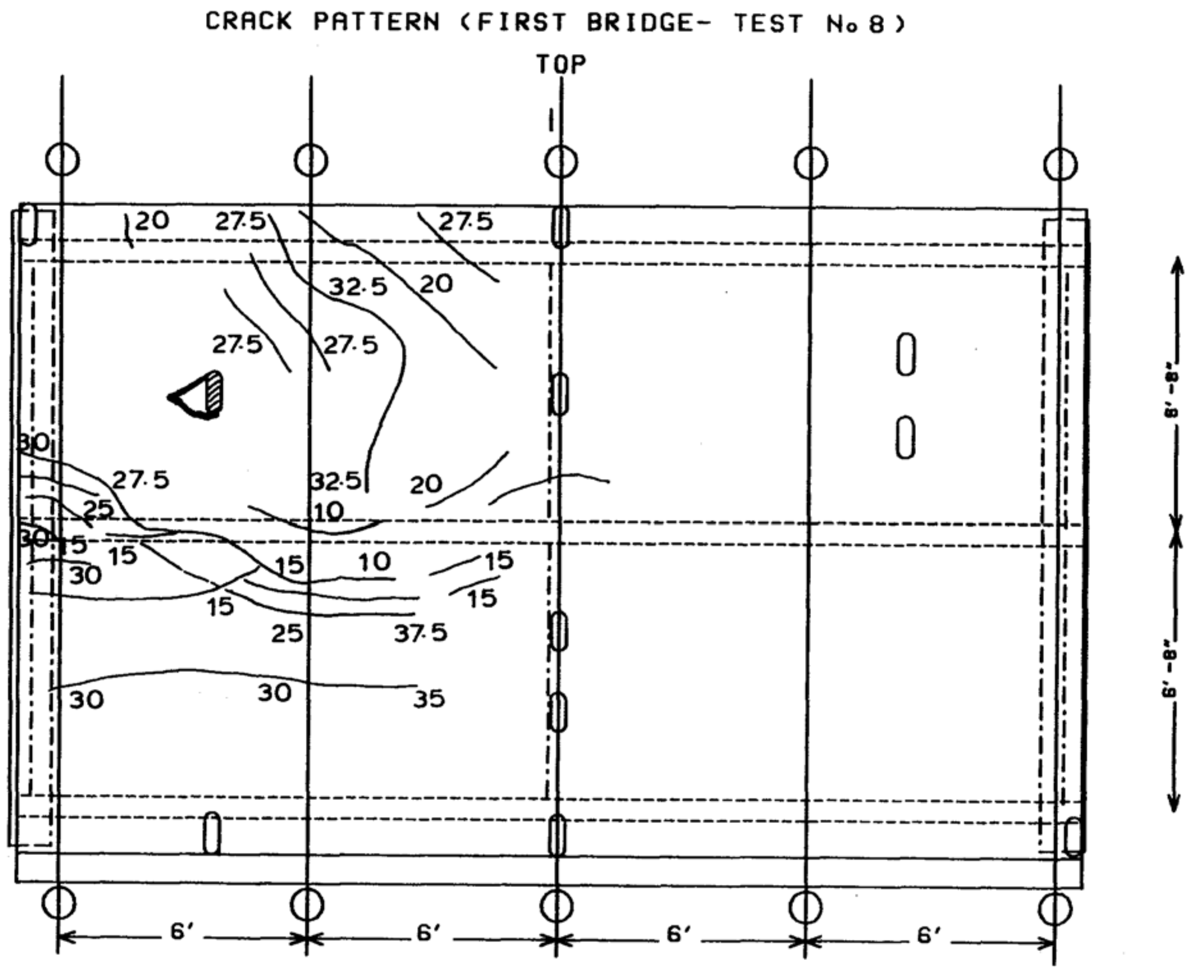

Figure E.15 Top Cracking Pattern (First Bridge - Test No. 8)

CRACK PATTERN (FIRST BRIDGE- TEST No 8)
BOTTOM

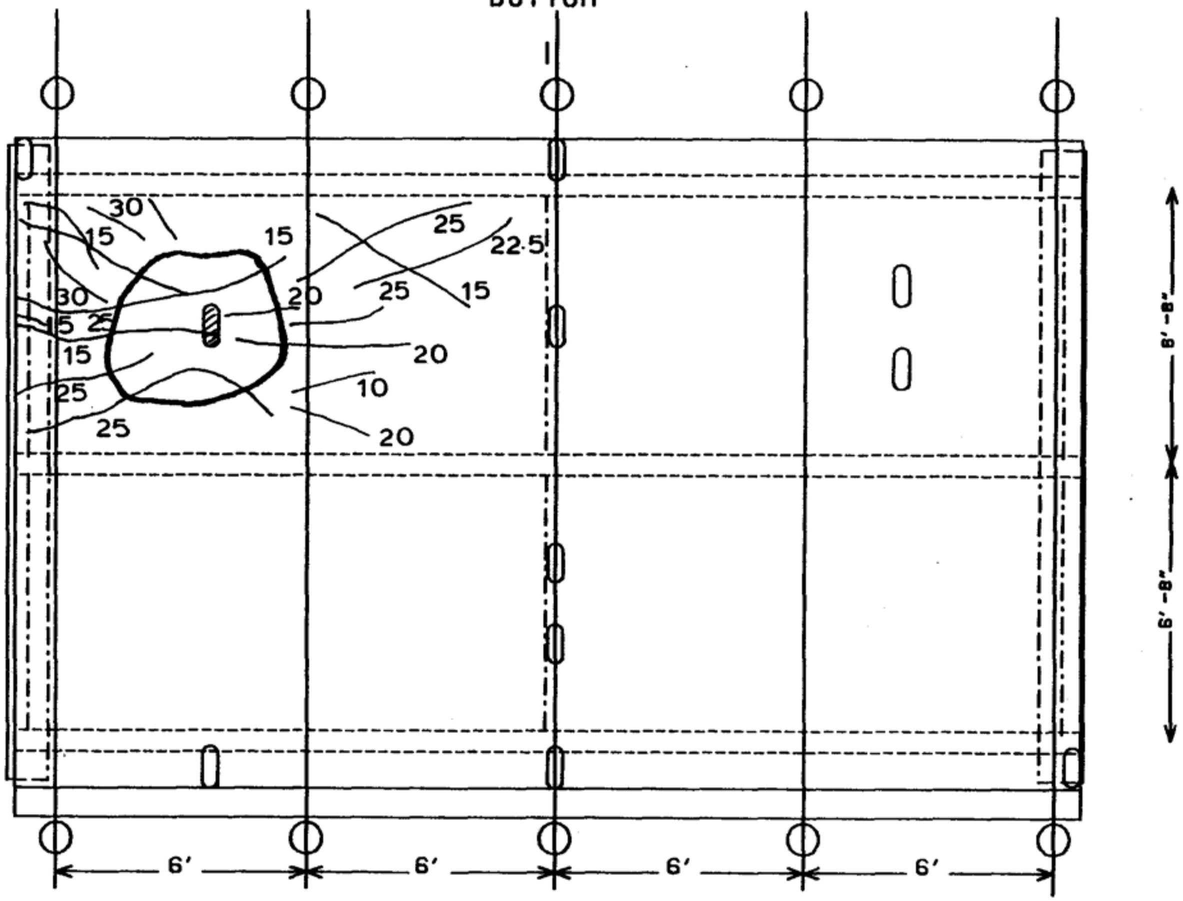

Figure E.16 Bottom Cracking Pattern (First Bridge - Test No. 8)

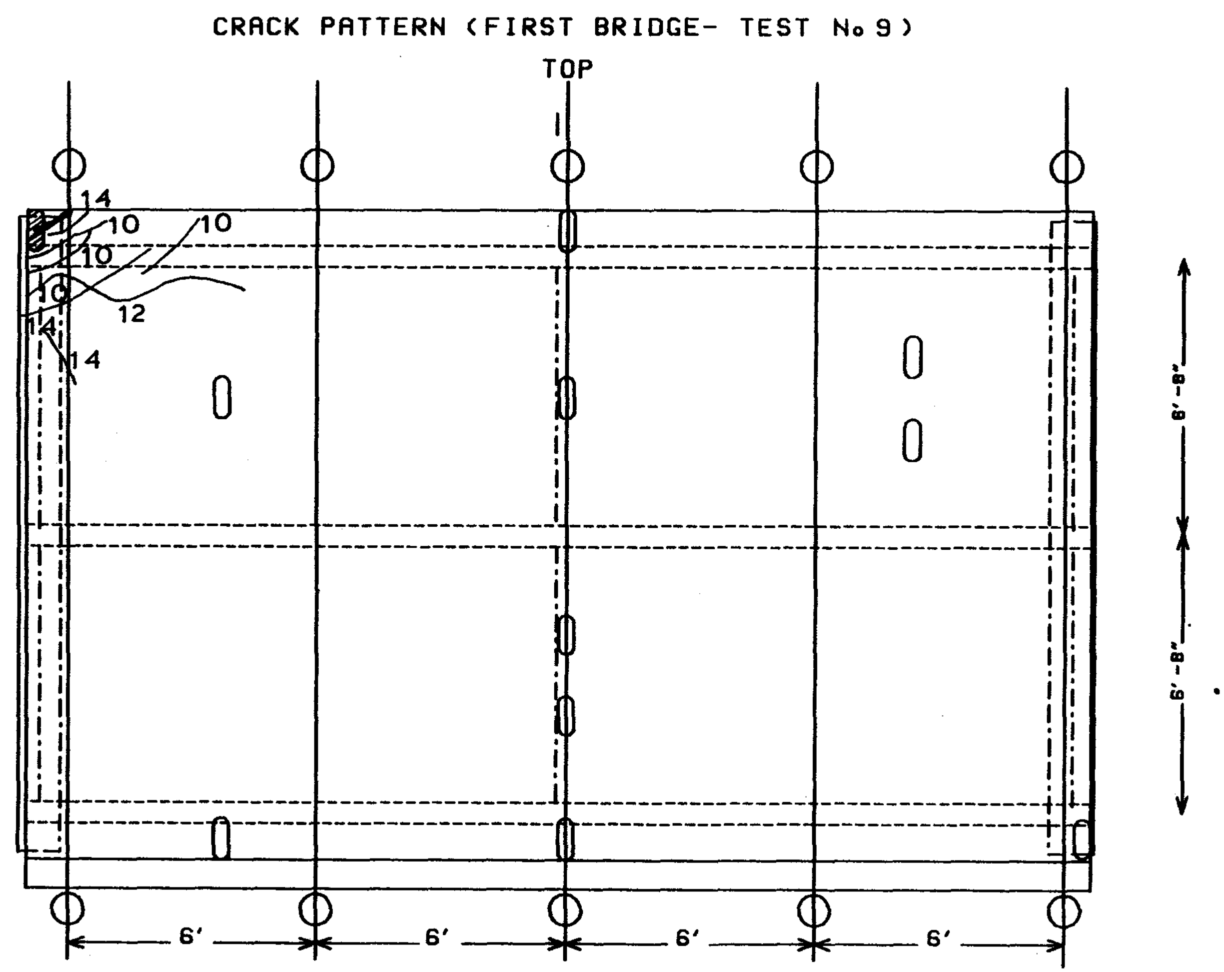

Figure E.17 Top Cracking Pattern (First Bridge - Test No. 9)

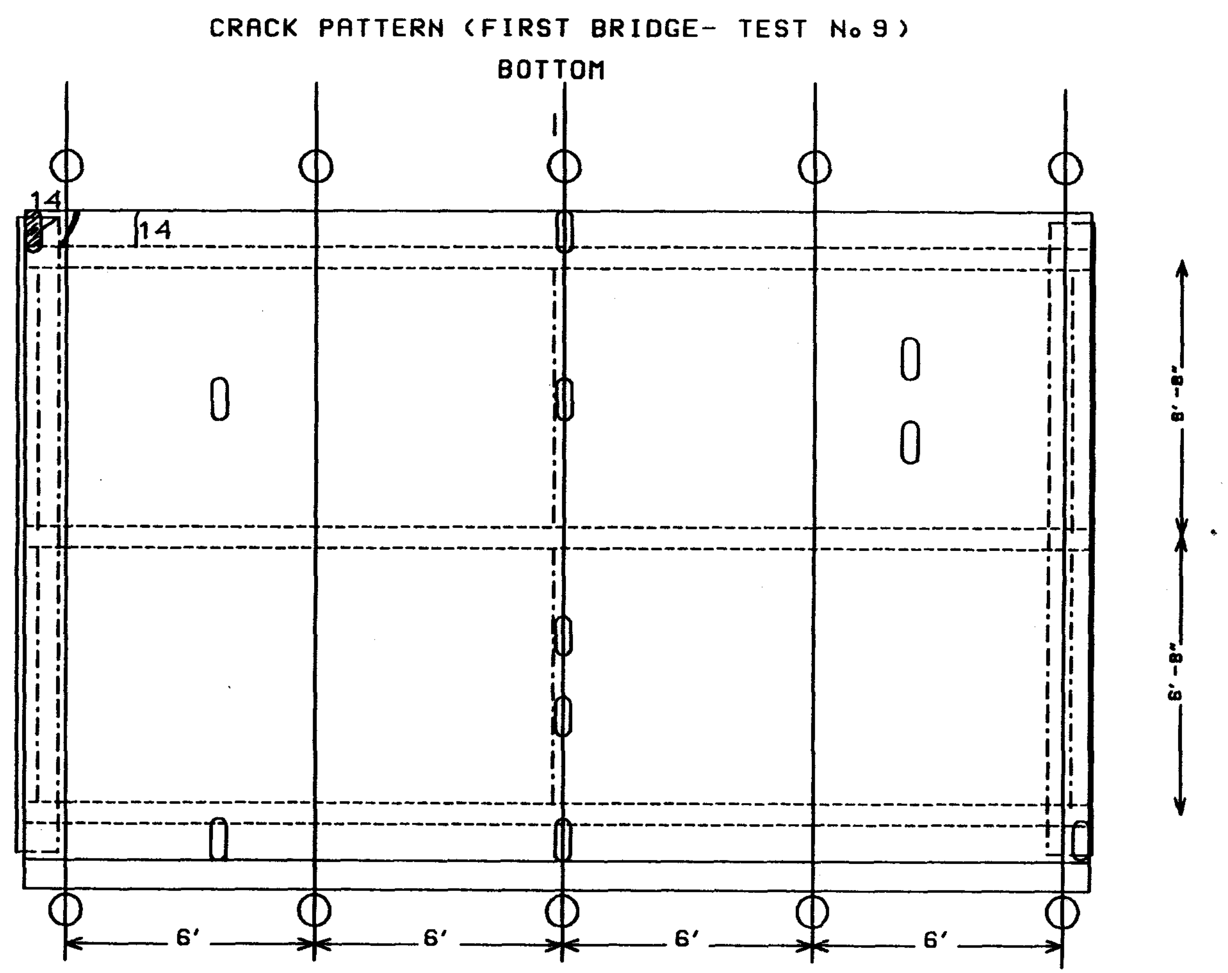

Figure E.18 Bottom Cracking Pattern (First Bridge - Test No. 9)

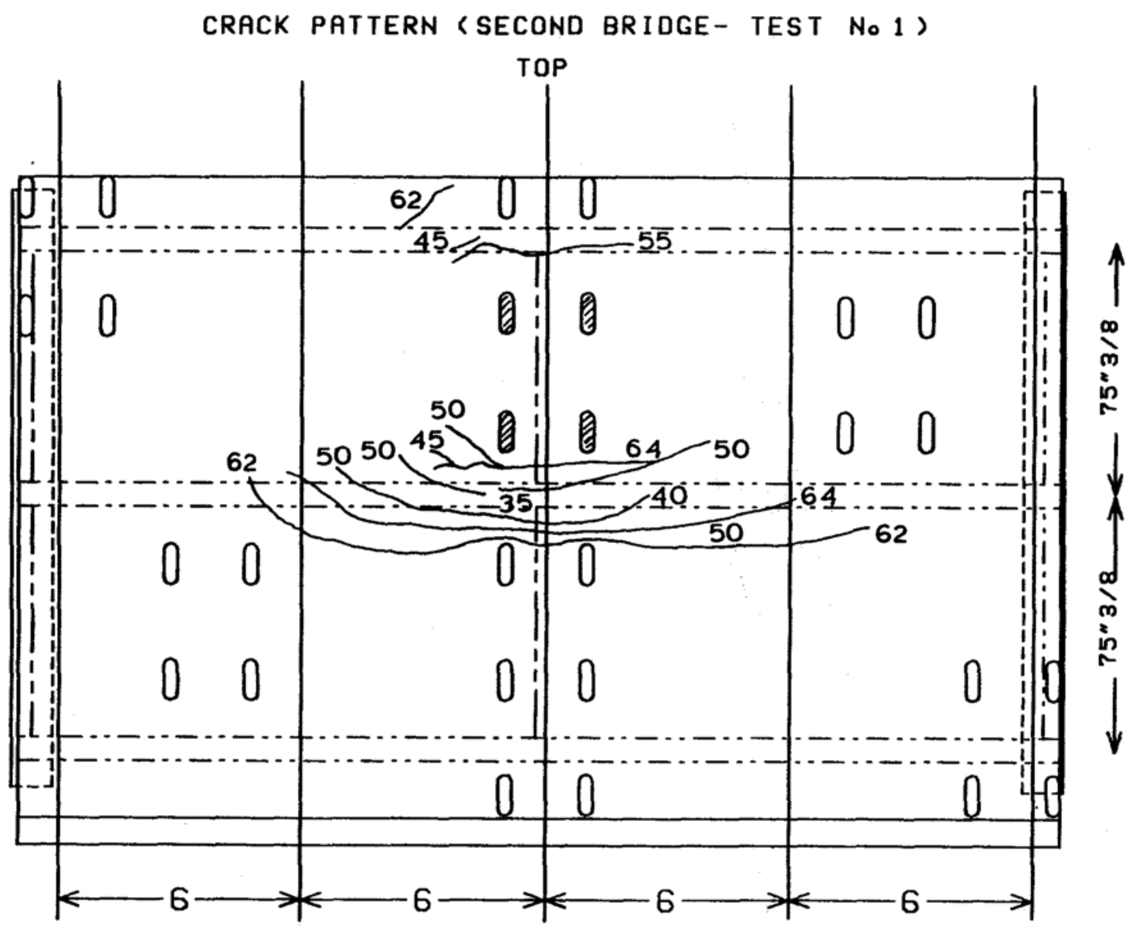

Figure E.19 Top Cracking Pattern (Second Bridge - Test No. 1)

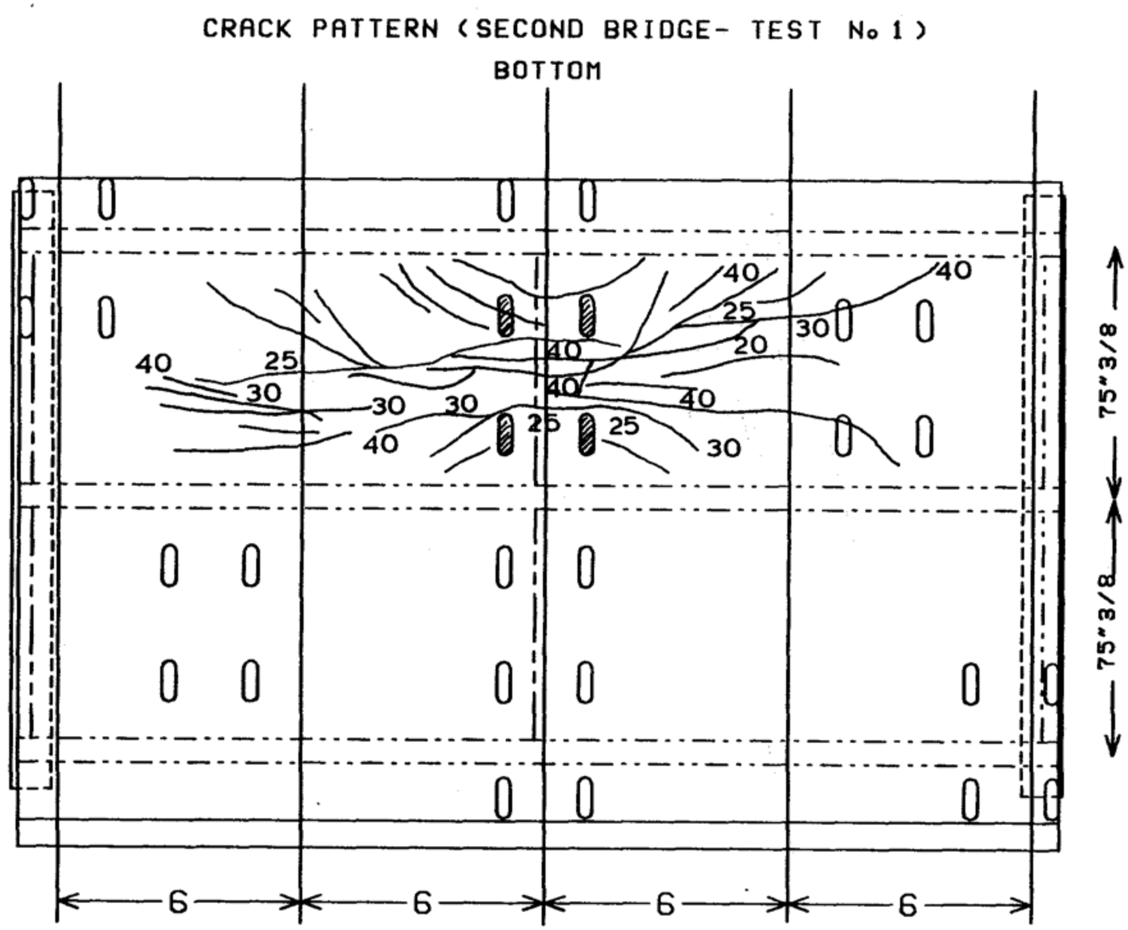

Figure E.20 Bottom Cracking Pattern (Second Bridge - Test No. 1)

CRACK PATTERN (SECOND BRIDGE- TEST No 2)

TOP

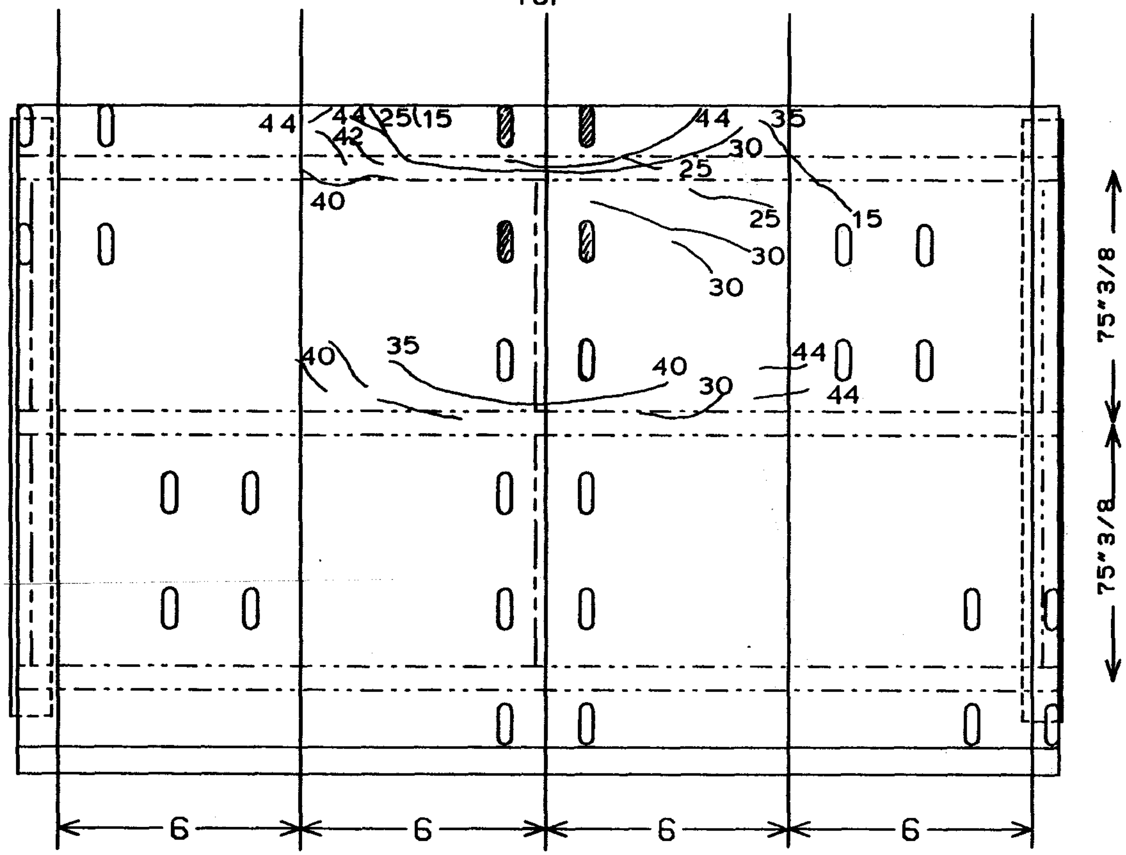

Figure E.21 Top Cracking Pattern (Second Bridge - Test No. 2)

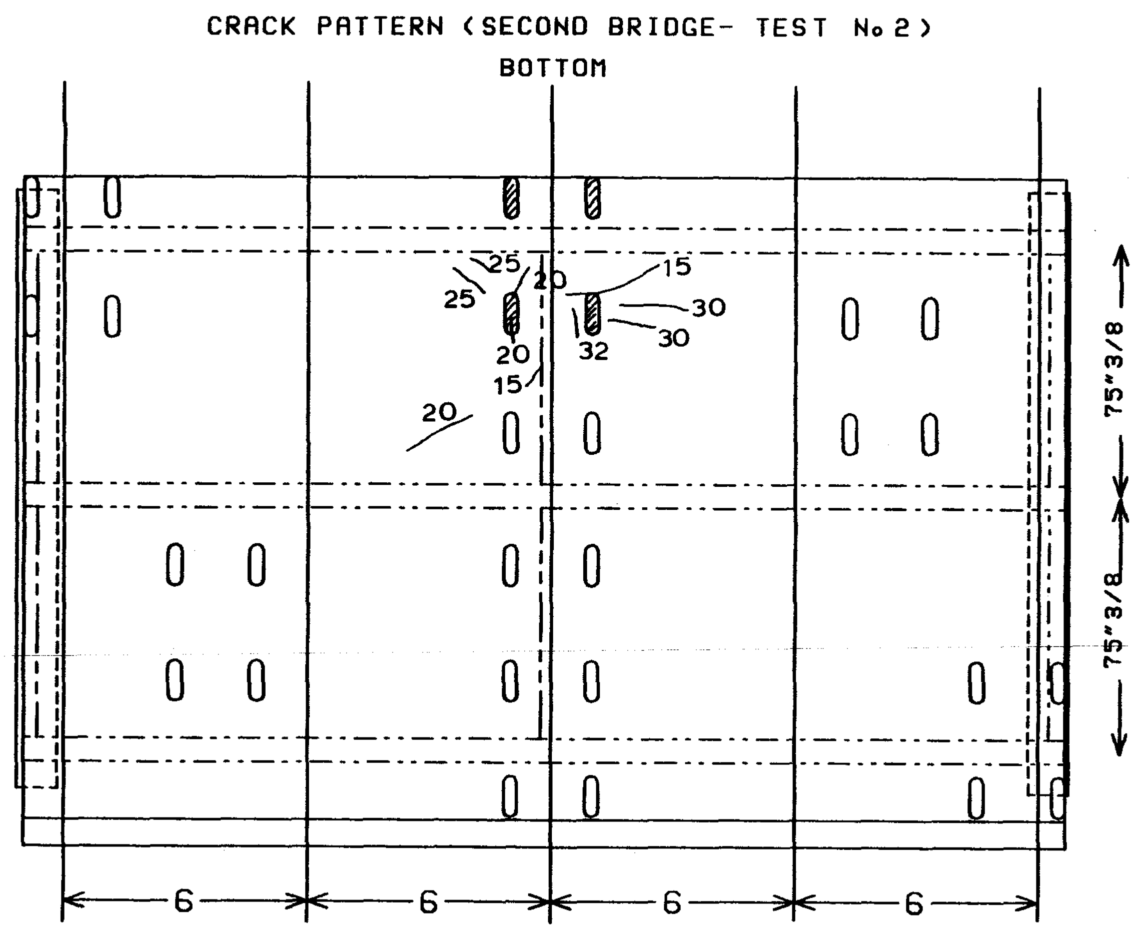

Figure E.22 Bottom Cracking Pattern (Second Bridge - Test No. 2)

CRACK PATTERN (SECOND BRIDGE- TEST No 3)

TOP

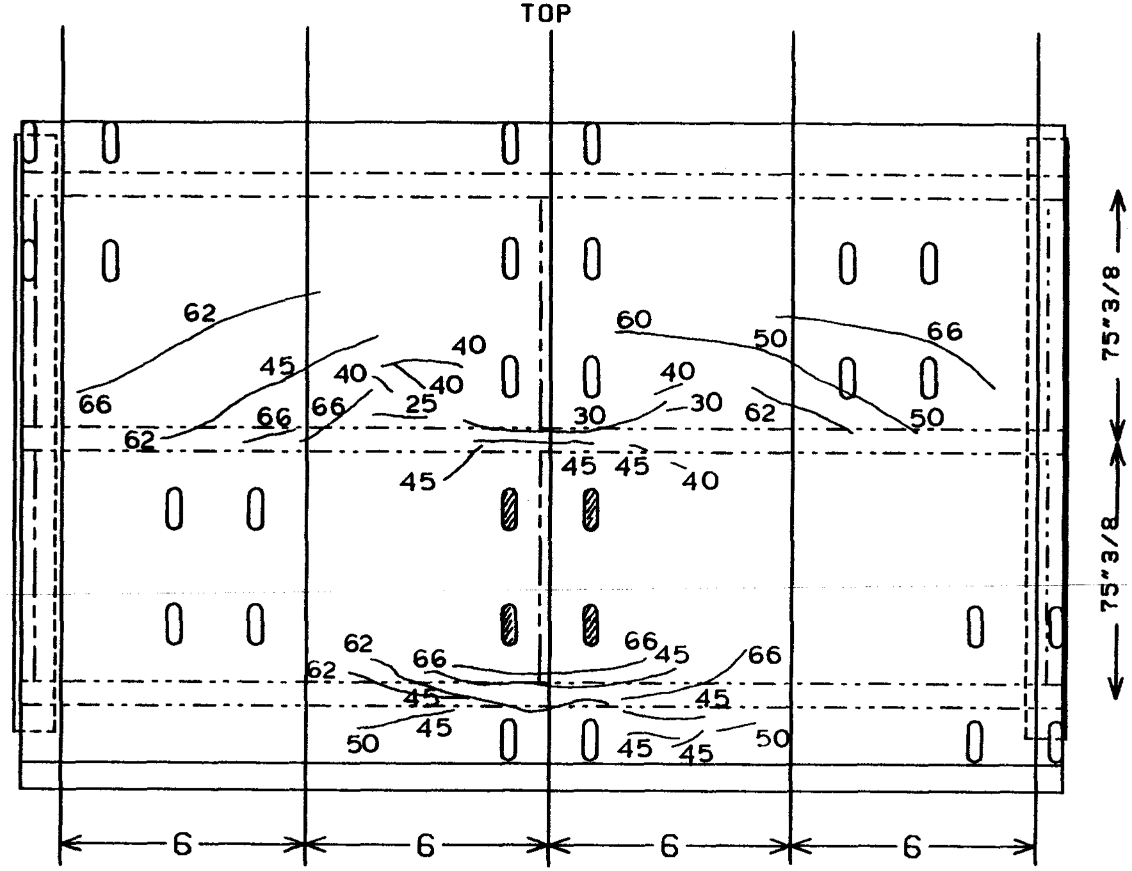

Figure E.23 Top Cracking Pattern (Second Bridge - Test No. 3)

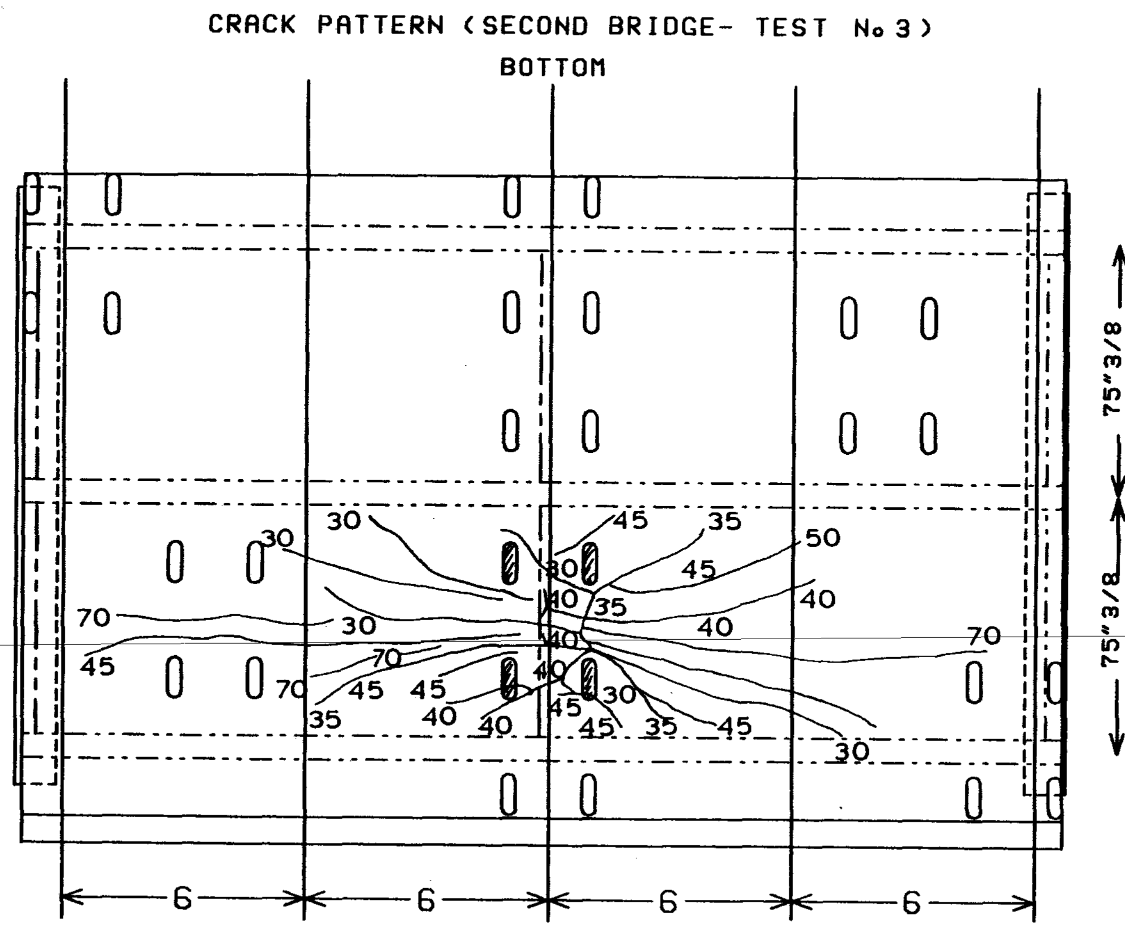

Figure E.24 Bottom Cracking Pattern (Second Bridge - Test No. 3)

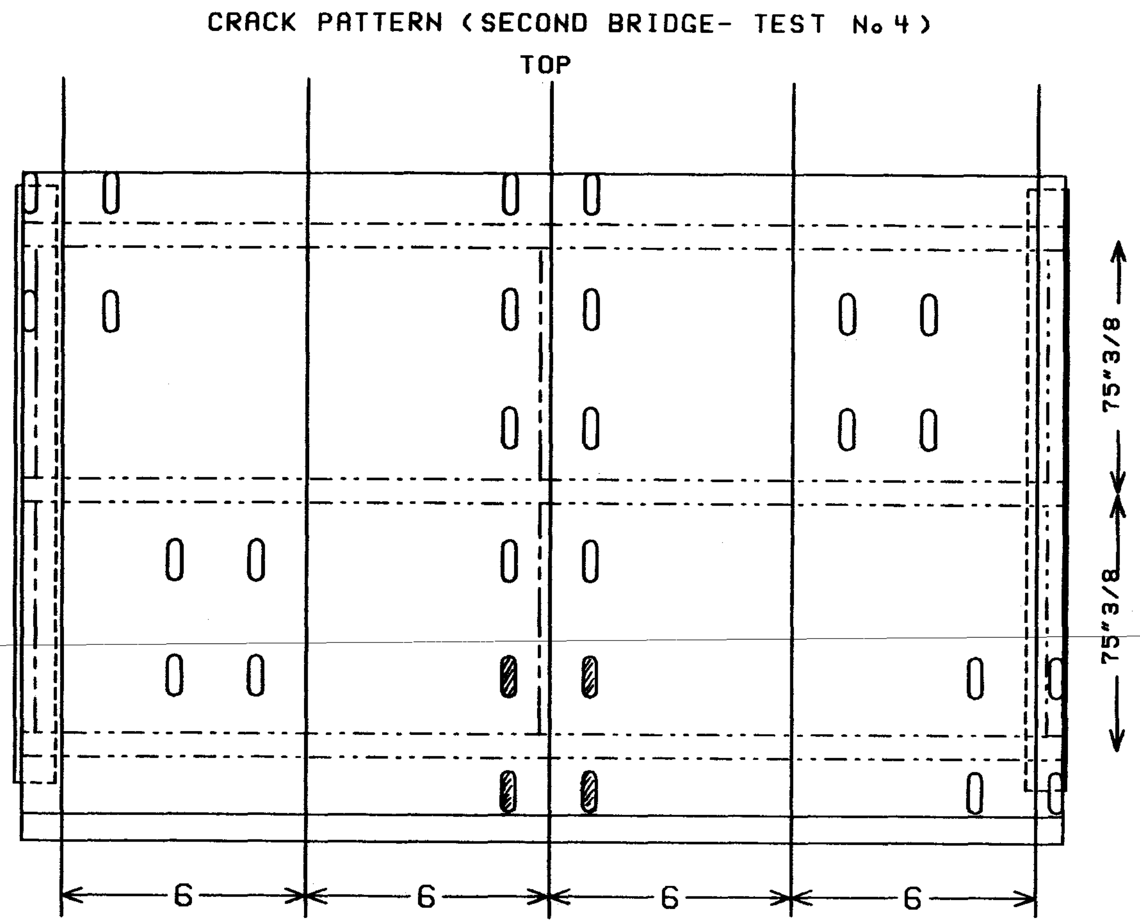

Figure E.25 Top Cracking Pattern (Second Bridge - Test No. 4)

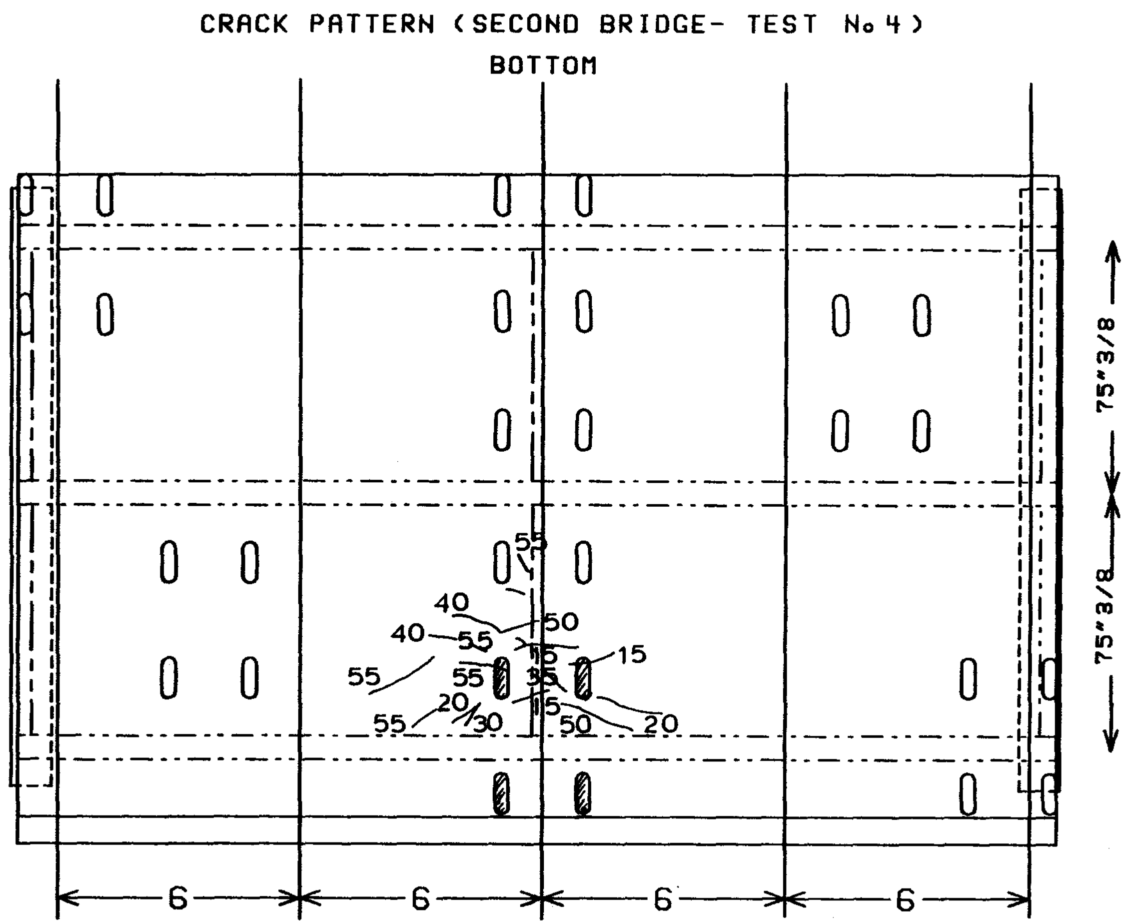

Figure E.26 Bottom Cracking Pattern (Second Bridge - Test No. 4)

CRACK PATTERN (SECOND BRIDGE- TEST No 5)

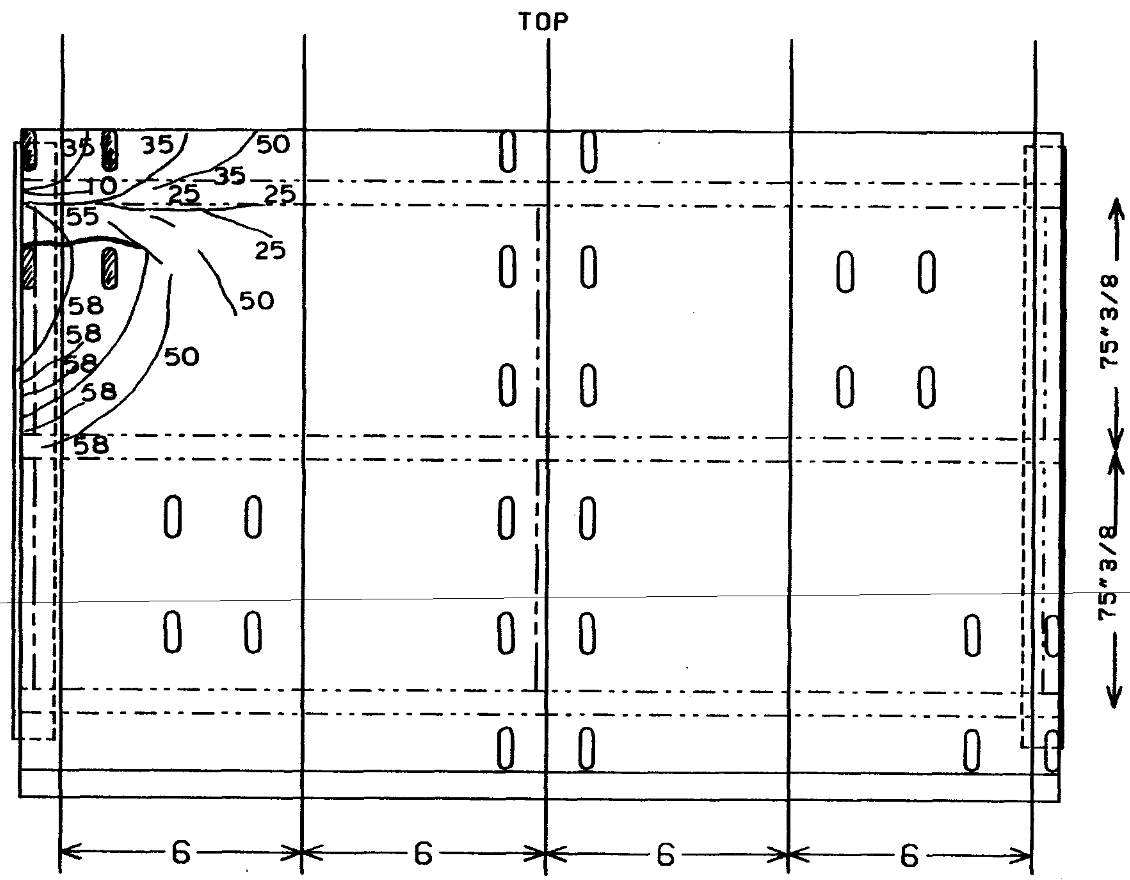

Figure E.27 Top Cracking Pattern (Second Bridge - Test No. 5)

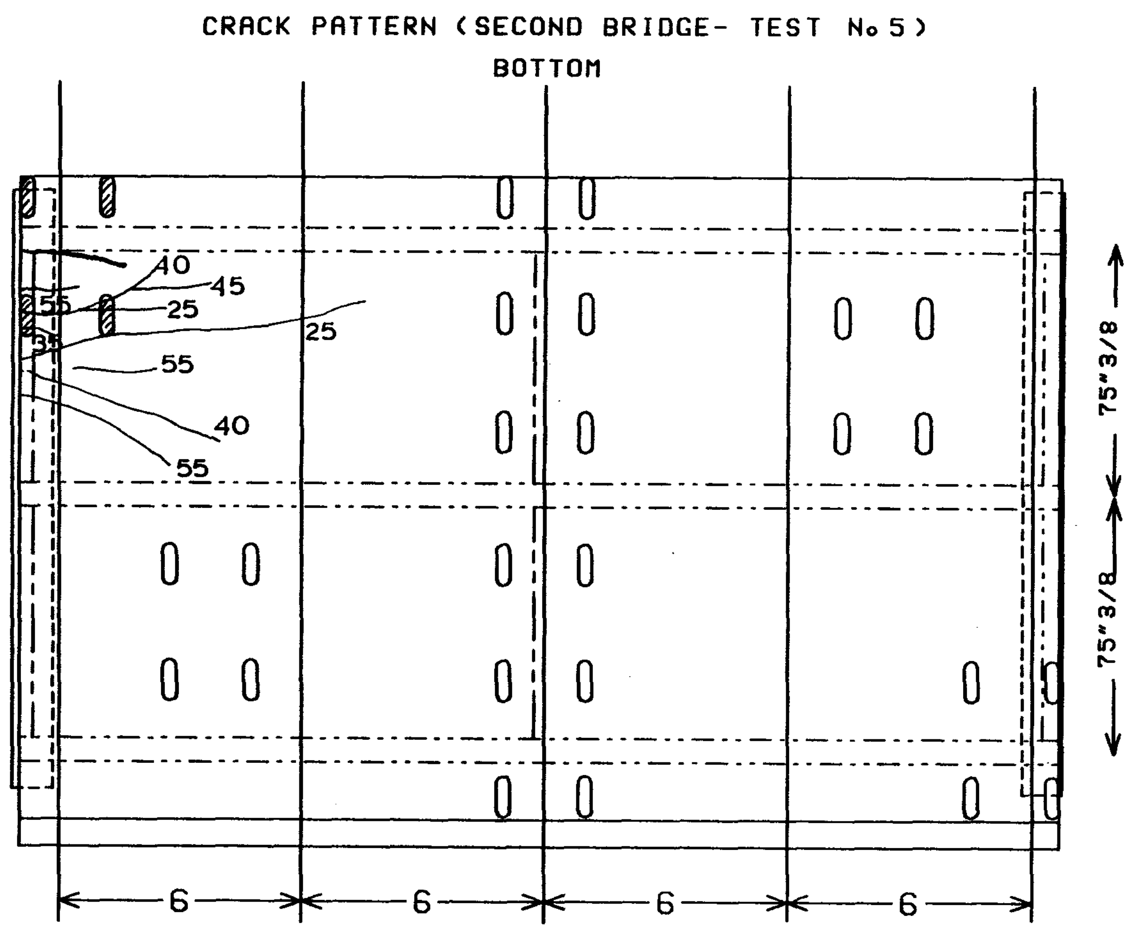

Figure E.28 Bottom Cracking Pattern (Second Bridge - Test No. 5)

CRACK PATTERN (SECOND BRIDGE- TEST No 6)

TOP

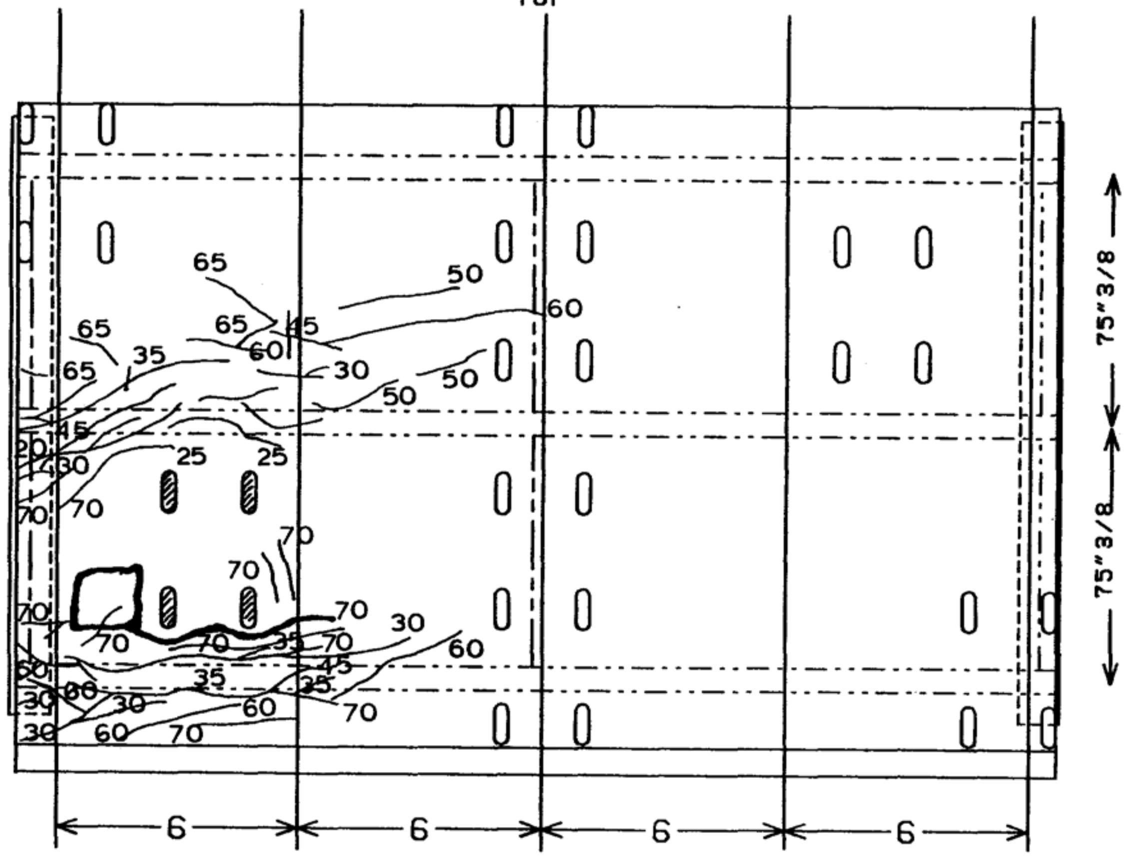

Figure E.29 Top Cracking Pattern (Second Bridge - Test No. 6)

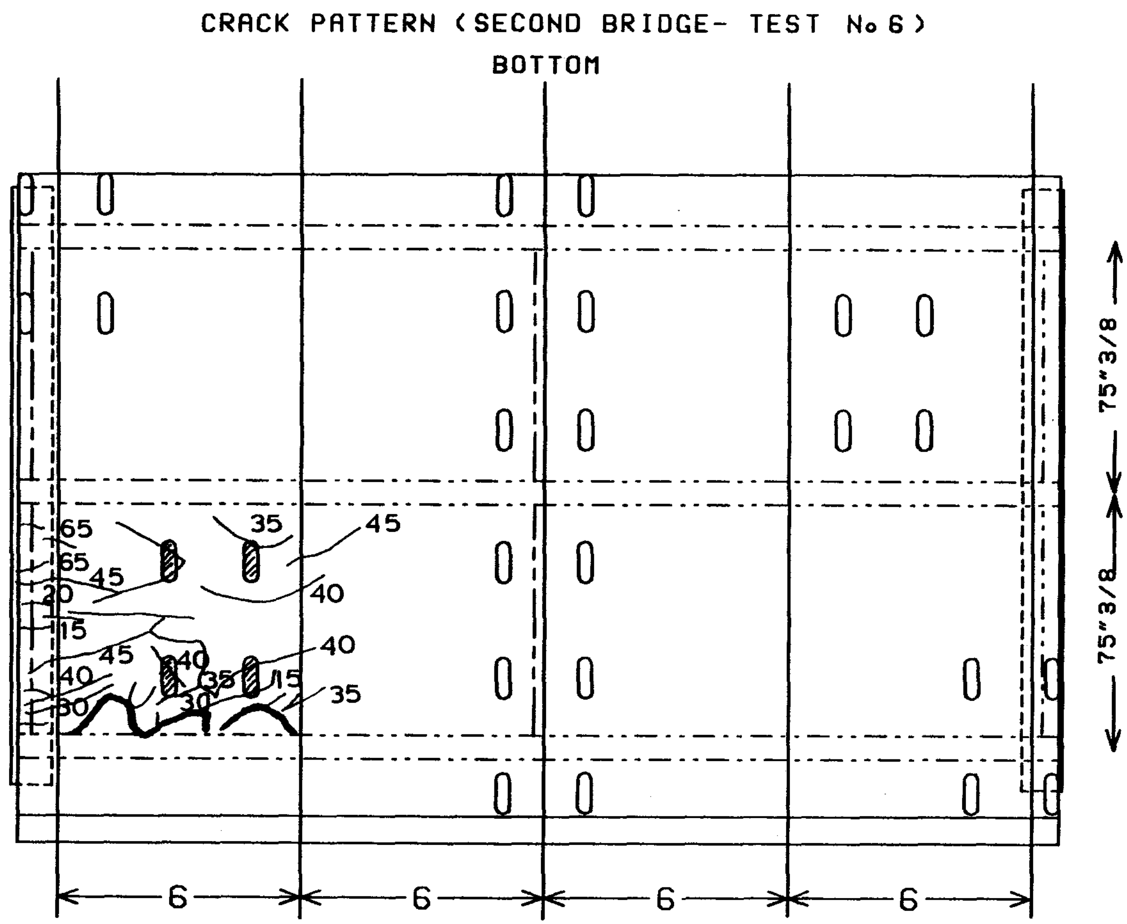

Figure E.30 Bottom Cracking Pattern (Second Bridge - Test No. 6)

CRACK PATTERN (SECOND BRIDGE- TEST No 7)

TOP

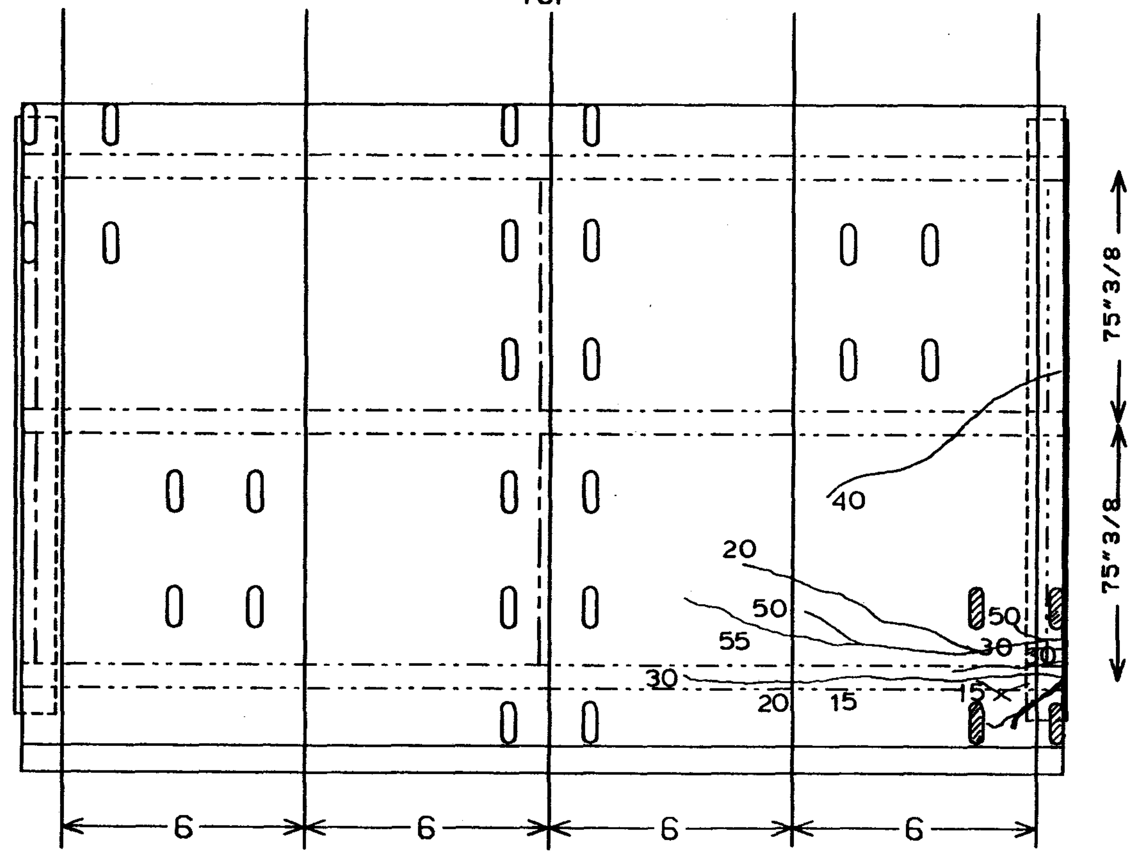

Figure E.31 Top Cracking Pattern (Second Bridge - Test No. 7)

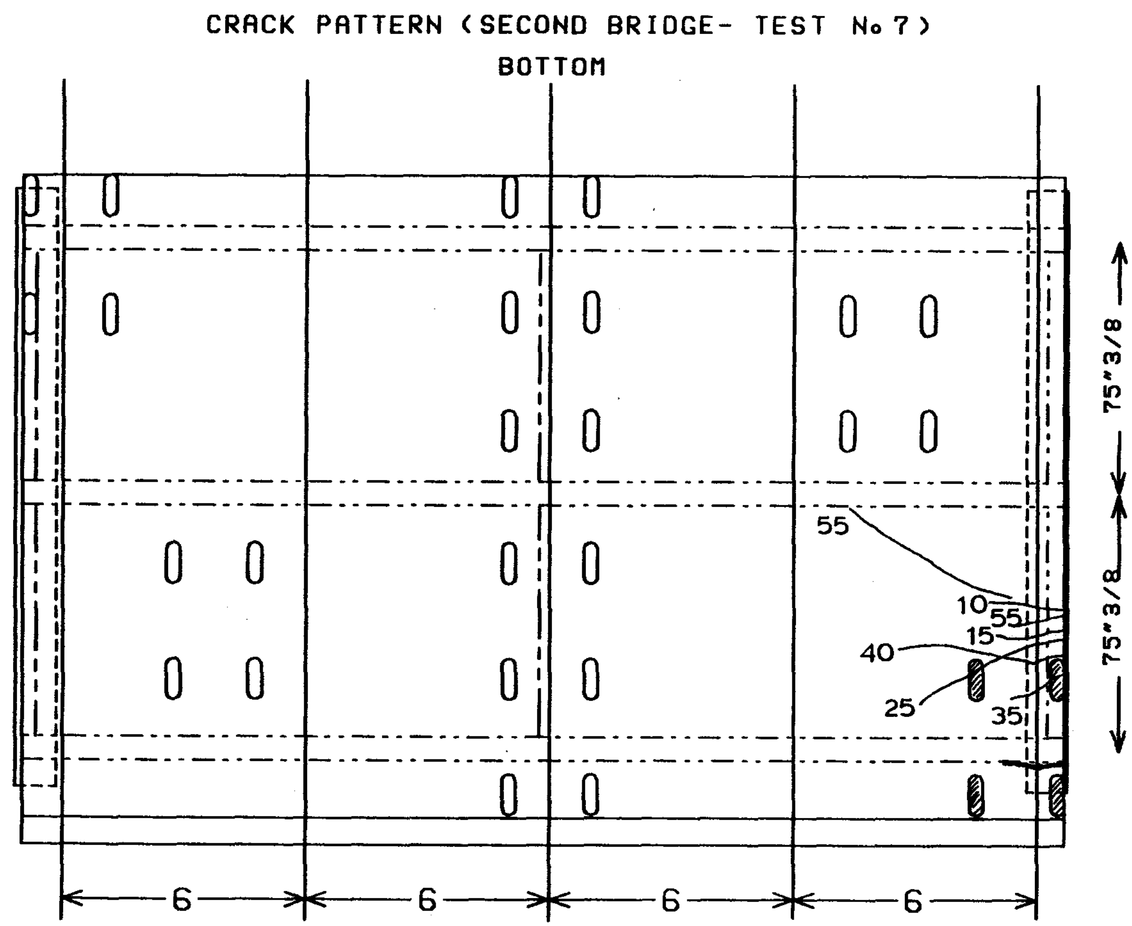

Figure E.32 Bottom Cracking Pattern (Second Bridge - Test No. 7)

CRACK PATTERN (SECOND BRIDGE- TEST No 8)
BOTTOM

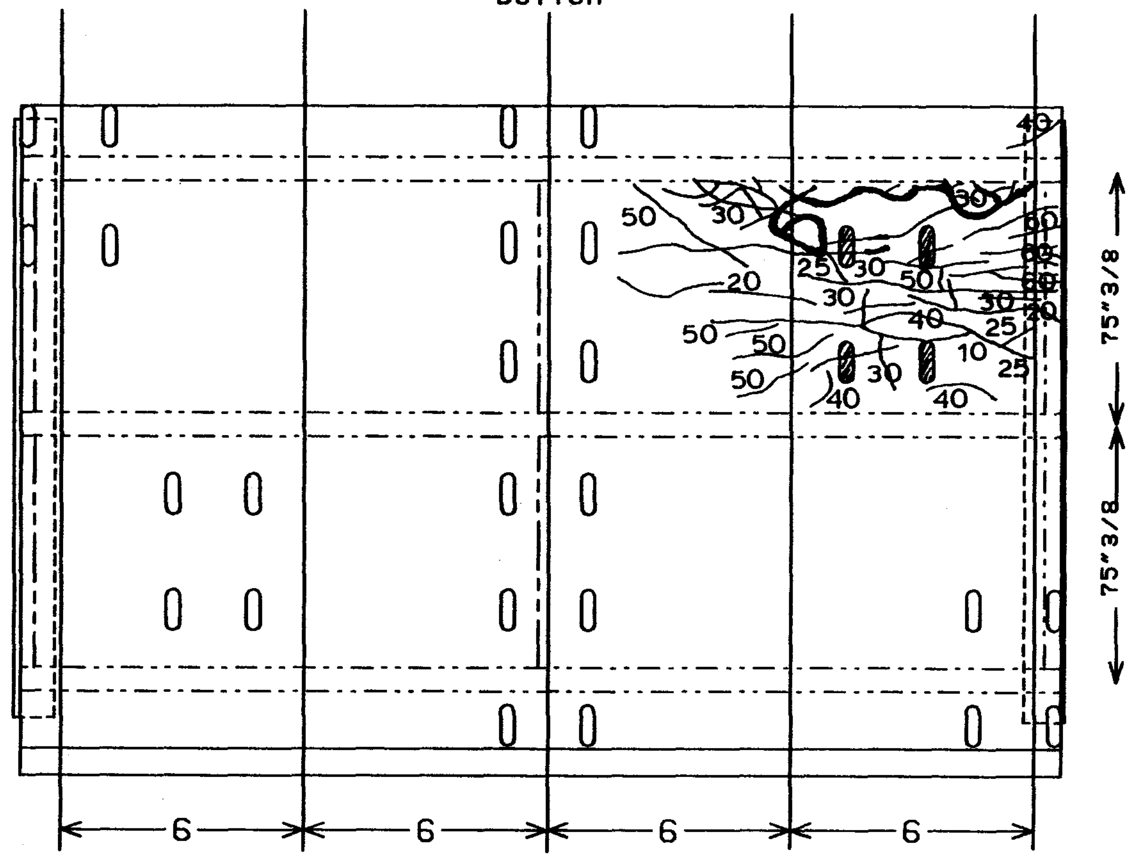

Figure E.34 Bottom Cracking Pattern (Second Bridge - Test No. 8)

CRACK PATTERN (SECOND BRIDGE- TEST No 8)

TOP

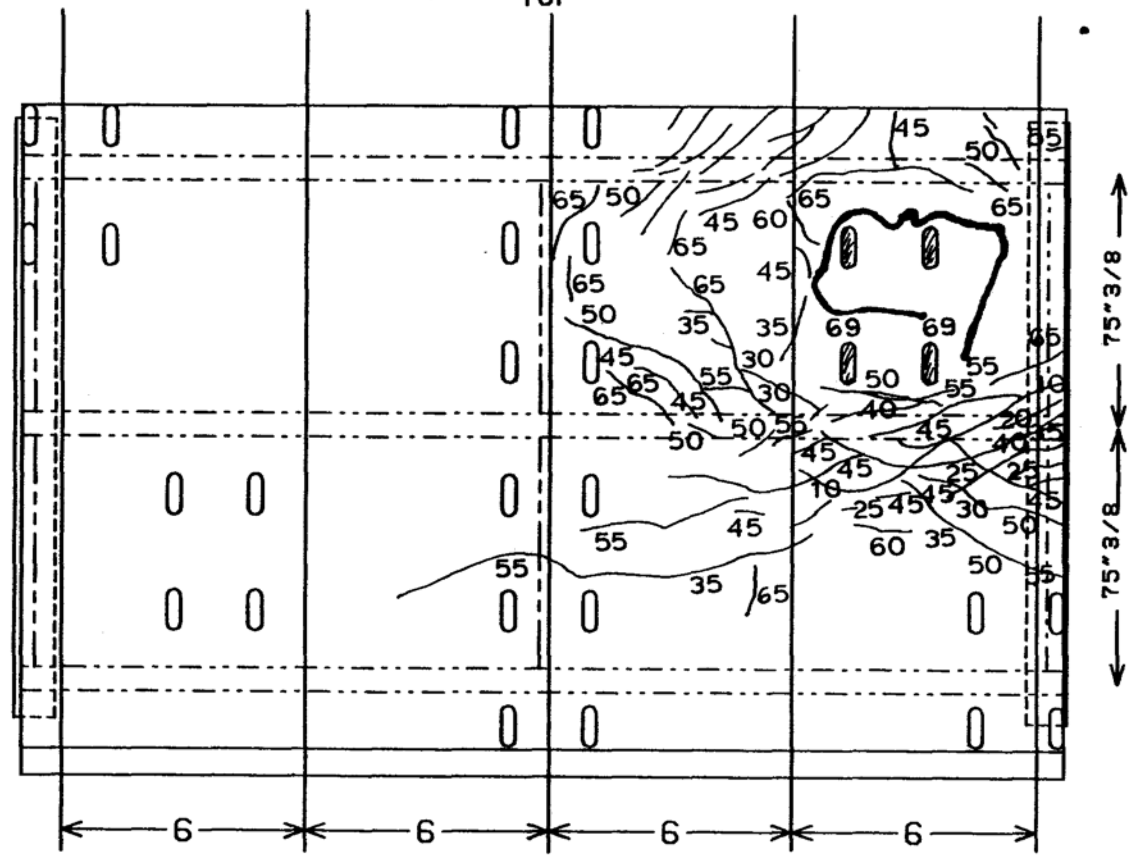

Figure E.33 Top Cracking Pattern (Second Bridge - Test No. 8)

CRACK PATTERN (THIRD BRIDGE -TEST No 1)

TOP

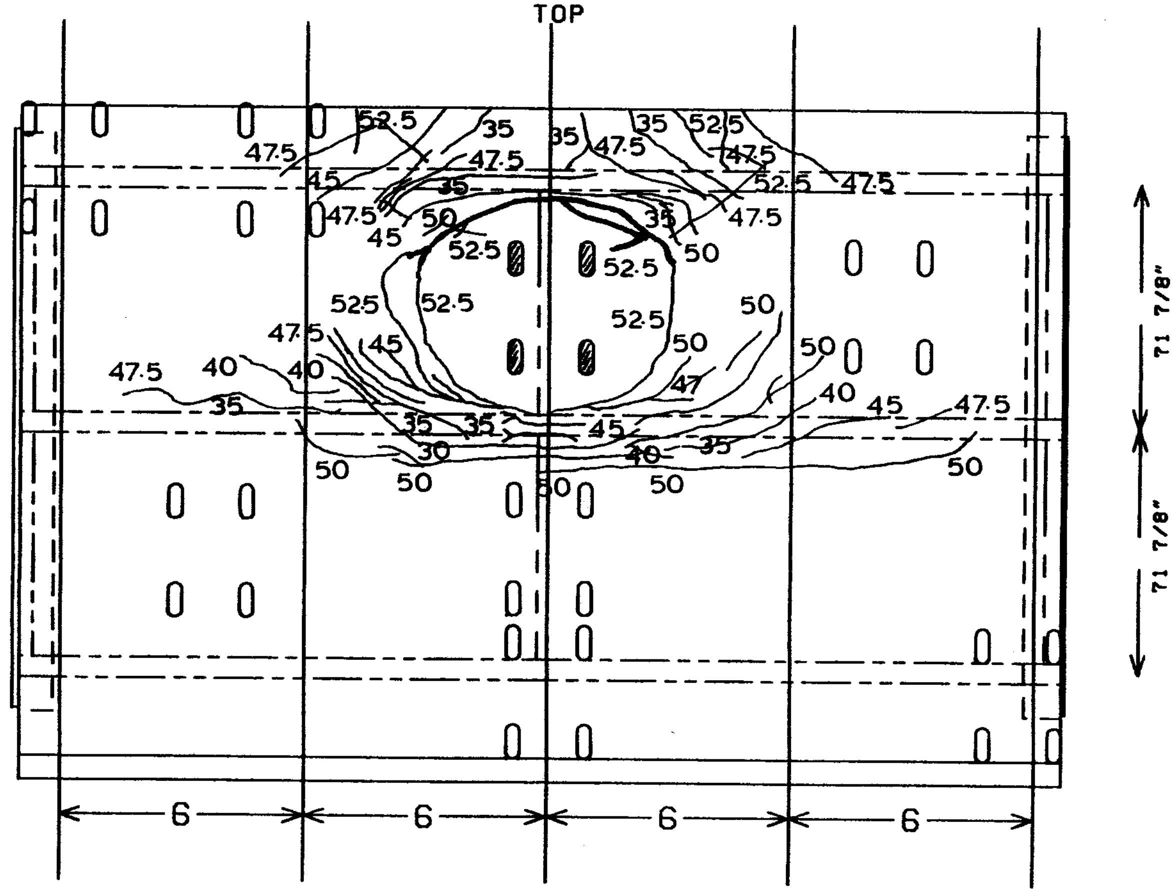

Figure E.35 Top Cracking Pattern (Third Bridge - Test No. 1)

CRACK PATTERN (THIRD BRIDGE -TEST No 1)

BOTTOM

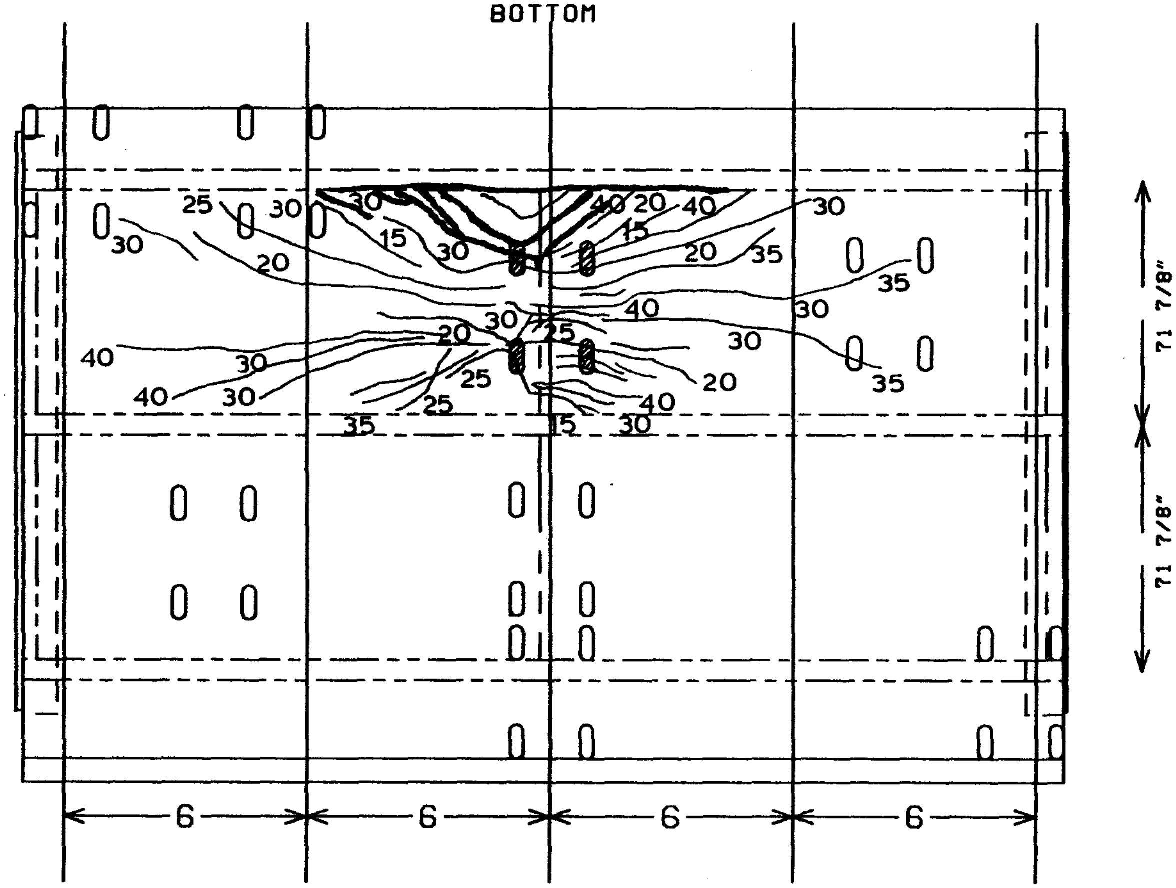

Figure E.36 Bottom Cracking Pattern (Third Bridge - Test No. 1)

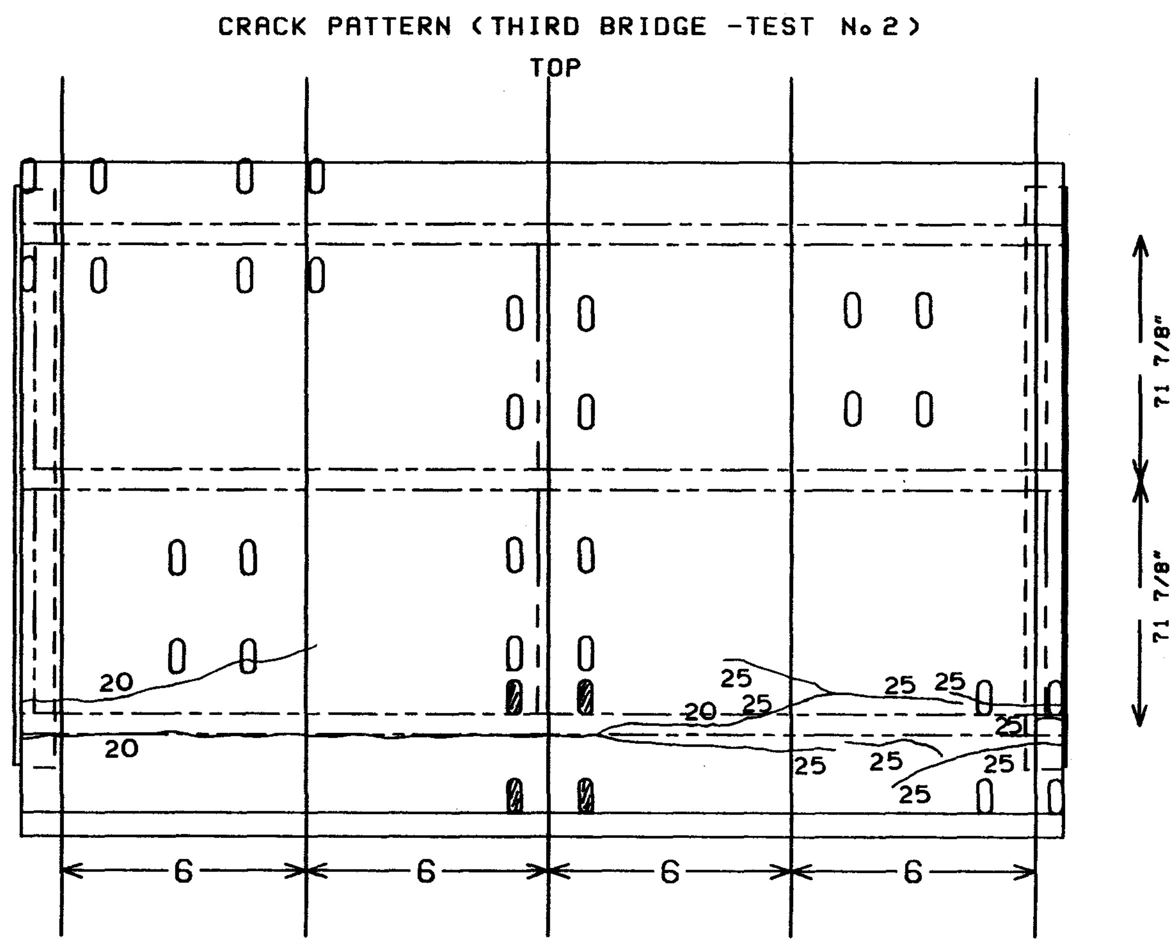

Figure E.37 Top Cracking Pattern (Third Bridge - Test No. 2)

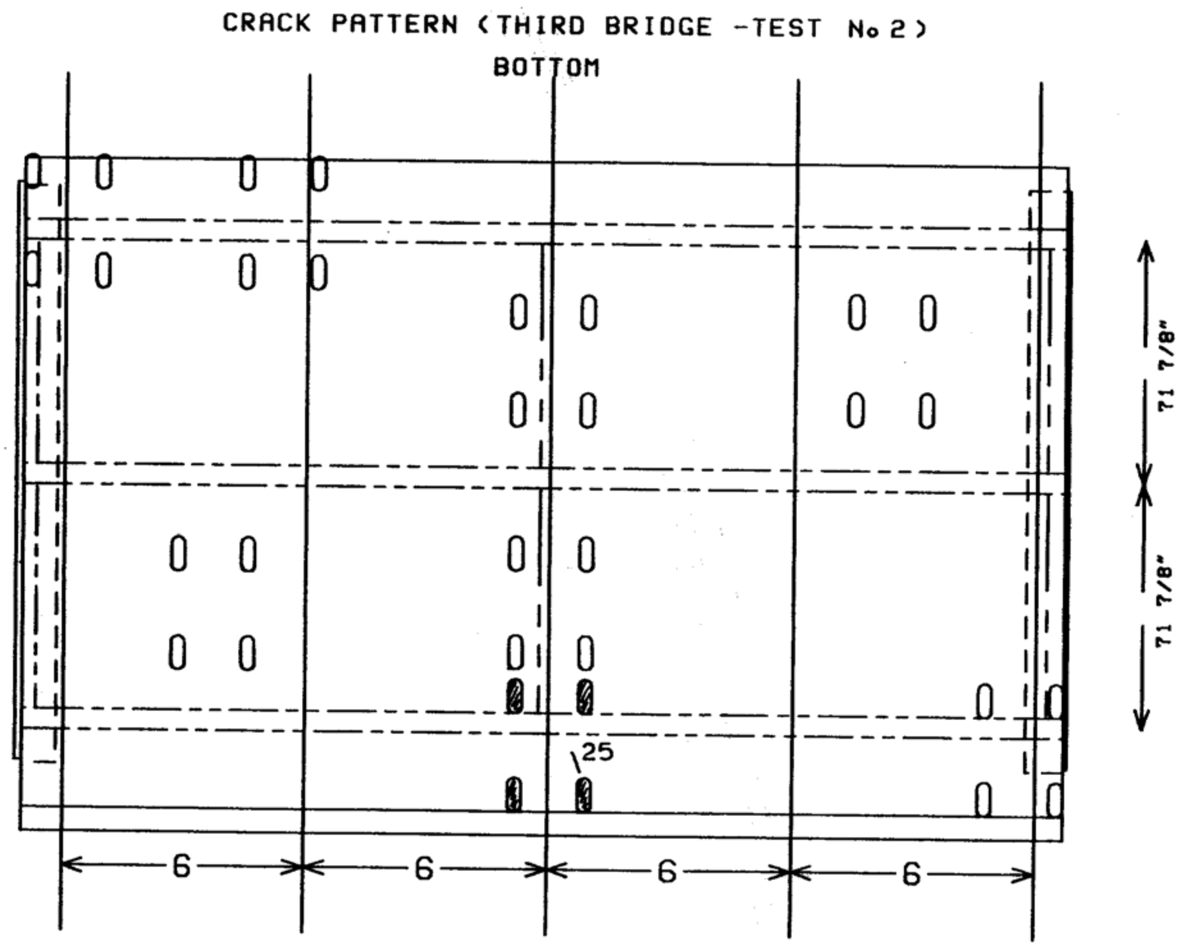

Figure E.38 Bottom Cracking Pattern (Third Bridge - Test No. 2)

CRACK PATTERN (THIRD BRIDGE - TEST No 3)

TOP

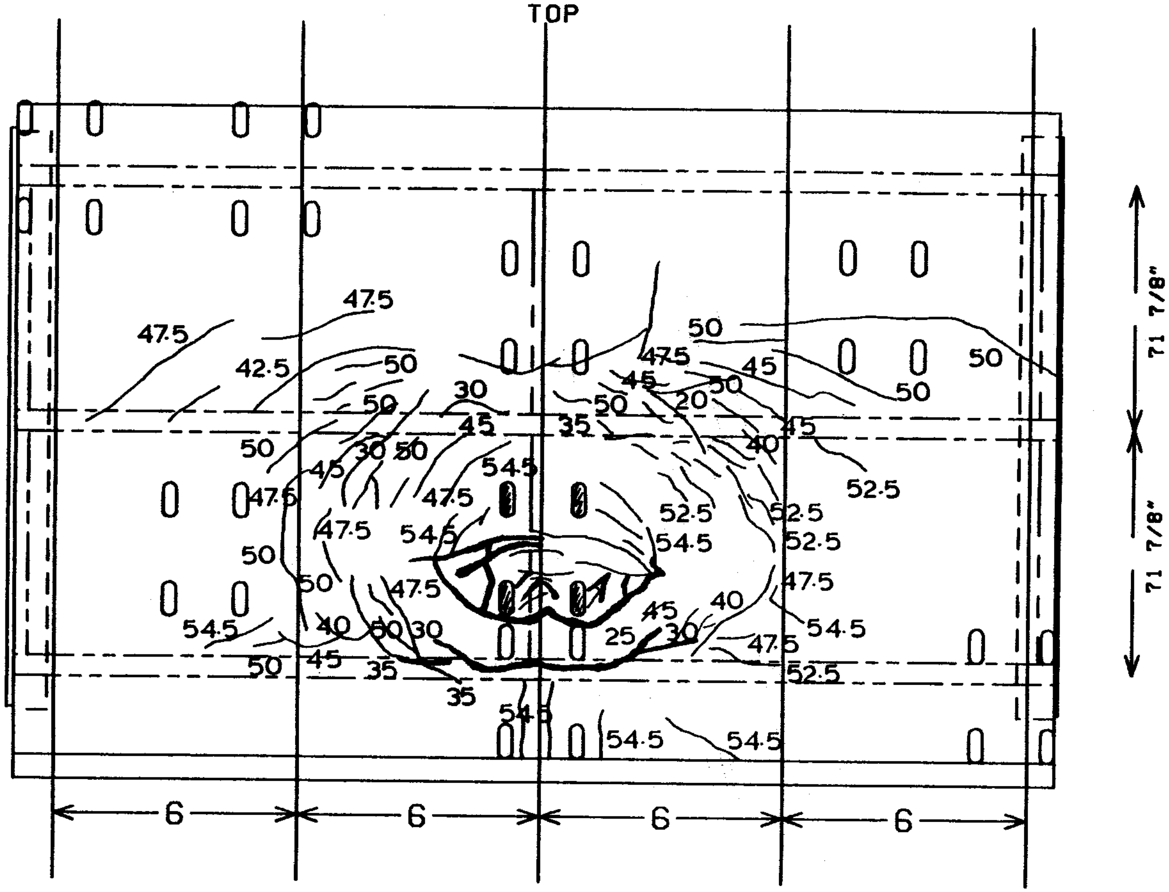

Figure E.39 Top Cracking Pattern (Third Bridge - Test No. 3)

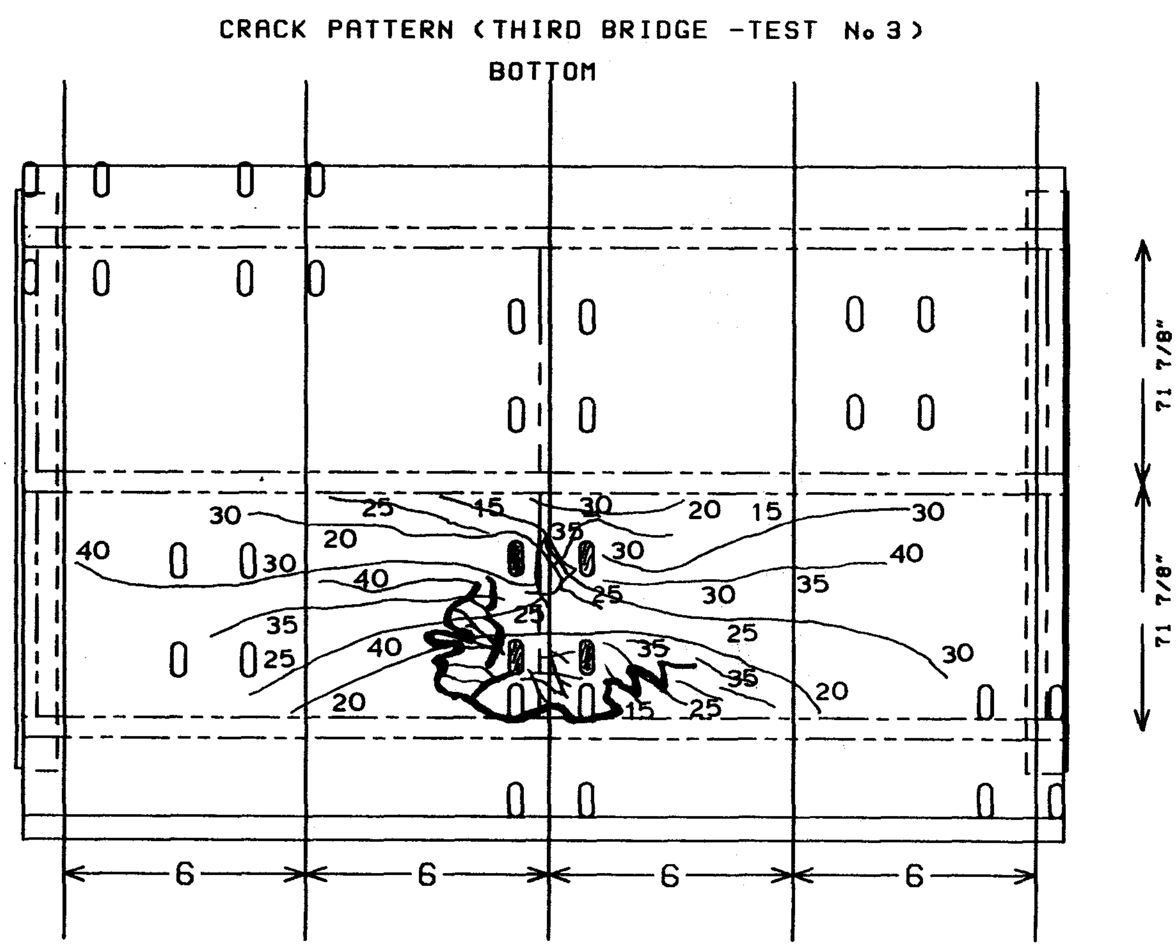

Figure E.40 Bottom Cracking Pattern (Third Bridge - Test No. 3)

CRACK PATTERN (THIRD BRIDGE -TEST No 4)

TOP

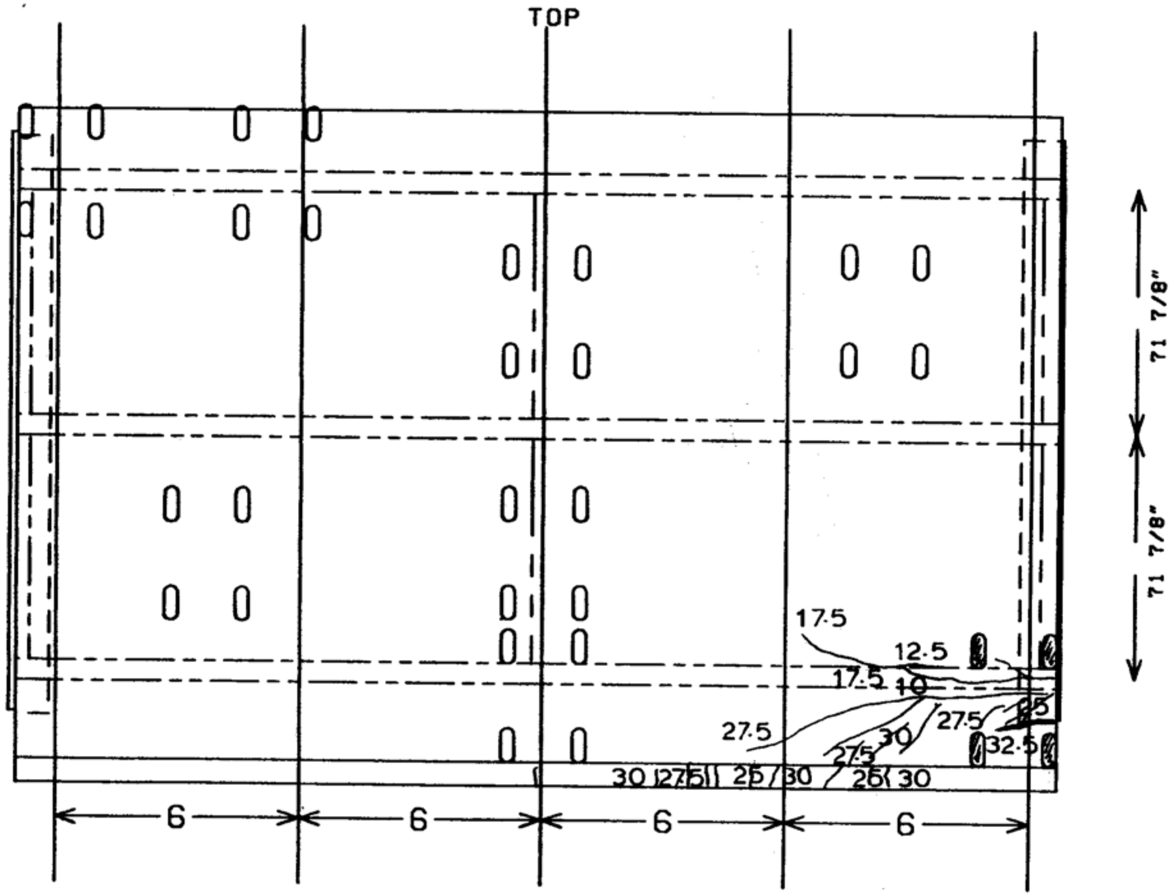

Figure E.41 Top Cracking Pattern (Third Bridge - Test No. 4)

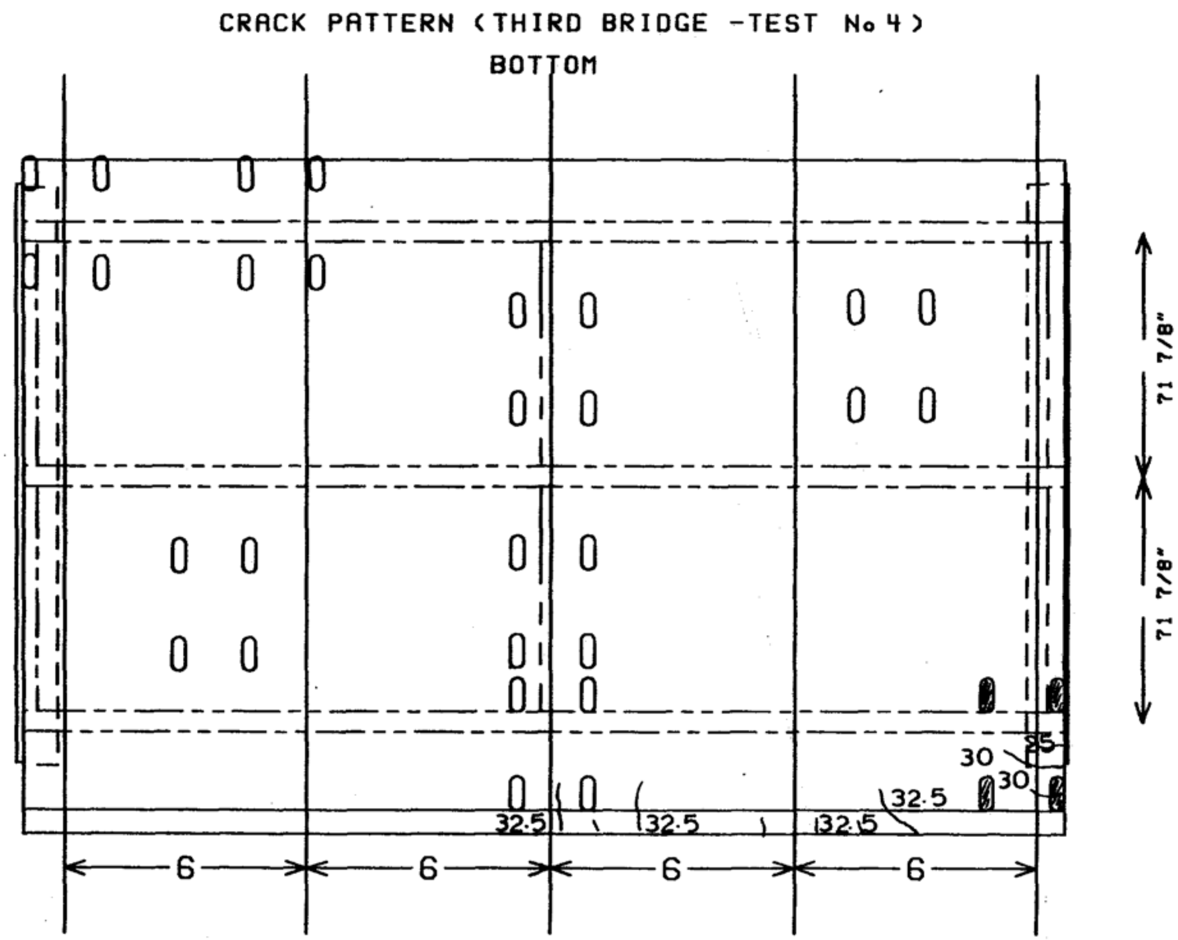

Figure E.42 Bottom Cracking Pattern (Third Bridge - Test No. 4)

CRACK PATTERN (THIRD BRIDGE -TEST No 5)

TOP

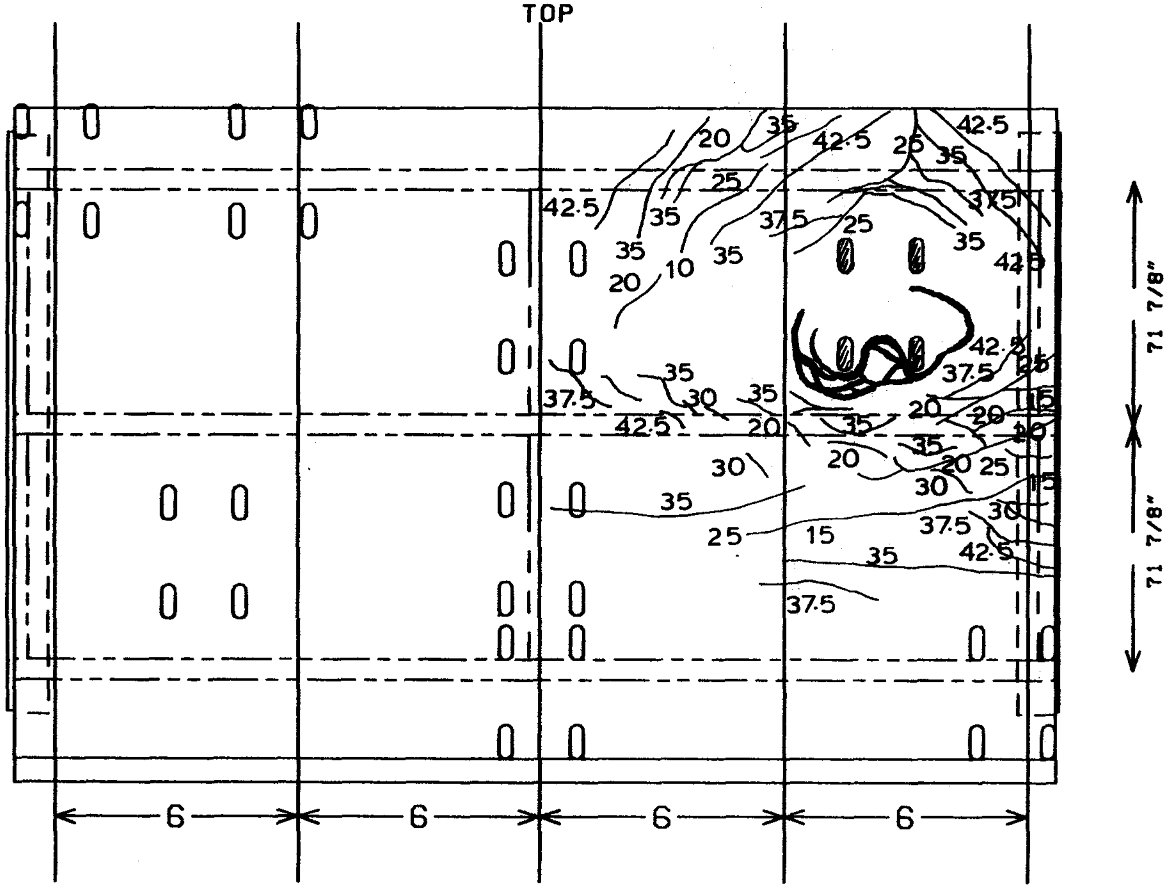

Figure E.43 Top Cracking Pattern (Third Bridge - Test No. 5)

CRACK PATTERN (THIRD BRIDGE -TEST No 5)

BOTTOM

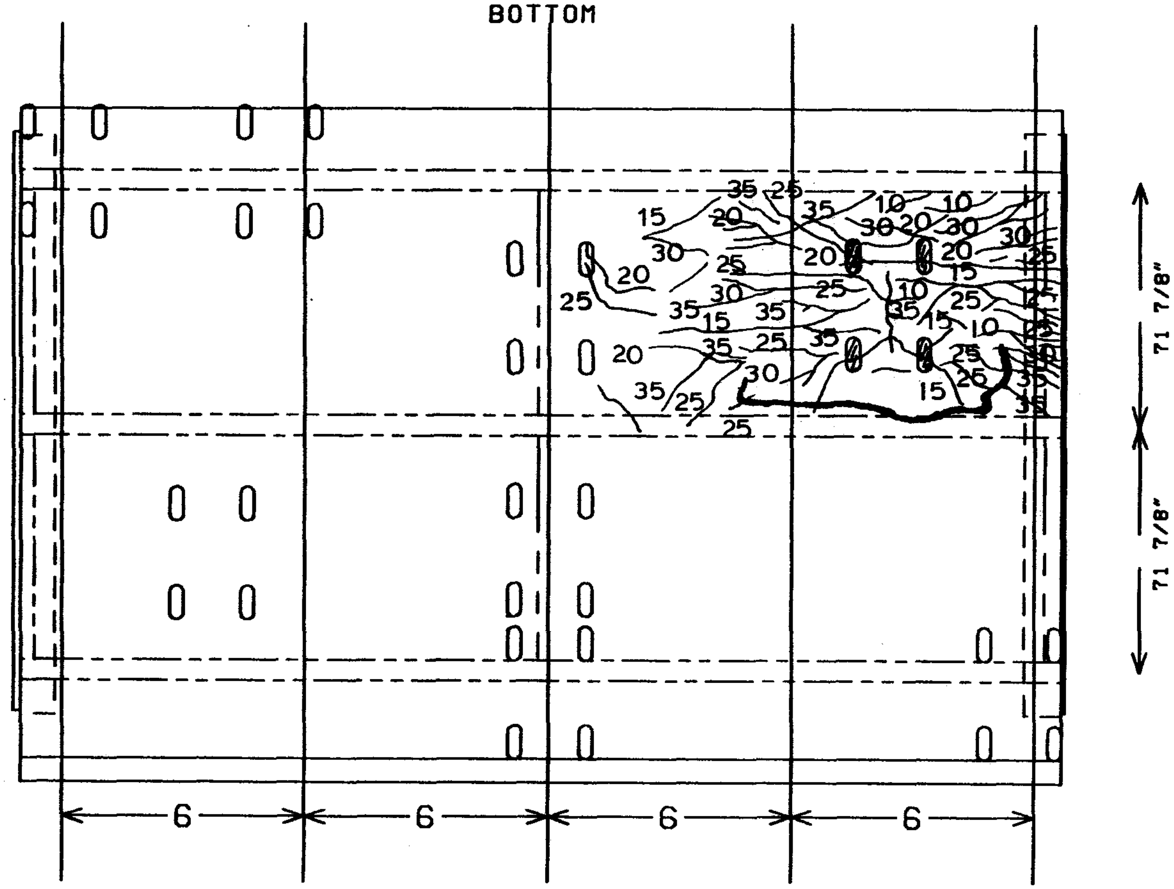

Figure E.44 Bottom Cracking Pattern (Third Bridge - Test No. 5)

CRACK PATTERN (THIRD BRIDGE -TEST No 6)

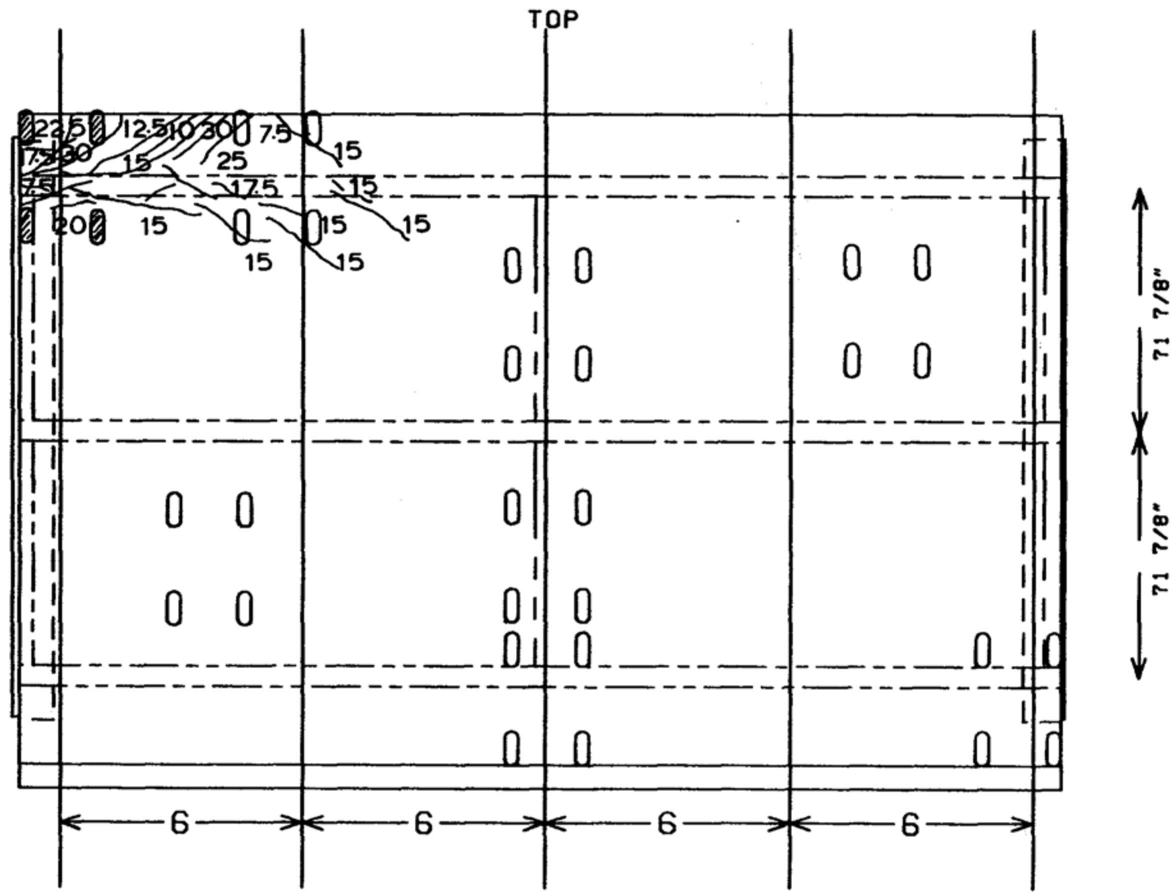

Figure E.45 Top Cracking Pattern (Third Bridge - Test No. 6)

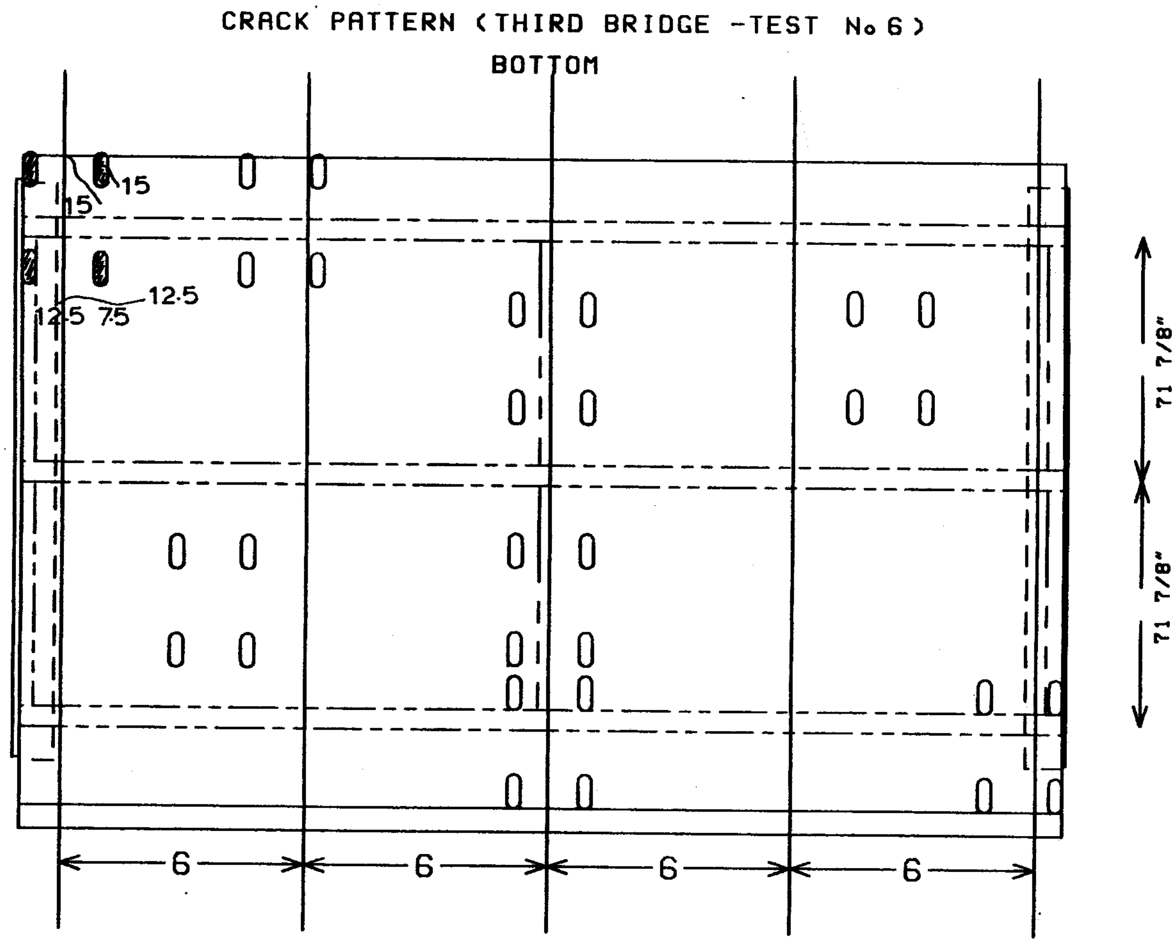

Figure E.46 Bottom Cracking Pattern (Third Bridge - Test No. 6)

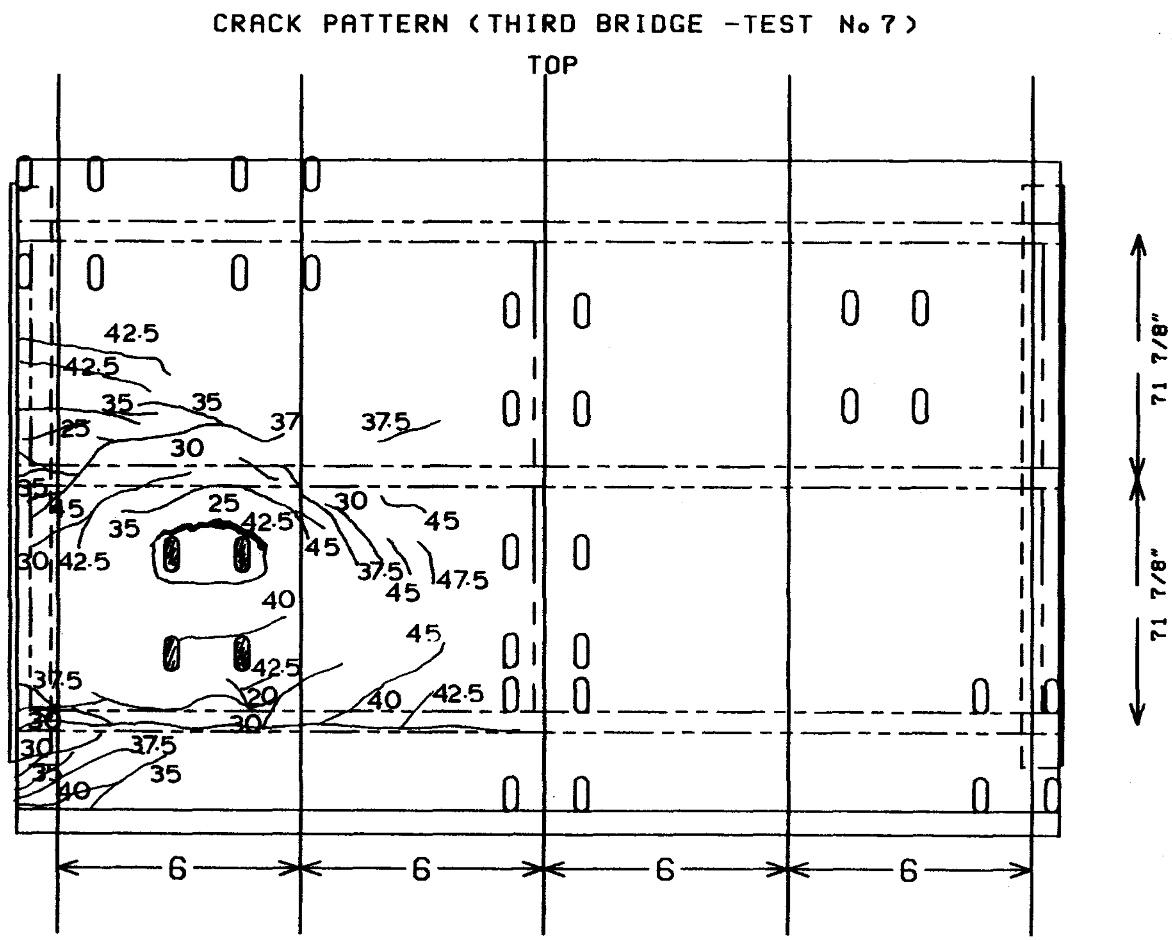

Figure E.47 Top Cracking Pattern (Third Bridge - Test No. 7)

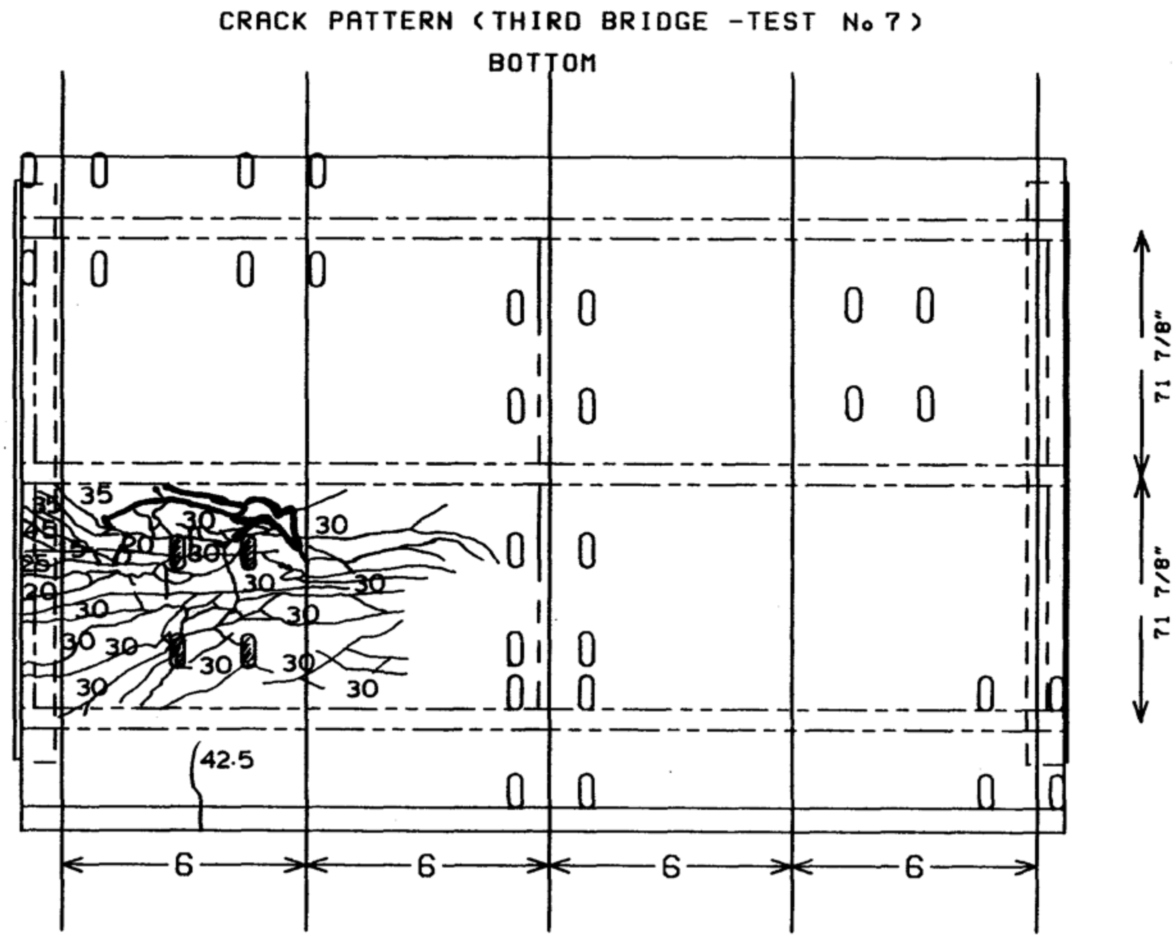

Figure E.48 Bottom Cracking Pattern (Third Bridge - Test No. 7)

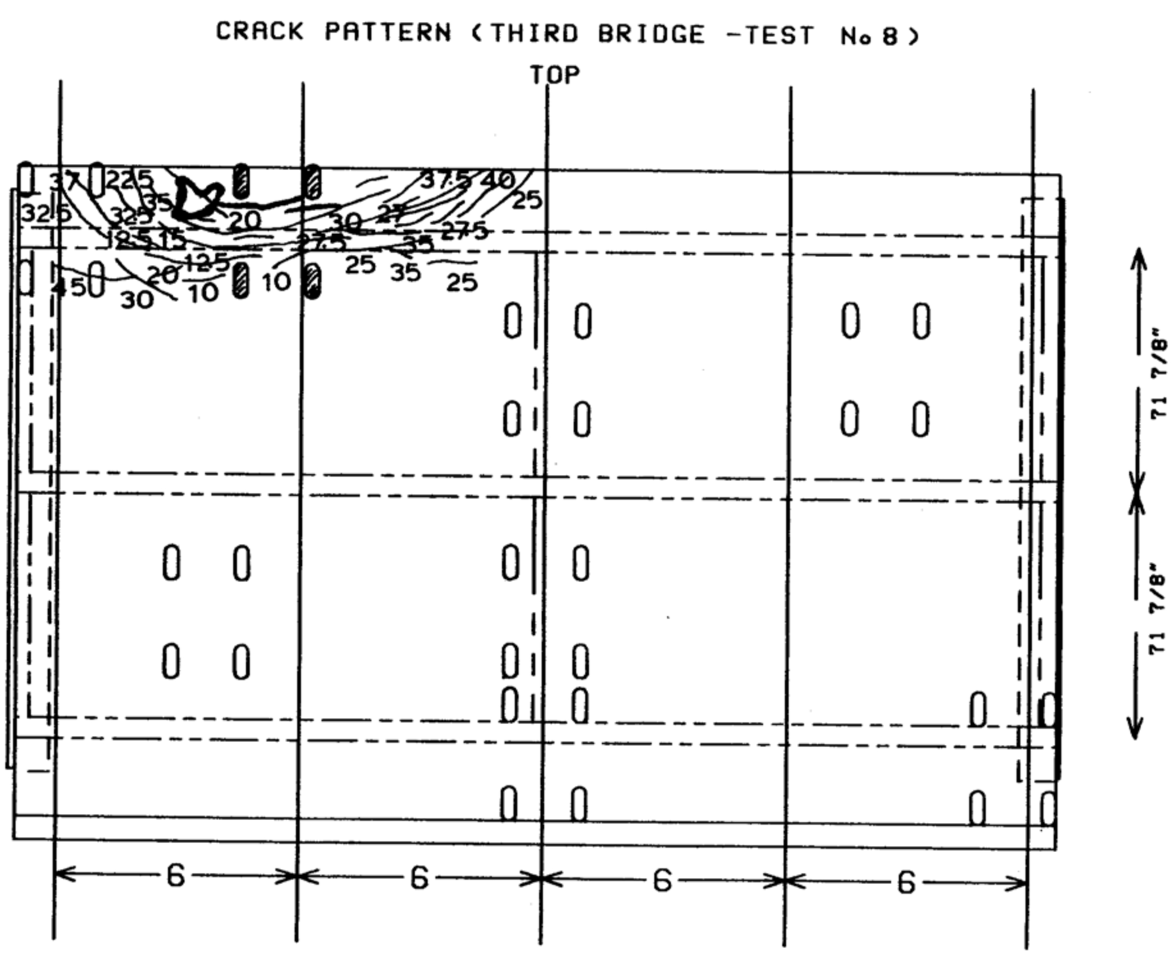

Figure E.49 Top Cracking Pattern (Third Bridge - Test No. 8)

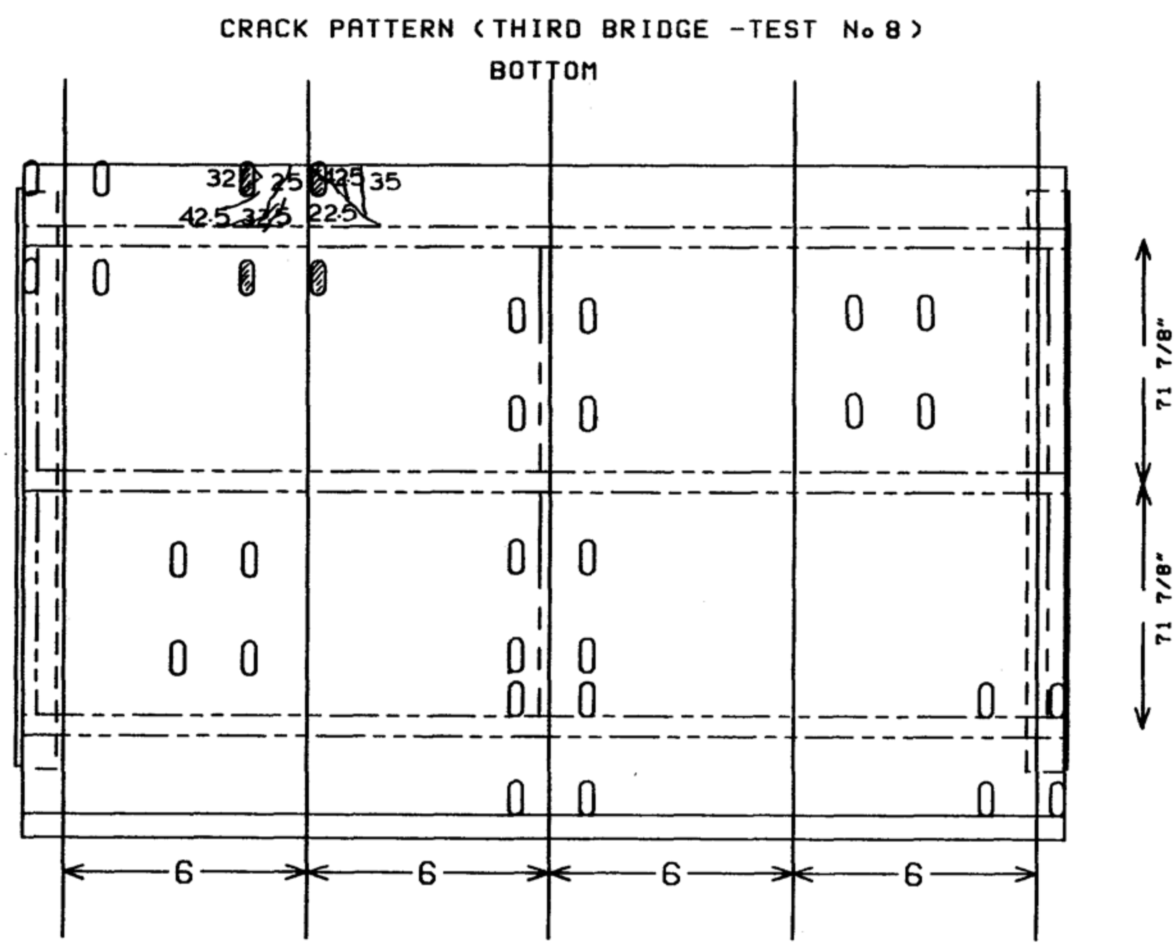

Figure E.50 Bottom Cracking Pattern (Third Bridge - Test No. 8)

APPENDIX F

Material Properties

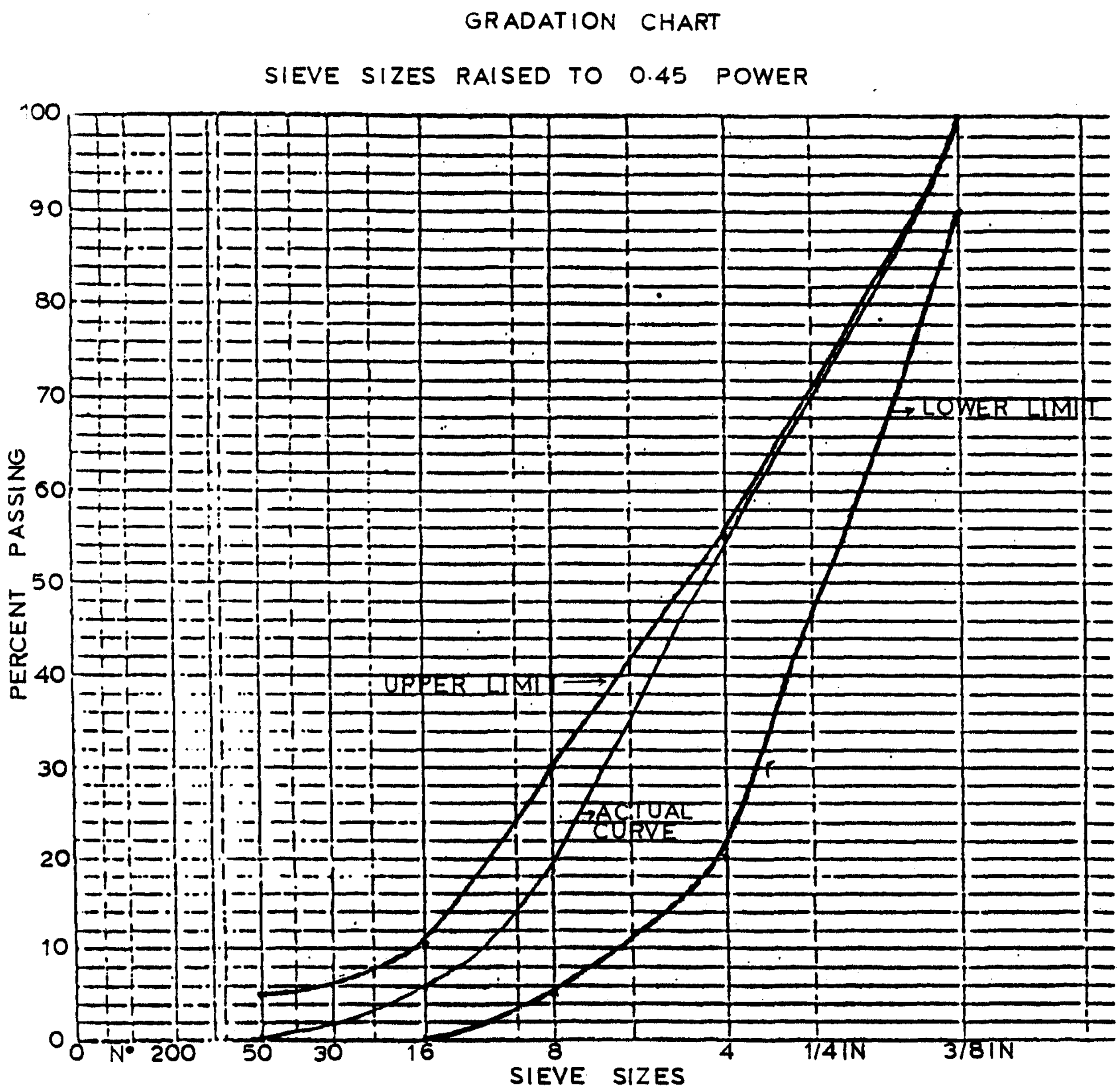

CONCRETE MIX
WEIGHT IN POUNDS OF AGGREGATE
(PER YARD)
1710 N° 89 ROCK 5% MOISTURE
1270 SILICA SAND 5% MOISTURE
564 CEMENT TYPE 1
24 GAL WATER
1.7 ml OF AIR (MBUR)
45 ml OF RETARDER (MBL 80)

Figure F.1 Aggregate Gradation Chart and Concrete Mix

FIRST BRIDGE

Cast of the Slab .. 9/25/87

COMPRESSION TEST (Slab)

Days	Strength
6	4360
21	5100
28	5587
59	5122
74	5970
109	5810
115	6410

TENSION TEST (Slab)

Days	Strength
28	499
59	505
74	536
115	538

BEAM TEST (Slab)

Days	Strength
28	456
59	517
74	682
115	721

Cast of the Parapet .. 10/2/87

COMPRESSION TEST (Parapet)

Days	Strength
14	5500
28	6480
103	7710

TENSION TEST (Parapet)

Days	Strength
28	507
59	525
74	560
103	566

Figure F.2 Concrete Test Results (First Bridge)

SECOND BRIDGE
Cast of the slab.. 2/23/88

COMPRESSION TEST (Slab)

Days	Strength
13	5102
28	5980
63	6339
71	6550
78	6574

TENSION TEST (Slab)

Days	Strength
28	465
64	486
71	479
78	543

BEAM TEST (Slab)

Days	Strength
28	419
65	463
79	544

Cast of the Parapet ..3/2/88

COMPRESSION TEST (Parapet)

Days	Strength
5	5337
28	6450
55	7638
70	7692

Figure F.3 Concrete Test Results (Second Bridge)

THIRD BRIDGE

Cast of the slab.. 6/10/88

COMPRESSION TEST (Slab)

Days	Strength
28	5721
38	6137
40	5967
42	6020
45	5899
47	6366
49	6345
54	6382
56	6295
59	6369

TENSION TEST (Slab)

Days	Strength
28	498
54	502
56	495
59	505

BEAM TEST (Slab)

Days	Strength
28	528
49	589
59	630

Cast of the Parapet .. 6/17/88

COMPRESSION TEST (Parapet)

Days	Strength
28	5651
49	6142
52	5949

TENSION TEST (Parapet)

Days	Strength
28	530
49	545

BEAM TEST (Parapet)

Days	Strength
28	522
52	630

Figure F.4 Concrete Test Results (Third Bridge)

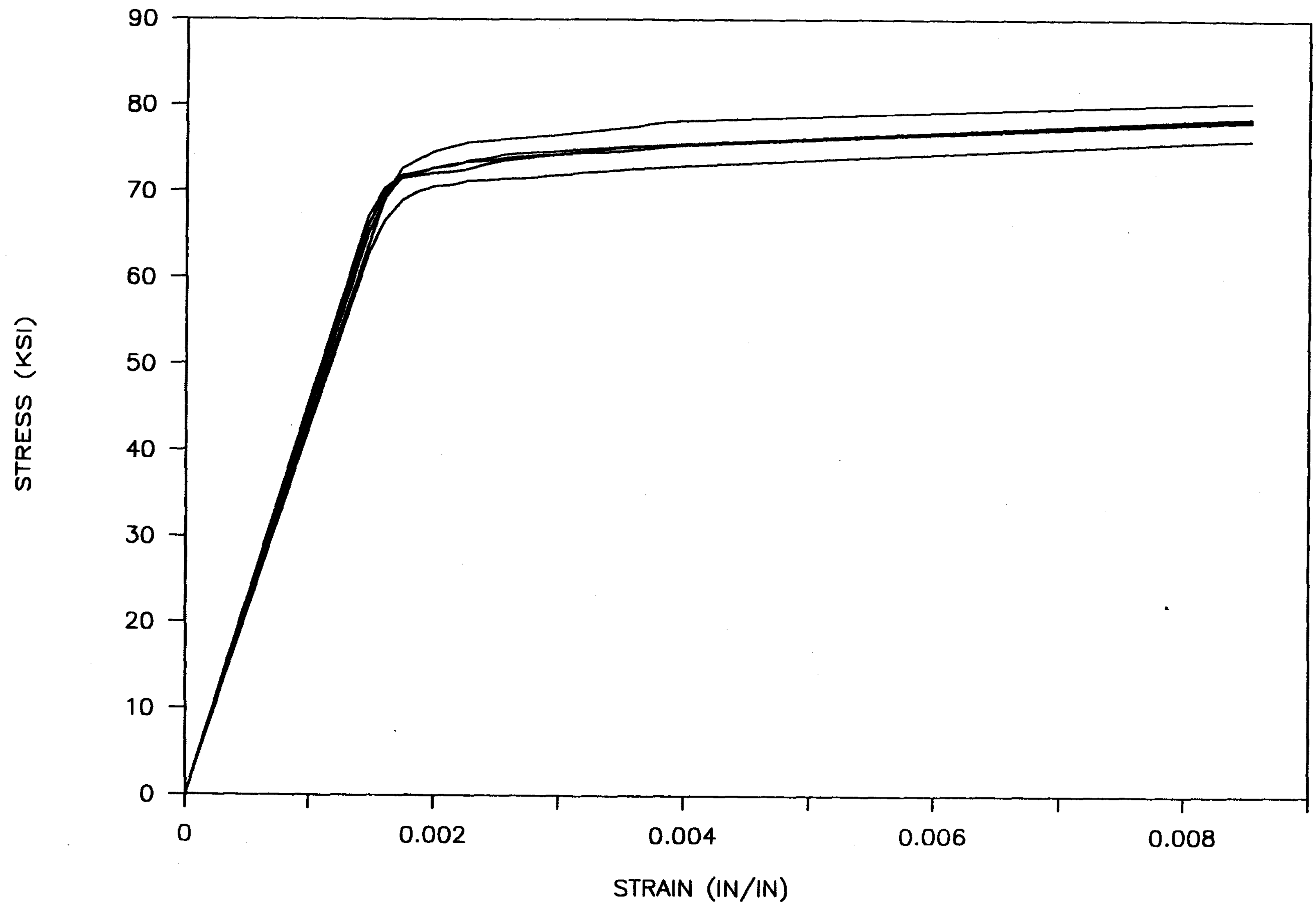

Figure F.5 Stress-Strain Curves for Deck Reinforcing Steel

APPENDIX G
Measured Thicknesses of Deck

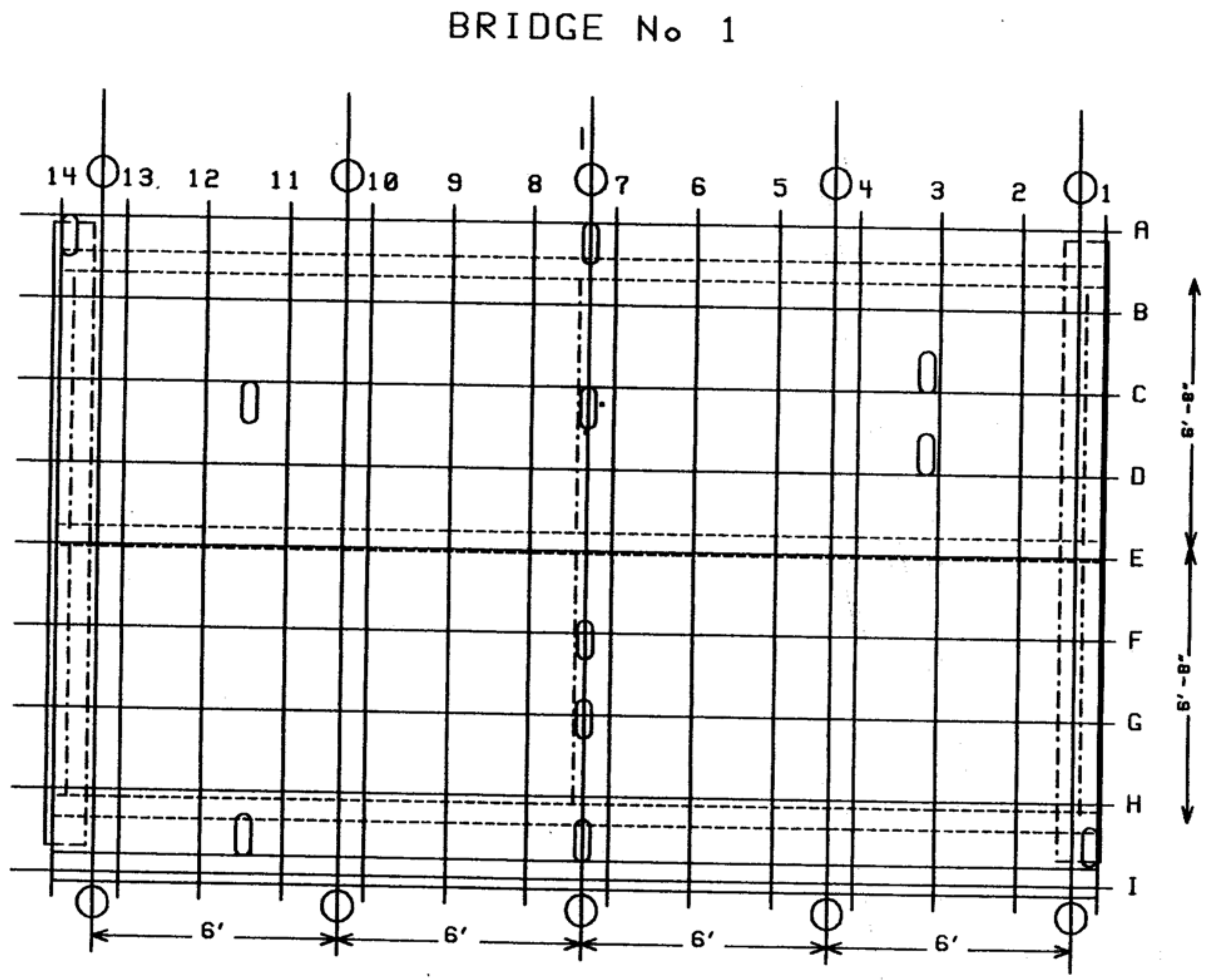

Figure G.1 Location of Reference Lines for Thickness Measurements (Bridge No. 1)

Table G.1 Thickness Variation (Bridge No. 1)

	1	2	3	4	5	6	7	8	9	10	11	12	13	14
A	4	4 3/32	4	4	4 1/16	4 5/32	4	4 1/8	4	4 1/8	4 5/32	4 5/32	4 1/32	4 3/16
B	4	4 7/32	4 5/16	4 9/32	4 9/32	4 17/32	4 11/32	4 13/32	4 11/32	4 11/32	4 13/32	4 13/32	4 7/16	4 3/16
C	4 7/32	4 3/8	4 13/32	4 3/8	4 13/32	4 15/32	4 15/32	4 9/16	4 1/2	4 19/32	4 17/32	4 15/32	4 3/8	4 5/16
D	4 5/16	4 1/2	4 1/2	4 7/16	4 17/32	4 5/8	4 19/32	4 3/4	4 23/32	4 23/32	4 7/16	4 17/32	4 3/8	4 3/16
E	4 5/16	4 3/8	4 7/16	4 11/32	4 13/32	4 19/32	4 15/32	4 9/16	4 5/8	4 9/16	4 9/16	4 1/2	4 5/16	4 7/32
F	4 1/4	4 7/32	4 3/8	4 13/32	4 19/32	4 3/4	4 21/32	4 5/8	4 11/16	4 13/32	4 19/32	4 1/2	4 1/4	4 1/8
G	4 1/8	4 9/32	4 11/32	4 15/32	4 19/32	4 5/8	4 5/8	4 1/2	4 19/32	4 11/32	4 15/32	4 3/16	4 1/16	4 3/32
H	4 5/32	4 1/4	4 5/16	4 11/32	4 21/32	4 5/8	4 21/32	4 11/32	4 13/16	4 5/32	4 1/32	4 1/16	4 1/32	4 5/32
I	4 1/8	4 1/16	4 1/16	4 1/8	4 3/16	4 3/16	4 3/16	4 3/16	4 1/4	4 1/8	4 1/16	4 1/16	4 1/8	4 3/16

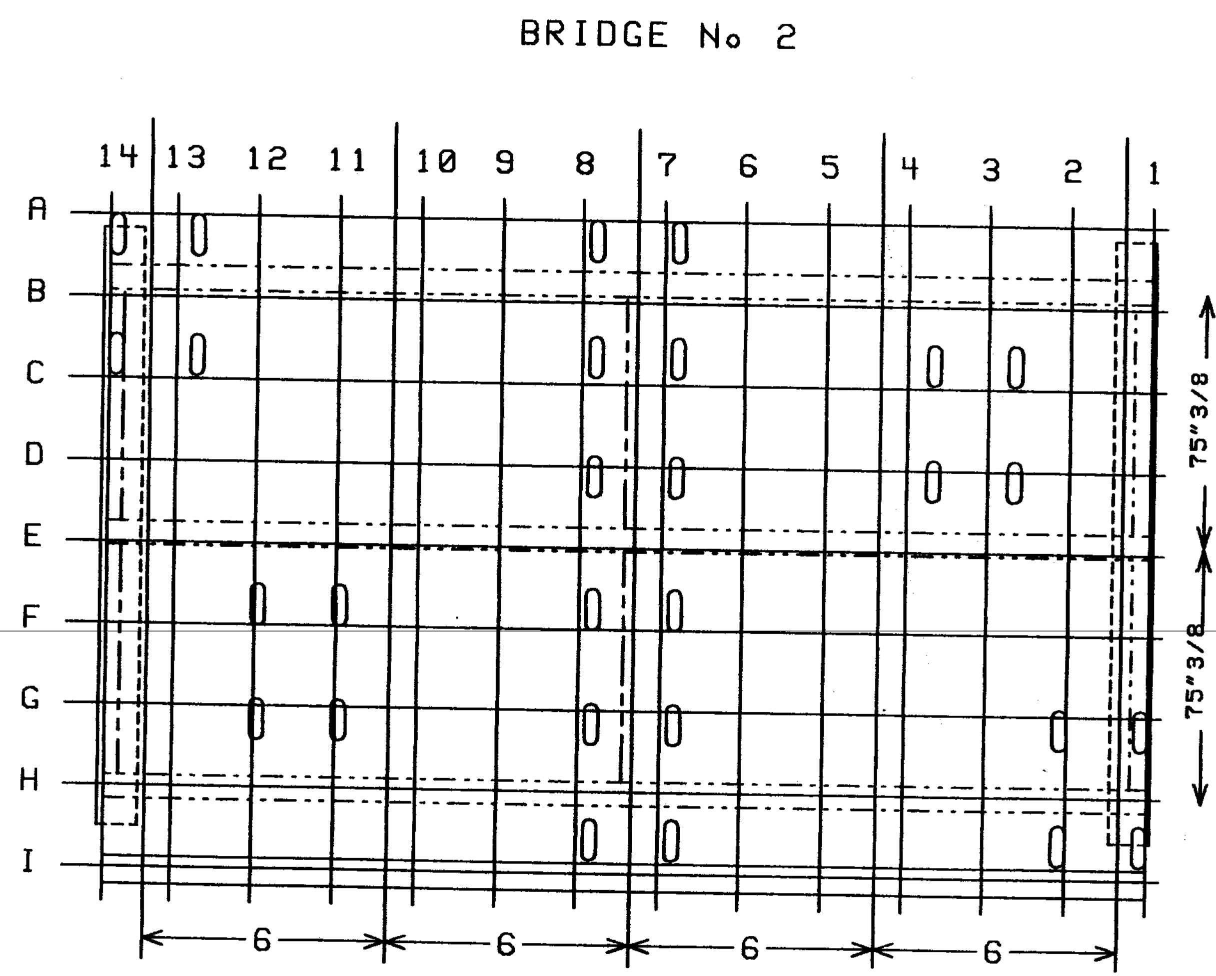

Figure G.2 Location of Reference Lines for Thickness Measurements (Bridge No. 2)

Table G.2 Thickness Variation (Bridge No. 2)

	1	2	3	4	5	6	7	8	9	10	11	12	13	14
A	3 13/16	3 3/4	3 3/4	3 3/4	3 3/4	3 13/16	3 13/16	3 3/4	3 3/4	3 13/16	3 7/8	3 3/4	3 13/16	3 3/4
B	3 13/16	3 13/16	3 11/16	3 5/8	3 9/16	3 9/16	3 1/2	3 5/8	3 5/8	3 1/2	3 9/16	3 11/16	3 13/16	3 3/4
C	3 3/4	3 13/16	3 3/4	3 5/8	3 1/2	3 1/2	3 5/8	3 9/16	3 11/16	3 11/16	3 3/4	3 3/4	3 13/16	3 7/8
D	3 3/4	3 3/4	3 5/8	3 3/4	3 13/16	3 7/8	3 3/4	3 11/16	3 11/16	3 13/16	3 13/16	3 13/16	3 3/4	3 13/16
E	3 3/4	3 11/16	3 5/8	3 9/16	3 9/16	3 1/2	3 9/16	3 9/16	3 11/16	3 5/8	3 11/16	3 11/16	3 11/16	3 3/4
F	3 7/8	3 5/8	3 5/8	3 9/16	3 1/2	3 7/16	3 7/16	3 9/16	3 5/8	3 11/16	3 11/16	3 11/16	3 13/16	3 13/16
G	3 7/8	3 13/16	3 11/16	3 3/4	3 11/16	3 11/16	3 5/8	3 3/4	3 15/16	3	3 15/16	3 7/8	3	3 7/8
H	3 13/16	3 11/16	3 11/16	3 5/8	3 5/8	3 9/16	3 1/2	3 9/16	3 11/16	3 5/8	3 11/16	3 3/4	3 13/16	3 13/16
I	3 7/8	3 5/8	3 9/16	3 1/2	3 1/2	3 11/16	3 7/16	3 9/16	3 3/4	3 7/8	3 15/16	3 3/4	3 13/16	3 3/4

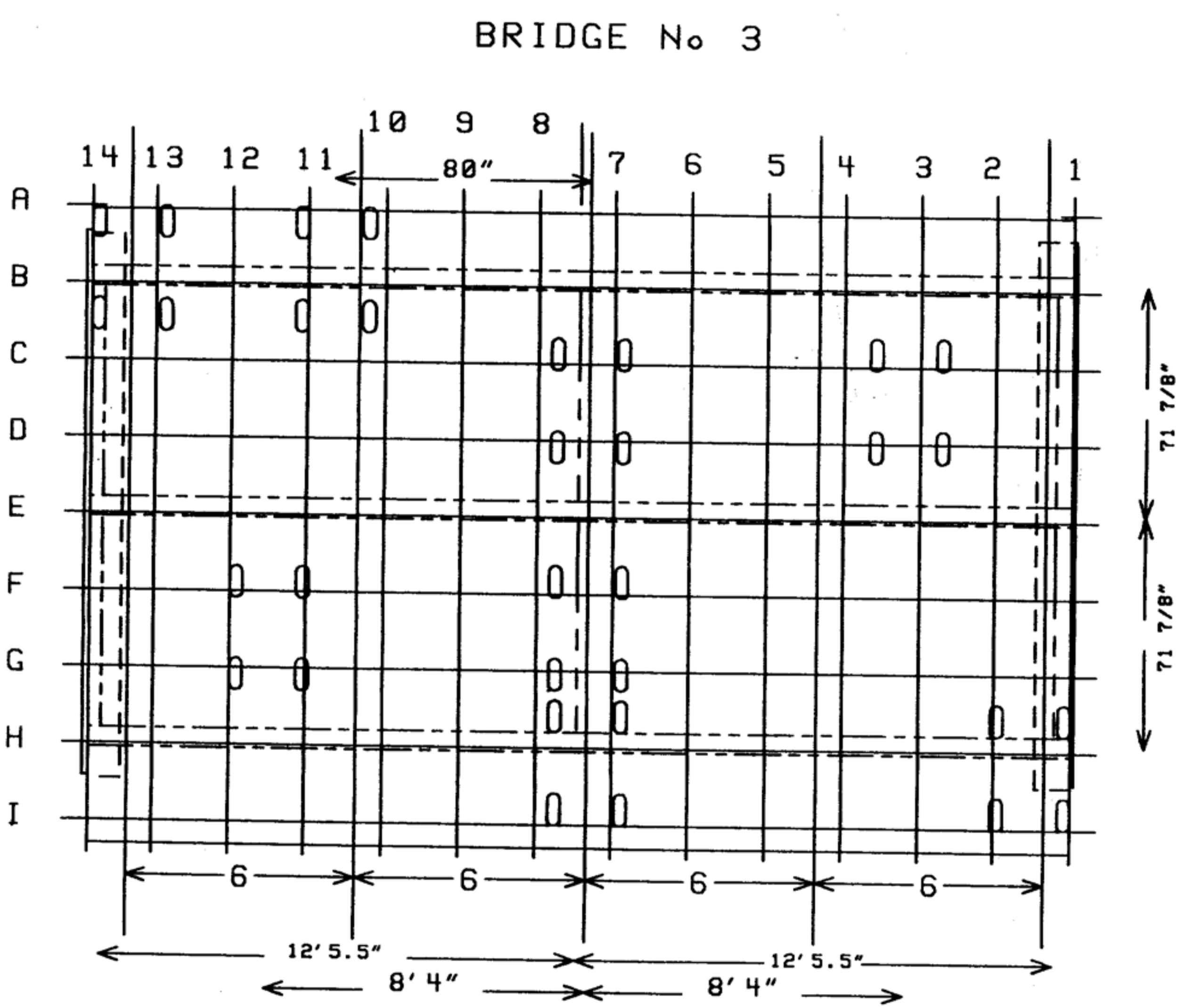

Figure G.3 Location of Reference Lines for Thickness Measurements (Bridge No. 3)

Table G.3 Thickness Variation (Bridge No. 3)

	1	2	3	4	5	6	7	8	9	10	11	12	13	14
A	3 3/8	3 11/32	3 1/2	3 17/32	3 1/2	3 1/2	3 7/32	3 7/32	3 7/32	3 11/32	3 13/32	3 13/32	3 7/16	3 7/16
B	3 5/16	3 9/32	3 5/16	3 7/32	3 1/32	3	3 1/32	3 1/4	3 5/32	3 7/32	3 5/32	3 3/32	3 5/32	3 9/32
C	3 3/8	3 1/4	3 11/32	3 3/16	3 3/32	3 1/8	3 1/32	3 3/32	2 15/16	2 29/32	3 1/32	2 31/32	3 1/16	3 1/4
D	3 3/8	3 1/4	3 5/16	3 5/32	3 5/32	3 3/32	3 1/8	3 5/32	3 1/16	3	3 3/32	3 1/32	3 5/32	3 5/16
E	3 9/32	3 7/32	3 7/32	3 3/32	3 1/32	3 3/32	3 3/32	3 7/32	3 1/32	3 1/32	3 1/8	3 1/32	3 5/32	3 11/32
F	3 7/32	3 1/8	3 3/32	2 31/32	3	3	2 29/32	2 29/32	3	3 9/32	3 5/32	3 1/16	3 3/16	3 5/16
G	3 3/16	3 7/32	3 5/32	3 1/16	3 3/32	3 1/32	3	3	3 3/32	3 3/16	3 1/8	3 1/16	3 1/8	3 5/16
H	3 9/32	3 1/4	3 3/32	3 5/32	3 5/32	3 7/32	3 1/8	3 1/4	3 5/32	3 1/8	3 1/16	3 3/32	3 3/16	3 5/16
I	3 11/32	3 5/16	3 1/4	3 1/4	3 3/8	3 5/16	3 1/4	3 5/16	3 11/32	3 11/32	3 3/8	3 11/32	3 5/16	3 7/16